Switchable Catalysis to make Multi-Block Copolymers

Shyeni Paul

Imperial College London

Department of Chemistry

A thesis submitted in partial fulfilment of the requirements for the degree of Doctor of Philosophy in Chemistry

Declaration

All work, unless otherwise stated, has been carried out by the author between October 2013 and October 2016.

Abstract

This thesis describes the development of methods to selectively generate block copolymers using a single catalyst and multiple different polymerisation cycles referred to as "switchable'' catalysis. It exploits the ability of various dinuclear zinc catalysts to selectively catalyse both ring opening copolymerisation of epoxides and carbon dioxide or anhydrides and ring opening polymerisation of lactones and lactide. The catalyst selectivity is proposed to arise from different rates of insertion into the key intermediate, a zinc alkoxide species, and from the different stabilities of the linkages formed. Chapters 2 and 3 describe the new switchable catalysis to link the ring opening copolymerisation of epoxides and carbon dioxide with the subsequent ring opening polymerisation of lactones (ε-caprolactone, ε-decalactone, δ-valerolactone). This method allows the formation of well-defined block copolymers. The block copolymers are characterised using *in-situ* infrared spectroscopy, nuclear magnetic resonance spectroscopy including diffusion ordered spectroscopy analysis and size exclusion chromatography analysis. Block copolymers are synthesised with a range of compositions from 1:0.5 – 1:10 carbonate:ester. The thermal properties of the copolymers are highly dependent on the proportion of polyester. The block copolymers containing ε-caprolactone and ε-decalactone were found to act as flexible plastics by tensile mechanical measurements. In contrast, the block copolymer containing δ-valerolactone was a soft, inflexible plastic. Chapter 4 describes the use of the switchable catalysis method to form multiblock copolymers compromising of up to seven blocks. The dizinc catalyst is able to switch between ring opening copolymerisation of cyclohexene oxide and carbon dioxide and ring opening polymerisation of ε-caprolactone reversibly and exclusively forms a multiblock copolymer. Chapter 5 describes the application of the method to a mixture of four monomers: epoxides, carbon dioxide, anhydrides and lactones or lactide. The dizinc catalyst selectively forms pentablock copolymers with predictable compositions and block sequences. The structure of the pentablock copolymer depends on whether lactone or lactide is applied as the monomer. Overall, this thesis presents a novel type of catalyst selectivity and a means to control it. The switchable catalysis is demonstrated with dizinc catalysts, and is used to form a variety of multiblock copolymers from mixtures of monomers.

Acknowledgements

I would like to thank my supervisor, Professor Charlotte Williams, for believing in me, for her support and all the work that has entailed.

I would like to thank all those people who conducted analysis for me. In particular, Peter Haycock and Richard Sheppard for conducting several NMR experiments; Lisa Haigh for her mass spectrometry service and Stephen Boyer, from London Metropolitan University, for elemental analysis.

I am extremely grateful to all the members of the Williams Group, for the support, expertise, company, laughter and cake. Thank you to Rachel Brooks, Dominic Myers, Frank Zhu, Jameel Marafie, Ni Yi, Gemma Trott, Charlie Coleman, Alice Leung, Arnaud Thevenon, Aaron Deacy, Tim Stoesser, Matthew Allinson, Yoni Wiener, Dr Prabhjot Saini, Dr Junjuda Unruangsri, Dr Andres Trenco Garcia, Dr Seb Pike, Dr Giulia Fiorani, Dr Anish Cyriac, Dr Sumesh Raman Kureppadathu and Dr Clare Bakewell. Especial thanks go to Dr Charles Romain, for answering every single question.

My friends deserve special recognition for all the times they have listened to me talk about my work (and it not working). I'd like to thank Ally and Amelia for giving me other things to talk about, Chris for making me smile and Suzi for taking me to dinner, helping me breathe and for pointing out I never choose the easy option.

Credit goes to my family for not making too much fun of me for spending my first 16 years promising that 'I'd never be a scientist and never ever a chemist'. So thank you to my wonderful family for their love and support; to my parents for showing me the world and my siblings for making me laugh.

Mostly I need to thank James, without whom I wouldn't have finished. Thank you for loving me, keeping me sane and doing the dishes.

List of Publications

Chemoselective Polymerizations from Mixtures of Epoxide, Lactone, Anhydride, and Carbon Dioxide

Romain C, Zhu Y, Dingwall P, Paul S, Rzepa HS, Buchard A, Williams CK, 2016, J.Am.Chem.Soc, **138**, 4120-4131.

Sequence Selective Polymerization Catalysis: A New Route to ABA Block Copoly(ester-b-carbonate-b-ester)

Paul S, Romain C, Shaw J, Williams CK, 2015, Macromolecules, **48**, 6047-6056.

Ring-opening copolymerization (ROCOP): synthesis and properties of polyesters and polycarbonates

Paul S, Zhu Y, Romain C, Brooks R, Saini PK, Williams CK, 2015, Chem. Commun., **51**, 6459-6479.

Formation of Pentablock copolymers from switch chemsitry

Shyeni Paul, Charlotte K. Williams, 2016, ACS Macro Lett, *in preparation*

A copy of the research papers is included in the appendix.

List of Abbreviations

ADMET	Acylic Diene Metathesis
AGE	Allyl Glycidyl Ether
ATR-IR	Attenuated Total Reflectance Infrared
ATRP	Atom Transfer Radical Polymerisation
BDI	β-Diiminate
BnOH	Benzyl Alcohol
C	Centigrade
CCU	Carbon Capture and Utilisation
CHD	Cyclohexane-1,2-diol
CHO	Cyclohexene Oxide
CO_2	Carbon Dioxide
$CoCp_2$	Bis(cyclopentadienyl)cobalt(II) (Cobaltocene)
COSY	Homonuclear Correlation Spectroscopy
CPA	Cyclopentane-1,2-Dicarboxylic Acid Anhydride
CPrA	Cyclopropane-1,2-Dicarboxylic Acid Anhydride
CSS	Carbon Capture and Storage
CTA	Chain Transfer Agent
D	Diffusion Coefficent
Đ	Dispersity
DBU	1,8-Diazabicycloundec-7-ene
DCM	Dichloromethane
DFT	Density Functional Theory
DGA	Diglycolic Anhydride
DMAP	4-Dimethylaminopyridine
DMC	Double Metal Cyanide
DMSO	Dimethyl Sulfoxide
DOSY	Diffusion Ordered Spectrosocopy
$\overline{DP}$	Degree of Polymerisation
DSC	Differential Scanning Calorimetry
E	Youngs Modulus

ee	Enantiomeric Excess
eq	Equivalent
ESI	Electrospray Ionisation
FcPF6	Ferricenium Hexafluorophosphate
GPC	Gel Permeation Chromatography
HMBC	Heteronuclear Multiple-Bond Correlation
HSQC	Heteronuclear Single Quantum Coherence
iBu	Iso-Butyl
iPr-OH	Iso -Propyl Alcohol
iPr	Iso-Propyl
IR	Infrared
k_{obs}	Observed Rate Constant
L	Ligand
LA	Lactide
LS	Light Scattering
M	Molar
MA	Maleic Anhydride
MALDI-ToF	Matrix Assisted Laser Desorption Ionisation Time of Flight
MALLS	Multi Angle Laser Light Scattering
MEG	Methoxy Ethylene Glycol
MeOH	Methanol
Meq	Equilibriation Concentration
M_n	Number Average Molecular Weight or Molar Mass
MPa	Mega Pascals
MS	Mass Spectrometry
N	Newtons
N_2	Nitrogen
NHC	N-heterocyclic
nm	nanometer
NMR	Nuclear Magnetic Resonance
OAc	Acetate

PA	Phthalic Anhydride
PCHC	Poly (cyclohexene carbonate)
PCHO	Poly (cyclohexene ether)
PCHPE	Poly (cyclohexene phthalic ester)
PCL	Poly (caprolactone)
PDI	Polydispersity Index
PDL	Poly (decalactone)
PDMS	Poly (dimethyl siloxane)
PE	Poly (ethylene)
PEG	Poly (ethylene glycol)
Ph	Phenyl
PI	Poly (isoprene)
PLA	Poly (lactide)
PLLA	Poly (l-lactide)
PO	Propylene Oxide
PPC	Poly (propylene carbonate)
PPC	Poly(propylene carbonate)
PPE	Poly (phosphoester)
ppm	Parts per Million
PPNCl	Bis(triphenylphosphine)iminium chloride
PS	Poly (styrene)
PU	Polyurethane
PVCHC	Poly (vinyl cyclohexene carbonate)
PVCHPE	Poly (vinyl cyclohexene phthalic ester)
PVL	Poly (valerolactone)
rac	Racemic
R_h	Hydrodynamic Radius
RI	Refractive Index
ROCOP	Ring Opening Copolymerisation
ROH	Alcohol
ROP	Ring Opening Polymerisation
SA	Succinic Anhydride

SBS	Poly (styrene-butadiene-styrene)
SEC	Size Exclusion Chromatography
SO	Styrene Oxide
TBD	Triazabicyclodecene
^{t}Bu	Tert-Butyl
T_C	Crystallisation Temperature
TCE	1,12,2-Tetrachloroethane
T_d	Decomposition Temperature
TFA	Trifluoroacetic Acid
T_g	Glass Transition Temperature
TGA	Thermogravimetric Analysis
THF	Tetrahydrofuran
T_m	Melting Temperature
TMC	Trimethylene Carbonate
TOF	Turnover Frequency
TON	Turnover Number
VCHO	Vinyl Cyclohexene Oxide
X	Co-ligand
α-CD	α-cyclodextrin
δ-VL	δ-Valerolactone
ε-CL	ε-Caprolactone
ε-DL	ε-Decalactone
χ_c	Percentage of Crystallinity

List of Figures, Schemes, Tables

Chapter 1

Chapter 2

Chapter 3

Chapter 4

Chapter 5

Chapter 6

Table of Contents

Chapter 1: Introduction

1.1 Carbon Dioxide as a Chemical Feedstock

1.1.1 Carbon Dioxide Utilisation

The amount of CO_2 we emit into the atmosphere has increased from 22 billion tonnes in 1990 to 25 billion tonnes in 2001.[1] The effect of this on the global climate is widely documented and in general the consensus is that CO_2 emissions need to be reduced dramatically to prevent irreversible changes to our climate. The European Union (EU) has set targets to reduce its emissions to 20 % below the 1990 levels by 2020 and by 80 % of the 1990 levels by 2050. Within the EU's plans to meet this target an integral part is the focus on CO_2 capture and the utilisation of CO_2 emissions from industrial processes.[2] The utilisation of CO_2 in chemical processes cannot make a huge impact on the absolute global atmospheric carbon dioxide levels because of the relative scales of the CO_2 emissions and chemical manufacture worldwide. However, the utilisation of captured carbon dioxide adds value to the CO_2 capture process, particularly from large scale industrial processes and thus provides an economic stimulus to carbon capture and storage (CSS).[3] It is likely there will be some form of carbon taxation in the future, which will also encourage using CO_2 as a raw material. Finally some technologies using CO_2 are able to replace more toxic or polluting reagents, e.g epoxides, thereby providing additional environmental benefits.

CO_2 as a chemical feedstock has some positive features such as its availability, non-toxicity and ease of use (gas). The key problem with using carbon dioxide as a feedstock is its thermodynamic stability, as it is the most highly oxidised form of carbon. However, chemists can utilise carbon dioxide in chemical processes, such as the formation of urea and cyclic carbonates, by exploiting the reactivity of the other reagents. Modern catalysts allow the transformation of carbon dioxide into a variety of complex products. Carbon dioxide is used as a chemical feedstock in processes as varied as the synthesis of urea, methanol, acrylic acid and polycarbonates.[4] The products with the highest commercial value are those that are both economically viable and more environmentally friendly than current processes. The utilisation of carbon dioxide does not necessarily ensure that the new process will be more environmentally friendly. This is because in order to react carbon dioxide, other energy

intensive reagents are usually required. One example is that in order to form methanol from carbon dioxide, hydrogen is required. Hydrogen is typically formed by the steam reforming of natural gas, an energy intensive process that produces large quantities of carbon dioxide.[1,5] The amount of carbon dioxide used in the formation of methanol is not enough to offset the amount of CO_2 produced by the formation of hydrogen.[5] Therefore the decision whether to use the CO_2 method depends on the method of producing hydrogen. Any chemical process that claims to be green, due to its use of carbon dioxide, must reduce overall CO_2 emissions and be less energy and material intensive, compared to the current process and it must also be economically viable.[6] Therefore, methods where the carbon dioxide is replacing a high energy chemical (like an epoxide) are generally the most promising for immediate deployment.

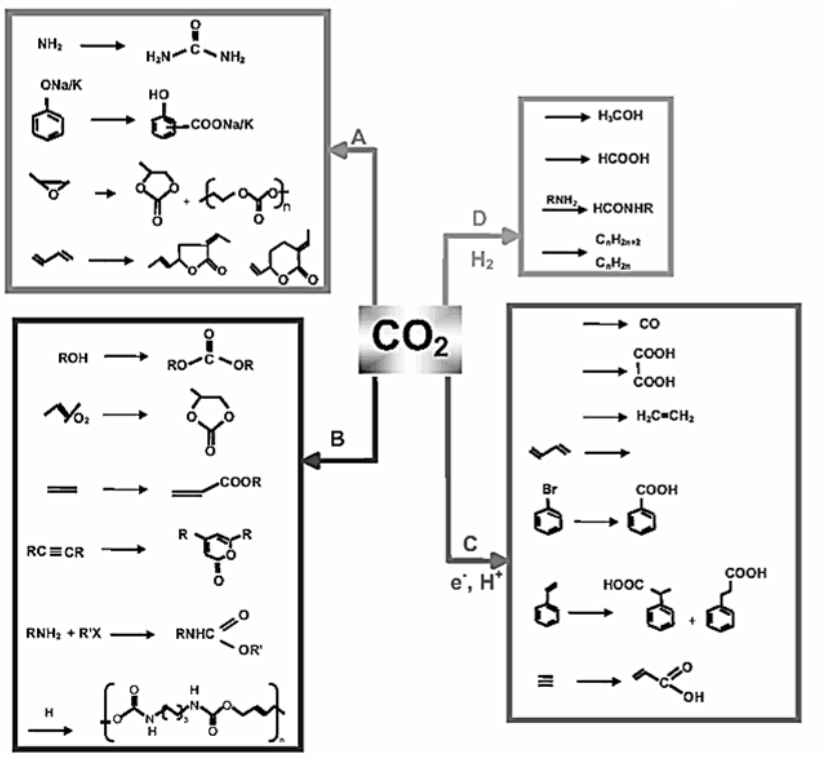

Figure 1.1.1: Potential products which incorporate carbon dioxide in the synthesis.

Taken from 'Carbon Dioxide: Utilization Options to Reduce its Accumulation in the Atmosphere' [6] with permission.

1.1.2 Polycarbonates from Carbon Dioxide: Polymer Industry

One of the most technologically viable uses for carbon dioxide is as a monomer in the production of polymers. Carbon dioxide is used as a monomer in the formation of aliphatic polycarbonates, *via* ring opening copolymerisation with epoxides. The polycarbonate formed can be used as polymeric material in its own right or used in the formation of higher polymers, like polyurethanes. Polyurethanes are manufactured on an 8 Mtonne scale per annum worldwide and have applications as foams, coatings and elastomers. They currently are synthesised from the coupling of a polyol, traditionally an epoxide derived polyether or polyester, and an isocyanate. Lifecycle analysis showed that the incorporation of carbon dioxide into the polyol portion of polyurethanes provides two improvements in the global warming impact of the process: a small contribution from the carbon dioxide capture and a considerably larger contribution from the utilisation of the carbon dioxide instead of the fossil fuel derived epoxide.[7] Covestro is industrialising the incorporation of carbon dioxide into the polyol, *via* the formation of polyether-carbonates, in its DREAM process.[7] This pilot scale plant uses carbon dioxide from a lignite power plant and incorporates up to 20 % carbon dioxide into the polymers. There are other companies working in the same area. Novomer is also commercialising polycarbonates with an alternative catalyst.[8] Econic technologies is commercialising the manufacture of catalysts enabling polyol manufacture and SK Energy provides poly(propylene carbonate) for high molar mass applications.[9]

1.2 Ring Opening Copolymerisation

The formation of aliphatic polycarbonates from the ring opening copolymerisation of epoxides and carbon dioxide is an attractive CCU approach due to the high proportion of CO_2 that can be incorporated, up to 43 % in polypropylene carbonate. ROCOP is catalysed by a variety of different metals, with Zn(II), Co(III) and Cr(III) being particularly common.[10-19] The more common initiating groups include alkoxides, carboxylates, halides and other anionic groups. General features of ROCOP catalysts are that the metals are Lewis acidic, with a low propensity for redox reactivity; the alkoxide and carboxylate intermediates need to

be labile. In general catalysts that are colourless, odourless and have a low toxicity are preferred. Therefore, potential contamination of the polymer product is not problematic.

1.2.1 Polymerisation Mechanism

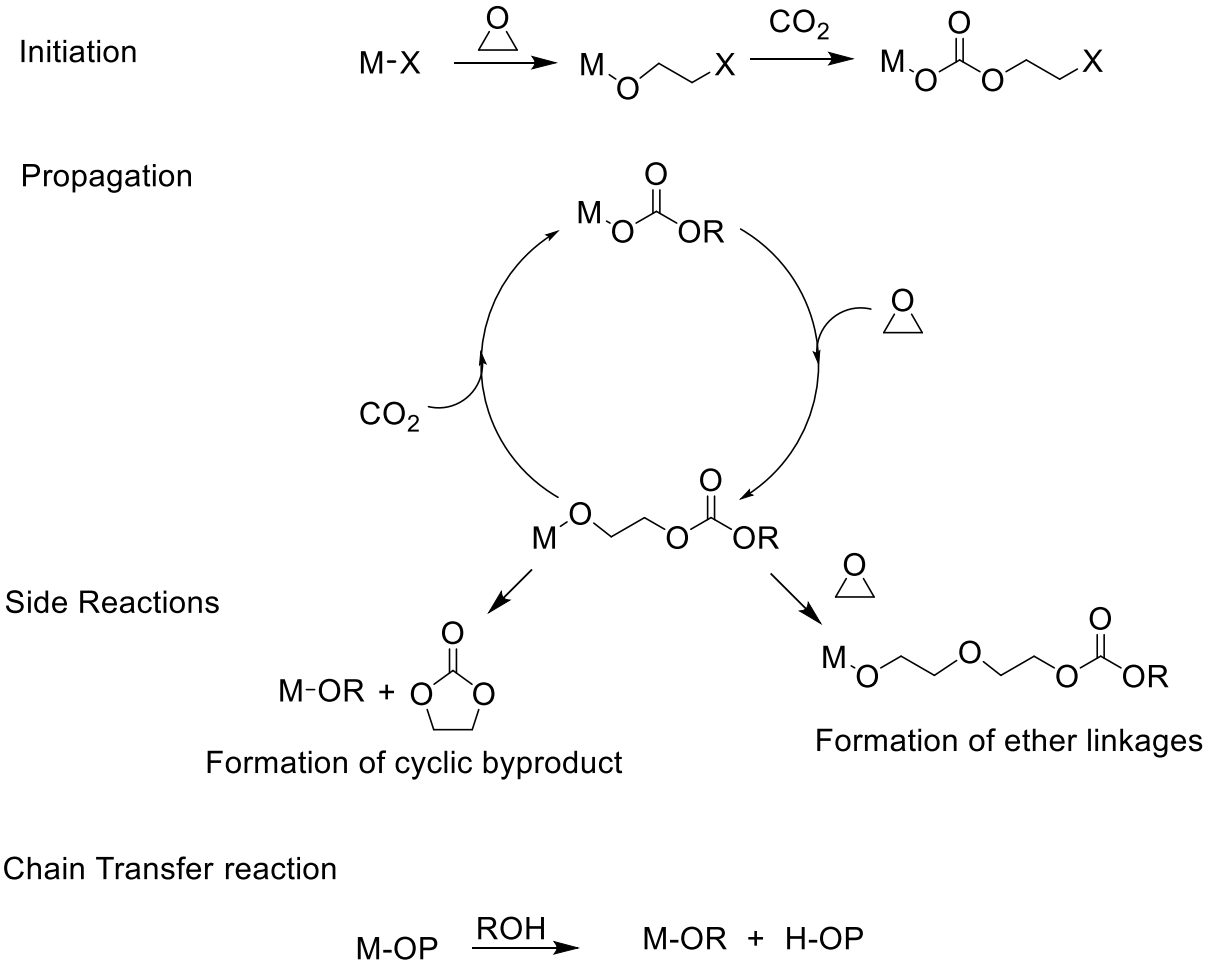

Chain Transfer reaction

Figure 1.2.1: Scheme showing the mechanism of ROCOP, with the initiation, propagation, side reactions and chain transfer reaction.

The polymerisation is initiated by co-ordination of an epoxide to the metal complex and subsequent nucleophilic attack to ring open the epoxide, which gives a metal alkoxide

species. Carbon dioxide can then insert into the metal alkoxide bond. In cases where the co-ligand is an alkoxide or aryl oxide, then the initiating step is the insertion of carbon dioxide. Propagation through the cycle involves co-ordination of an epoxide and nucleophilic attack by the metal bound carbonate group, which ring opens the epoxide. The formation of the new metal alkoxide allows the insertion of carbon dioxide. In ideal situation this leads to a perfect alternating chain, with 100 % carbonate linkages. In a controlled copolymerisation, the initiation occurs much faster than the propagation and the degree of polymerisation ($\overline{DP}$) is dependent on the concentration of catalyst. The $\overline{DP}$ correlates with the number average molar mass, M_n. A controlled polymerisation should show: a linear increase of M_n with % conversion, a linear increase of M_n with $1/[\text{initiator}]_0$, a narrow polydispersity index ($Đ = M_w/M_n$), the ability to undergo sequential monomer addition (i.e. to enable block copolymer construction), the rate of initiation should be faster than the rate of propagation and the rate of chain transfer should be faster than the rate of propagation.

However, in most cases, side reactions can occur. If the metal alkoxide bond ring opens another epoxide, instead of inserting carbon dioxide, ether linkages occur. The presence of ether linkages can modify the polymer properties but reduces the percentage of carbon dioxide being sequestered.[7] Five membered cyclic carbonates can also form. These are the thermodynamic product of the reaction between CO_2 and epoxides, so often form under forcing conditions. Cyclic carbonates form *via* backbiting or depolymerisation reactions, and the extent of their formation depends on the catalyst and the polymer being formed (bulky epoxides are less likely to form cyclic carbonates).[20] The formation of cyclic carbonates can be particularly problematic when ionic additives or co-catalysts are added, as they can also form 'off metal'. This is most common in the case of salen catalysts, where ionic co-ligands are common, and the formation of free anionic polymer chains occurs. These free anionic chains can undergo cyclization to form the cyclic carbonates.[13 21]

When polymerisations are carried out under immortal conditions, i.e. with an excess of protic compounds present (chain transfer agent, CTA), chain transfer reactions can occur.[22-24] It is proposed that the metal-alkoxide polymer chain is in constant and rapid exchange with the protic reagent, resulting in new metal-alkoxide species and hydroxyl terminated polymer chains. The chain transfer is proposed to be considerably faster than propagation, resulting in

highly controlled polymerisations, with the molar mass of the polymer being determined by the combined catalyst and CTA concentration and with narrow dispersities.

In ROCOP it is common for molar masses to be lower than would be expected for a living polymerisation, where the molar mass is dependent only on the catalyst concentration.[23] This is due to the presence of protic impurities which can cause the formation of diols *via* the ring opening of the epoxides.[25-28 29] Previous hypotheses suggested that the water reacted directly with the catalyst to form a hydroxide species, which then acts as the active centre.[30] However, there has been little evidence for this hypothesis.[28,29,31-36] Recently, the formation of diols from the ring opening of epoxides was elegantly shown by Darensbourg and co-workers.[37] They studied the effect of the addition of water on the ROCOP of PO/CO_2, using a cobalt salen catalyst with a trifluoroacteate co-ligand. Detailed studies using *in-situ* ATR-IR spectroscopy, showed that the addition of water causes a lag time in the formation of PPC.[37] During this lag time, there is a significant change in the infrared region of 3000-3800 cm^{-1}. The absorption band for water (3600 cm^{-1}) decreases steadily and a new sharp band arises at 3500 cm^{-1}. These changes were assigned to the consumption of water and the formation of a new alcohol species. Because the addition of the water causes the inhibition of the polymerisation until this new species is formed, it was hypothesised that the catalyst must be involved in the conversion of water and the conversion must be significantly faster than the polymerisation. The new species was shown to be 1,2-propane diol (by ^{1}H NMR spectroscopy and isolation of the compound), which was formed by the ring opening of PO by water as catalysed by the salen complex. Once all the water has been consumed, the copolymerisation of PO/CO_2 occurs, and the diol acts as the chain transfer agent, forming an alkoxide initiating group on the catalyst.

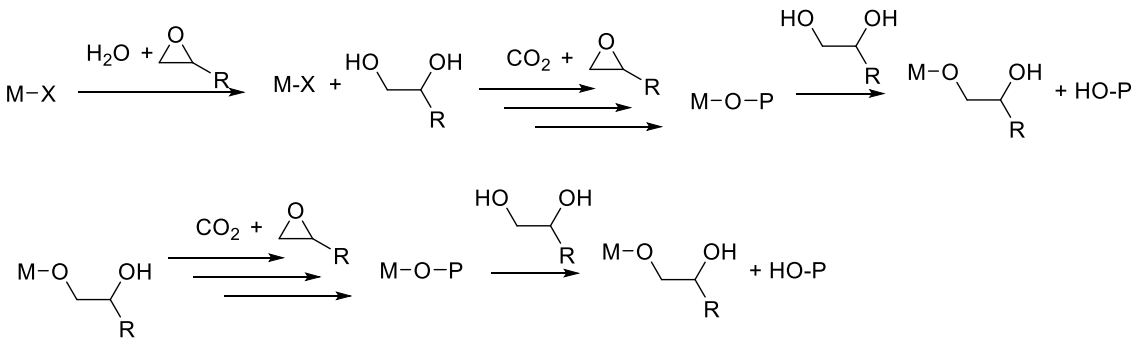

Figure 1.2.3: Scheme showing the proposed mechanisms for the formation of hydroxyl terminated polycarbonate using salen catalysts.[37]

The ability of catalysts to work effectively in the presence of protic impurities is required for the use of captured carbon dioxide and for the formation of the polyols for polyurethane production.[7,38]

1.2.2 Early Discoveries

The discovery that propylene epoxide and carbon dioxide could be combined to give a polycarbonate was made by Inoue and co-workers in 1969.[39,40] They initially used a 1:1 mixture of diethyl zinc and water, but later went on to investigate a wide range of diprotic sources.[41-44] These systems required high pressures and only achieved TOF's of up to 0.43 h^{-1}. The polymers produced contained a large quantity of ether linkages. Following Inoue's discoveries, further developments were made, with new heterogeneous catalysts based on $ZnEt_2$ or ZnO and alcohols. The turnover frequencies increased up to $1h^{-1}$ but the lack of information on the catalyst structure or active sites hindered any catalyst design.[45-48] Therefore, further development focused on well-defined homogeneous catalysts. The first homogeneous catalyst was an aluminium tetraphenylporphyrin (tpp) complex **(1)**, reported by Takeda and Inoue, in 1978. With the addition of $EtPh_3PBr$ as a co-ligand, it was found to be active for the copolymerisation of PO and CO_2. It took 19 days to form polycarbonate but was the first example of a monodisperse polymer with a narrow dispersity.[49,50]

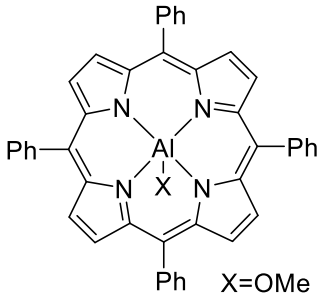

1

Figure 1.2.4: Aluminium tetraphenylporphyrin (1).

1.2.3 Main Catalyst Classes

Since then there has been an explosion of research into catalysts which are active for the ROCOP of epoxides and carbon dioxides. In general the best catalysts belong to the following classes: Heterogeneous catalysts, bi-component catalysts that require a co-ligand and dinuclear catalysts. A brief overview of the key developments will be given below.

Heterogeneous Catalysts

There are two main classes of heterogeneous catalyst, zinc glutarates and Double Metal Cyanides (DMC) ($Zn_3[M(CN)_6]_2$, where M = Fe(III) or Co(III)). Zinc glutarate is the most widely applied heterogeneous catalyst, due to its ease of production and because it produces polypropylene carbonate of a high molar mass. Two features have been found, which increase the activity of zinc glutarate: increasing the crystallinity of the catalyst and the addition of ethylsulfinate groups.[51-58] The most common DMC is $Zn_3(Co(CN)_6)_2$, and is often applied with complexation agents, such as salts and alcohols. Unlike zinc glutarates, DMC's perform best when they have an amorphous structure. Typically DMC's have a very high activity but only incorporate small quantities of CO_2 as they are effective epoxide homopolymerisation catalysts. [59-64]

Bicomponent Catalysts

Bicomponent catalysts are metal(III) complexes that require the addition of a co-catalyst, typically an ionic compound e.g. PPNCl or DMAP, to be effective. Common metals include Co(III), Cr(III), Mn(III) or Al(III) and the most common ligand frameworks are salens and porphyrins.

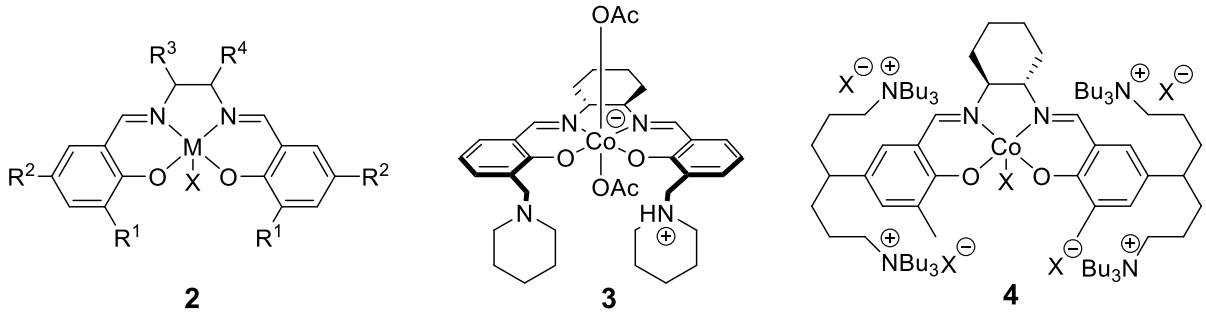

Figure 1.2.5: Bicomponent catalysts.

Porphyrin complexes were the first well-defined homogeneoushomogeneous catalysts for ROCOP[49] and subsequent work has shown that the use of Co(III) and electron withdrawing substituents gives the best activities.[29,33,36,65-71] However typically porphyrin catalysts can not compete in terms of activity and selectivity with the other catalysts available .

Salen catalysts **(2)** were first used for ROCOP in 2000,[31,72,73] and since then have become one of the most widely developed catalytic systems in the field of ROCOP.[19,26-28,32,74-94] There have been several developments in the field of salen catalysis.[13] The first chromium salen catalysts showed a high activity and selectivity, when combined with a co-catalyst.[73] The use of cobalt also further increased the activity of the catalysts (especially in PO/CO_2 ROCOP).[32,87,95,96] The ease of making chiral salen catalyst was exploited by Coates *et al*, who applied chiral [Co(salen)] complexes as CO_2/PO ROCOP catalysts.[97,98] These chiral cobalt salen catalysts show high activities as well as precise levels of regio- and stereochemical control. Recently they have been used to form stereocomplex polycarbonates, starting from a racemic mixture of epoxides.[81-83,99,100] The co-ligand plays several important roles in the catalytic cycle. It is proposed to bind to the metal centre and aid the disassociation of the initiating or propagating group. It may also act as an external nucleophile and initiate polymerisation.

However there is no consensus on the precise role played.[13] In general 1-2 equivalents are the optimum quantity. This is due to excess equivalents competing against the epoxide at binding to the metal centre. [101-103]

In order to get round the entropic difficulties caused by two component systems, catalysts with the co-ligands covalently bonded to the ligand framework were developed. The first system was developed by Nozaki and was a Co(III) salen complex, substituted with piperidinium 'arms'**(3).**[76] This catalyst showed very high selectivity and turnovers (250 h^{-1}) even under mild conditions (14 bar, r.t.). Lee *et al* subsequently synthesised a variety of bifunctional catalysts, substituted with ionic groups **(4)**.[26,27,75] These catalysts are among the most active catalysts to date (26000 h^{-1}) and are active under very low catalyst loadings (1:25000).

A significant amount of mechanistic work has been carried out on salen catalysts. Recent kinetic studies showed the polymerisation rate is dependent on a catalyst concentration to a fractional order, between **1** and **2**.[85] This occurs when the polymerisation pathway involves two catalyst complexes or dimerization in the rate-limiting step. The rate limiting step has been shown to be the ring opening of the epoxide. The study suggested that a combination of two pathways may be occurring for the ring opening of the epoxide.

Dinuclear Catalysts

One of the key findings of the field of ROCOP was the discovery of highly active Zinc β-diiminate catalysts **(5)** [104-108] and the study into their mechanism that showed the most active catalysts existed in a dimeric form.[109]

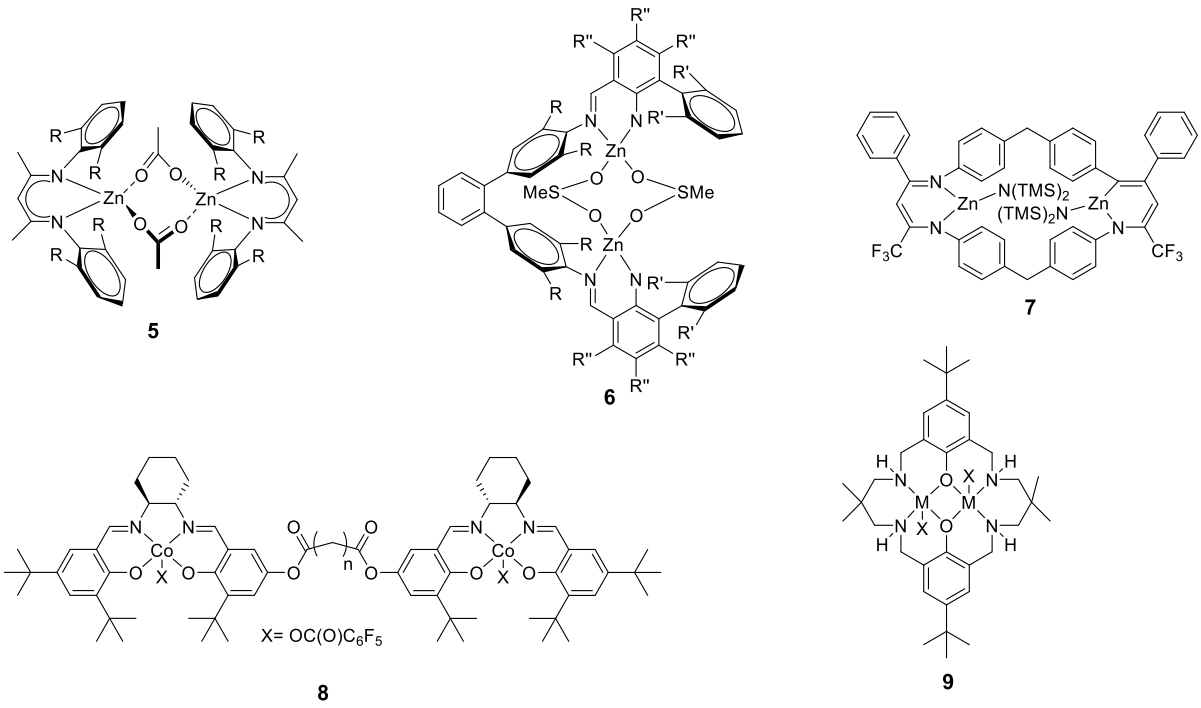

Figure 1.2.6: Dinuclear catalysts for ROCOP.

This study inspired the development of many bimetallic catalysts, in order to achieve higher activities. Many attempts at tethering [ZnBDI]'s have been attempted, and this causes a variety of effects depending on the position and type of tether.[110-113] The best system, with a methylenediphenyl tether **(7)** achieves a TOF of 155,000 h^{-1}. [110] Lee developed a series of zinc (II) bis anilido-aldimine complexes **(6)**, which showed high activities (2860 h^{-1}).[114] Nozaki and Reiger targeted the tethering of salen complexes **(8)**.[87,93] This resulted in higher activities than the corresponding monometallic complex, especially at lower loadings. Our group has focused on the synthesis of dinuclear catalysts coordinated by a macrocyclic diphenolate ancillary ligand, with Zn (II), Mg (II), Fe(III) and Co(III) metal centres **(9).**[115-121] The dizinc catalysts were the first to be active for the ROCOP of CHO/CO_2 at 1 atm of carbon dioxide, and there are still very few catalysts that can operate at this pressure.[117] Kinetic studies of CO_2/epoxide ROCOP, using the di-zinc acetate complex, showed a first-order dependence on CHO and catalyst concentrations and zero-order dependence on CO_2 (1–40 bar). [115,122]Analysis of the mechanism showed co-operativity between the two metal centres, with each performing a distinct role (ring opening the epoxide or insertion of the

carbon dioxide). This lead to the development of a hetero-metallic catalyst, with an improvement of the activity. [123,124]

1.3 Polycarbonate Properties

The two most common polycarbonates produced *via* ROCOP are poly(propylene carbonate) (PPC) and poly(cyclohexene carbonate) (PCHC), which are derived from propylene oxide (PO) and cyclohexene oxide (CHO), respectively. One of the key advantages of ROCOP is that a wide variety of epoxides can be incorporated into the polymer chain, including epoxides such as styrene oxide,[39] indene oxides,[125] limonene oxide,[105] isomers of butane oxide,[40] epichlorohydrin[39] and dioxaepoxides[126] as well as many other functionalised epoxides.[127-131] This huge variation in the potential backbone structure allows access to a wide variety of different polymer properties, including the thermal properties (glass transition temperature (T_g), thermal decomposition temperature (T_d) and material properties (e.g. Tensile strength and elongation at break).

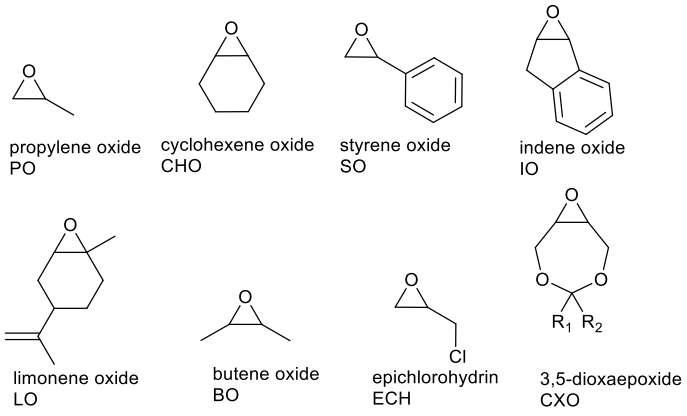

Figure 1.3.1: Structures of common epoxides.

1.3.1 Thermal Properties

Both PPC and PCHC are amorphous materials but have different thermal properties. PPC has a T_g of 30-40 °C, but the increased rigidity of the PCHC backbone increases its T_g to between 80-115 °C.[11] Recent work has shown that the T_g of PCHC can be increased by control of the tacticity of the polymer.[25,84,97,132-137] Isotactic PCHC can be synthesised using chiral salen catalysts or chiral [ZnBDI] catalysts.[84,107] The highest *ee* values were reached by Lu et at *via* the modification of a cobalt salen system.[84] Isotactic PCHC (*ee* >99 %) no longer had a glass transition, as it is a crystalline material and instead shows a T_m of 272 °C. Highly isoenriched PCHC (*ee* > 92 %), however, shows a T_g of 124 °C. Similar results were achieved with a [ZnBDI] catalyst.[107] It is also possible to make isoenriched PCHC *via* the ROP of *trans*-cyclic cyclohexene carbonate.[138] Isotactic PPC has been widely investigated and can be prepared using various chiral cobalt and chromium salens.[27,28,32,96,98,137,139-144] A stand out result was achieved by Nozaki and coworkers who formed a tapered stereoblock (isotactic) PPC from *rac*-PO.[145] It had not been previously known that PPC could form a stereoblock. The stereoblock PPC had a T_g of 33°C and were semicrystalline. It is also possible to synthesise syndiotactic PPC using cobalt salen catalysts.[28]

The use of rigid epoxides can increase the glass transition temperature even further. Indene oxide has been investigated, by Darensbourg and co-workers, and the polycarbonate has been shown to have very good thermal properties.[125] A T_g of 134 °C was achieved, despite the molar masses of the polymer being moderate. The molar mass had a strong effect on the T_g, with a variation of >20 °C occurring depending on the molar mass. Lu *et al* copolymerised a dimethyl substituted dioxaepoxide and carbon dioxide to form an isotactic polycarbonate using a cobalt salen catalyst.[84] The isotactic polycarbonate was crystalline with a T_m of 242 °C. In contrast, the atactic polycarbonate, synthesised by an achiral version of the cobalt salen, had a T_g of 140 °C. This is the highest T_g reported for a polycarbonate synthesised *via* ROCOP.

Another method of increasing the T_g of a polymer is to form stereocomplex, where two chains with opposite chirality co-crystallise. It requires the formation of a 1:1 mixture of each orientation. The co-crystallisation often increases the melting temperature and the amount of crystallinity. The most studied system is PLA, and the formation of a stereoblock can cause

the T_m to increase by about 50 °C.[146-148] Coates and co-workers discovered that while enantiopure poly(limonene carbonate) (PLC) was not crystalline, if the two enantiomers were co-crystallised then a crystalline material was produced.[81,82] The *R* and *S* chains of PLC were found to interdigitate when crystallised, which leads to an increased rigidity of the chains. The T_g of the stereocomplex was 122 °C,[81] compared to the previously reported T_g 110 °C for atactic PLC.[105]

1.3.2 Material Properties

The material properties of polycarbonates have not been studied in much detail. One problem is the strong correlation between the properties and the molar mass of the polymers. Only a few catalysts can produce polymers of a sufficient molar mass for bulk mechanical measurements.[11]

Polypropylene carbonate (PPC) is an amorphous polymer, with a low T_g. It is a thermoplastic and has a similar modulus of elasticity (~800 MPa) and yield strength (10-20 MPa) to low density polyethylene (LDPE).[149] Due to its long elongation at break, PPC could show potential as an elastomer, although this is hindered by the low T_g.[51] PCHC is also an amorphous polymer, but the increased rigidity in the backbone increases the T_g and properties, such as tensile strength and tensile modulus (compared to PPC). However PCHC has a very low elongation at break and is brittle. The restricted conformation of the cyclohexene rings means the polymer chains can not entangle, causing the brittleness.[150] Polycarbonate from bis-phenol A (PC) is a tough, rigid aromatic polymer that is formed by the condensation of bis-phenol A and phosgene. PC is partially crystalline, transparent, with a high impact strength (9.1 N cm^1), and a high glass transition temperature (T_g = 149 °C).[151] It is used for applications as diverse as bullet proof glass to mobile phone cases. In comparison polycarbonates from ROCOP are hindered by their moderate thermal stability and the ease of deformation, which prevents widespread applications. [150-152]

Table 1.1: Thermal and mechanical properties of polycarbonates.

Polymer	T_g /°C	T_d /°C	Tensile strength, σ_{break} (MPa)	Tensile modulus, E (MPa)	Elongation at break (%)	Ref.
Poly(propylene carbonate)	42	252	7-30	700-1400	600-1200	[51,149]
Poly(cyclohexene carbonate)	118	310	40-44	3599-3700	1.1-2.3	[150]
Polycarbonate (PC)	149	458	43-51	2000-2800	15-75	[151,153]

1.4 ROCOP to form Block Copolymers

There are many ways to alter the properties of a polymer, but one of the most interesting methods is the formation of block copolymers. By combining blocks of different polymers into a single material it is possible to moderate and overcome issues such as brittleness, low thermal resistance and rigidity. The most common example is of SBS (Poly(styrene-butadiene-styrene)), a hard rubber which derives its favourable properties from a combination of the hardness of polystyrene and the flexibility of polybutadiene.[154] Another favourable feature of block copolymers is their propensity to self-assemble on the nm scale. By attaching chemically different blocks together, the polymers are brought into close proximity, and self-assembly is encouraged. The driving force for self-assembly is the non-covalent interactions, hydrogen bonding, π-π stacking and hydrophobic interactions between the polymer chains. The reversible nature of these interactions means that there is the potential for self-assembled structures to be reversible and sensitive to stimuli. The self-assembled structures can be used as scaffolds for nanomaterials or for biomedical applications including drug delivery.[155] There are many ways to synthesise block copolymers: sequential addition methods, terpolymerisations with kinetic control, the use of polymeric chain transfer agents and the formation of macroinitators. Yet despite all the research into ROCOP, there are limited examples of block copolymers which contain polycarbonate from ROCOP.

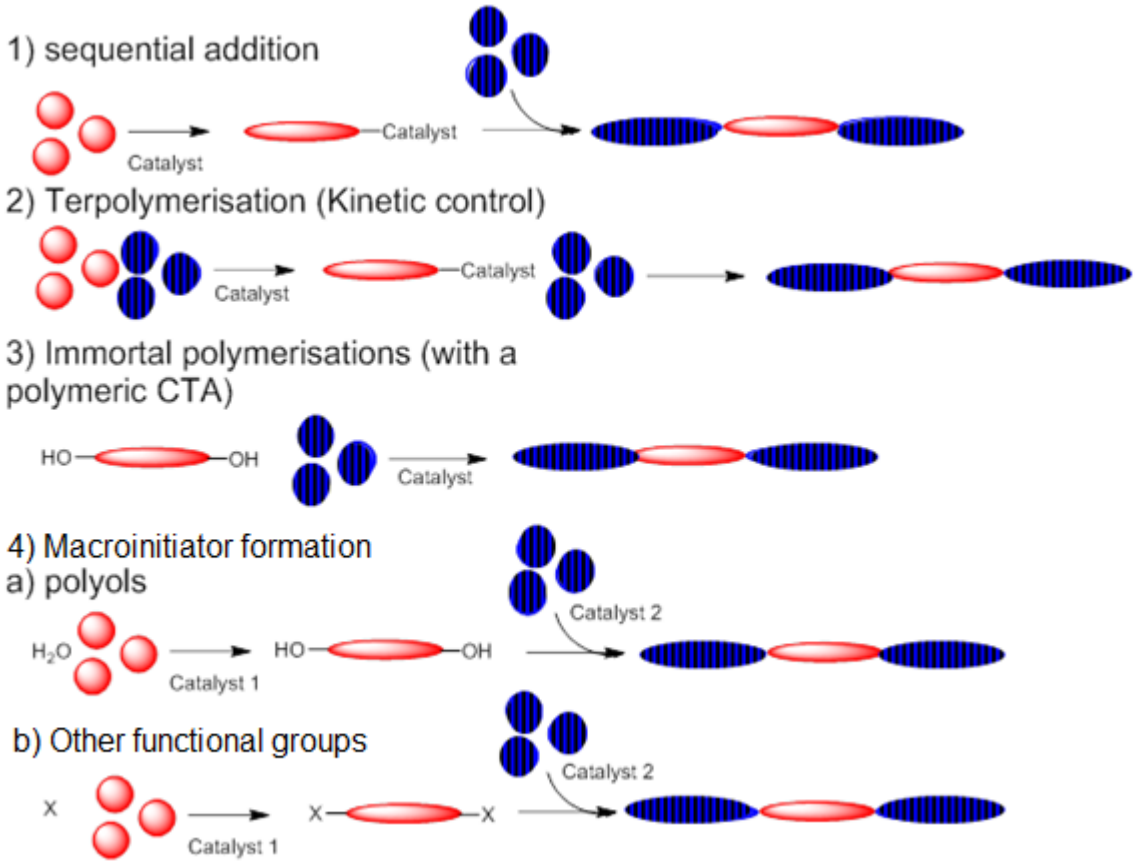

Figure 1.4.1: Scheme showing the potential methods of forming block copolymers.

1.4.1 Sequential Addition to Living Polymerisations

A living polymerisation is a controlled polymerisation with no termination reactions. The lack of termination means that if more monomer is added to the catalyst, then the reaction will resume.[23] The first example of this was discovered in 1956, for the anionic polymerisation of styrene with organo-alkali metal compounds.[156] Since then living polymerisation catalysts have been developed for many polymerisation mechanisms. Living polymerisations can be used to make block copolymers, *via* the sequential addition of various monomers. This requires the catalyst, not only to be capable of living polymerisation, but also to be capable of polymerising multiple monomers and fully consuming the monomer – to prevent tapering. This technique has been used with great effect in radical polymerisation, affording multiblock copolymers with up to 20 blocks, as achieved by Perrier.[157]

Many ROCOP catalysts exhibit living characteristics. However, there is often a limit on the variety of epoxides that can be copolymerised by a single catalyst and most catalysts are most effective when used with a large excess of epxoide. In 2006, Nozaki developed a cobalt salen complex with piperidinium capped arms **(11)**, that was able to completely consume PO when a solvent was utilised.[76] This allowed the addition of 1-hexene oxide, forming a block copolymer. However the catalyst was not able to fully consume the 1-hexene oxide (89 %), so this prevents further blocks being added. Darensbourg and co-workers worked around the fact their chromium salan catalyst **(12)** did not reach full conversions, by removing any unreacted epoxide before the addition of the next monomer. They synthesised a diblock and a triblock using PO, CHO and VCHO.[158] Coates *et al*, used a [ZnBDI] catalyst **(10)** and 6 different functionalised cyclohexene oxides, to form a hexablock copolymer.[159] The high activity of the [ZnBDI] catalyst means that all monomer was consumed regardless of epoxide structure, allowing the formation of multiblock copolymers. The hexablock copolymer is a rare example of a multiblock copolymer that contains more than 4 non-equivalent blocks.[160] When the [ZnBDI] has a norbornene initiating group further manipulation of the block copolymer can be done. The polymer chains contain a double bond in the norbornene endgroup so a Grubbs catalyst can be employed to catalyse the Ring Opening Metathesis Polymerisation, forming a graft copolymer.[161]

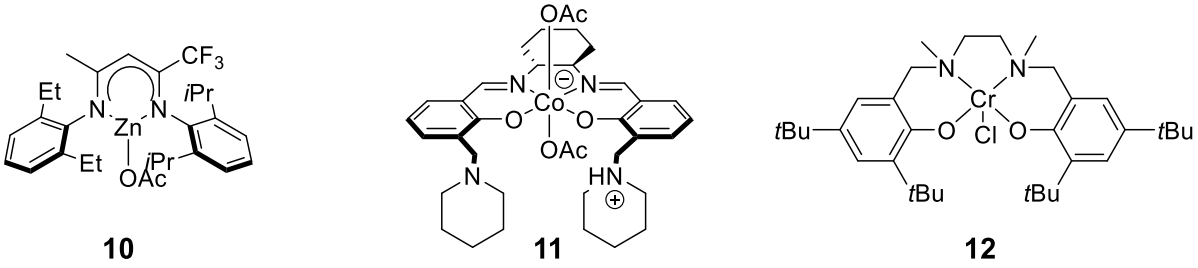

10 **11** **12**

Figure 1.4.2: Catalysts used for the formation of block copolymers *via* sequential addition.

There have been many attempts at the terpolymerisation of two or more epoxides with carbon dioxide, but there are no reported examples of this resulting in block copolymers.[135,162-165] In most cases a copolymer forms. Lee and co-workers used the Fineman Ross method to determine the structure of the copolymers from the terpolymerisation of CO_2/PO with CHO, Hexene oxide and 1-butene oxide, using a cobalt salen complex with tethered quaternary ammonium salts.[90] In all cases $r_{PO} >> 1 >> r_{epoxide}$. When $r > 1$ then the monomer (in this case considered as epoxide enchainment after carbon dioxide insertion) preferentially self-propagates. When $r < 1$, the monomer preferentially copolymerises. In the terpolymerisations, regardless of which epoxide was previously enchained, it was preferential for PO to be enchained next. This results in a gradient copolymer, with the initial section of the polymer being PO enriched and the latter section containing more of the second epoxide.

1.4.2 Terpolymerisation of Anhydrides/Epoxides/Carbon Dioxide using ROCOP

It is also possible to polymerise anhydrides with epoxides to form polyesters, *via* ROCOP. The similarity of the mechanism means that catalysts for CO_2/epoxide ROCOP are often also good catalysts for anhydride/epoxide ROCOP. [108,166-174] The first detailed report of the terpolymerisation of epoxides/anhydrides/carbon dioxide was carried out by Coates *et al*, using a [ZnBDI] catalyst **(13).**[108] The terpolymerisation of diglycolic anhydride (DGA), CO_2 and CHO, resulted in the formation of a block copolymer. Detailed *in-situ* ATR-IR spectroscopic analysis revealed that epoxide/anhydride ROCOP occurred first, and it was only once the anhydride was completely consumed, that the epoxide/CO_2 ROCOP began to occur. This was surprising because when conducted independently the epoxide/CO_2 copolymerization occurs significantly faster than epoxide–anhydride copolymerization. It was proposed that the selectivity is due to a relative faster rate of anhydride insertion *vs*. CO_2 insertion into the zinc alkoxide intermediate; both reactions are pre-rate determining steps in the catalytic cycles.

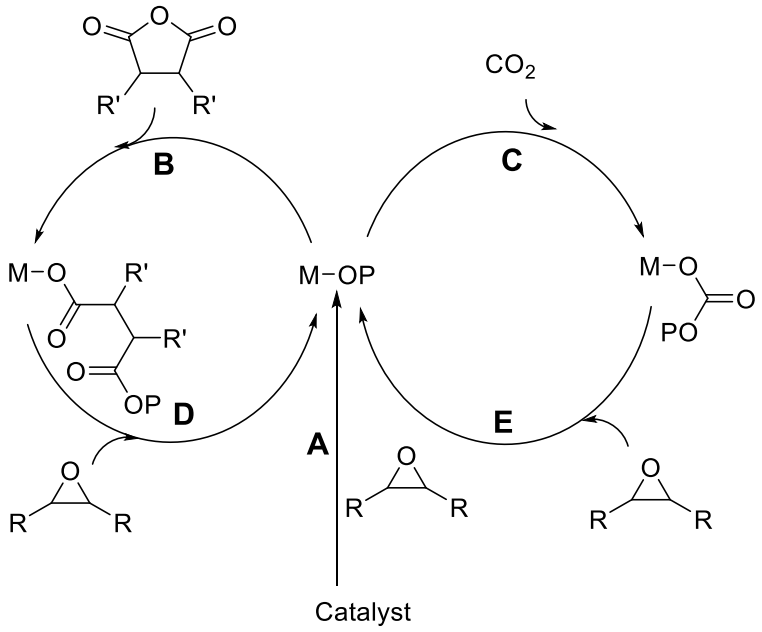

Figure 1.4.3: Scheme showing the mechanism of the terpolymerisation of anhydrides/epoxides/CO_2 and how it results in block copolymers.

During initiation, the [(BDI)ZnOAc] complex reacts with an equivalent of epoxide to generate the zinc alkoxide species (A). At this stage, the insertion of anhydride (B) is proposed to occur faster than the insertion of CO_2 (C), leading to the dominant intermediate in terpolymerisations being a zinc carboxylate species. This intermediate reacts with epoxide (D) to form a zinc-alkoxide and the polymerization cycle progresses around the ester cycle (steps B, D). Only when the anhydride is almost fully consumed, does the insertion of CO_2 into the zinc alkoxide intermediate (C) become competitive. Once this occurs, a zinc carbonate intermediate is formed, which ring opens an epoxide to re-generate the alkoxide species (E). The rate limiting step of the second cycle (E), is faster than the rate limiting step of the 1st cycle (D), so the second (polycarbonate) block forms faster. The same selectivity was found to result from a wide range of catalysts, and block poly(ester-carbonates) can be formed with a wide range of epoxides and anhydrides. [166-174]

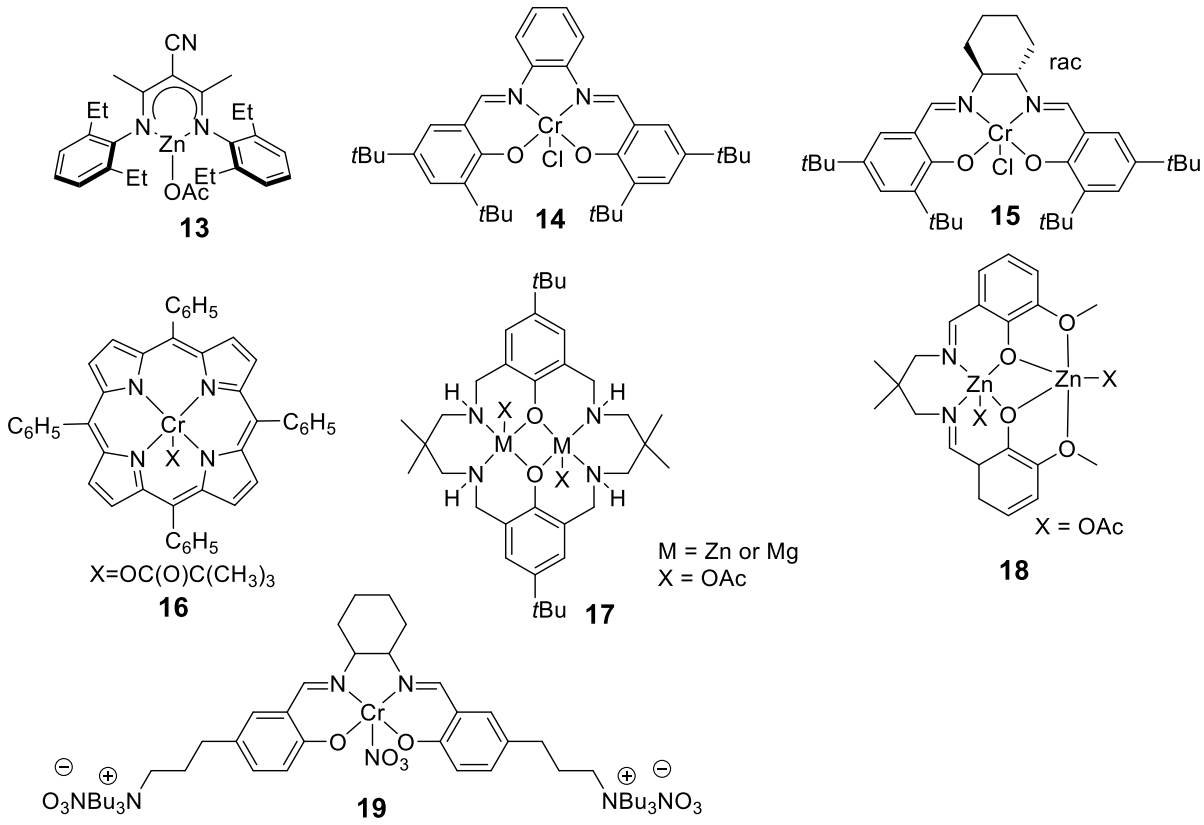

Figure 1.4.4: Catalysts used for the terpolymerisation of anhydrides/epoxides/CO_2.

Duchateau and co-workers used a chromium salophen complex **(14)** with DMAP as the co-catalyst for the terpolymerisation of CHO/anhydrides (SA, CPrA, CPA or PA)/CO_2.[166,167] ~90 % of the anhydride is converted before any carbonate functionalities are formed. It was discovered that the presence of CO_2, suppresses the formation of ether linkages, even in the ester blocks. It was suggested that the coordination of CO_2 to the metal may reduce its Lewis acidity and thereby quench sequential epoxide enchainment. The resulting copolymers show a single glass transition temperature, due to blocks being miscible. Darensbourg and co-workers also prepared block copolymers from CHO/PA/CO_2, using a chromium salen catalyst with PPNCl/N_3 as the co-catalyst, however, in this case two glass transition temperatures were observed, consistent with phase separation of the blocks (T_g = 48 °C and 115 °C).[170] The variety in the thermal properties of the different block copoly (ester-carbonates) being reported is due to the range of different epoxides and anhydrides available.

This is one of the positive points for ROCOP method of forming polyesters. A Co(III)salen catalyst with a tethered ammonium co-catalyst **(19),** was also successfully applied, to copolymerize PO/NA/CO_2.[172] Duchateau and co-workers reported that metal porphyrin catalyst **(16)** with DMAP (as co-catalyst), was effective for the terpolymerisation of CHO/CO_2/anhydrides (SA, CPrA, CPA or PA).[167] In this case however, there was concurrent carbonate linkage formation during the enchainment of ester linkages, leading to a tapered block structures. This is due to the relatively similar rates of anhydride and CO_2 insertion into the metal-alkoxide bonds. In contrast, Chisholm *et al*. also used the same catalyst, **(16)** with PPNCl as co-catalyst, for the terpolymerisation of PO/SA/CO_2 and reported the formation of diblock copoly(ester–carbonates).[66] This highlights how the insertion of anhydride affects the selectivity, with more effective catalysts for the anhydride insertion resulting in the formation of block copolymers. Our group have reported that the di-zinc and di-magnesium catalysts, **(17)** and a dinuclear zinc salen complex **(18)** are also selective in the terpolymerisations of CHO, PA and CO_2 producing block copoly(ester–carbonates).[168,169]

Heterogeneous catalysts, such as zinc glutarate or double metal cyanides (DMC) have been investigated. Using zinc glutarate for the PO/MA/CO_2 terpolymerisation produced tapered block copoly(ester–carbonates).[173] This is proposed to be due to similarities in the rate of insertion of the anhydride and CO_2. A similar result occurs using double metal cyanide catalysts.[174] The polymerisation of CHO/MA/CO_2 gave a sequence where initially polyester forms, together with the random insertion of carbon dioxide. Once the MA is mostly consumed (~90 %), the carbonate block forms. In contrast, a polymer supported double metal cyanide showed a different selectivity.[171] During the polymerisation of PO/MA/CO_2, only polycarbonate formed, with occasional, random insertion of MA, there was no formation of polyester blocks.

1.4.3 Immortal Polymerisations

An immortal polymerisation is a living polymerisation, which is not terminated by the addition of protic substances.[23] Instead, the addition of protic substance increases the number of polymer chains being produced, in line with the amount of protic substance added. This

occurs by chain transfer reactions, and for an immortal polymerisation the chain transfer reactions are faster than the propagation reaction. This results in all chains being similar lengths with a very narrow dispersity. Because the chain transfer agent ends up as a unit of the polymer, the use of polymeric chain transfer agents, or macroinitiators results in the formation of block copolymers. If the macroinitiator is monofunctional, then AB type block copolymers form, whereas if it is difunctional then ABA type block copolymers are likely to form

The most common form of macroinitator is a dihydroxyl terminated polymer or polyol. When used as a chain transfer agent, polyols result in the formation of ABA type block copolymers. In 2010, Lee and co-workers showed that the activity of a cobalt salen catalyst with tethered co-ligands **(20),** for the copolymerisation of PO/CO_2 was unaffected by the presence of up to 500 equiv. of chain transfer agent *vs* catalyst.[22] They then used polyols as the chain transfer agents within the ROCOP. Several different types of polyols were successfully used to form triblock copolymers: polyethers (PEG), polyesters (PCL) and polycarbonates (poly hexamethylene carbonate). They also used polyethylene and polystyrene (PE, PS) with only one hydroxyl group to form diblock copolymers. The different polyols had a wide variety of effects on the properties, when compared to PPC. The PPC-PEG-PPC block copolymer was significantly less brittle than PPC, but retained a similar flexibility. The PS-PPC block copolymer resulted in a translucent material that was tougher than PPC.

Recently, Rieger and co-workers used a hydroxy methyl siloxane as a chain transfer agent in the ROCOP of CHO/CO_2 using [ZnBDI] catalysts **(21)**.[175] This resulted in the formation of PCHC-PDMS-PCHC triblock copolymers. The methyl siloxanes were chosen as a central block in order to provide a flexible central block that may reduce the brittleness of PCHC. The block copolymers showed a single glass transition temperature, 65-102 °C depending on the composition. The blends of PCHC and PDMS resulted in two T_gs (90 and -120 °C, respectively).

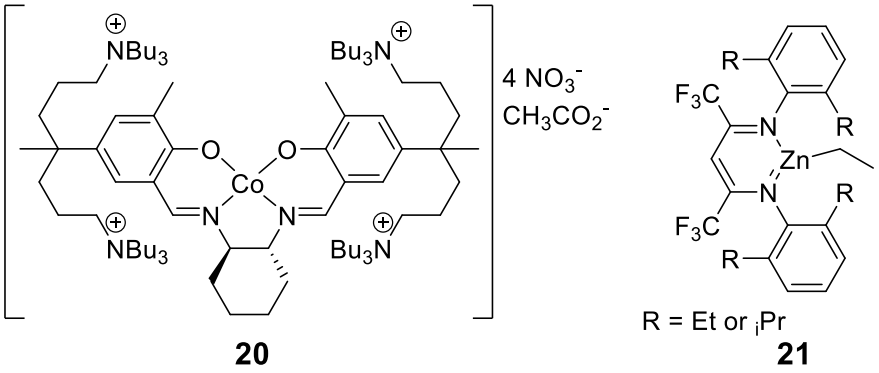

Figure 1.4.5: Catalysts used to form block copolymers *via* Immortal polymerisation.

A DMC was used by Müller and co-workers for the ROCOP of CO_2/PO/MA and allyl glycidyl ether (AGE) in the presence of a polypropylene oxide polyol.[176] The resulting polymer had an ABA structure with the B block being a random poly (ether-ester-carbonate). The MA, CO_2, PO and AGE all have a similar reactivity and therefore there is random insertion of the monomers. Ester units are formed when MA is inserted after PO or AGE, carbonate units are formed when CO_2 inserts after PO or AGE, and the ether units form when PO or AGE inserts after another PO or AGE. The group also reported an ABCBA structure where the C group is the polypropylene oxide but the MA and AGE are added sequentially. This results in the B block being a random poly (ester-carbonate-ether) (ether units result from sequential PO enchainment) and the A block being a random poly (ether-carbonate).

1.4.4 Macroinitator Formation

Polyols

In 2012, a bimetallic zinc catalyst with trifluoroacetate co-ligands **(22)** was discovered to produce only polycarbonate polyols from the copolymerisation CHO/CO_2, without the addition of a chain transfer agent.[177] There was no indication that the trifluoroacetate group was retained on any of the polymer chains (NMR spectroscopy and MALDI-ToF analysis). This was proposed to be due to the ease of hydrolysis of the trifluoroacetate groups. Once the

PCHC polyols were isolated, they were used as the macroinitator with a yttrium catalyst in the ROP polymerisation of lactide to form ABA triblock copolymers. The formation of a block copolymer was confirmed by the significant increase in molar mass and the disappearance of the PCHC end group signals in the ^{1}H NMR spectrum. The reaction was successful using PCHC blocks of various molar masses (2,000 -10,000 g mol^{-1}) and a range of lactide loadings (100-400 equiv.). In all cases a T_g was observed at 60 °C, corresponding to the PLA blocks. In the ABA block copolymers with the longer PCHC blocks, a second T_g was observed at 80-95 °C, indicating that the blocks are not miscible.

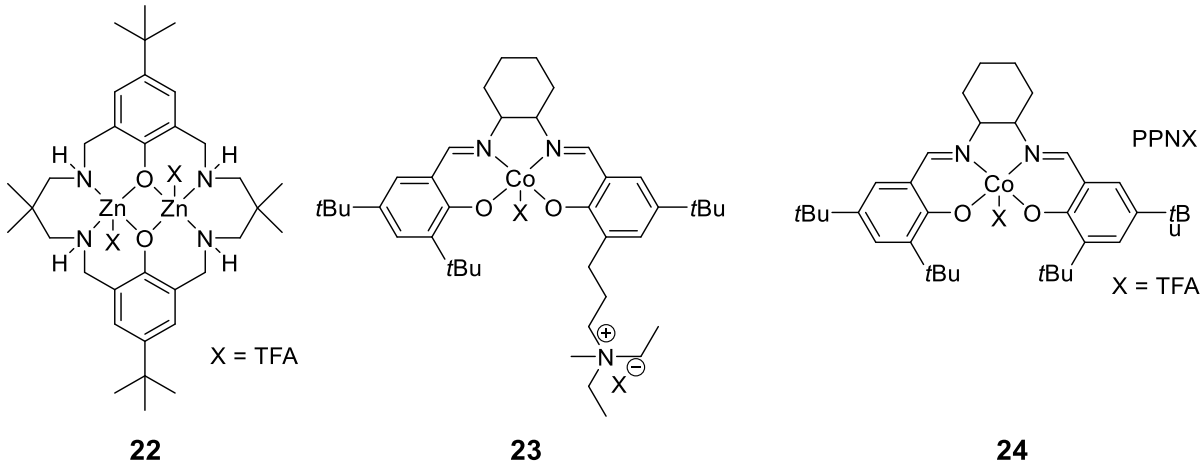

22 **23** **24**

Figure 1.4.6: Catalysts used to form block copolymers *via* polyol formation.

Darensbourg and co-workers were inspired to apply the same approach, with a trifluoroacetate ligand co-ordinated to a cobalt salen catalyst **(23)**.[30] They discovered that the addition of water to the completed polymerisation, resulted in the formation of hydroxyl terminated PSC. Then the method was used to form PSC-PLA block copolymers, in a two-step, one-pot method. Initially PSC was formed, followed by the addition of water to form the hydroxyl end group. This is then followed by the addition of lactide and DBU, an organocatalyst. The hydroxy end groups act as macroinitiators in the ROP of lactide. Subsequently, a salen catalyst with a trifluoroacetate co-ligand **(24)**, was reported, which was

capable of copolymerising PO/CO_2 in the presence of water.[178] This resulted in the in-situ formation of dihydroxyl terminated polymers. Once the ROCOP was complete, DBU and lactide could be added and the polycarbonate polyol acted as a macroinitiator for the ROP of lactide. The resulting triblock copolymers showed a much greater thermal deformation resistance (T_g = 45 °C and T_m >110 °C), compared to both PPC and PLA (T_g = 35 °C and T_m = 60 °C respectively). The cobalt salen catalyst has also been used to form PPC and PCHC polyols that were used as the macroinitators for the ROP of a cyclic phosphate, catalysed by DBU.[37] The polyphosphoester (PPE) blocks are hydrophilic, whereas the polycarbonate blocks are hydrophoblic, so the ABA block copolymers are amphiphillic and self-assemble into micelles. PPE-PPC-PPE forms spherical micelles, whereas PPE-PCHC-PPE forms spherical micelles at low PPE molar fractions, but rod-like micelles at higher PPE molar fractions. Both the polycarbonate and the polyphosphoester blocks are biodegradable; therefore the block copolymers are attractive for biomedical applications.

Other Functional Groups

As well as modifying polycarbonate to form polyols, other functional end groups can be incorporated, allowing the polymers to act as macroinitiators for other polymerisations. Feng *et al* used lithium ion species as an initiator, along with Al(*i*Bu)$_3$ and an alcohol, to form an active catalyst system for the ROCOP of CHO/CO_2.[179] The Al(*i*Bu)$_3$ activates the epoxide. The PCHC chains were found to be endcapped by the anion from the lithium ion pair. The use of a lithium ion pair of Polystyrene (PS) or Polyisoprene (PI) resulted in the formation of a block copolymer (PS-PCHC, PI-PCHC).

1.5 Switch Catalysis

Switch catalysis is where a single catalyst has the ability to switch between two, or more, distinct mechanistic cycles, in response to an external stimulus. The stimuli can include changes to the catalysts allosteric (changing the structure of the catalyst), redox, chemical, electrochemical, photochemical or mechanochemical states.[180-182] The switch alters the

catalysts structure or electrochemical state and this causes it to behave in a different way. A true switch should be both reversible and repeatable. There are two key types of switchable catalysts, those that are switched "on'' or "off'' by the external stimuli and those which are switched from one reaction to another. The on/off type of switch is more commonly applied but the switch between reactions has significantly more potential to deliver useful materials and processes. In the field of polymerisation catalysts, switchable catalysts have been developed in the fields of ring opening metathesis polymerisation, atom transfer radical polymerisation but the majority of switchable catalysts can be found in the field of ring opening polymerisation.[183]

Ring opening polymerisation is a versatile and facile method of synthesising polyesters. Over the years many catalysts have been developed, both with organocatalysts and transition metal catalysts, providing impressive levels of control. However the quest for highly tailored polymeric structures has resulted in the development of switchable ROP catalysts, which will be discussed below. To date only one example of a switchable ROCOP catalyst has been developed, and as it switches from ROCOP to ROP it will be discussed in the relevant section (1.5.2).[184]

The appeal of switch chemistry in polymerisations is that it allows high levels of control over the reactions. In the case of one/off switches, this can allow the control of molar mass, or for other reactions to occur during the 'off' periods. Potentially one could swap or add monomers during this time or even perform sidechain modifications. For switches between monomers, this allows the formation of block copolymers, in a one pot method, a key goal for advanced material properties.

1.5.1 Redox Control

Metals that have relatively low redox potentials can be altered from one oxidation state to another *via* the addition of chemical oxidants/ reductants or electrochemically. For use within switchable catalysis it is important the redox process is reversible. The difference in oxidation state can have a dramatic effect on the catalytic activity. Changing the oxidation state can

also have a structural as well as an electronic effect on the catalyst.[183] There are two main types of redox switches, one where the redox active switch is remote from the catalyst centre and where the catalyst centre is the redox active switch.

The most common remote redox active switches feature a ferrocene unit, because its redox chemistry as well as its chemical and electronic properties are well understood. In 2006, Gibson, Long and co-workers were the first to report a ferrrocenyl functionalised titanium salen polymerisation catalyst **(25).**[185] It could readily be oxidised (by silver triflate), and (the oxidised form) reduced (by decamethyl ferrocene.) Both the oxidised and reduced forms were tested for the ROP of lactide (with the addition of iPrOH), and the reduced catalyst was significantly more active (~30x) than the oxidised catalyst. It was also possible to oxidise the catalyst, while under polymerisation conditions, by the addition of silver triflate. This slowed the rate of polymerisation, and subsequent reduction of the catalyst was accompanied by an increase in the rate of polymerisation. The rate of polymerisation after the re-reduction was approximately the same as the original rate.

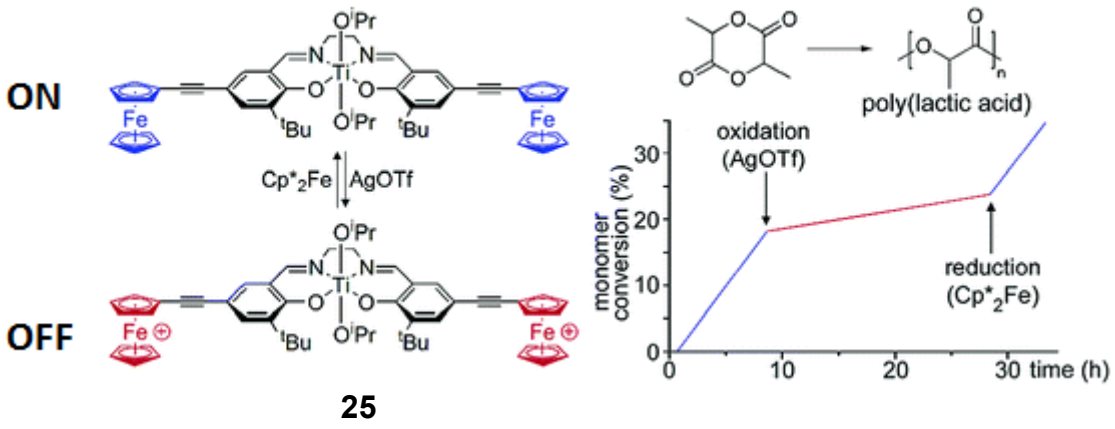

25

Figure 1.5.1: The first example of a redox switchable ROP catalyst.[185]

Diaconescu and co-workers reported another series of ferrocene based switchable polymerisation catalysts, based on a phosfen ligand and a trivalent metal (Y and In) **(26).**[186]

For the yttrium catalyst **(26a)**, oxidation halts the ROP of lactide, but reduction allows the polymerisation to restart, with no effect on the rate of polymerisation. This cycling can be repeated multiple times with no adverse effect.

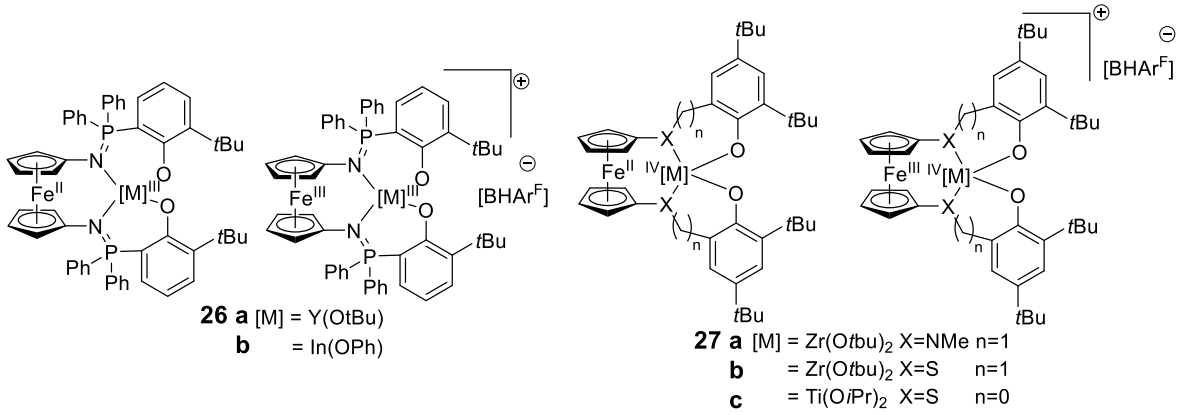

Figure 1.5.2: Redox switchable catalysts developed by Diaconsecu and co-workers.[186,187]

In order to determine if it was possible to create a system whereby the oxidised form is the more active species, an indium complex **(26 b)** was synthesised. This was chosen because while it is known that electron withdrawing groups, have a negative effect on yttrium catalysts, there have been reports of electron withdrawing groups increasing the activity of aluminium catalysts. Both the oxidised and reduced form of the indium catalyst **(26b)** were barely active for the ROP of lactide and ε-caprolactone. However, for the ROP of TMC, the oxidised form was significantly more active than the reduced (>40x), albeit still very slow (TOF = 2 h^{-1}). The yttrium catalyst **(26a)** showed the opposite behaviour, with the oxidised catalyst being less active for the ROP of TMC than the reduced form, despite both versions being more active than the indium complex.

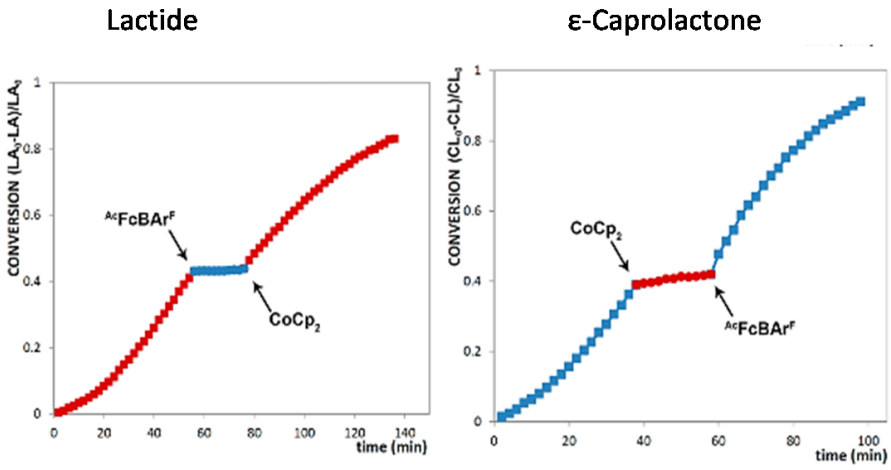

Figure 1.5.3: Plots showing the orthogonal reactivity of 27c with the ROP of ε-CL and Lactide.

The previous results showed that the cationic complexes of the early transition metals have stronger bonds with the polar monomers (lactide etc.), compared to the neutral complexes. Diaconescu and co-workers next focused on group 4 metals as there may be a better balance between the oxidised and reduced states, allowing the oxidised states to still be active.[187] Titanium and zirconium alkoxide complexes with salan and thiolfan based ligands were developed **(27).** All complexes were highly active for lactide polymerisation in their reduced form, but considerably less active as oxidised complexes. However, for the ROP of ε-CL the opposite reactivity was observed: with the oxidised complexes being active towards ε-CL ROP. The titatium thiolafan complex **(27c)** was able to undergo both lactide and ε-CL ROP in a one pot fashion. Initially, the reduced complex polymerises lactide from a mixture of monomers and once the oxidising agent is added, the complex is oxidised and caprolactone is polymerised. The oxidised complex is not as selective as the reduced form, so while the oxidised complex predominantly polymerises ε-CL some lactide is incorporated. The actual structure of the block copolymer is reported as poly[*b*-(LA-minor-CL)-*b*-(CL-minor-LA)]. There is an increase in the molar mass of the polymer after the oxidation step and the distribution remains narrow (M_n goes from 2,300 gmol^{-1} (1.11) to 3,200 gmol^{-1} (1.12)). The ^{1}H NMR spectroscopy shows signals for the junction units of both PCL and PLA. The titanium thiolafan complex **(27c)** was the only catalyst that was able to catalyse a block

copolymer from a mixture of monomers. With the zirconium salafan **(27a)**, the polymerisation of ε-CL did not occur after addition of the oxidant. The lack of activity is thought to be due to the strong co-ordination of lactide to the oxidised complex.

The binding of lactide to the oxidised form of **27a** highlights the potential complications when trying to form block copolymers with switch chemistry. The more species present in a system, the more likely they are to interact and cause problems. The addition of oxidising and reducing agents means that it is unlikely to be easy to form multiblock copolymers using redox switch chemistry, as at some point the concentration of these switching agents becomes inhibiting.

The first example of a catalyst, where the catalytic centre is the redox active centre, was in 2011 by Diaconescu and co-workers.[186] A cerium (III) salen complex **(28)** was active for the ROP of lactide, but the oxidised form was inactive. The redox chemistry was reversible allowing the on/off switching of lactide ROP with no loss of catalytic activity. Another cerium based catalyst **(29)** was developed by Okuda and co-workers.[188] The reduced complex was the active form, with the oxidised form being inactive. Initiation of the ROP occurs *via* lactide insertion into one of the aryl oxide bonds. The reduced complex has a larger ionic radius, which is proposed to allow easier co-ordination and insertion of the lactide, hence the increase in activity.

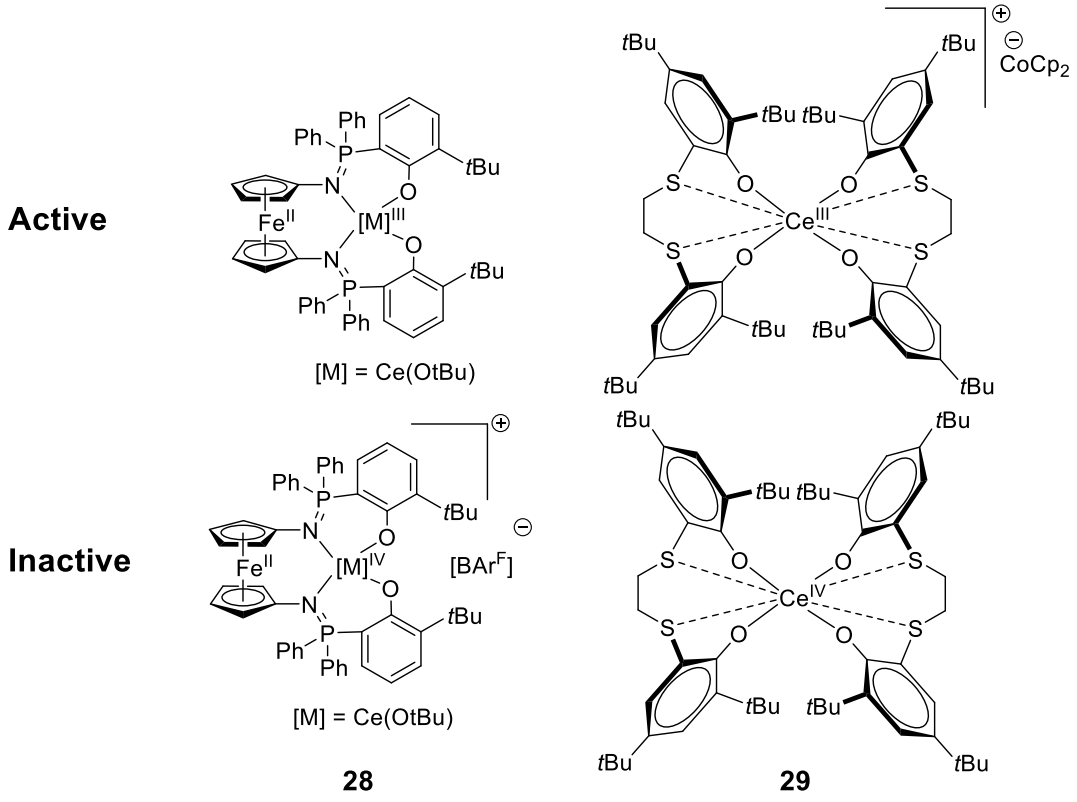

Figure 1.5.4: Catalysts where the active centre is the redox switch.[186,188]

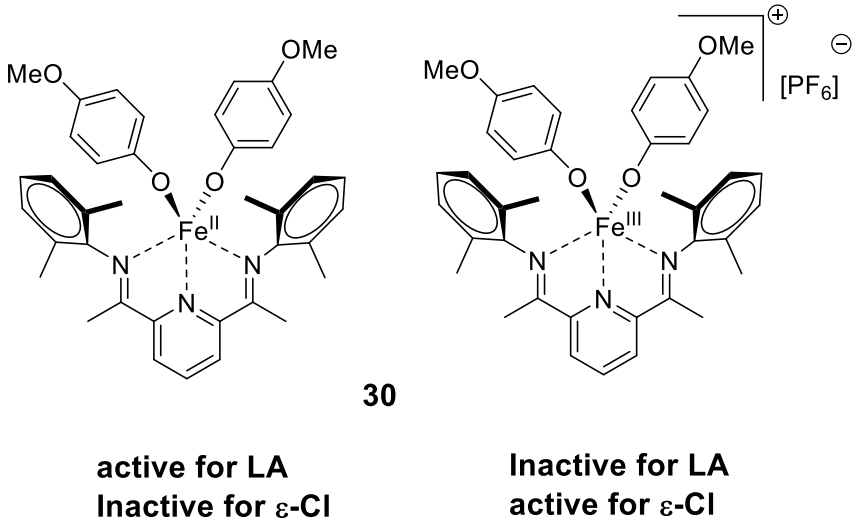

Figure 1.5.5: Structure of the bis(imino)pyridine iron diaryloxide developed by Byers.[189,190]

In 2013, a bis(imino)pyridine iron diaryloxide complex **(30)** was shown to be redox-switchable,by Byers and co-workers.[189] The reduced form was an effective catalyst for lactide polymerisation, but the rate could be reduced by the formation of the oxidised complex, achieved by the addition of $Fc(PF_6)$. The reduction and oxidation could be carried out *in-situ* multiple times with no effect on the rate of ring opening. A structurally similar catalyst was reported by Lang for the ROP of ε-CL.[190] The reduced Fe(II) complex was inactive for the ROP of ε-CL but oxidation to the Fe(III) complex produced an effective catalyst in the presence of alcohol. This is similar to the results discovered by Diaconescu, where the oxidised complexes were active for ε-CL ROP and the reduced complexes are active for lactide ROP.

Byers and co-workers recently showed that while the oxidised version of their catalyst **(30)** was inactive for lactide ROP, it was active for the ROP of epoxides.[191] The Fe(II) complex is active for lactide polymerisation, while the Fe(III) is the active for epoxide polymerisation. This is hypothesised to be due to the electron rich Fe(II) species being better at the nucleophilic activation of the alkoxides in lactide polymerisation; whereas the electron deficient Fe(III) species centre is more suited to the electrophilic activation required for epoxide polymerisations. The ROP of epoxide was not a controlled polymerisation, resulting in a disperse polymer. The catalyst is proposed to act *via* a co-ordination – insertion mechanism as the polymerisation is so dramatically affected (polymerisation stops) by the reduction of the catalyst. They hypothesise that a cationic polymerisation mechanism would not be affected by the redox state of the metal centre, as the growing polymer chain end is away from the metal centre. The oxidation and reduction of **(30)** could be carried out successfully *in-situ*, in the presence of both lactide and CHO. **(30)** was then used to make block copolymers, by *in-situ* reduction or oxidation. PLA-PCHO was formed by starting from the Fe(III) complex and *in-situ* reduction to the Fe(II) complex by $FcPF_6$. $FcPF_6$ is able to homopolymerise CHO, but at a much slower rates than the reduced complex **(30).** PCHO-PLA was formed by starting with the Fe(II) complex and *in-situ* reduction by $CoCp_2$. In both cases significant amounts of homo polyether are formed, but the major product is the block copolymer, as indicated by an increase in the molar mass and a single species being detected by DOSY NMR spectroscopy that contains both PLA and PCHO. The formation of such

large quantities of homopolymer is not ideal but this is still a significant report as the catalyst is fully chemoselective.

All of the current redox switchable catalysts require the addition of external reductants and oxidants, and this will become a limitation, particularly in the quest towards block copolymers, especially multiblocks copolymers. While the switches are added in low concentrations, with multiple switches, the levels will build up and may cause adverse side reactions and limit the number of monomers or processes that are tolerant. However, there is the potential to oxidise/reduce many metals *via* electrochemical means if a suitable set up could be derived.

1.5.2 Chemical Control

The addition of chemicals which do not affect the oxidation state of the catalyst but rather alter the structure of the catalyst have also been used as switches.[184,192,193] Mirkin and co-workers developed a complex aluminium salen catalyst **(31)** that had functionalised side arms each bearing a rhodium complex.[192] The catalyst was designed so that the activity would be modulated by the co-ordination sphere at the rhodium complex. The catalyst can be switched from a flexible open structure, to a closed structure where π stacking, results in a conformation where the Al centre is obstructed. While the open structure is active for the ROP of ε-CL, the closed structure is inactive, due to the inaccessible Al (III) centre. The switch can be facilitated by chloride abstraction through the addition of sodium or lithium salts. The change between the open and closed structures takes up to 20 minutes and the closed structure does eventually decompose to the open structure over time.

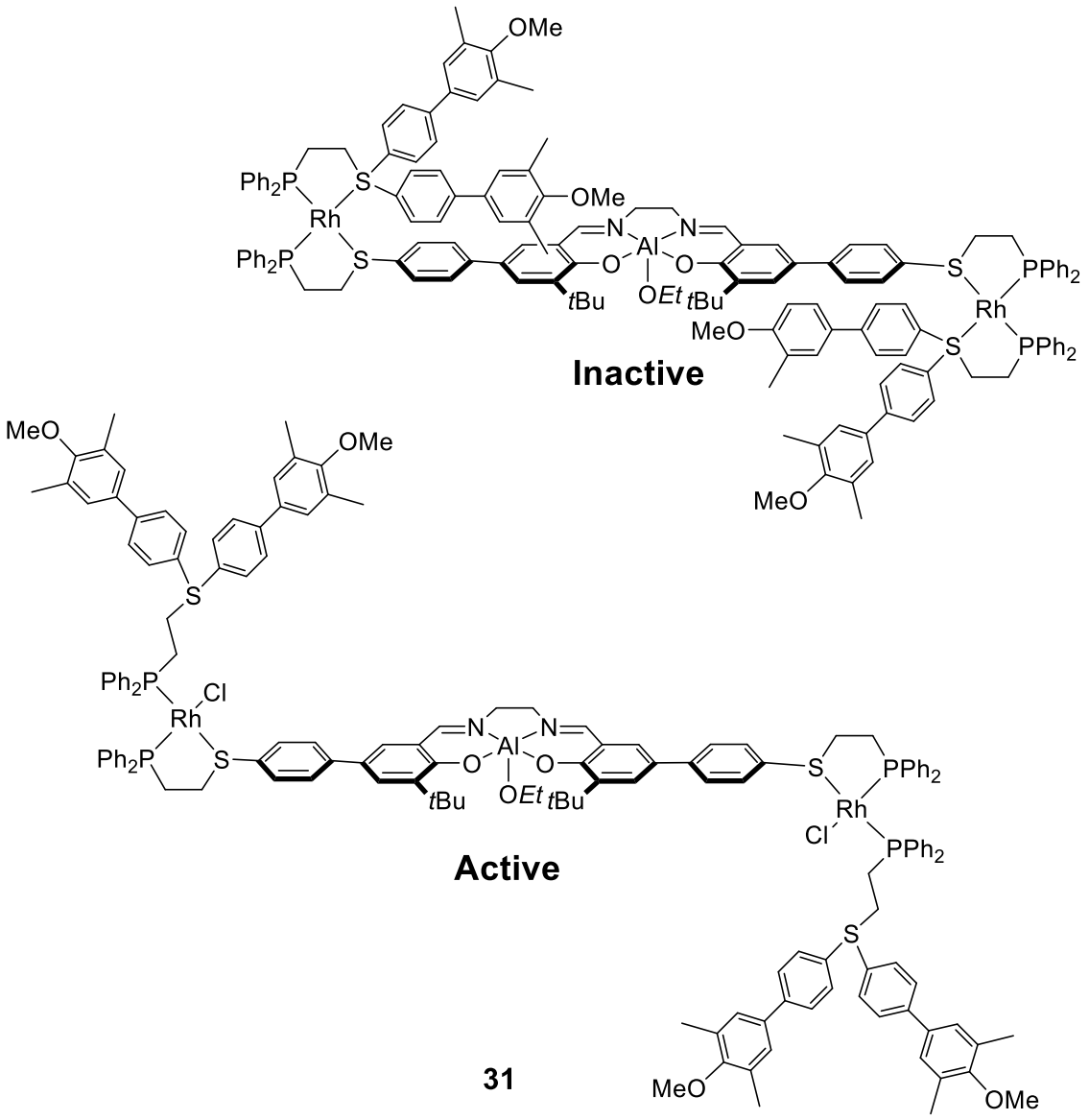

Figure 1.5.6: Functionalised Aluminium salen catalyst developed by Mirkin.[192]

Gases make an ideal switch reagent, due to the relative ease with which they can be added and removed from a system. In 2014, Dubois and co-workers reported that the addition of carbon dioxide to an organocatalytic system resulted in switching the polymerisation off.[193] They used a catalytic system of triazabicyclodecene (TBD), 1,8-Diazabicyclo[5.4.0]undec-7-ene (DBU) and benzyl alcohol (BnOH) (10:1:1), which was an active catalyst for the ROP of ε-CL. DBU is a well-known organocatalyst for ROP but requires a co-catalyst, usually thio-

urea; on its own or with alcohol, it was inactive for ε-CL ROP. TBD is also known to catalyse ROP in the presence of alcohol. DBU is known to form an ionic iminium carbonate species when in the presence of carbon dioxide and an alcohol. This effectively removes the hydroxyl group from the catalytic system, meaning the TBD is no longer able to polymerise ROP. The switch worked considerably better at lower monomer loadings (50:1 [M]:[I] compared to 200:1), where it could be switched multiple times, with minimal loss of activity.

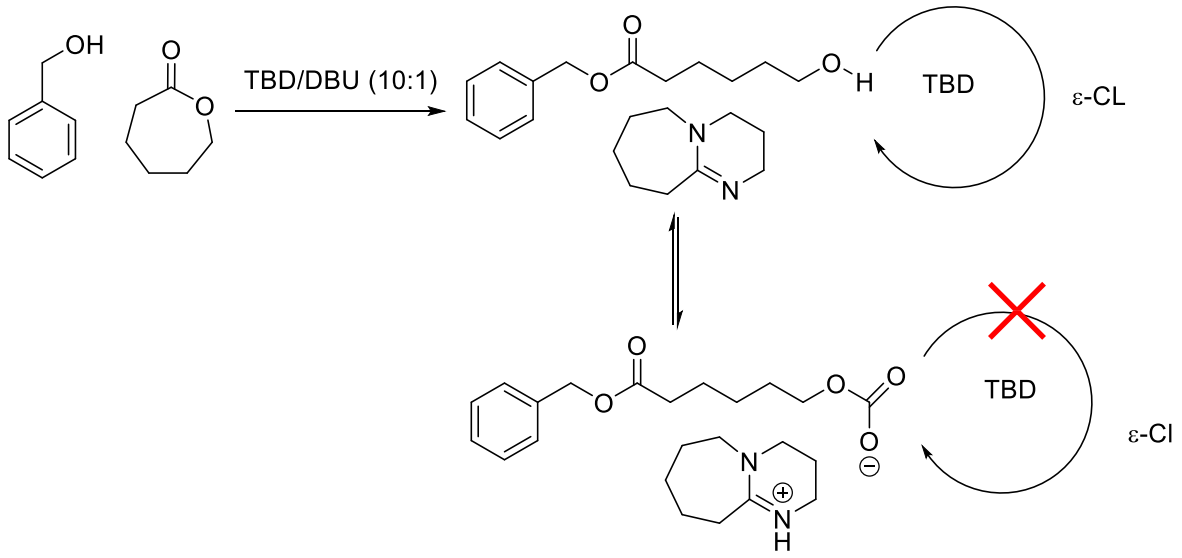

Figure 1.5.7: The switch mechanism developed by Dubois and co-workers.[193]

In 2014 our group discovered a switchable catalysis using a chemoselective method. While $[LZn_2(OAc)_2]$ was inactive for the ROP of ε-CL, a catalyst system from $[LZn_2(OAc)_2]$ and cyclohexene oxide was active.[184,194] $[LZn_2(OAc)_2]$ contains a zinc carboxylate bond as the active centre, which is unable to ring open ε-CL, but the reaction between $[LZn_2(OAc)_2]$ and CHO results in the formation of a zinc alkoxide bond. This zinc alkoxide bond can ring open ε-Cl, allowing ROP to occur. This catalyst system can be turned off by the addition of carbon dioxide. The carbon dioxide readily inserts into the zinc alkoxide bond, forming a zinc carbonate species, which is also inactive for ROP. $[LZn_2(OAc)_2]$ is an active catalyst for the ROCOP of epoxide and carbon dioxide, even at 1 atm pressure, therefore when carbon

dioxide is present ROCOP occurs. This allows block copolymers to made in one pot and using a single catalyst, which would otherwise require complex synthetic strategies. This system mimics the redox switchable systems in that a different switch reagent is required depending on the direction of the switch, in this case CHO switches the catalyst from ROCOP to ROP, and CO_2 which switches the catalyst from ROP to ROCOP. But the key difference, with the redox switch methods, is that here the switches are also reagents in the copolymerisation, so no additional species need to be introduced and very rapid and reversible switching is possible.

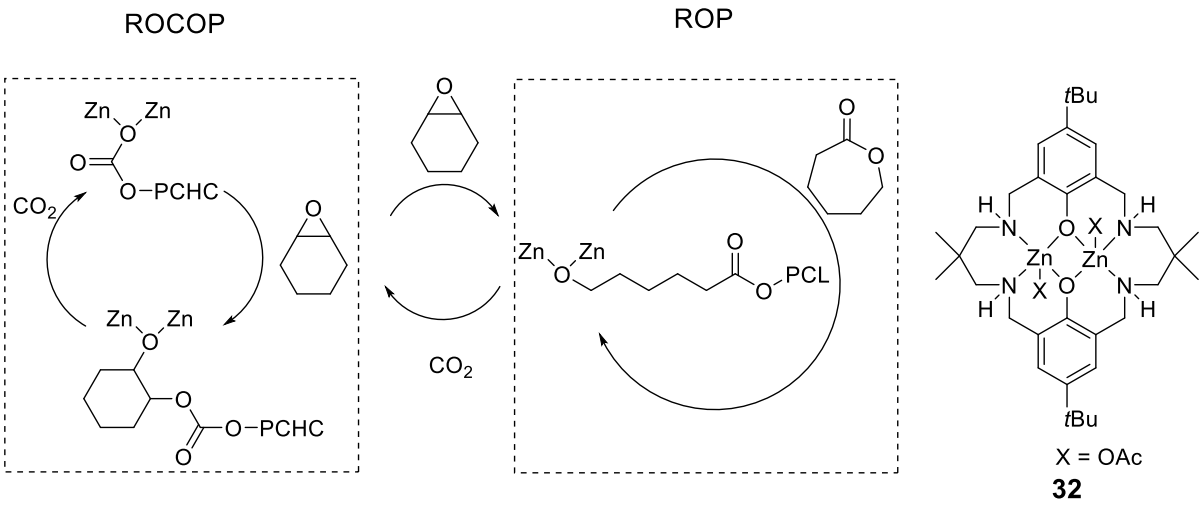

Figure 1.5.8: The switch mechanism for di-zinc catalyst 32.[184]

1.5.3 Photochemical Control

Light is, theoretically, an attractive means to switch reactions as it is non-invasive, selective to the chromaphore and the switch can occur near instantaneously. Photochemical switches are widely used in radical based polymerisations, especially those which are photo initiated, and in the photoredox catalysis of small molecule organics.[180,181] However, the use of light as switch is limited in the field of ring opening polymerisation. In 2006 Osaki *et al*, used

cinnamoyl α-cyclodextrin (α-CD) to polymerise δ-valerolactone.[195] α-CD was only active for the polymerisation if the cinnamoyl group had the *trans* isomer (Figure 1.5.7), although the polymerisation was very slow (TOF = 0.2 h^{-1}). The polymerisation of δ-VL occurs within the cavity of the cyclodextrin host and the access is blocked if the cinnamoyl group has the *cis* form. The switch between the *trans* (active) and the *cis* (inactive form) could be induced by UV radiation at 280 nm.

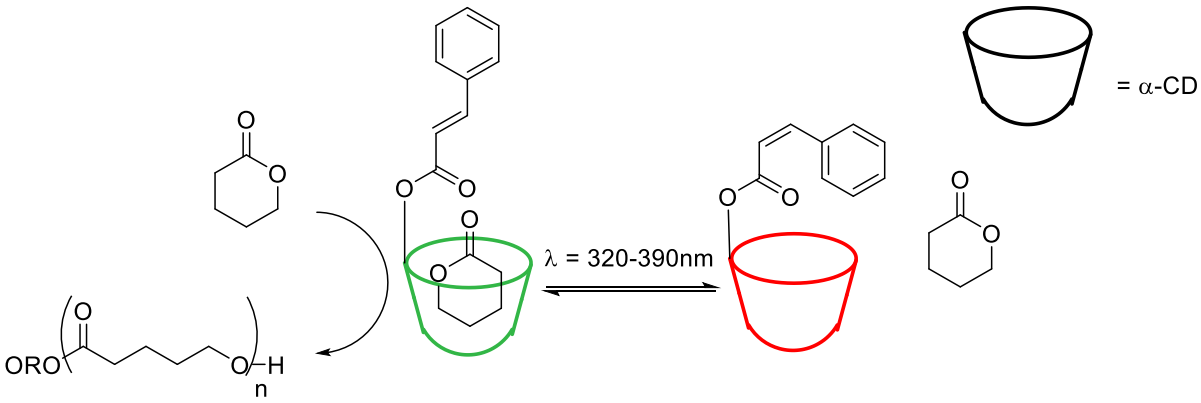

Figure 1.5.9: Photochemical switch developed by Osaki *et al.*[195]

In 2013, Nielson and Bielawaski reported a photoswitchable organocatalyst for the ROP of ε-Cl and δ-VL. [196] The catalytic system consisted of an *in-situ* generated N-hetrocyclic carbine (NHC). The NHC efficiently catalysed the ring opening of ε-CL in the presence of an alcohol initiator, *via* the formation of an imidazolium alkoxide, with a turnover frequency of >200 h^{-1}. The PCL formed is of a high molar mass (M_n = 12,500 g mol^{-1}) and narrow dispersity (Đ = 1.15).The photochromic nature of the NHC meant that under UV radiation (313 nm) a covalently bound NHC –alcohol adduct was formed. This species was inactive for ε-CL ROP, due to the extended conjugation of the backbone, which results in a more electron deficient carbenoid centre. This means the release of the alkoxide unit is prevented, so catalysis cannot occur. Subsequent exposure to visible light causes the reformation of the active NHC species.

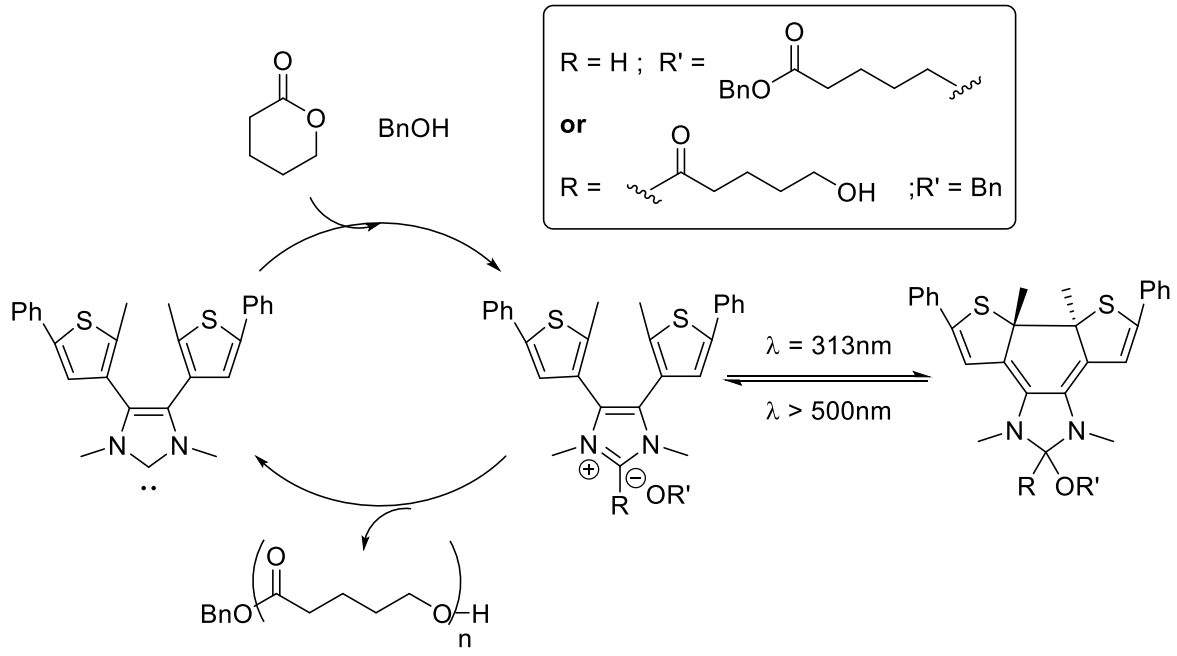

Figure 1.5.10: The photochemical switch developed by Nielson and Bielawaski.

1.5.4 Thermal Control

A thermal switch should deliver more than simply being able to stop or start a catalytic system because a certain amount of energy is required to overcome the thermodynamic barrier of the process. While this first strategy can be used in clever ways to form complex polymers,[197] the temperature has no effect on the catalyst itself. A true switch should change the catalyst structure, so as to deliver altered performance.

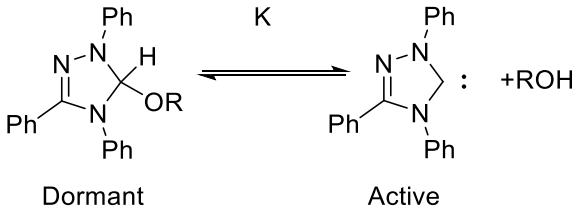

Figure 1.5.11: The thermal switch discovered by Hedrick and co-workers.[198]

Hedrick and co-workers developed a NHC based catalytic system, from the reaction between a triazolylidene and an alcohol, which was only active for the ROP of Lactide and β-butyrolactone at 90 °C.[198,199] While the alcohol readily reacts with the triazolylidene to form a covalent adduct, the NHC is only formed at 90 °C. The active species is the NHC, so the polymerisation only occurs at 90 °C. The catalyst is slow, with turnover frequencies of ~2 h^{-1}, but with good levels of control. The PLA produced is of a high molar mass (M_n = 10,000 $gmol^{-1}$) and narrow dispersity (Đ = 1.09). The system can be heated and cooled repeatedly, and still retain full control of the polymerisation and a polymer with a narrow dispersity.

Conclusion

Switchable polymerisation catalysis is currently held back by the time taken for the catalyst to switch and the potential build-up of any additional reagents used to initiate the switch. If the switch is not instantaneous or is not quantitative, then gradient or random copolymers form. While these polymers can have interesting properties, the polymerisation is not as well controlled, which makes it harder to repeat or scale up. When additional reagents are required to initiate the switch between catalytic states (e.g. oxidisers and reducing agents in redox controlled switch catalysis), there is the potential for them to build up in the system. This will become problematic as more complicated structures are targeted, such as multiblock copolymers. One potential work around this limitation is the use of electrochemical potentials to trigger the redox switch. While this has been achieved in the field of ATRP,[200] it is as of yet unreported within the field of ROP. When switch chemistry works successfully it is a very promising method of making block copolymers as it is truly one pot, requires a single catalyst and allows control of when to start and stop each polymerisation.

1.6 Outlook

While the utilisation of carbon dioxide as a monomer to form polycarbonates is feasible, there remains a considerable opportunity to improve catalytic selectivity and monomer scope. Research teams all over the world are dedicated to developing catalysts with ever increasing

activity for ROCOP. However, when highlighting ROCOP, many people cite its ease in forming structurally diverse backbones, and the corresponding range of properties, through the use of different epoxides. Yet the majority of catalysts reported so far are only tested with a limited range of epoxides, typically PO and CHO. Although the resulting polymers do have some attractive properties (e.g. T_g of PCHC and flexibility of PPC), they also have some draw-backs (the mechanical properties of PCHC and thermal properties of PPC). Catalysts that can polymerise other epoxides and mixture of epoxides will be fundamental to the future of the field. It will also be necessary to ensure that the full range of properties of different polycarbonates are measured and standardised. For instance, while the effect of the increased stereoselectivity on the thermal properties has been studied, there have been limited studies into whether or not this translates into an improvement in the mechanical properties.

Attempts to combine polymers from ROCOP into block copolymers are still at a very early stage, with truly one pot methods being even rarer. The ability to form block copolymers is important as it provides a method of moderating the properties of the polycarbonates and shows that ROCOP is as controllable a method as alternative polymerisation mechanisms. Another attraction of block copolymers is the ability to undergo self-assembly and the potential applications this enables. While these block copolymers are unlikely to become commodity materials, due to the complex synthesis, they may exhibit specialist properties that make them ideal for smaller scale applications, including as scaffolds for nano-structures, biomedical applications including drug delivery and specialist coatings.

The ability to use a single catalyst and switch between reactions is very attractive but in ROP and ROCOP this research is still in its infancy. While catalysts which can switch on and off are intrinsically interesting and can better inform the switch mechanism, a greater interest lies in catalysts which can switch between multiple monomers and/or reactions. Catalysts with such a multi-functional ability could provide a facile route to block copolymers and hopefully other more interesting architectures. The ideal switch needs to be instantaneous, removable, reversible and quantitative: taken together these are tough criteria.

1.7 Aims and Objectives

The aims and objectives of this thesis are as follows:

1 To gain an in-depth understanding of the mechanism employed by catalysts of the form $[LZn_2(X)_2]$ to switch between the ring opening copolymerisation of CHO/CO_2 and ring opening polymerisation of ε-CL. In particular to determine whether the switch between the two polymerisation mechanisms results in the formation of block copolymers. The structure of the copolymers will be investigated in detail.

2 To understand the effect of using alternative monomers in a switchable process using catalysts of the form $[LZn_2(X)_2]$. To determine if the selectivity is only specific to cyclohexene oxide, carbon dioxide and ε-caprolactone as monomers or can be widely applied. To understand how the rate of polymerisation of the monomers within a particular polymerisation cycle affects the overall catalyst selectivity. The thermal and mechanical properties of any copolymer synthesised using the switch method will be determined.

3 To determine whether the selectivity of catalysts of the form $[LZn_2(X)_2]$ can be used to form multiblock copolymers. This will require the catalysts to be able to switch between the ring opening copolymerisation and ring opening polymerisation in both directions, with complete control of the selectivity and should only result in block copolymer formation.

4 To uncover whether the switchable catalysis displayed the catalysts of the form $[LZn_2(X)_2]$ can be combined with the kinetic selectivity between anhydride/epoxide and carbon dioxide/epoxide copolymerisation, to result in block copolymers containing at least three distinct blocks. This will involve investigations of four different monomers.

References

(1) Song, C. *Catal. Today* **2006**, *115*, 2.
(2) Commission, E.; Commission, E., Ed. 2011.
(3) Poliakoff, M.; Leitner, W.; Streng, E. S. *Faraday Discuss.* **2015**, *183*, 9.
(4) North, M.; Styring, P. *Faraday Discuss.* **2015**, *183*, 489.
(5) Pérez-Fortes, M.; Schöneberger, J. C.; Boulamanti, A.; Tzimas, E. *Applied Energy* **2016**, *161*, 718.
(6) Aresta, M. In *Carbon Dioxide as Chemical Feedstock*; Wiley-VCH Verlag GmbH & Co. KGaA: 2010, p 1.
(7) Langanke, J.; Wolf, A.; Hofmann, J.; Bohm, K.; Subhani, M. A.; Muller, T. E.; Leitner, W.; Gurtler, C. *Green Chem.* **2014**, *16*, 1865.
(8) DeBolt, M.; Kiziltas, A.; Mielewski, D.; Waddington, S.; Nagridge, M. J. *J. Appl. Polym. Sci.* **2016**, *133*, n/a.
(9) Broadwith, P. Chemsitry World, 2015; Vol. 2016.
(10) Darensbourg, D. J.; Holtcamp, M. W. *Coord. Chem. Rev.* **1996**, *153*, 155.
(11) Kember, M. R.; Buchard, A.; Williams, C. K. *Chem. Commun.* **2011**, *47*, 141.
(12) Trott, G.; Saini, P. K.; Williams, C. K. *Phil. Trans. R. Soc. A* **2016**, *374*.
(13) Darensbourg, D. J. *Chem. Rev.* **2007**, *107*, 2388.
(14) Darensbourg, D. J.; Wilson, S. J. *Green Chem.* **2012**, *14*, 2665.
(15) Romain, C.; Thevenon, A.; Saini, P. K.; Williams, C. K. In *Carbon Dioxide and Organometallics*; Lu, X.-B., Ed.; Springer International Publishing: Cham, 2016, p 101.
(16) Nozaki, K. In *Pure Appl. Chem.* 2004; Vol. 76, p 541.
(17) Lu, X.-B.; Ren, W.-M.; Wu, G.-P. *Acc. Chem. Res.* **2012**, *45*, 1721.
(18) Klaus, S.; Lehenmeier, M. W.; Anderson, C. E.; Rieger, B. *Coord. Chem. Rev.* **2011**, *255*, 1460.
(19) Coates, G. W.; Moore, D. R. *Angew. Chem. Int. Ed.* **2004**, *43*, 6618.
(20) Darensbourg, D. J.; Wei, S.-H. *Macromolecules* **2012**, *45*, 5916.
(21) Wu, G.-P.; Wei, S.-H.; Ren, W.-M.; Lu, X.-B.; Li, B.; Zu, Y.-P.; Darensbourg, D. J. *Energy Environ Sci* **2011**, *4*, 5084.
(22) Cyriac, A.; Lee, S. H.; Varghese, J. K.; Park, E. S.; Park, J. H.; Lee, B. Y. *Macromolecules* **2010**, *43*, 7398.
(23) Inoue, S. *J. Polym. Sci., Part A: Polym. Chem.* **2000**, *38*, 2861.
(24) Yi, N.; Unruangsri, J.; Shaw, J.; Williams, C. K. *Faraday Discuss.* **2015**, *183*, 67.
(25) Nakano, K.; Nakamura, M.; Nozaki, K. *Macromolecules* **2009**, *42*, 6972.
(26) Na, S. J.; S, S.; Cyriac, A.; Kim, B. E.; Yoo, J.; Kang, Y. K.; Han, S. J.; Lee, C.; Lee, B. Y. *Inorg. Chem.* **2009**, *48*, 10455.
(27) Noh, E. K.; Na, S. J.; S, S.; Kim, S.-W.; Lee, B. Y. *J. Am. Chem. Soc.* **2007**, *129*, 8082.
(28) Cohen, C. T.; Chu, T.; Coates, G. W. *J. Am. Chem. Soc.* **2005**, *127*, 10869.
(29) Chatterjee, C.; Chisholm, M. H. *Inorg. Chem.* **2011**, *50*, 4481.
(30) Wu, G.-P.; Darensbourg, D. J.; Lu, X.-B. *J. Am. Chem. Soc.* **2012**, *134*, 17739.
(31) Mang, S.; Cooper, A. I.; Colclough, M. E.; Chauhan, N.; Holmes, A. B. *Macromolecules* **2000**, *33*, 303.

(32) Qin, Z.; Thomas, C. M.; Lee, S.; Coates, G. W. *Angew. Chem.* **2003**, *115*, 5642.
(33) Chatterjee, C.; Chisholm, M. H. *Inorg. Chem.* **2012**, *51*, 12041.
(34) Chatterjee, C.; Chisholm, M. H.; El-Khaldy, A.; McIntosh, R. D.; Miller, J. T.; Wu, T. *Inorg. Chem.* **2013**, *52*, 4547.
(35) Liu, J.; Ren, W.-M.; Liu, Y.; Lu, X.-B. *Macromolecules* **2013**, *46*, 1343.
(36) Xia, W.; Vagin, S. I.; Rieger, B. *Chem. Eur. J.* **2014**, *20*, 15499.
(37) Wu, G.-P.; Darensbourg, D. J. *Macromolecules* **2016**, *49*, 807.
(38) Chapman, A. M.; Keyworth, C.; Kember, M. R.; Lennox, A. J. J.; Williams, C. K. *ACS Catal.* **2015**, *5*, 1581.
(39) Inoue, S.; Koinuma, H.; Tsuruta, T. *J. Polym. Sci., Part B: Polym. Phys* **1969**, *7*, 287.
(40) Inoue, S.; Koinuma, H.; Tsuruta, T. *Macromol. Chem. Phys.* **1969**, *130*, 210.
(41) Kobayashi, M.; Inoue, S.; Tsuruta, T. *Macromolecules* **1971**, *4*, 658.
(42) Kobayashi, M.; Tang, Y.-L.; Tsuruta, T.; Inoue, S. *Macromol. Chem. Phys.* **1973**, *169*, 69.
(43) Kobayashi, M.; Inoue, S.; Tsuruta, T. *J. Polym. Sci., Part A: Polym Chem* **1973**, *11*, 2383.
(44) Inoue, S.; Kobayashi, M.; Koinuma, H.; Tsuruta, T. *Macromol. Chem. Phys.* **1972**, *155*, 61.
(45) Kuran, W.; Pasynkiewicz, S.; Skupińska, J.; Rokicki, A. *Macromol. Chem. Phys.* **1976**, *177*, 11.
(46) Góarecki, P.; Kuran, W. *J. Polym. Sci. Polym. Lett. Ed.* **1985**, *23*, 299.
(47) Kuran, W.; Listoś, T. *Macromol. Chem. Phys.* **1994**, *195*, 977.
(48) Soga, K.; Imai, E.; Hattori, I. *Polym. J.* **1981**, *13*, 407.
(49) Takeda, N.; Inoue, S. *Macromol. Chem. Phys.* **1978**, *179*, 1377.
(50) Aida, T.; Inoue, S. *Macromolecules* **1982**, *15*, 682.
(51) Luinstra, G. A. *Polym. Rev.* **2008**, *48*, 192.
(52) Ree, M.; Hwang, Y.; Kim, J.-S.; Kim, H.; Kim, G.; Kim, H. *Catal. Today* **2006**, *115*, 134.
(53) Kim, J.-S.; Kim, H.; Ree, M. *Chem. Mater.* **2004**, *16*, 2981.
(54) Kim, J.-S.; Ree, M.; Shin, T. J.; Han, O. H.; Cho, S. J.; Hwang, Y.-T.; Bae, J. Y.; Lee, J. M.; Ryoo, R.; Kim, H. *J. Catal.* **2003**, *218*, 209.
(55) Kim, J. S.; Ree, M.; Lee, S. W.; Oh, W.; Baek, S.; Lee, B.; Shin, T. J.; Kim, K. J.; Kim, B.; Lüning, J. *J. Catal.* **2003**, *218*, 386.
(56) Ree, M.; Bae, J. Y.; Jung, J. H.; Shin, T. J. *J. Polym. Sci., Part A: Polym. Chem.* **1999**, *37*, 1863.
(57) Eberhardt, R.; Allmendinger, M.; Zintl, M.; Troll, C.; Luinstra, G. A.; Rieger, B. *Macromol. Chem. Phys.* **2004**, *205*, 42.
(58) Klaus, S.; Lehenmeier, M. W.; Herdtweck, E.; Deglmann, P.; Ott, A. K.; Rieger, B. *J. Am. Chem. Soc.* **2011**, *133*, 13151.
(59) Varghese, J. K.; Park, D. S.; Jeon, J. Y.; Lee, B. Y. *J. Polym. Sci., Part A: Polym. Chem.* **2013**, *51*, 4811.
(60) Sebastian, J.; Srinivas, D. *Appl. Catal., A* **2013**, *464–465*, 51.
(61) Zhang, X.-H.; Wei, R.-J.; Sun, X.-K.; Zhang, J.-F.; Du, B.-Y.; Fan, Z.-Q.; Qi, G.-R. *Polymer* **2011**, *52*, 5494.
(62) Sun, X.-K.; Zhang, X.-H.; Liu, F.; Chen, S.; Du, B.-Y.; Wang, Q.; Fan, Z.-Q.; Qi, G.-R. *J. Polym. Sci., Part A: Polym. Chem.* **2008**, *46*, 3128.

(63) Kim, I.; Yi, M. J.; Lee, K. J.; Park, D.-W.; Kim, B. U.; Ha, C.-S. *Catal. Today* **2006**, *111*, 292.
(64) Chen, S.; Qi, G.-R.; Hua, Z.-J.; Yan, H.-Q. *J. Polym. Sci., Part A: Polym. Chem.* **2004**, *42*, 5284.
(65) Sugimoto, H.; Ohshima, H.; Inoue, S. *J. Polym. Sci., Part A: Polym. Chem.* **2003**, *41*, 3549.
(66) Bernard, A.; Chatterjee, C.; Chisholm, M. H. *Polymer* **2013**, *54*, 2639.
(67) Xia, W.; Salmeia, K. A.; Vagin, S. I.; Rieger, B. *Chem. Eur. J.* **2015**, *21*, 4384.
(68) Harrold, N. D.; Li, Y.; Chisholm, M. H. *Macromolecules* **2013**, *46*, 692.
(69) Anderson, C. E.; Vagin, S. I.; Hammann, M.; Zimmermann, L.; Rieger, B. *ChemCatChem* **2013**, *5*, 3269.
(70) Sugimoto, H.; Kuroda, K. *Macromolecules* **2008**, *41*, 312.
(71) Anderson, C. E.; Vagin, S. I.; Xia, W.; Jin, H.; Rieger, B. *Macromolecules* **2012**, *45*, 6840.
(72) Jacobsen, E. N. *Acc. Chem. Res.* **2000**, *33*, 421.
(73) Darensbourg, D. J.; Yarbrough, J. C. *J. Am. Chem. Soc.* **2002**, *124*, 6335.
(74) Darensbourg, D. J.; Moncada, A. I.; Wei, S.-H. *Macromolecules* **2011**, *44*, 2568.
(75) S, S.; Min, J. K.; Seong, J. E.; Na, S. J.; Lee, B. Y. *Angew. Chem. Int. Ed.* **2008**, *47*, 7306.
(76) Nakano, K.; Kamada, T.; Nozaki, K. *Angew. Chem. Int. Ed.* **2006**, *45*, 7274.
(77) Klaus, S.; Vagin, S. I.; Lehenmeier, M. W.; Deglmann, P.; Brym, A. K.; Rieger, B. *Macromolecules* **2011**, *44*, 9508.
(78) Darensbourg, D. J. In *Synthetic Biodegradable Polymers*; Rieger, B., Künkel, A., Coates, W. G., Reichardt, R., Dinjus, E., Zevaco, A. T., Eds.; Springer Berlin Heidelberg: Berlin, Heidelberg, 2012, p 1.
(79) Darensbourg, D. J.; Yeung, A. D. *Polym. Chem.* **2015**, *6*, 1103.
(80) Darensbourg, D. J.; Moncada, A. I.; Choi, W.; Reibenspies, J. H. *J. Am. Chem. Soc.* **2008**, *130*, 6523.
(81) Auriemma, F.; De Rosa, C.; Di Caprio, M. R.; Di Girolamo, R.; Coates, G. W. *Macromolecules* **2015**, *48*, 2534.
(82) Auriemma, F.; De Rosa, C.; Di Caprio, M. R.; Di Girolamo, R.; Ellis, W. C.; Coates, G. W. *Angew. Chem. Int. Ed.* **2015**, *54*, 1215.
(83) Liu, Y.; Ren, W.-M.; Wang, M.; Liu, C.; Lu, X.-B. *Angew. Chem. Int. Ed.* **2015**, *54*, 2241.
(84) Liu, Y.; Ren, W.-M.; Liu, J.; Lu, X.-B. *Angew. Chem.* **2013**, *125*, 11808.
(85) Ohkawara, T.; Suzuki, K.; Nakano, K.; Mori, S.; Nozaki, K. *J. Am. Chem. Soc.* **2014**, *136*, 10728.
(86) Niu, Y.; Li, H. *Colloid. Polym. Sci.* **2013**, *291*, 2181.
(87) Nakano, K.; Hashimoto, S.; Nozaki, K. *Chem. Sci.* **2010**, *1*, 369.
(88) Jeon, J. Y.; Lee, J. J.; Varghese, J. K.; Na, S. J.; Sujith, S.; Go, M. J.; Lee, J.; Ok, M.-A.; Lee, B. Y. *Dalton Trans.* **2013**, *42*, 9245.
(89) Yoo, J.; Na, S. J.; Park, H. C.; Cyriac, A.; Lee, B. Y. *Dalton Trans.* **2010**, *39*, 2622.
(90) Seong, J. E.; Na, S. J.; Cyriac, A.; Kim, B.-W.; Lee, B. Y. *Macromolecules* **2010**, *43*, 903.
(91) Kim, B.-E.; Varghese, J. K.; Han, Y.-G.; Lee, B.-Y. *Bull. Korean Chem. Soc.* **2010**, *31*, 829.

(92) Luinstra, G. A.; Haas, G. R.; Molnar, F.; Bernhart, V.; Eberhardt, R.; Rieger, B. *Chem. Eur. J.* **2005**, *11*, 6298.
(93) Vagin, S. I.; Reichardt, R.; Klaus, S.; Rieger, B. *J. Am. Chem. Soc.* **2010**, *132*, 14367.
(94) Eberhardt, R.; Allmendinger, M.; Rieger, B. *Macromol. Rapid Commun.* **2003**, *24*, 194.
(95) Niu, Y.; Li, H.; Chen, X.; Zhang, W.; Zhuang, X.; Jing, X. *Macromol. Chem. Phys.* **2009**, *210*, 1224.
(96) Lu, X.-B.; Shi, L.; Wang, Y.-M.; Zhang, R.; Zhang, Y.-J.; Peng, X.-J.; Zhang, Z.-C.; Li, B. *J. Am. Chem. Soc.* **2006**, *128*, 1664.
(97) Cohen, C. T.; Thomas, C. M.; Peretti, K. L.; Lobkovsky, E. B.; Coates, G. W. *Dalton Trans.* **2006**, 237.
(98) Cohen, C. T.; Coates, G. W. *J. Polym. Sci., Part A: Polym. Chem.* **2006**, *44*, 5182.
(99) Wu, G.-P.; Zu, Y.-P.; Xu, P.-X.; Ren, W.-M.; Lu, X.-B. *Chem. Asian J.* **2013**, *8*, 1854.
(100) Wu, G.-P.; Xu, P.-X.; Lu, X.-B.; Zu, Y.-P.; Wei, S.-H.; Ren, W.-M.; Darensbourg, D. J. *Macromolecules* **2013**, *46*, 2128.
(101) Paddock, R. L.; Nguyen, S. T. *J. Am. Chem. Soc.* **2001**, *123*, 11498.
(102) Darensbourg, D. J.; Bottarelli, P.; Andreatta, J. R. *Macromolecules* **2007**, *40*, 7727.
(103) Darensbourg, D. J.; Mackiewicz, R. M.; Rodgers, J. L.; Phelps, A. L. *Inorg. Chem.* **2004**, *43*, 1831.
(104) Cheng, M.; Lobkovsky, E. B.; Coates, G. W. *J. Am. Chem. Soc.* **1998**, *120*, 11018.
(105) Byrne, C. M.; Allen, S. D.; Lobkovsky, E. B.; Coates, G. W. *J. Am. Chem. Soc.* **2004**, *126*, 11404.
(106) Allen, S. D.; Moore, D. R.; Lobkovsky, E. B.; Coates, G. W. *J. Am. Chem. Soc.* **2002**, *124*, 14284.
(107) Ellis, W. C.; Jung, Y.; Mulzer, M.; Di Girolamo, R.; Lobkovsky, E. B.; Coates, G. W. *Chem. Sci.* **2014**, *5*, 4004.
(108) Jeske, R. C.; Rowley, J. M.; Coates, G. W. *Angew. Chem. Int. Ed.* **2008**, *47*, 6041.
(109) Moore, D. R.; Cheng, M.; Lobkovsky, E. B.; Coates, G. W. *J. Am. Chem. Soc.* **2003**, *125*, 11911.
(110) Kissling, S.; Lehenmeier, M. W.; Altenbuchner, P. T.; Kronast, A.; Reiter, M.; Deglmann, P.; Seemann, U. B.; Rieger, B. *Chem. Commun.* **2015**, *51*, 4579.
(111) Piesik, D. F. J.; Range, S.; Harder, S. *Organometallics* **2008**, *27*, 6178.
(112) Kissling, S.; Altenbuchner, P. T.; Lehenmeier, M. W.; Herdtweck, E.; Deglmann, P.; Seemann, U. B.; Rieger, B. *Chem. Eur. J.* **2015**, *21*, 8148.
(113) Lehenmeier, M. W.; Kissling, S.; Altenbuchner, P. T.; Bruckmeier, C.; Deglmann, P.; Brym, A.-K.; Rieger, B. *Angew. Chem. Int. Ed.* **2013**, *52*, 9821.
(114) Lee, B. Y.; Kwon, H. Y.; Lee, S. Y.; Na, S. J.; Han, S.-i.; Yun, H.; Lee, H.; Park, Y.-W. *J. Am. Chem. Soc.* **2005**, *127*, 3031.
(115) Jutz, F.; Buchard, A.; Kember, M. R.; Fredriksen, S. B.; Williams, C. K. *J. Am. Chem. Soc.* **2011**, *133*, 17395.
(116) Kember, M. R.; Williams, C. K. *J. Am. Chem. Soc.* **2012**, *134*, 15676.

(117) Kember, M. R.; Knight, P. D.; Reung, P. T. R.; Williams, C. K. *Angew. Chem. Int. Ed.* **2009**, *48*, 931.
(118) Kember, M. R.; White, A. J. P.; Williams, C. K. *Inorg. Chem.* **2009**, *48*, 9535.
(119) Kember, M. R.; White, A. J. P.; Williams, C. K. *Macromolecules* **2010**, *43*, 2291.
(120) Buchard, A.; Kember, M. R.; Sandeman, K. G.; Williams, C. K. *Chem. Commun.* **2011**, *47*, 212.
(121) Kember, M. R.; Jutz, F.; Buchard, A.; White, A. J. P.; Williams, C. K. *Chem. Sci.* **2012**, *3*, 1245.
(122) Buchard, A.; Jutz, F.; Kember, M. R.; White, A. J. P.; Rzepa, H. S.; Williams, C. K. *Macromolecules* **2012**, *45*, 6781.
(123) Saini, P. K.; Romain, C.; Williams, C. K. *Chem. Commun.* **2014**, *50*, 4164.
(124) Garden, J. A.; Saini, P. K.; Williams, C. K. *J. Am. Chem. Soc.* **2015**, *137*, 15078.
(125) Darensbourg, D. J.; Wilson, S. J. *Macromolecules* **2013**, *46*, 5929.
(126) Liu, Y.; Wang, M.; Ren, W.-M.; He, K.-K.; Xu, Y.-C.; Liu, J.; Lu, X.-B. *Macromolecules* **2014**, *47*, 1269.
(127) Hirano, T.; Inoue, S.; Tsuruta, T. *Macromol. Chem. Phys.* **1976**, *177*, 3245.
(128) Inoue, S.; Matsumoto, K.; Yoshida, Y. *Macromol. Chem. Phys.* **1980**, *181*, 2287.
(129) Takanashi, M.; Nomura, Y.; Yoshida, Y.; Inoue, S. *Macromol. Chem. Phys.* **1982**, *183*, 2085.
(130) Inoue, S. *J. Macromol. Sci. Chem.* **1979**, *13*, 651.
(131) Geschwind, J.; Frey, H. *Macromolecules* **2013**, *46*, 3280.
(132) Childers, M. I.; Longo, J. M.; Van Zee, N. J.; LaPointe, A. M.; Coates, G. W. *Chem. Rev.* **2014**, *114*, 8129.
(133) Lu, X.-B.; Darensbourg, D. J. *Chem. Soc. Rev.* **2012**, *41*, 1462.
(134) Kielland, N.; Whiteoak, C. J.; Kleij, A. W. *Adv. Synth. Catal.* **2013**, *355*, 2115.
(135) Shi, L.; Lu, X.-B.; Zhang, R.; Peng, X.-J.; Zhang, C.-Q.; Li, J.-F.; Peng, X.-M. *Macromolecules* **2006**, *39*, 5679.
(136) Wu, G.-P.; Ren, W.-M.; Luo, Y.; Li, B.; Zhang, W.-Z.; Lu, X.-B. *J. Am. Chem. Soc.* **2012**, *134*, 5682.
(137) Li, B.; Zhang, R.; Lu, X.-B. *Macromolecules* **2007**, *40*, 2303.
(138) Guerin, W.; Diallo, A. K.; Kirilov, E.; Helou, M.; Slawinski, M.; Brusson, J.-M.; Carpentier, J.-F.; Guillaume, S. M. *Macromolecules* **2014**, *47*, 4230.
(139) Li, B.; Wu, G.-P.; Ren, W.-M.; Wang, Y.-M.; Rao, D.-Y.; Lu, X.-B. *J. Polym. Sci., Part A: Polym. Chem.* **2008**, *46*, 6102.
(140) Lu, X.-B.; Liang, B.; Zhang, Y.-J.; Tian, Y.-Z.; Wang, Y.-M.; Bai, C.-X.; Wang, H.; Zhang, R. *J. Am. Chem. Soc.* **2004**, *126*, 3732.
(141) Paddock, R. L.; Nguyen, S. T. *Macromolecules* **2005**, *38*, 6251.
(142) Sugimoto, H.; Kuroda, K. *Macromolecules* **2007**, *41*, 312.
(143) Ren, W.-M.; Liu, Y.; Wu, G.-P.; Liu, J.; Lu, X.-B. *J. Polym. Sci., Part A: Polym. Chem.* **2011**, *49*, 4894.
(144) Lu, X.-B.; Wang, Y. *Angew. Chem. Int. Ed.* **2004**, *43*, 3574.
(145) Nakano, K.; Hashimoto, S.; Nakamura, M.; Kamada, T.; Nozaki, K. *Angew. Chem. Int. Ed.* **2011**, *50*, 4868.
(146) Ikada, Y.; Jamshidi, K.; Tsuji, H.; Hyon, S. H. *Macromolecules* **1987**, *20*, 904.
(147) Tsuji, H. *Macromolecular Bioscience* **2005**, *5*, 569.

(148) Cartier, L.; Okihara, T.; Lotz, B. *Macromolecules* **1997**, *30*, 6313.
(149) Luinstra, G. A.; Borchardt, E. In *Synthetic Biodegradable Polymers*; Rieger, B., Künkel, A., Coates, W. G., Reichardt, R., Dinjus, E., Zevaco, A. T., Eds.; Springer Berlin Heidelberg: Berlin, Heidelberg, 2012, p 29.
(150) Koning, C.; Wildeson, J.; Parton, R.; Plum, B.; Steeman, P.; Darensbourg, D. J. *Polymer* **2001**, *42*, 3995.
(151) Stevens, M. P. *Polymer Chemistry: An Introduction* Third ed.; Oxford University Press, 1999.
(152) Thorat, S. D.; Phillips, P. J.; Semenov, V.; Gakh, A. *J. Appl. Polym. Sci.* **2003**, *89*, 1163.
(153) Li, X.-G.; Huang, M.-R. *Polym. Int.* **1999**, *48*, 387.
(154) Brydson, J. A. *Thermoplastic Elastomers - Properties and Applications*; iSmither Rapra Publishing 1995.
(155) Huang, F.; O'Reilly, R.; Zimmerman, S. C. *Chem. Commun.* **2014**, *50*, 13415.
(156) Szwarc, M. *Nature* **1956**, *178*, 1168.
(157) Gody, G.; Zetterlund, P. B.; Perrier, S.; Harrisson, S. *Nat Commun* **2016**, *7*.
(158) Darensbourg, D. J.; Ulusoy, M.; Karroonnirum, O.; Poland, R. R.; Reibenspies, J. H.; Çetinkaya, B. *Macromolecules* **2009**, *42*, 6992.
(159) Kim, J. G.; Cowman, C. D.; LaPointe, A. M.; Wiesner, U.; Coates, G. W. *Macromolecules* **2011**, *44*, 1110.
(160) Hadjichristidis, N.; Pitsikalis, M.; Iatrou, H. In *Block Copolymers I*; Abetz, V., Ed.; Springer Berlin Heidelberg: Berlin, Heidelberg, 2005, p 1.
(161) Kim, J. G.; Coates, G. W. *Macromolecules* **2012**, *45*, 7878.
(162) Wu, G.-P.; Xu, P.-X.; Zu, Y.-P.; Ren, W.-M.; Lu, X.-B. *J. Polym. Sci., Part A: Polym. Chem.* **2013**, *51*, 874.
(163) Ren, W.-M.; Zhang, X.; Liu, Y.; Li, J.-F.; Wang, H.; Lu, X.-B. *Macromolecules* **2010**, *43*, 1396.
(164) Li, H.; Niu, Y. *Polym. J.* **2011**, *43*, 121.
(165) Xu, Y.; Xiao, M.; Wang, S.; Pan, M.; Meng, Y. *Polym. Chem.* **2014**, *5*, 3838.
(166) Koning, C. E.; Sablong, R. J.; Nejad, E. H.; Duchateau, R.; Buijsen, P. *Prog. Org. Coat.* **2013**, *76*, 1704.
(167) Huijser, S.; HosseiniNejad, E.; Sablong, R.; Jong, C. d.; Koning, C. E.; Duchateau, R. *Macromolecules* **2011**, *44*, 1132.
(168) Saini, P. K.; Romain, C.; Zhu, Y.; Williams, C. K. *Polym. Chem.* **2014**, *5*, 6068.
(169) Thevenon, A.; Garden, J. A.; White, A. J. P.; Williams, C. K. *Inorg. Chem.* **2015**, *54*, 11906.
(170) Darensbourg, D. J.; Poland, R. R.; Escobedo, C. *Macromolecules* **2012**, *45*, 2242.
(171) Liu, Y.; Huang, K.; Peng, D.; Wu, H. *Polymer* **2006**, *47*, 8453.
(172) Duan, Z.; Wang, X.; Gao, Q.; Zhang, L.; Liu, B.; Kim, I. *J. Polym. Sci., Part A: Polym. Chem.* **2014**, *52*, 789.
(173) Liu, Y.; Xiao, M.; Wang, S.; Xia, L.; Hang, D.; Cui, G.; Meng, Y. *RSC Advances* **2014**, *4*, 9503.
(174) Sun, X.-K.; Zhang, X.-H.; Chen, S.; Du, B.-Y.; Wang, Q.; Fan, Z.-Q.; Qi, G.-R. *Polymer* **2010**, *51*, 5719.
(175) Reiter, M.; Kronast, A.; Kissling, S.; Rieger, B. *ACS Macro Letters* **2016**, *5*, 419.

(176) Subhani, M. A.; Köhler, B.; Gürtler, C.; Leitner, W.; Müller, T. E. *Angew. Chem. Int. Ed.* **2016**, *55*, 5591.
(177) Kember, M. R.; Copley, J.; Buchard, A.; Williams, C. K. *Polym. Chem.* **2012**, *3*, 1196.
(178) Darensbourg, D. J.; Wu, G.-P. *Angew. Chem., Int. Ed.* **2013**, *52*, 10602.
(179) Zhang, D.; Zhang, H.; Hadjichristidis, N.; Gnanou, Y.; Feng, X. *Macromolecules* **2016**.
(180) Leibfarth, F. A.; Mattson, K. M.; Fors, B. P.; Collins, H. A.; Hawker, C. J. *Angew. Chem. Int. Ed.* **2013**, *52*, 199.
(181) Blanco, V.; Leigh, D. A.; Marcos, V. *Chem. Soc. Rev.* **2015**, *44*, 5341.
(182) Teator, A. J.; Lastovickova, D. N.; Bielawski, C. W. *Chem. Rev.* **2016**, *116*, 1969.
(183) Guillaume, S. M.; Kirillov, E.; Sarazin, Y.; Carpentier, J.-F. *Chem. Eur. J.* **2015**, *21*, 7988.
(184) Romain, C.; Williams, C. K. *Angew. Chem. Int. Ed.* **2014**, *53*, 1607.
(185) Gregson, C. K. A.; Gibson, V. C.; Long, N. J.; Marshall, E. L.; Oxford, P. J.; White, A. J. P. *J. Am. Chem. Soc.* **2006**, *128*, 7410.
(186) Broderick, E. M.; Guo, N.; Vogel, C. S.; Xu, C.; Sutter, J.; Miller, J. T.; Meyer, K.; Mehrkhodavandi, P.; Diaconescu, P. L. *J. Am. Chem. Soc.* **2011**, *133*, 9278.
(187) Wang, X.; Thevenon, A.; Brosmer, J. L.; Yu, I.; Khan, S. I.; Mehrkhodavandi, P.; Diaconescu, P. L. *J. Am. Chem. Soc.* **2014**, *136*, 11264.
(188) Sauer, A.; Buffet, J.-C.; Spaniol, T. P.; Nagae, H.; Mashima, K.; Okuda, J. *ChemCatChem* **2013**, *5*, 1088.
(189) Biernesser, A. B.; Li, B.; Byers, J. A. *J. Am. Chem. Soc.* **2013**, *135*, 16553.
(190) Fang, Y.-Y.; Gong, W.-J.; Shang, X.-J.; Li, H.-X.; Gao, J.; Lang, J.-P. *Dalton Trans.* **2014**, *43*, 8282.
(191) Biernesser, A. B.; Delle Chiaie, K. R.; Curley, J. B.; Byers, J. A. *Angew. Chem. Int. Ed.* **2016**, n/a.
(192) Yoon, H. J.; Kuwabara, J.; Kim, J.-H.; Mirkin, C. A. *Science* **2010**, *330*, 66.
(193) Coulembier, O.; Moins, S.; Todd, R.; Dubois, P. *Macromolecules* **2014**, *47*, 486.
(194) Zhu, Y.; Romain, C.; Poirier, V.; Williams, C. K. *Macromolecules* **2015**, *48*, 2407.
(195) Osaki, M.; Takashima, Y.; Yamaguchi, H.; Harada, A. *Organic & Biomolecular Chemistry* **2009**, *7*, 1646.
(196) Neilson, B. M.; Bielawski, C. W. *Chem. Commun.* **2013**, *49*, 5453.
(197) Olsén, P.; Odelius, K.; Keul, H.; Albertsson, A.-C. *Macromolecules* **2015**, *48*, 1703.
(198) Coulembier, O.; Dove, A. P.; Pratt, R. C.; Sentman, A. C.; Culkin, D. A.; Mespouille, L.; Dubois, P.; Waymouth, R. M.; Hedrick, J. L. *Angew. Chem. Int. Ed.* **2005**, *44*, 4964.
(199) Coulembier, O.; Lohmeijer, B. G. G.; Dove, A. P.; Pratt, R. C.; Mespouille, L.; Culkin, D. A.; Benight, S. J.; Dubois, P.; Waymouth, R. M.; Hedrick, J. L. *Macromolecules* **2006**, *39*, 5617.
(200) Magenau, A. J. D.; Strandwitz, N. C.; Gennaro, A.; Matyjaszewski, K. *Science* **2011**, *332*, 81.

Chapter 2 : Formation of ABA Triblock Copolymers using Switchable Catalysis

2.1 Introduction

[$LZn_2(OAc)_2$] is a well-known catalyst for the ROCOP of CHO/CO_2.[1,2] It was one of the first catalysts to show good activity at 1 atm CO_2 pressure.[3] [$LZn_2(OAc)_2$] is also an interesting catalyst as it doesn't form ether linkages under ROCOP conditions, due to its very slow rate of epoxide ring opening. This lack of ether formation means that investigations into switch chemistry are simpler as this pathway can be ignored. In 2014, the Williams group showed that [$LZn_2(OAc)_2$] was a selective pre-catalyst for the ROP of ε-caprolactone; the true catalyst was formed in the presence of CHO, and is a dizinc alkoxide complex.[4] The ring opening polymerisation of cyclic esters is a desirable route to polyesters as it is both faster and more thermodynamically favourable than polycondensation routes.[5] In general ROP can produce high molar mass aliphatic polyesters.[5] The best ROP catalysts are typically homogeneous metal complexes.

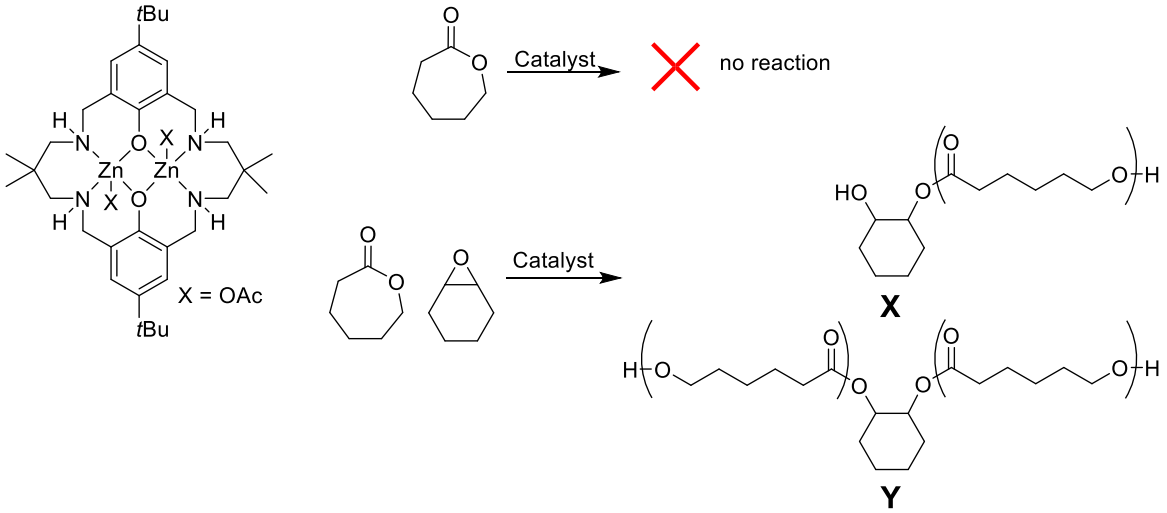

Figure 2.1.1: Scheme showing the structure of [$LZn_2(OAc)_2$] and the ring opening polymerisation to form two types of PCL: X = endcapped by diol Y = chain extended.

Given that [$LZn_2(OAc)_2$] will catalyse ROP and ROCOP separately, it was relevant to consider whether it would catalyse both processes at once. There are very few examples of catalysts which have the ability to catalyse both ROCOP and ROP processes and all those

that have been reported, do so independently.[6-10] Inoue *et al* tested aluminium metalloporphyrins for both ROCOP and ROP using several different monomers.[6] There is also an example of an aluminium amino-phenolate complex that was reported for both CHO/CO_2 ROCOP and ε-CL ROP in 2012.[7] The complexes with a methyl group were more active for the ROP of ε-CL (in the presence of BnOH) but only the complexes with chloro initiating groups were active for the ROCOP of CHO/CO_2. A dinuclear zinc complex was also tested for CHO/CO_2 ROCOP and the ROP of various cyclic esters.[8] The [ZnBDI] catalysts were reported by Coates and co-workers in separate papers for both lactide ROP and CHO/CO_2 ROCOP.[9,10] The most active ROP [ZnBDI] catalyst was actually the least selective for ROCOP, whereas the least active [ZnBDI] ROP catalyst is among the more selective ROCOP catalysts. The majority of these catalysts form poly(ether-carbonates) when undergoing ROCOP and so are clearly more suited to ROP than ROCOP since epoxide ROP is a competing pathway. In fact, preventing the ROP of epoxides and the formation of ether linkages is a driving force in the development of better ROCOP catalysts.

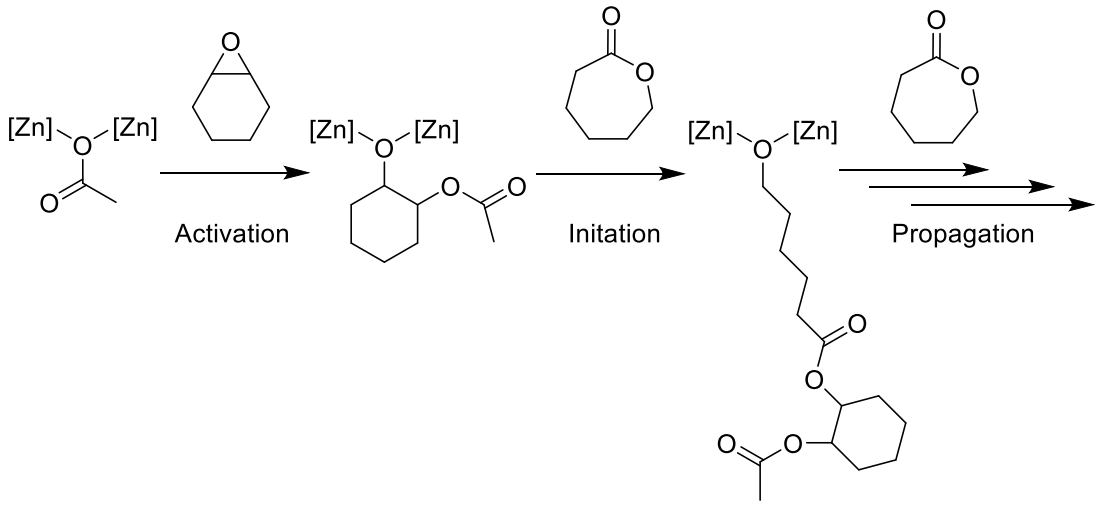

Figure 2.1.2: Scheme showing the proposed mechanism by which the ROP of ε-CL occurs when catalysed by [$LZn_2(OAc)_2$]/CHO.

The catalyst system derived from [$LZn_2(OAc)_2$] and CHO has already been shown to selectively catalyse the ROP of ε-CL, in a controlled manner.[4,11] Control experiments

revealed that ε-CL ROP by [$LZn_2(OAc)_2$] did not occur under any experimental conditions, including under forcing conditions such as high temperatures (130 °C), high monomer concentrations (up to 8 M) or for long times (16 h). Computational density functional theory (DFT) studies also failed to find a pathway whereby [$LZn_2(OAc)_2$] can successfully ring open ε-CL.[4,11,12] On the other hand [$LZn_2(OAc)_2$], with either a large or small excess CHO, showed excellent activity and control for the ROP of ε-CL. *In-situ* ATR-IR spectroscopy suggested that a single cyclohexene oxide monomer reacts with the zinc carboxylate bond, to form a zinc alkoxide species.

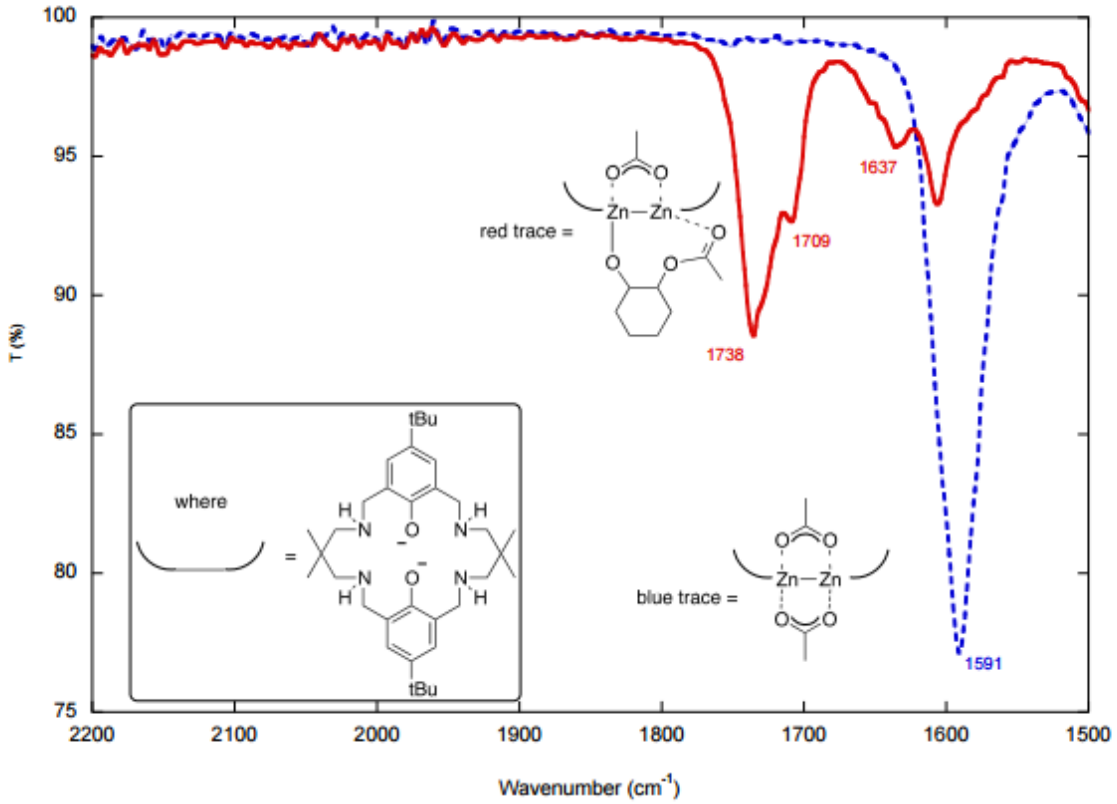

Figure 2.1.3: Plot showing the IR spectra of [$LZn_2(OAc)_2$] (blue dots) and the zinc alkoxide species from the reaction of [$LZn_2(OAc)_2$] and CHO (red line).

Taken from Angew. Chem. Int. Ed., 2014, 53, 1607–1610 [4] with permission.

The formation of the alkoxide was calculated to be the thermodynamically favourable option, when compared to the starting species, $[LZn_2(OAc)_2]$ (Stabilisation = ΔG_{353} = -5.2 kcal·mol^{-1}) , according to DFT calculations.[11] The DFT studies showed that the ROP of ε-CL by the alkoxide species has a moderate activation barrier ($\Delta G^{\ddagger}$ = 30.7 kcal·mol^{-1}), which is in line with the reaction requiring temperatures of 80 °C to proceed. There was no experimental observation of the formation of ether linkages in the PCL (by ^{1}H NMR or IR spectroscopy), indicating that competitive ring opening of CHO does not occur, within detection limits. By DFT, the sequential enchainment of CHO was found to have a very high activation barrier ($\Delta\Delta G_{353}$ = 39.1 kcal·mol^{-1}).There is a significant lag time when $[LZn_2(OAc)_2]$/CHO was used as the catalyst. This is because the rate of initiation (insertion of the 1st ε-CL into the zinc alkoxide bond) is considerably slower than the rate of propagation (insertion of subsequent ε-CL) (Figure 2.1.2). The activation barrier for the initiation step is considerably higher than the activation barrier for the subsequent steps ($\Delta\Delta G^{\ddagger}$ = +33.6 *vs* +25.8 kcal mol^{-1}).[12] This is hypothesised to be due to the alkoxide from the cyclohexene oxide being a secondary alkoxide while the alkoxides from caprolactone insertion are primary alkoxides and less hindered. Detailed kinetic analysis carried out on the $[LZn_2(OAc)_2]$/CHO system by Zhu showed that while the rate of propagation is always faster than the rate of initiation, the rate of initiation is highly dependent on the nature of the zinc alkoxide species formed. When the zinc alkoxide species is primary alkoxide, the rate of initiation is approximately 1.4 times of the rate of initiation from a secondary alkoxide.[11]

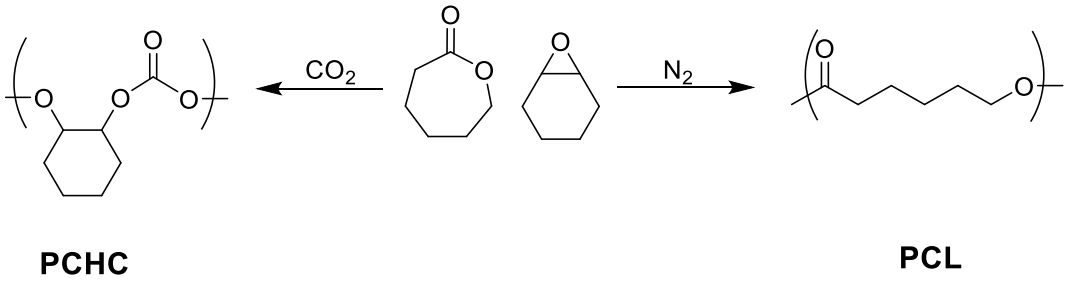

Figure 2.1.4: Scheme showing the orthogonal behaviour of $[LZn_2(OAc)_2]$ when subjected to a mixture of monomers (CHO, ε-CL).

When carbon dioxide is present, only PCHC forms, without carbon dioxide, only PCL forms.

The next experiments revealed interesting selectivity when a mixture of monomers was used. When a mixture of both ε-CL and CHO are polymerised under carbon dioxide, only PCHC forms. This is orthogonal to the result obtained under nitrogen where only PCL forms. Mechanistic studies of the ROCOP of CHO/CO_2 using [$LZn_2(OAc)_2$] showed that polymerisation proceeds *via* the ring opening of CHO followed by the insertion of carbon dioxide. The ring opening of CHO is the rate determining step, so the resting state of the catalytic cycle is the zinc carbonate species.[2,13] Computational investigations showed that once the zinc alkoxide species has been formed, the insertion of carbon dioxide has a low activation barrier and leads to a stable intermediate. This pathway has a much lower activation barrier than the insertion of ε-CL ($\Delta\Delta G^{\ddagger}$ = +11.4 *vs* +33.6 kcal mol^{-1}). There is no evidence (computational or experimental) that the zinc carbonate species can ring open ε-caprolactone. Therefore when both ε-CL and CO_2 are present, it appears that it is considerably more favourable for carbon dioxide to insert into the zinc alkoxide bond compared to the insertion of ε-CL. This leads to the exclusive formation of an alternating polycarbonate as the sole reaction product. The inability of the key intermediate of the ROCOP cycle, the zinc carboxylate species, to insert ε-CL means that no ROP can occur. It is only when CO_2 is removed, that the ROP of ε-CL is catalysed.

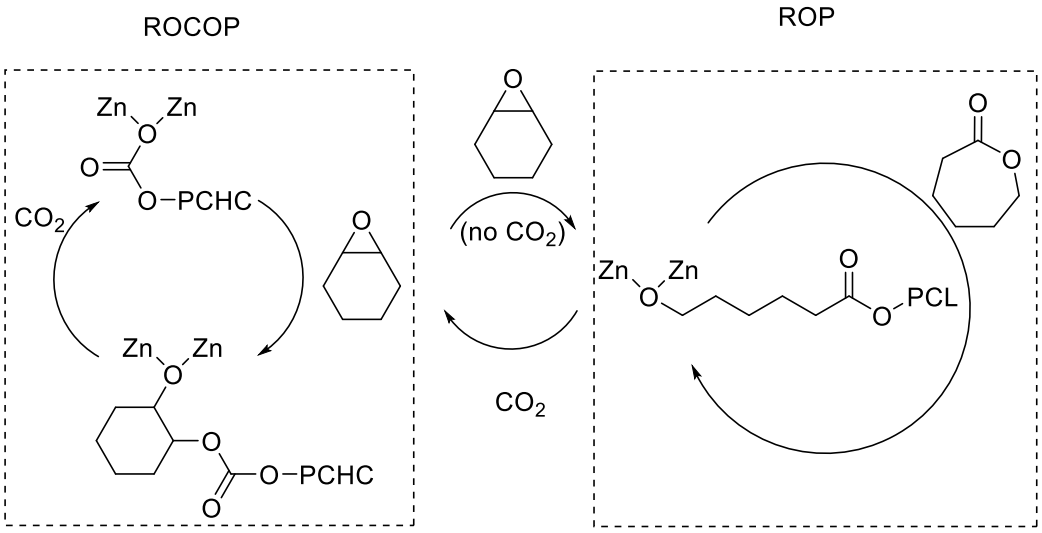

Figure 2.1.5: Diagram showing the mechanisms for ROCOP and ROP and the switch between the two cycles.

In the selective catalysis, carbon dioxide "switches'' the ROP "off'' and the ROCOP process "on''. On the other hand the ROP is switched "on'' by the presence of cyclohexene oxide. As carbon dioxide is a gas, it can easily be removed from or added to the system and the switch reaction can occur near instantaneously. As both the cyclohexene oxide and the carbon dioxide are monomers, their presence does not result in any contamination of the system, making them near ideal switches. The results indicate that the $[LZn_2(X)_2]$ system is an interesting starting point for the development of block copolymers.

2.2 Aims

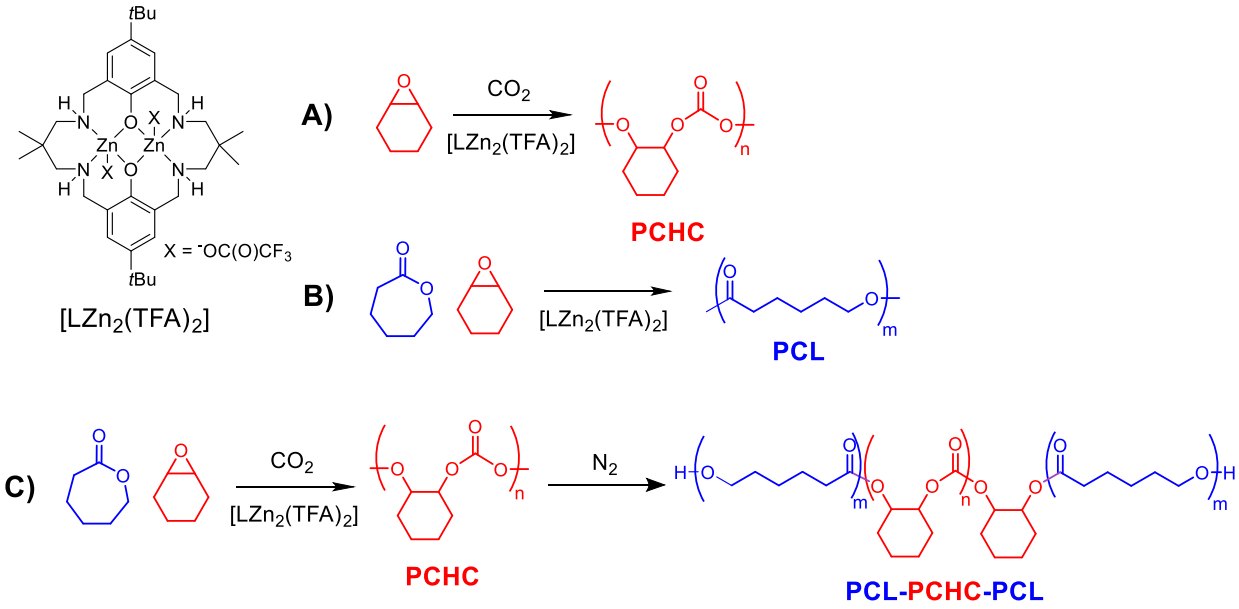

Figure 2.2.1: Scheme showing the objectives of this project.

Poly(ester – carbonates) are an attractive target as they combine the properties of both oxygenated aliphatic polymers and allow a modification of the properties. The aim of this project is to synthesise poly(caprolactone-*b*-cyclohexene carbonate-*b*-caprolactone) in a one pot method. In order to be able to form an ABA triblock in a one pot method the following conditions are required: a catalyst that can control which monomer is being polymerised

from a mixture of the monomers; both polymerisations must occur in a living manner with no (or minimal) termination reactions; the central block should be dihydroxyl terminated in order to ensure all chains are of an ABA structure.

The Aims of this research project can be summarised as:

A) To investigate the ROCOP of CHO/CO_2 catalysed by [$LZn_2(OCOCF_3)_2$]. PCHC, produced in conditions suitable for block formation, should have dihydroxyl end groups. The dihydroxyl end groups are required to ensure both ends of the PCHC chain are equivalent and the polyester will form evenly (*via* chain transfer) from both sides.

B) To determine whether [$LZn_2(OCOCF_3)_2$] can catalyse the ROP of ε-CL. The microstructure of the polyester will be analysed.

C) To determine whether [$LZn_2(OCOCF_3)_2$] displays the same selectivity as [$LZn_2(OAc)_2$] when subjected to a mixture of CHO/ε-CL/CO_2 or if the trifluoroacetate coligand changes the selectivity. Once a system has been developed that allows the selective formation of PCHC followed by the formation of PCL, the structure of the resulting polymer will be investigated (see section 2.3 for details).

D) To analyse the thermal properties of poly(caprolactone-*b*-cyclohexene-*b*-caprolactone), which will be measured across a series of compositions, to understand how the proportions of ester: carbonate affects the polymer. The mechanical properties, including the Young's modulus and elasticity, of the ABA poly(ester-carbonate) will be compared to the properties of the homopolymers.

2.3 Techniques

In the formation of block copolymers, accurate analysis and determination of the structure is vital. In particular, for ABA block copolymers it is very important that the selectivity *vs* AB type copolymers is determined and that endgroup *versus* main chain analysis confirms the

structure. The main methods which are used to identify the structure of the polymers are described in the sections below:

2.3.1 ^{1}H NMR Spectroscopy

NMR spectroscopy of polymeric species is complicated by the fact that the polymer chains have a range of M_n values. This leads to a broadening of resonances. If the chain end groups are hydroxyls, it is often possible to characterise the final repeat unit at the chain end as the protons have a distinct chemical shift or coupling. It may be possible to calculate the molar mass of the polymer from the normalised integrals of the ^{1}H NMR signals of the end groups *versus* the main chain signals.

For some block copolymers the monomer unit at a junction between two distinct blocks will also show a different chemical shift to the main chain units. This results in distinct signals corresponding to these junction units in the NMR spectra. Clearly the signals for the junction units will not be present in an NMR spectrum of the homopolymer and are also likely to be dependent on the nature of the second block. For a typical ABA type block copolymer, there will be junction units corresponding to both the A and B blocks and these are expected to be present in equal proportions (Figure 2.3.2, oval units depict junction units). The end group signals for the central block will not be present for any triblock copolymer, rather these are replaced by the new junction units. However there may be polymers where the resonance for the end group is not clearly distinguishable from the main chain. Another problem that can occur if there is long polymer chain, is that the intensity of the end group signal becomes too low to be detected. These same issues can also complicate analysis of junction units.

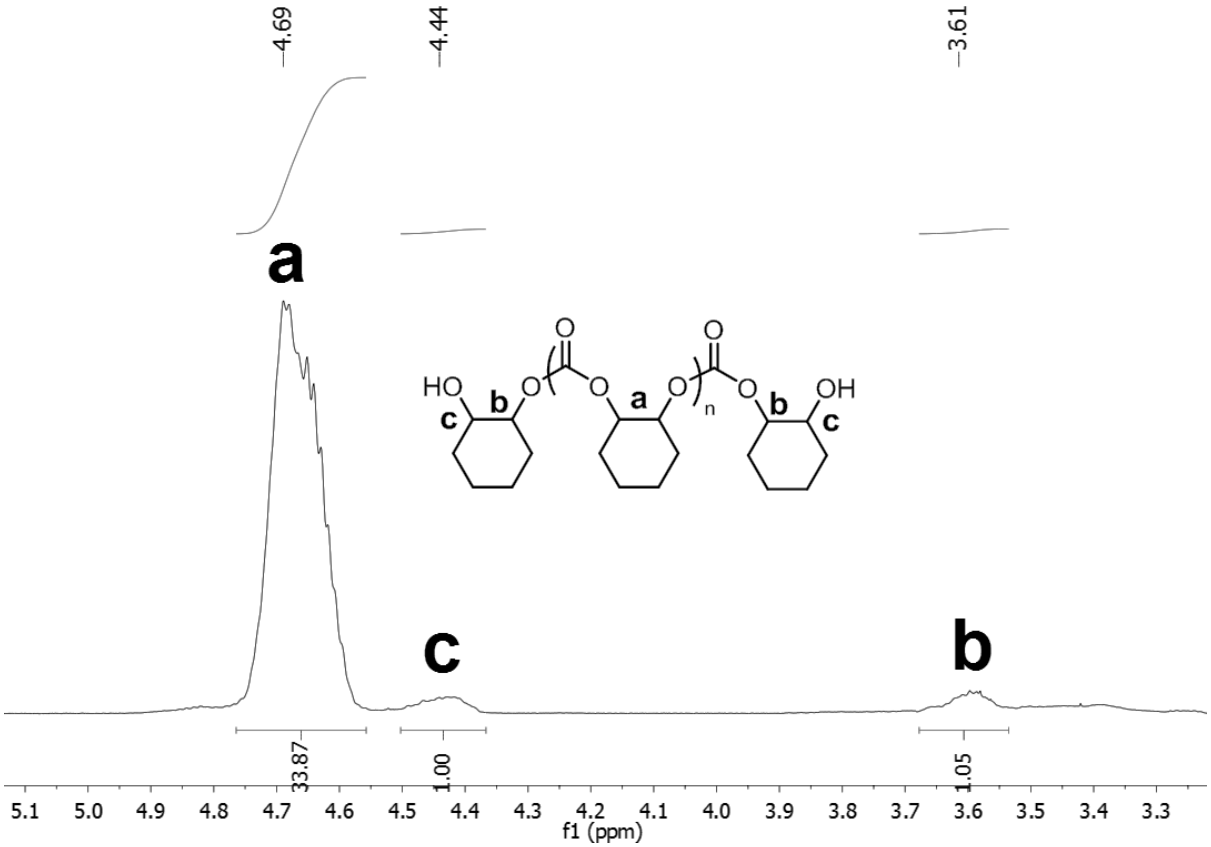

Figure 2.3.1: Excerpt of a ^{1}H NMR spectrum of PCHC.

Showing the main chain methine protons at 4.65 ppm and the end group methine protons at 4.44 ppm and 3.61 ppm. Using this example there are 34 main chain units (integral of a) in each chain, giving a total of 35 repeat units (includes the end group unit). The molar mass for this polymer would be 142 x 35 = 4,900 g mol^{-1}.

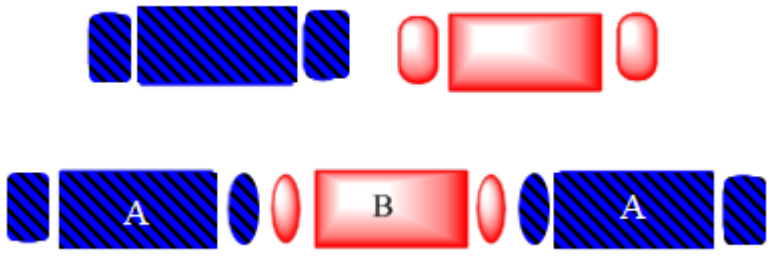

Figure 2.3.2: Scheme showing the end groups of polymers and the presence of junction units in block copolymers.

2.3.2 MALDI-ToF Analysis

Matrix-assisted laser desorption/ionisation time of flight analysis (MALDI-ToF) is a soft ionisation technique for mass spectrometry. It provides a good method of analysing polymers, and typically results in a spectrum whereby each polymer chain of a particular molar mass gives rise to a separate signal. The difference in *m/z* between the signals should be equivalent to the mass of the repeat unit of the polymer. If all the chains have the same structure but differ only in length, a single series is usually observed. If there is a range of different end groups then several series will arise, separated by the same repeat unit but differing in the end group mass. The polymer composition can be proposed by comparison of the theoretical molar masses to the observed *m/z* values. Under the experimental techniques used in this work (Chapter 6), potassium ions are used as the ionising agent. In order to be detected, the polymer chains have to be ionised, so the K^+ ion must be included in the theoretical mass calculation. Polymers which have the potential to form an anionic end group, e.g. $P\text{-}COO_2^-$, then there is the potential for the first potassium ion to form a salt and another potassium ion to act as the ionising agent, resulting in a polymer structure of P^-2K^+ being detected. While MALDI-ToF is a powerful method of determining the composition of a polymer, it is important to emphasise that not all species are ionised or accelerated in the same way. The intensity of a signal correlates with volatile ionisation products and should not be used to quantify concentration of the polymeric species

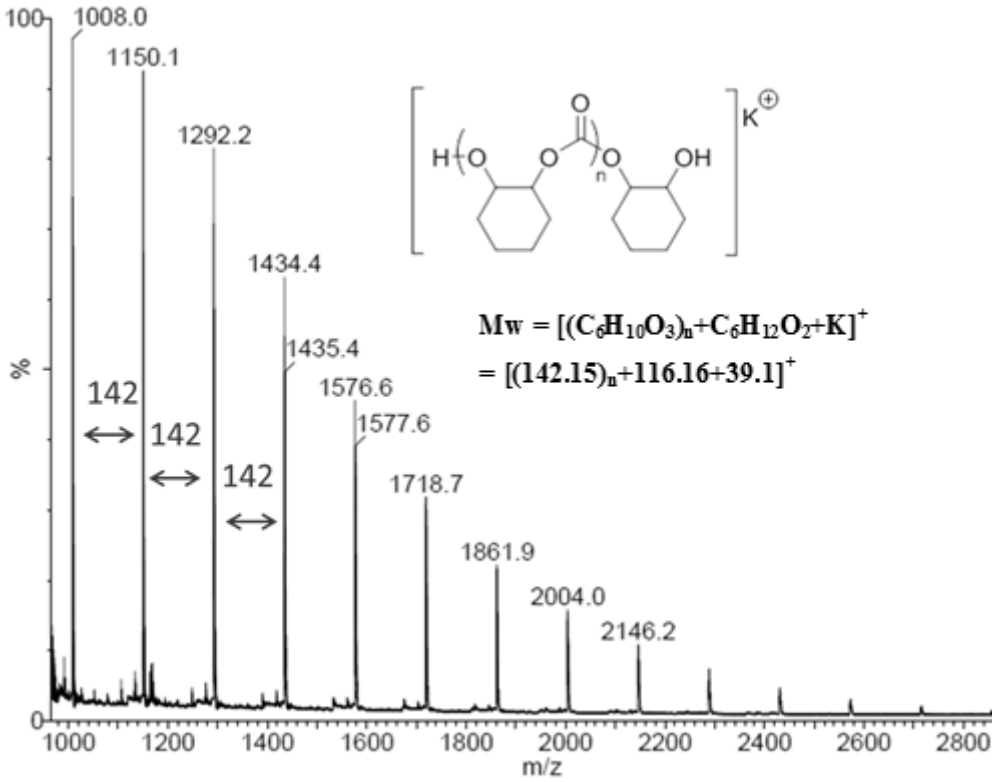

Figure 2.3.3: Example of a MALDI-ToF spectrum of PCHC.

Each signal is separated by 142 m/z, the molar mass of the repeat unit.

2.3.3 ^{31}P NMR Spectroscopy as a Quantitative Technique in End Group Analysis

The fast proton exchange of hydroxyl groups with residual water or other protic sources means that they are not always observed in ^{1}H NMR spectroscopy. Therefore in order to determine the presence of hydroxyl groups an alternative technique is required. Spyros *et al* showed that the reaction between hydroxyl groups and 2-chloro-4,4,5,5-tetra-methyldioxaphospholane results in phosphinic esters, whose chemical shift in the ^{31}P NMR spectrum is very responsive to the type of hydroxyl group.[14] The difference between a primary and secondary hydroxide was shown to be up to 5ppm, with primary hydroxides giving higher chemical shifts.

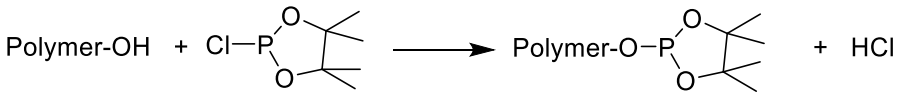

Figure 2.3.4: The reaction between hydroxyl endgroups and the diaoxaphospholane species.

The phosphinic ester produced is the species being detected in the ^{31}P endgroup analysis.

This method can be used to characterise polymeric species featuring hydroxyl end groups. Hydroxyl terminated polymers can be reacted with a dioxaphospholane, in the presence of a standard (Bis-phenol A, BPA). The ^{31}P spectrum of the products allows the primary and secondary hydroxyl groups to be distinguished as they appear in different regions of the NMR spectrum (Figure 2.3.4). Typically hydroxyl groups result in a ^{31}P signal in the region 146-148 ppm, with the primary hydroxyls appearing downfield (146.4-147.8 ppm for primary hydroxyls compared to 146.1-146.2 for secondaryhydroxyls). Carboxylic acid end groups also result in a ^{31}P signal, between 135.5-135.7 ppm. There is significantly less variation in the chemical shift regardless of the structure of the carboxylic end group.

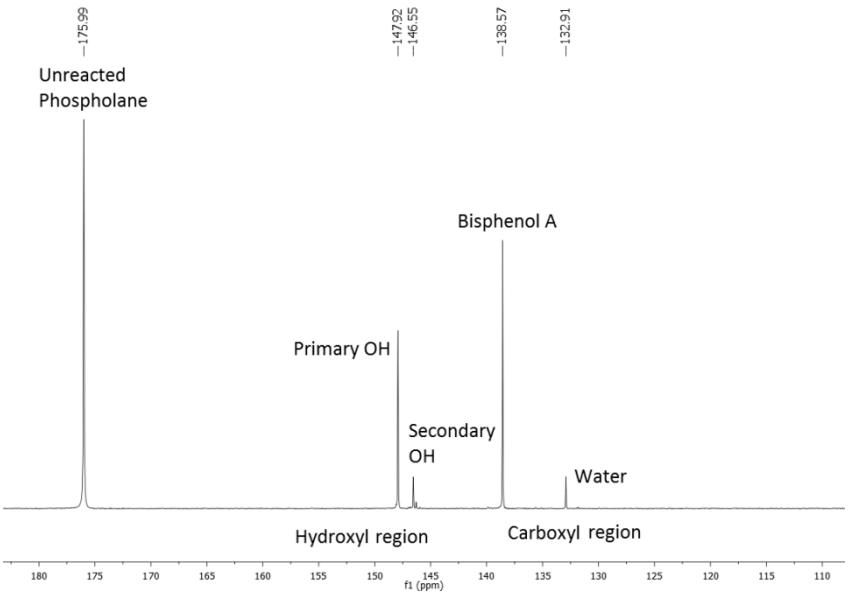

Figure 2.3.5: Example ^{31}P spectrum used for end group analysis.

The standard Bisphenol A occurs at 138.57 ppm. Unreacted phospholane occurs at 175.99 ppm. The carboxyl region is between 135.5-135.7 ppm. The hydroxyl region is between 146.1-147.8 ppm.

The test is carried out in the presence of a significant amount of pyridine, which scavenges any acidic protons produced and solubilises the BPA standard. The basic nature of the test means that appreciable amounts of polycarbonate degradation can occur over the timescale of the reaction, making it unsuitable for the analysis of polycarbonate end groups.

2.3.4 Size Exclusion Chromatography

Size Exclusion Chromatography (SEC) is used to determine the number averaged molecular weight (M_n) and dispersity (Đ) of a sample. In this work the IUPAC definition 'molar mass' is used when referring to M_n. The analysis separates species according to their hydrodynamic volume. This is achieved by allowing the sample to pass through a column containing a porous phase. The smaller species can enter the pores and therefore have to travel across a greater volume (of the column). The larger species can not enter the pores and so have less volume to travel across and are released earlier.

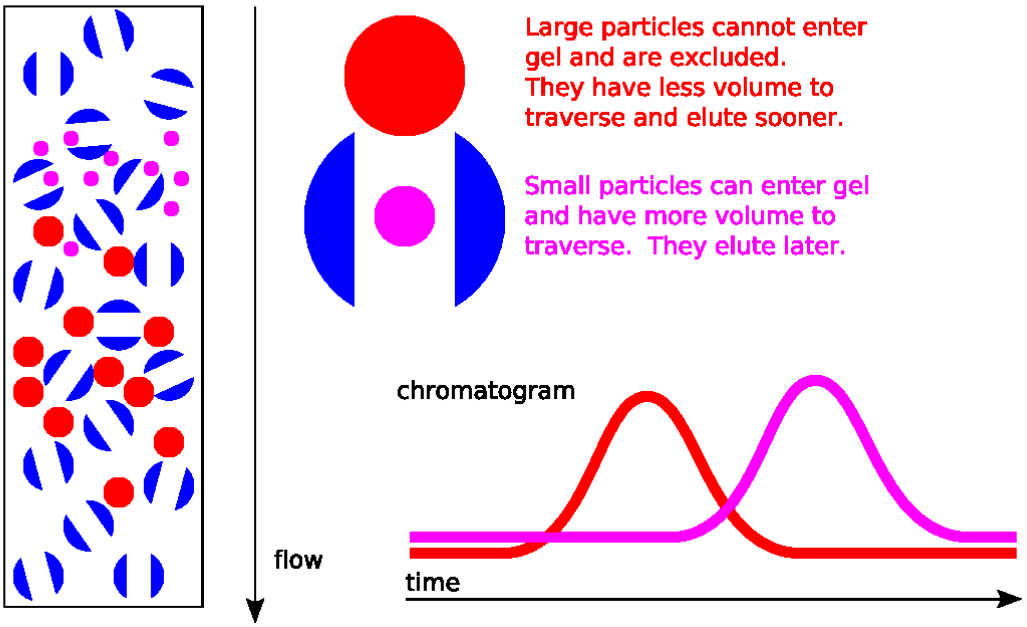

Figure 2.3.6: Scheme showing the mechanism of size exclusion chromatography.

The time taken for the sample to be eluted is therefore related to its hydrodynamic radius and can be correlated to the molar mass *via* the use of standards to calibrate the instrument. This correlation presumes that all the polymer chains are spherical in solution. Throughout this work, narrow polystyrene standards have been used to calibrate the SEC instrument therefore, the assumption is that all polymers interact with the solvent (THF) and coil in the same manner as polystyrene. SEC actually measures the hydrodynamic volume of a species, so it is dependent on the structure of the polymer. Polystyrene (PS) is a rigid plastic, and polymers which coil more or less tightly will elute through the column at the different rates. For well-known polymers, correction factors can be applied to the molar masses calculated from the PS standards.

$$M_{n\,(corrected)} = X \cdot M_{n\,(SEC)}$$

The correction factor is calculated using the Mark Houwink equation above. The Mark Houwink equation relates the intrinisic viscosity (η) and molecular weight (M) of a polymer.

$$[\eta] = KM^{\alpha}$$

The Mark-Houwink parameters α and K depend on the polymer-solvent system. K and α can be determined by monitoring molar mass and viscosity of series of monodisperse samples and fitting to the following equation. The absolute molar mass can be measured using light scattering or osmotic pressure.[15]

$$\log \eta = \log K + \alpha \log M$$

If the Mark-Houwink parameters are known for one polymer system, the following equation can be used in order to determine the molecular weight of a second polymer. The Mark Houwink parameters for polystyrenene in THF(25 °C) are K = 0.706, α = 0.000160

$$K_1 M_1^{1+\alpha_1} = K_2 M_2^{1+\alpha_1}$$

As every polymeric sample contains chains of different lengths, SEC analysis gives a distribution of lengths. In circumstances, where chains have closely related lengths the trace would be a Gaussian distribution with a narrow width. An SEC trace that is broad or lopsided indicates that not all of the chains have grown at the same rate, and therefore are different lengths. This is most often due to the presence of different chain structures. Using the catalyst [$LZn_2(OAc)_2$] for the ROCOP of CHO/CO_2, results in both dihydroxyl terminated and acetate terminated polymer species. The presence of both species can be observed in the SEC traces as a bimodal molar mass distribution.

SEC analysis is the most common method of confirming that block copolymers have formed. SEC traces of the final copolymer should be shifted to a higher molar mass than that of the

central block and still be of a narrow dispersity. This indicates that all of the central blocks have been converted to copolymer, rather than a second polymer species forming as mixture.

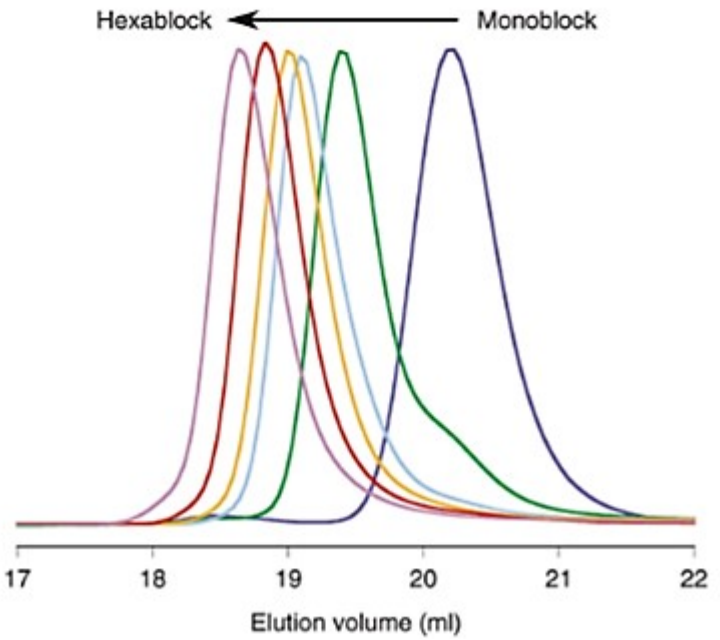

Figure 2.3.7: SEC traces from the formation of a hexablock copolymer by Coates and co-workers.[16]

With the formation of each block, there is a clear shift of the SEC trace to a higher molar mass, with the trace remaining monomodal and narrow. Picture reproduced with permission from Macromolecules, 2011, **44**, 1110-1113 [16]

2.3.5 *In-Situ* ATR-IR Spectroscopy

In-situ ATR-IR spectroscopy allows the change in components of a reaction to be monitored in real time. An ATR-IR probe is situated inside the reaction mixture and spectra recorded at regular intervals. By monitoring the changes in intensity of specific signals in the IR spectra over time, the change in concentration of the species present can be observed. In this work it is very useful to observe whether or not the two polymerisations are occurring simultaneously or in sequence. The silver halide probe records absorptions between 2500 - 650 cm^{-1} but is only accurate between 1900-650 cm^{-1} due to the materials optical bandgap. The probe records

the change in all wavelengths at set time intervals (down to 15 seconds) (top right of Figure 2.3.8). By selecting specific time points, the change in the overall spectrum can be observed (bottom of Figure 2.3.8). The intensity of specific wavenumbers (or bands) can be chosen and plotted against time (Top left Figure 2.3.8). Characteristic wavelengths are assigned to the species under consideration (monomers or polymers) from control experiments whereby pure reagent is analysed. Typical wavelengths for polymers and monomers are described in appendix B. As the polymeric species are structurally very similar to the monomers, the wavelengths being monitored often correspond to small changes in the fingerprint region or the formation of shoulders on peaks. This means the precise wavelength being followed is very dependent on the conditions of the reaction.

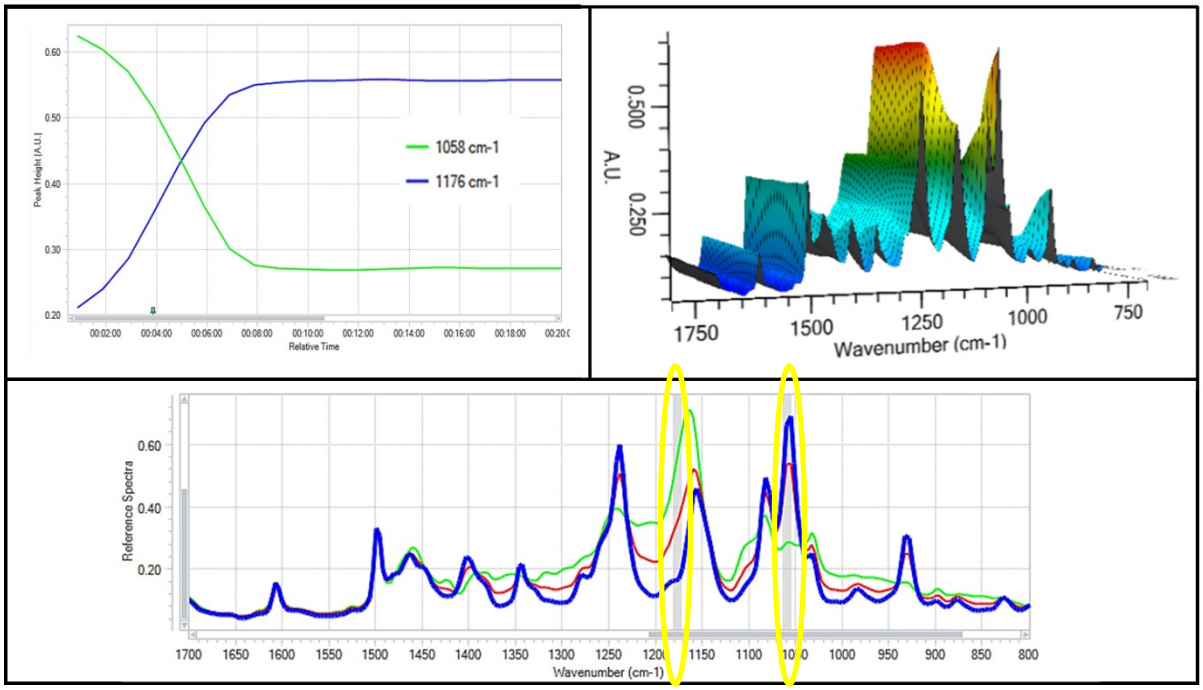

Figure 2.3.8: Plots recorded by the *in-situ* ATR-IR Probe.

Top Left: A plot of the absorbance of specific wavenumbers *versus* time. The wavenumbers selected are highlighted in the bottom spectra Top Right: A spectrum showing the change in absorption of all wavenumbers against time. Bottom: Spectra from specific time points are plotted.

The absorption can be easily converted to the concentration, using Beers law:

$$A = \varepsilon\, l\, C$$

[A = absorption ε = molar extinction co-efficient ($Lmol^{-1}cm^{-1}$) l = path length (cm) C = concentration ($mol\ L^{-1}$)]

The conversion at specific time points can be determined using ^1H NMR spectroscopy of aliquots and the following relation used.

$$Conversion = \frac{I - I_0}{I_{max}} \times conversion\ at\ I_{max}$$

[I = Intensity, I_0 = Intensity at time 0, I_{max} = Intensity at final conversion]

Using both IR and NMR spectroscopy allows plots of conversion against time to be plotted. The rate of the reaction can be determined from the absorption. For a first order reaction rate dependence on the monomer concentration should fit the following equations

$$\ln\,[A] = -kt + \ln[A_0]$$

$$\ln\frac{[A]}{[A_0]} = -kt$$

$$\ln\frac{[A_0]}{[A]} = kt$$

[[A] = absorption k = rate constant t = time]

A plot of $\ln\frac{[A_0]}{[A]}$ *versus* time should result in a straight line, where the gradient is equal to k. Both ROP and ROCOP processes are well known to often be first order in monomer.[2,4] Detailed kinetic studies have shown that when $[LZn_2(OAc)_2]$ is used for CHO/CO_2 ROCOP, the reaction is first order in [CHO].[2]

Carbon dioxide absorbs at 2340 cm^{-1} and although this peak can be detected, its intensity can not be used to determine concentration because it is partially obscured by the AgX

absorbance. However monitoring the presence or absence of the peak can be used to confirm the presence or absence of carbon dioxide in the solution (Figure 2.3.9).

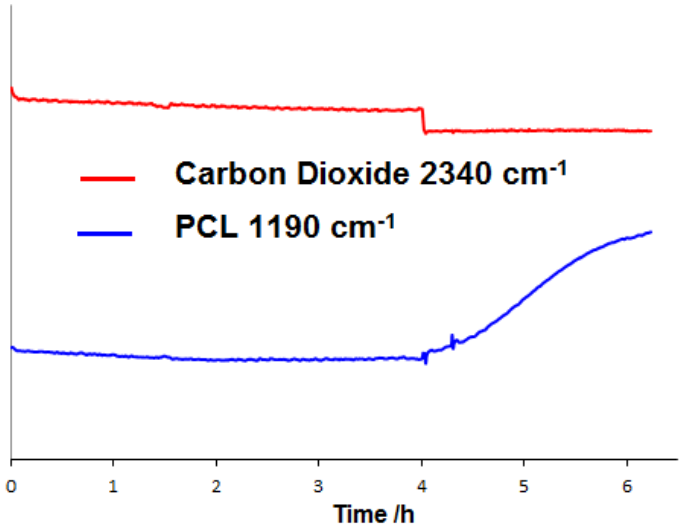

Figure 2.3.9: A plot of absorption *versus* time from the formation of an ABA block copolymer.

The absorption of carbon dioxide is shown and a drop in the absorption can be observed when the vacuum/nitrogen cycles are applied**.**

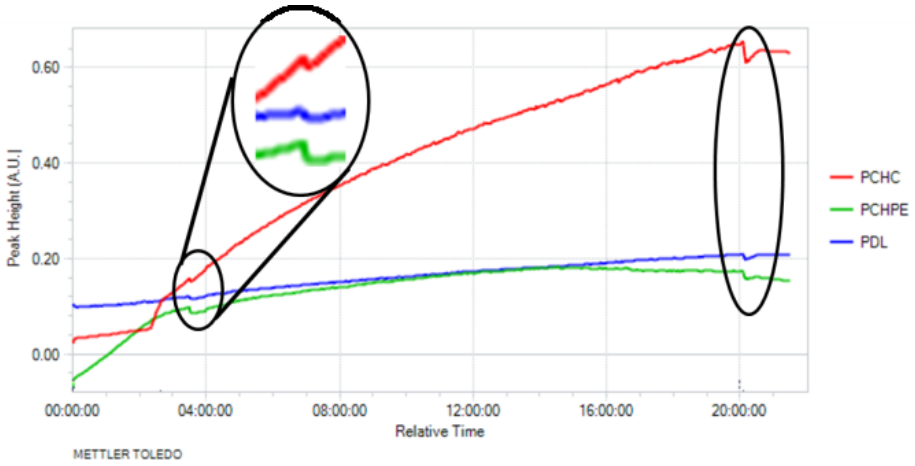

Figure 2.3.10: A plot absorption *versus* time for the formation of a copolymer.

There are two occasions when some variances in the absorptions are observed. At 4 h, an aliquot was taken, resulting in a small change to overall concentration. At 20 h, the vacuum/nitrogen cycle was applied and a decrease in the absorbance is observed due to a small decrease in monomer and solvent.

It is worth observing also that sometimes when aliquots are withdrawn (> 0.1 mL) from an overall volume of 2 mL, a small decrease in intensity of all resonances can be observed (Figure 2.3.10). This can be overcome by limiting aliquot volume to <0.1 mL. Additionally, cycles of vacuum/nitrogen can also disturb the baseline, this is overcome by limiting the evacuation time to 3s.

2.3.6 ^{1}H DOSY NMR Spectroscopy

Diffusion ordered spectroscopy (DOSY) differentiates the NMR signals according to the diffusion co-efficients of the species. DOSY provides a measure of the translational motion of molecular species in solution. Spin-echo spectra, with different pulsed field gradient strengths are collected and the signal decays measured. The spin-echo intensity of a spin active nucleus, (I) is related to the diffusion coefficient (D) of the molecule by the following equation:

$$\ln\left(\frac{I}{I_0}\right) = -\gamma^2\delta^2G^2\left(\Delta - \frac{\delta}{3}\right)D$$

[γ is the gyromagnetic ratio, δ is the length of the gradient pulse, G is the gradient strength, and Δ is the delay between gradient midpoints, D is diffusion coefficient, I is spin echo intentsity]

From the diffusion co-efficient of a species, its hydrodynamic radius (R_H) can be calculated using Stokes Law.

$$R_H = \frac{k_BT}{6\pi\eta D}$$

[k_B is the Boltzmann constant, T is the temperature, and η is the solvent viscosity at the measured temperature, D is the diffusion coefficient, R_H is the hydrodynamic radius]

In small molecule chemistry ^{1}H DOSY is regularly used to determine nuclearity and to study aggregation phenomena. If standard compounds are used, of known nuclearity, a calibration

can be used to estimate molar mass. In concept this is similar to how SEC correlates the hydrodynamic radius of the species to its molar mass and therefore suffers from the same limitations. In polymer chemistry there are several examples of DOSY spectroscopy being used to determine the molar mass or the number of species present.[17-19] The hydrodynamic radius of a block copolymer differs from that of the parent polymers, due to its increased molar mass and because of the interactions between the blocks. Therefore the ^{1}H DOSY NMR spectrum can be used to characterise block copolymers and in particular should show a single diffusion coefficient which correlates with all the ^{1}H NMR signals of the block components. If there are any contaminating homopolymers, these show as signals with different diffusion rates and correlate with specific ^{1}H NMR signals (Figure 2.3.11).

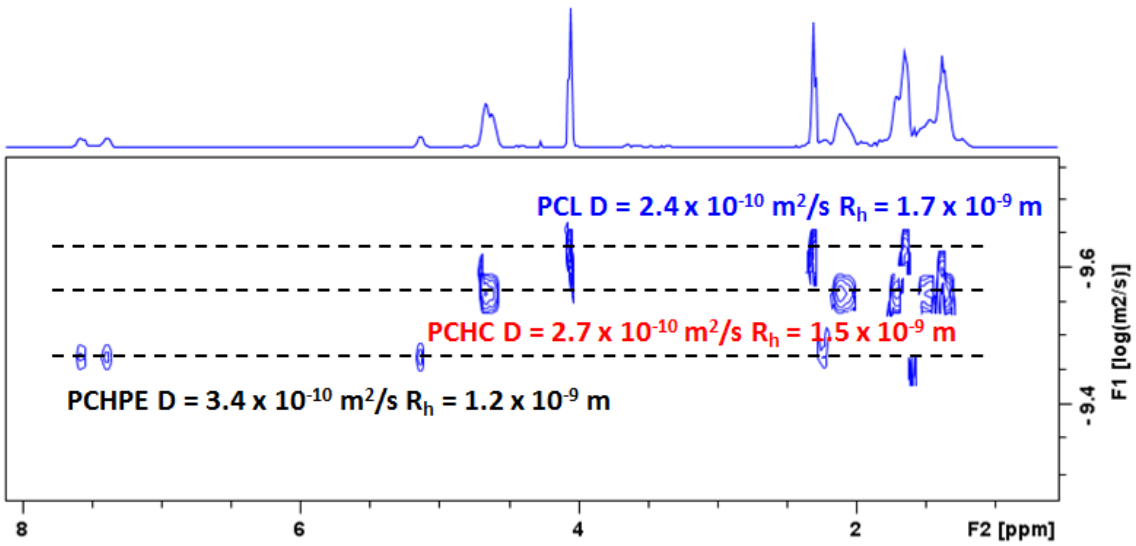

Figure 2.3.11: A ^{1}H DOSY plot of a mixture of polymers.

Each polymer displays an individual diffusion coefficient due to their different hydrodynamic radii.

In this thesis DOSY experiments and the data processing to give two-dimensional plots were carried out by Mr P. Haycock, Imperial College London, further details are provided in the experimental section.

2.3.7 Differential Scanning Calorimetry

Differential Scanning Calorimetry (DSC) compares the heat required to increase the temperature of a sample against a reference material. It is used to study thermal transitions of polymers. Typically the sample and reference are maintained at the same temperature, and the temperature is increased in a linear fashion. The amount of energy required to maintain the zero temperature difference is measured. When the polymer sample undergoes a thermal transition, more or less energy will be required to maintain the zero temperature difference depending on the type of transition. Melting is an endothermic process and therefore requires an increase in the amount of energy provided. Crystallisation is an exothermic process and requires the provision of less energy. The output of a typical DSC experiment is a plot of heat flow *versus* temperature. The enthalpies associated with the transitions can be calculated by integration of a given transition.

$$\Delta H = KA$$

[ΔH is the enthalpy of transition, K is the calorimetric constant and A is the transition area.]

For the semi-crystalline and amorphous polymers studied in this thesis, the main transitions determined by DSC for a polymeric sample are glass transition temperatures (T_g) and melting temperatures (T_m). Amorphous polymers or the amorphous regions of a semi crystalline polymers transition from a glassy state, where the material is hard and often brittle, to a rubbery state as the temperature is increased. The transition temperature is the glass transition temperature (T_g). It is typically indicated by a step change in the baseline of the DSC curve. Above the glass transition temperature, chains have sufficient energy to rearrange, resulting in rubber like properties. The glass transition temperature is dependent on the ease of mobility of the chains and it is influenced by backbone, side chain and endgroup chemistry. The T_g therefore provides some insight into the rigidity of the polymer. Polymers which have a high T_g are usually rigid, structural plastics and polymers with a T_g below room temperature are elastomers. For plastic applications, the polymer T_g should be above the normal range of

temperatures experienced by the product. However the T_g should fall within a reachable range of temperatures as polymers are often processed above the T_g.

Crystalline polymers, e.g. polypropylene, do not possess a glass transition, but instead exhibit melting temperatures (T_m) and crystallisation temperatures (T_c). Semicrystalline polymers contain both amorphous and crystalline regions. In such cases, it is possible to calculate the percentage of crystallinity, using the enthalpy of crystallisation.[20]

$$\chi_c = \frac{\Delta H_c}{\Delta H_{c\,100\%}}\ 100\%$$

[χc = Degree of crystallisation ΔH_c = Enthalpy of crystallisation $\Delta H_{c\ 100\%}$ = Enthalpy of crystallisation of the fully crystalline polymer]

The thermal properties of a copolymer give an indication of its structure. For example, if the blocks are immiscible then two distinct T_g values are anticipated and these should be observed in similar regions to the T_g values of the homopolymers. When the blocks are fully miscible a single T_g is expected. For a random copolymer, a single T_g is expected regardless of whether the individual polymers are miscible. For miscible polymers the Fox-Flory equation can be used to predict the T_g value.

$$\frac{1}{T_g} = \frac{w_1}{T_{g,1}} + \frac{w_2}{T_{g,2}}$$

[w_1 = weight fraction of 1st homopolymer; $T_{g,1}$ = glass transition temperature of 1st homopolymer at infinite chain length; w_2 = weight fraction of 2nd homopolymer; $T_{g,2}$ = glass transition temperature of 2nd homopolymer at infinite chain length; T_g = glass transition temperature of the copolymer]

The Fox-Flory equation is only reliably applied if the two polymers are fully miscible. If the block copolymer shows a single T_g that is in poor agreement with the Fox-Flory result, this

suggests the blocks are only partially miscible. In these cases the T_g is usually very sensitive to the composition of the polymer.

2.4 Ring Opening Copolymerisation of CHO and CO_2

2.4.1. Ring Opening Copolymerisation

The catalyst [$LZn_2(OAc)_2$] showed the first example of chemoselectivity between the zinc alkoxide and carbonate chain ends.[4] It has already been well studied for the ROCOP of CHO and CO_2.[1,2,21] It was highly selective towards the formation of polycarbonate (>99 %), and highly active (TOF = 140 h^{-1})[1]. The polycarbonate was a mixture of hydroxyl terminated chains and acetate terminated chains and both structures are observed by MALDI-ToF spectroscopy. The SEC trace was bimodal in line with the two polymer series. The formation of the acetate end capped polycarbonate series makes [$LZn_2(OAc)_2$] an unsuitable catalyst for the formation of ABA triblock copolymers, as a mixture of AB and ABA block copolymers would result.

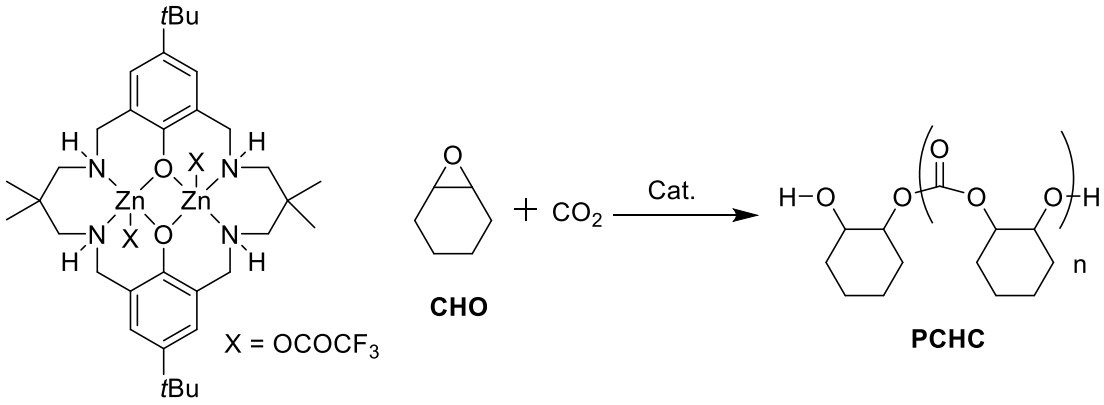

Figure 2.4.1: Scheme showing the structure of [$LZn_2(OCOCF_3)_2$] and the ROCOP of CHO/CO_2.

The Williams group have previously published an alternative catalyst [$LZn_2(OCOCF_3)_2$] which is known to only produce dihydroxyl terminated PCHC.[22] The selectivity was attributed to the trifluoroacetate group being more easily hydrolysed than the acetate group (See 1.2.1 and 1.4.3.1). [$LZn_2(OCOCF_3)_2$] was synthesised according to literature procedures[22] (See Chapter 6), and was utilised for the ring opening copolymerisation of CHO and CO_2 under various conditions.

Table 2.1: Shows the data obtained for poly(cyclohexene carbonate) (PCHC) produced by the ring opening copolymerization (ROCOP) of cyclohexene oxide (CHO) and CO_2.

Run #	Catalyst:CHO (eq)	ε-CL (eq)	Toluene	[Cat] / mM	% conversion of CHO [a]	TON [b]	TOF / h^{-1} [c]	M_n / g mol^{-1} (Đ) [d]
1	1:1000	-	N	10	59	590	33	4830 (1.20)
2	1:500	-	Y	10	44	220	12	2910 (1.20)
3	1:500	400	Y	8	16	80	5	1670 (1.20)

Ring opening copolymerization runs were carried out at 80 °C, under 1 atm of CO_2 for 18 h, with 1.1 mL of toluene added to runs 2-3. a) determined by ^{1}H NMR spectroscopy by comparing the normalised integrals for the CH signals at 3.05 ppm (CHO) and at 4.58 ppm (PCHC) b) TON = mol of epoxide consumed/mol of catalyst. c) TOF = TON/h. d) determined by SEC, in THF, using narrow molar mass polystyrene standards to calibrate the instrument.

[$LZn_2(OCOCF_3)_2$] was able to catalyse the ROCOP of CHO and CO_2, using either neat CHO or toluene as the solvent. The TOF was reduced when toluene was used as the solvent, due to the reduction in CHO concentration, which given that the ROCOP of CHO/CO_2 is first order in epoxide concentration, is unsurprising.[13] Under both conditions, the polycarbonate produced has a high selectivity for carbonate linkages (>99 %), as evidenced by the lack of

ether signals at 3.54 ppm in the ^{1}H NMR spectrum (Figure 2.4.3). [$LZn_2(OCOCF_3)_2$] was also highly selective towards polymer formation, with less than 5 % cyclic carbonate formation when using CHO as the solvent (less than 10 % when using toluene as the solvent). The molar masses of the polymers were controllable and had a narrow dispersity. The molar mass of the polymer increased linearly as the conversion of CHO increased (Figure 2.4.2).

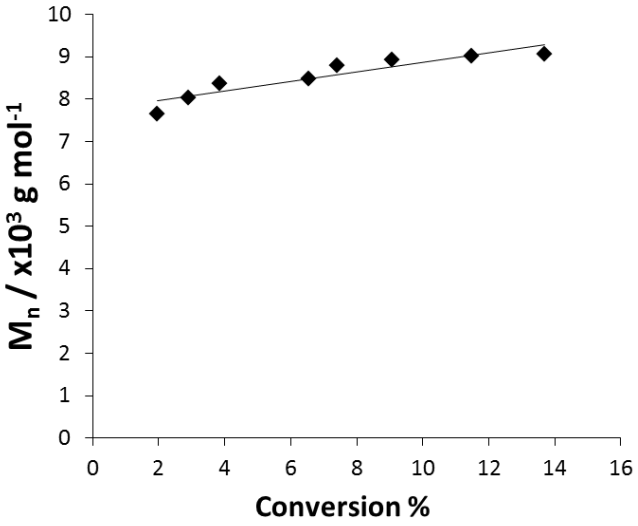

Figure 2.4.2: Plot showing the relationship between conversion and molar mass.

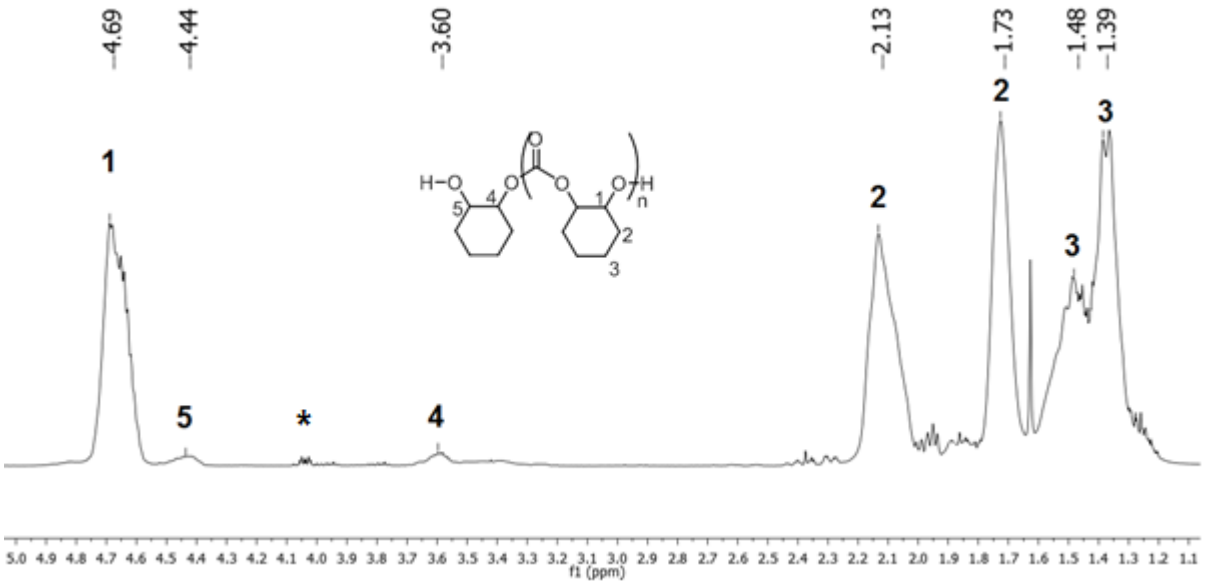

Figure 2.4.3: ^{1}H NMR ($CDCl_3$) spectrum of PCHC synthesised according to Table 2.1, Run 1.

The signals are assigned according to the diagram. The peaks at 4.44 ppm and 3.60 ppm correspond to the methine protons of the end groups. There is a lack of signal at 3.45-3.55 ppm, indicating no ether linkages have formed. *cyclic carbonate.

The low molar masses of the polymers was due to inherent chain transfer reactions, caused by 1,2 cyclohexene diol (CHD) which was proposed to form from the reaction of CHO and water (discussed in section 1.2).[22] The water was likely to be introduced by the carbon dioxide which is applied as a dynamic gas to the system. The PCHC was analysed by MALDI-TOF mass spectrometry which revealed that only dihydroxyl terminated polymers were produced (Figure 2.4.3). The formation of α,ω-dihydroxyl terminated polymers was also suggested by ^{19}F NMR spectroscopy, which showed that no resonances corresponding to trifluoracetate groups were present in the spectrum of the polymer.

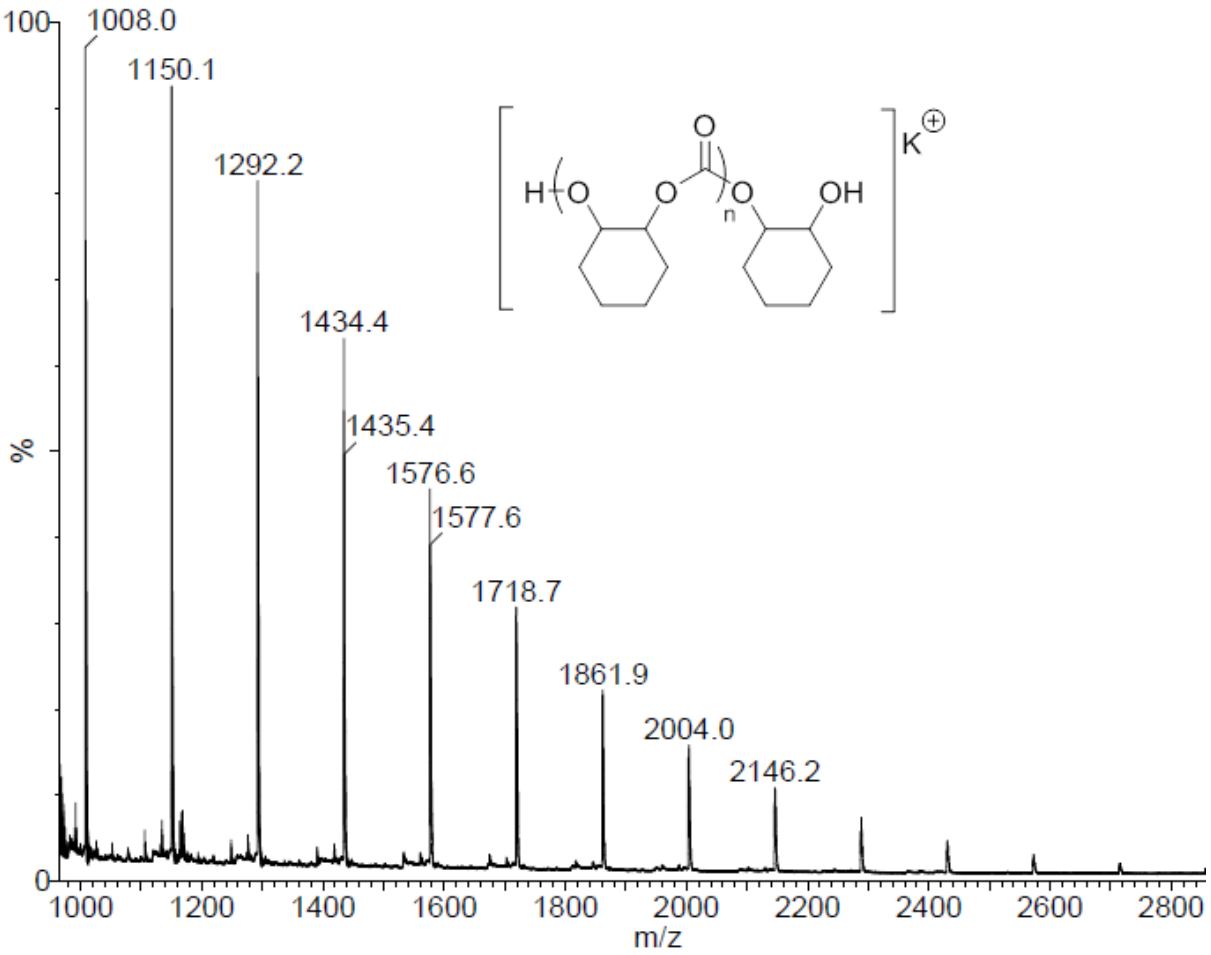

Figure 2.4.4: MALDI-ToF spectrum of PCHC synthesised according to Table 2.1 Run 1.

Series calculated for $[(C_7H_{10}O_3)_n+C_6H_{12}O_2+K]^+ = [(142.15)_n+116.16+39.1]^+$.

It has been hypothesised that the trifluoroacetate group is more readily hydrolysable than the corresponding acetate group.[22] Therefore, the trifluoroacetate group might be cleaved from the polymer chain or replaced by an alcohol (CHD) at the catalyst centre.[22,23] Such processes are proposed to occur during the reaction, rather than during the work-up (precipitation from THF by MeOH). MALDI-ToF analysis of aliquots taken at the beginning of the polymerisation showed that at 2 hours there were still trifluoracetate terminated chains present, but by 6 hours all the chains were dihydroxyl terminated (Figure 2.4.4).

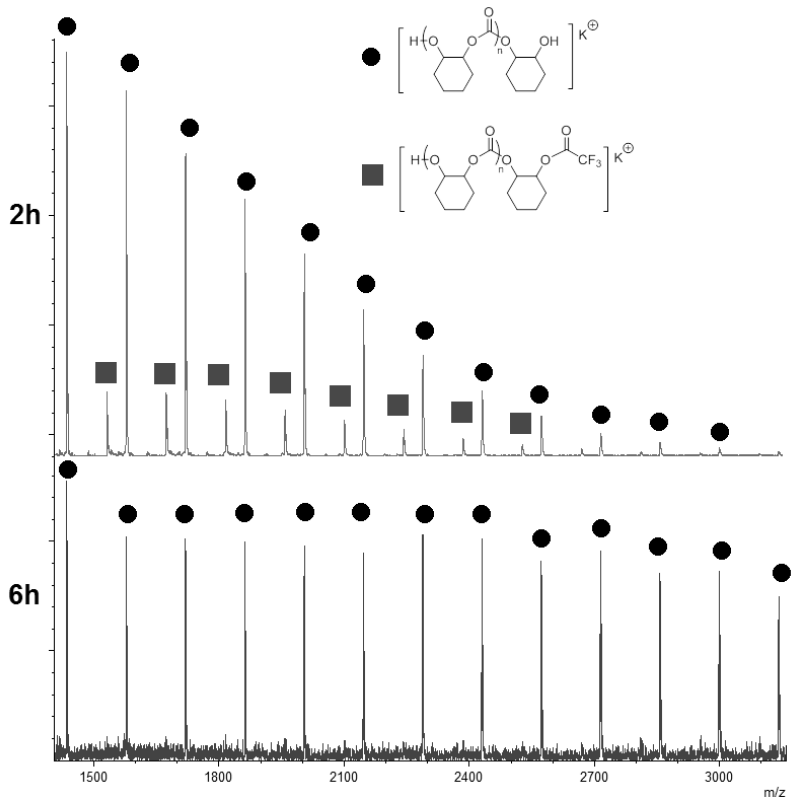

Figure 2.4.5: MALDI-ToF spectra taken from aliquots during the ROCOP CHO/CO_2. The top spectrum was taken at 2 h, and shows two series, The bottom spectrum was taken at 6 hours and only showed a single series. The dots represent the dihydroxyl terminated series $[(C_6H_{10}O_3)_n+C_6H_{12}O_2+K]^+=[(142.15)_n+116.16+39.1]^+$. The squares represent the acetate terminated series $[(C_6H_{10}O_3)_n+C_8H_{14}O_3+K]^+ = [(142.15)_n+158.09+39.1]^+$.

2.4.2 Chain Transfer Agents

The polymerisation wsa also performed in the presence of alcohols, such as methoxy ethylene glycol (MEG), which resulted in the formation of end capped polymers. These polymers could be useful as macro initiators as the presence of a single functional end group could be exploited to select for AB block copolymers. Polymerisations were conducted using 32 equivalents of MEG, without any loss of catalyst activity or selectivity. As more MEG was added, the molar mass of the polycarbonate produced decreased in line with the immortal polymerisation theory. The result was that an increased number of chains were formed as more chain transfer agent was added. The molar mass of the polymer, formed in the presence

of 32 equivalents of MEG, was low (M_n = 590 g mol^{-1}). It is notable that such a low molar mass is ideal for polyurethane production, in particular for rigid foam production.

Table 2.2: The data obtained for poly(cyclohexene carbonate) (PCHC) produced by the ring opening copolymerization (ROCOP) of cyclohexene oxide (CHO) and CO_2 in the presence of methoxy ethylene glycol.

#	LZn_2TFA_2:CHO:MEG	Conversion %	M_n / gmol^{-1} (Đ)	% of Endcapped polymers
1	1:500:0	56	3703 (1.16)	0
2	1:500:16	57	994 (1.10)	71
3	1:500:32	56	590 (1.06)	92

ROCOP carried out at 80°C for 24h. Determined by ^{1}H NMR analysis by comparing the normalised integrals for the CH signals at 3.05 ppm (CHO) 4.58 ppm (PCHC) d) determined by SEC in THF using narrow molar mass polystyrene standards to calibrate the instrument. e) Determined by ^{1}H NMR analysis; described below.

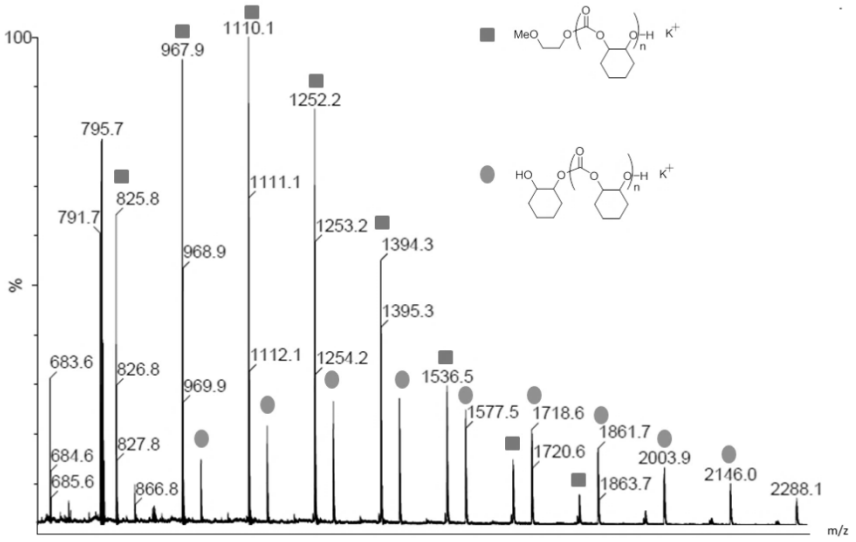

Figure 2.4.6: MALDI-ToF spectrum of PCHC synthesised in the presence of MEG (Table 2.2, Run 2).

Squares mark the series calculated for $[(C_7H_{10}O_3)_n+C_3H_8O_2+K]^+ = [(142.06)_n+76.05+39.1]^+$. Circles mark the series calculated for $[(C_7H_{10}O_3)_n+C_6H_{12}O_2+K]^+ = [(142.06)_n+116.16+39.1]^+$.

However, despite the addition of a large quantity of chain transfer agent, the MALDI-ToF analysis showed that there were still two series of chains (Figure 2.4.5). There were a series which has a methoxy ethanol unit end group, and there was also a dihydroxyl terminated series. The methoxy ethanol end group was clearly observed by ^{1}H NMR spectroscopy (4.26 and 3.37 ppm) and it was quantified by integration. The ^{1}H NMR spectrum showed there were 4 signals corresponding to the end groups. The methoxy ethanol end capped chains showed resonances at 3.37 (A - CH_3), 3.60 (B - CH_2) and 4.26 (C - CH_2) ppm. The methine protons from the cyclohexene unit with the terminal hydroxyl groups were also distinct with resonances at 4.40 (D) and 3.56 (E) ppm (Figure 2.4.6). The methoxy ethanol end capped species (I) contains only one of the cyclohexene units, whereas the dihydroxyl terminated species (II) contains two such units, one at each end of the polymer. A ^{1}H NMR spectrum containing only species I would show signals D:C:A in the ratio 1:2:3. The signals for B and E overlap, but together the integral should be three protons. However if species II is present the signals for D and E show higher intensities, as each polymer chain contributes an additional two protons to each signal. For a 50:50 mixture of I:II, the expected ratio of signals D:C:A, would be 3:2:3. By calculating the increase in intensity of signal D the percentage of species I and II can be calculated. In order to carry out the analysis, the integrals were normalised against signal A (integral = 3H). The integral of D can then be used to determine the composition of the mixture:

$$\text{Percentage of species I} = (1/(1 + (\int D - 1)/2)) \times 100$$

$$\int D = \text{relative integral of D (A = 3H)}$$

To illustrate this empirical relationship: When $\int D = 2.5$. The quantity of D protons responsible for $\int D$ is 0.75 and the percentage of species I is 57%. $I = 1/(1 + (2.5 - 1)/2) = 1/(1 + (0.75))$ x 100 = 57%

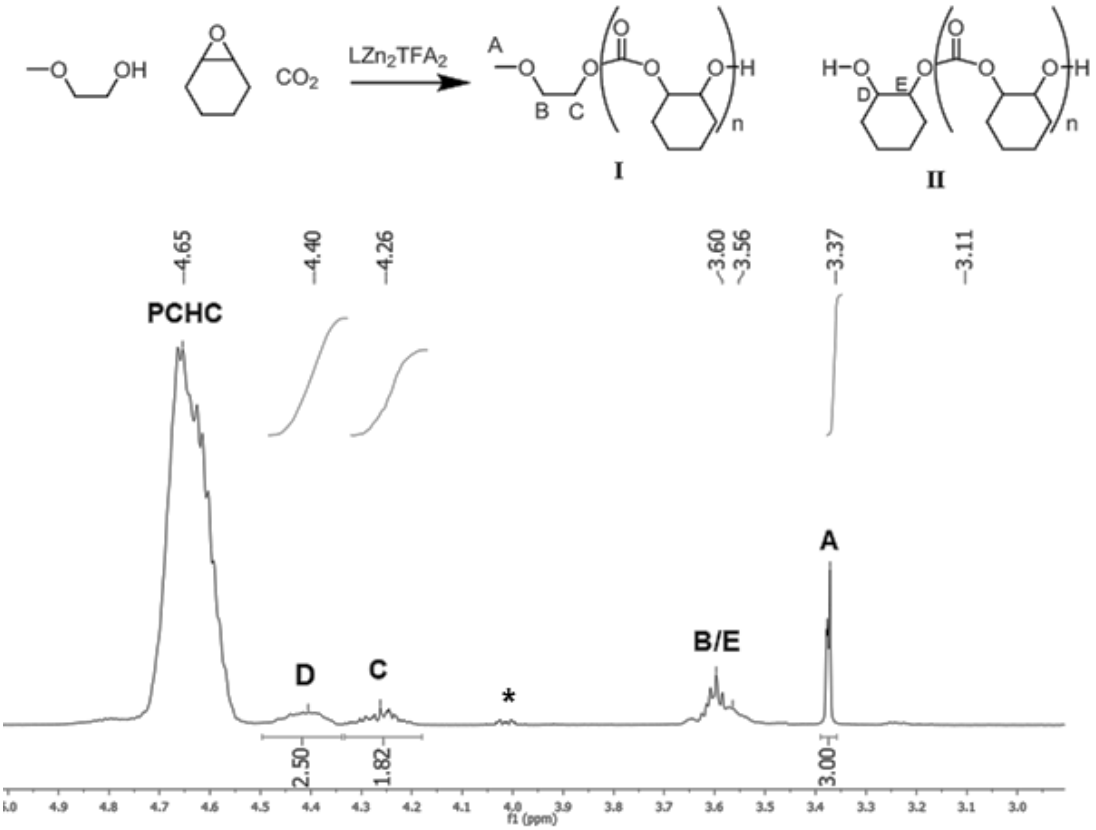

Figure 2.4.7: Excerpt of the ^{1}H NMR spectrum of end capped PCHC.

The scheme shows the ROCOP of CHO in the presence of MEG and the resulting polymer structures I and II. * cyclic carbonate.

The experiments using MEG (up to 32 equiv. *vs* catalyst) demonstrated that only 92 % selectivity to mono-ethylene glycol end capped chains can be achieved. This is due to the presence of 1,2-cyclohexene diol. In the current system there was always 1,2 cyclohexene diol present, due to the use of a dynamic carbon dioxide atmosphere. In order to use the end capped chains as macroinitiators, the proportion of end capped chains should be >99 %; at such a proportion the majority of the block copolymers would have the desired AB structure. Given the low molar mass and lower selectivity using MEG, it was decided impractical to continue with AB type block copolymers.

2.4.3 Ring Opening Copolymerisation in the Presence of ε-CL

In order to determine if [$LZn_2(OCOCF_3)_2$] displayed similar levels of control to [$LZn_2(OAc)_2$], the ROCOP of CHO/CO_2 was carried out in the presence of ε-caprolactone (Table 2.1, Run 3). Despite the presence of ε-CL, only PCHC was produced. The TOF was slightly reduced due to the decrease in catalyst concentration by the addition of ε-CL. The ^{1}H NMR spectrum of the crude polymer showed the exclusive formation of PCHC with no formation of PCL. The lower conversion meant that the molar mass of the polymer has been slightly reduced to 1670 g mol^{-1} (Đ = 1.2). MALDI-ToF analysis of the PCHC produced in the presence of ε-CL, showed only polycarbonate chains with up to 4 ether linkages present (Figure 2.4.7). This quantity of ether linkages was undetectable by ^{1}H NMR spectroscopy, due to partial signal overlap from the PCHC end groups at 3.45 ppm and 3.55 ppm respectively. However they can be detected in the $^{13}C\{^1H\}$ NMR spectroscopy of the polymer in d_6-DMSO (Figure 2.4.7). The use of $CDCl_3$ obscured the ether signal which was observed at 77 – 76 ppm. The formation of ether linkages is likely due to the high dilution of the catalyst and may also arise from the carbon dioxide being less soluble in toluene than CHO.

[$LZn_2(OCOCF_3)_2$] was an efficient catalyst for the ROCOP of CHO/CO_2, which selectively and efficiently produced only dihydroxyl terminated PCHC. The dihydroxyl end groups are a key requirement for the formation of block copolymers. [$LZn_2(OCOCF_3)_2$] was also capable of forming the dihydroxyl terminated polycarbonate, in the presence of ε-CL, with limited side reactions. If [$LZn_2(OCOCF_3)_2$] is capable of catalysing the ROP of ε-CL in the presence of CHO, it is expected to be a suitable and ideal catalyst for the formation of ABA type block copolymers.

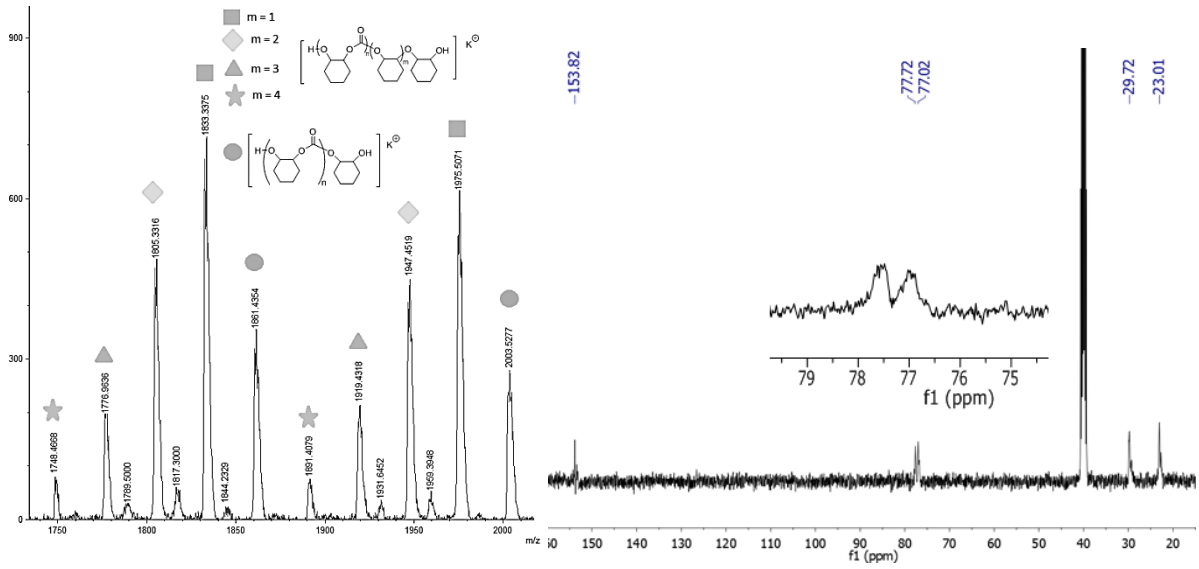

Figure 2.4.8 Analysis showing the formation of ether linkages in polycarbonate.

Left: Selected region of the MALDI-ToF spectrum for the polycarbonate polyol (Table 2.1, Run 3). The circles represent the polycarbonate polyol series, repeat unit of $[(C_6H_{10}O_3)_n+C_6H_{12}O_2+K]^+$ = $[(142.15)_n+116.16+39.1]^+$. The squares, diamonds, triangles and stars represent polyol series containing 1, 2, 3 and 4 ether linkages, respectively represented (where m=1-4, respectively): $[(C_6H_{10}O_3)_n+(C_6H_{10}O_2)_m+C_6H_{12}O_2+K]^+$ = $[(142.15)_n+(114.08)_m+116.16+39.1]^+$. Right: ^{13}C NMR spectrum of PCHC, in *d*$_6$-DMSO, showing the presence of peaks at 77 and 76 ppm, corresponding to (low proportions) of ether linkages in PCHC. The low intensity is due the low proportion of ether in the polymer (indistinguishable in ^{1}H NMR due to overlap with the endgroup signal).

2.5 Ring Opening Polymerisation

Next, $[LZn_2(OCOCF_3)_2]$ was investigated for its ability to catalyse the ROP of ε-CL with CHO present as the switch reagent. The reaction between only $[LZn_2(OCOCF_3)_2]$ and ε-CL in toluene failed to result in the formation of polyester. The addition of alcohol (isopropanol) also failed to result in an active catalyst system. However, the reaction between $[LZn_2(OCOCF_3)_2]$, CHO and ε-CL resulted in an active catalyst system that exclusively produced polycaprolactone. The polymerisation was rapid with a TOF of >800 h^{-1} and controlled with the molar mass increasing linearly with increasing equivalents of caprolactone, and the dispersities remaining narrow throughout (Figure 2.5.1).

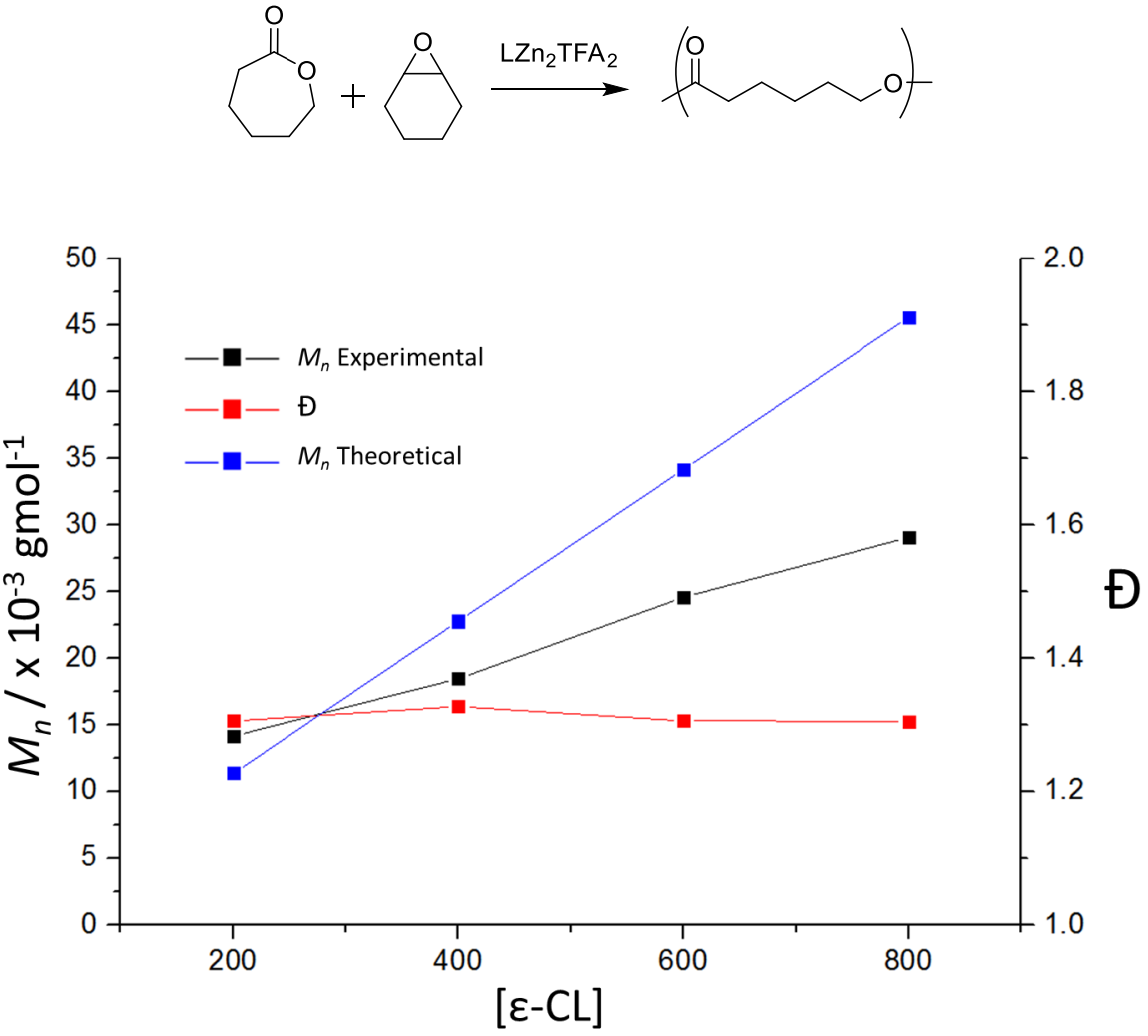

Figure 2.5.1: Scheme showing the ROP of ε-CL by [$LZn_2(OCOCF_3)_2$] and CHO. Graph showing the linear correlation between molar mass and caprolactone concentration.

Polymerisations carried out at a 1:1000:X loading of [$LZn_2(OCOCF_3)_2$]:CHO:ε-CL, at 80 °C, for 1 h (Table 2.3, Run 3-7).

Table 2.3: The ring opening polymerizations (ROP) of ε-caprolactone, using [$LZn_2(OCOCF_3)_2$].

Run #	**1**: ε-CL:CHO: IPA	% conversion ε-CL[a)]	M_n (Đ)[b)] / g mol^{-1}	M_n calc.[c)] / g mol^{-1}
1	1:400:0:0	-	-	-
2	1:400:0:10	-	-	-
3	1:200:500:0	>99%	14,200 (1.33)	11,400
4	1:400:500:0	>99%	18,500 (1.40)	22,800
5	1:600:500:0	>99%	24,600 (1.33)	34,200
6	1:800:500:0	>99%	29,100 (1.31)	45,600
7	1:400:500:0[d)]	>99%	17,000 (1.39)	22,800
8	1:400:500:5	>99%	7,320 (1.35)	9120
9	1:400:500:10	>99%	3,400 (1.47)	4560

All polymerizations were conducted in toluene, using 4 mM catalyst concentrations (1.6 M concentration of ε-CL), at 80 °C for 1 h. a) Determined by ^{1}H NMR spectroscopy by comparing the normalized integrals of the signals at 4.05 ppm (methylene protons of PCL) *vs*. 4.15 ppm (methylene protons of ε-CL). b) Determined by SEC, in THF, using narrow molar mass polystyrene standards to calibrate the instrument. A correction factor of 0.56 was applied, as described by Penczek and co-workers.[24] c) The theoretical molar mass was determined according to: [(#moles ε-CL converted) / 2(#moles catalyst **1**) x 114], assuming both trifluoroacetate groups on the catalyst initiate polymerization. When iso-propyl alcohol is present: [(#moles ε-CL converted) / (#moles iso-propyl alcohol) x 114]. d) Polymerization conducted using a solution that was pre-saturated with carbon dioxide.

The lack of activity when [$LZn_2(OCOCF_3)_2$] and *i*-PrOH were used showed that the CHO played an active role in the switching on of the ROP of ε-CL, and that the diol alone would not be able to act as the initiating species for the polymerisation. It has previously been reported that the reaction between [$LZn_2(OAc)_2$], CHD, and ε-CL does not result in the formation of polyester, even after extended reaction times.[11] It has also been previously observed, using *in-situ* ATR-IR spectroscopy, that the di-zinc catalyst (X = OAc) reacts only once with an epoxide molecule, even in the presence of excess epoxide, to generate a dizinc alkoxide complex.[11] It is proposed that the di-zinc alkoxide species can react with ε-CL to

initiate the ring-opening polymerisation. The reaction with ε-CL generates a new propagating zinc alkoxide complex (Section 2.1).

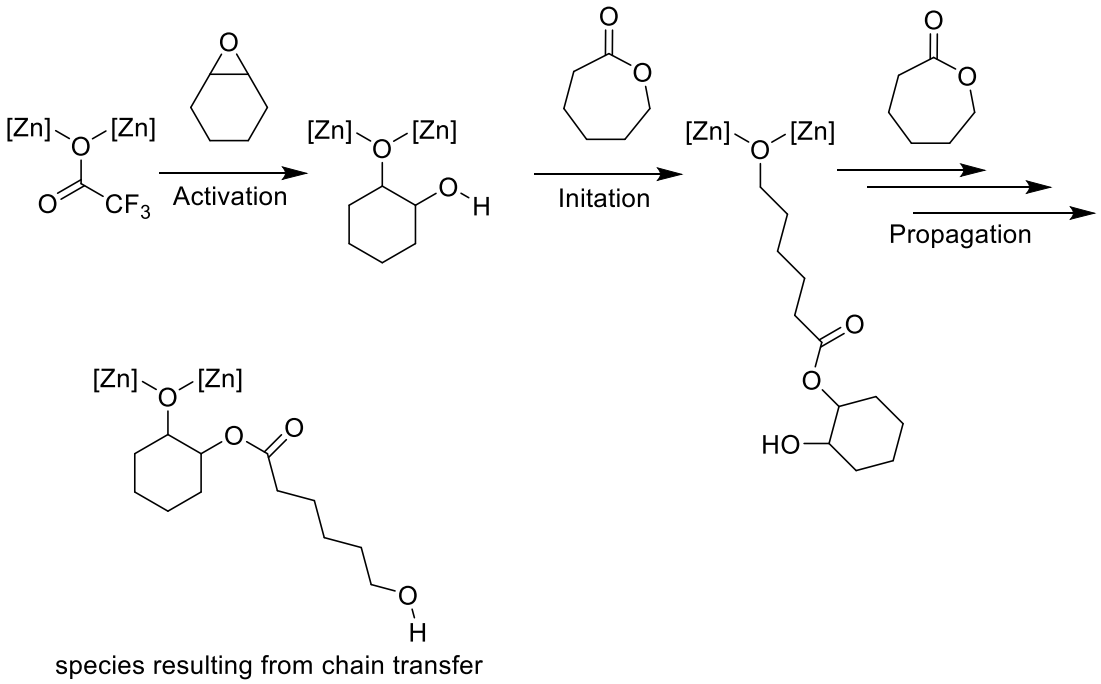

Figure 2.5.2: Scheme showing the proposed mechanism for ROP catalysed by $[LZn_2(OCOCF_3)_2]$/CHO.

The activation, initiation and propagation steps shown. The trifluoroacetate group is hydrolysed at some point during the reaction.

When bifunctional chain transfer agents or initiators are used it is conventional to assume that both functional groups are equivalent and will react in the same manner, resulting in polymer chains growing at the same rate from all active sites of the chain transfer agent. However, this requires chain transfer to be faster than propagation. If propagation is faster, the majority of the polymer may be formed at a single functional site. Detailed kinetic analysis carried out on the $[LZn_2(OAc)_2]$/CHO system by Zhu *et al*, showed that the rate of propagation is significantly faster from a primary alkoxide *versus* a secondary species.[11] Given that the alkoxide formed by CHO ring-opening is a secondary alkoxide, but the alkoxide formed from the ε-CL ring-opening is a primary alkoxide, it is clear there may be a difference in the

relative rates of propagation. Furthermore, as discussed in the introduction, DFT analysis showed that the insertion of ε-CL into a secondary zinc alkoxide species (formed by the ring opening of CHO) has a significantly higher activation barrier than its insertion into a primary zinc alkoxide species (formed from the ring opening of ε-CL).[12] This implies that once a caprolactone unit has ring opened by the secondary alkoxide, it will be much more favourable for further propagation to occur from that site compared to the other secondary hydroxyl group of the cyclohexylene species. Using the $[LZn_2(OAc)_2]$/CHO catalyst, two different polymer architectures were observed in PCL formation: one with the cyclohexene ring as an end group (X) and the other with the cyclohexene ring as a chain extender (Y) (Figure 2.5.3).[11]

The structure of the PCL formed using $[LZn_2(OCOCF_3)_2]$/CHO catalyst system was analysed by NMR spectroscopy and MALDI-ToF spectrometry (Figure 2.5.3). The MALDI-ToF spectrum showed a single series of chains, separated by 114 m/z (corresponding to the PCL repeat unit), with a single cyclohexene oxide unit included in the polymer structure. The mass spectrometry data cannot be used to determine the precise location of the cyclohexylene unit. However as CHO is involved during the initiation step of the ROP (Figure 2.5.2), it is expected that it is either located at the end of the polymer chain (Species X, Figure 2.5.3) or somewhere along the chain (acting as a chain extender – Species Y, Figure 2.5.3).^{1}H NMR spectroscopy showed multiple end groups, in accordance with the presence of multiple structures. The different end groups present in the NMR spectra were assigned using 2D spectroscopy. The methylene protons near the hydroxyl group on the terminal caprolactone unit appear at 3.60 ppm. When the cyclohexene unit is an end group (X), the methine protons appear as signals at 4.59 and 3.55 ppm. When the cyclohexene unit is a chain extender (Y), the methine protons appear at 4.80 ppm.

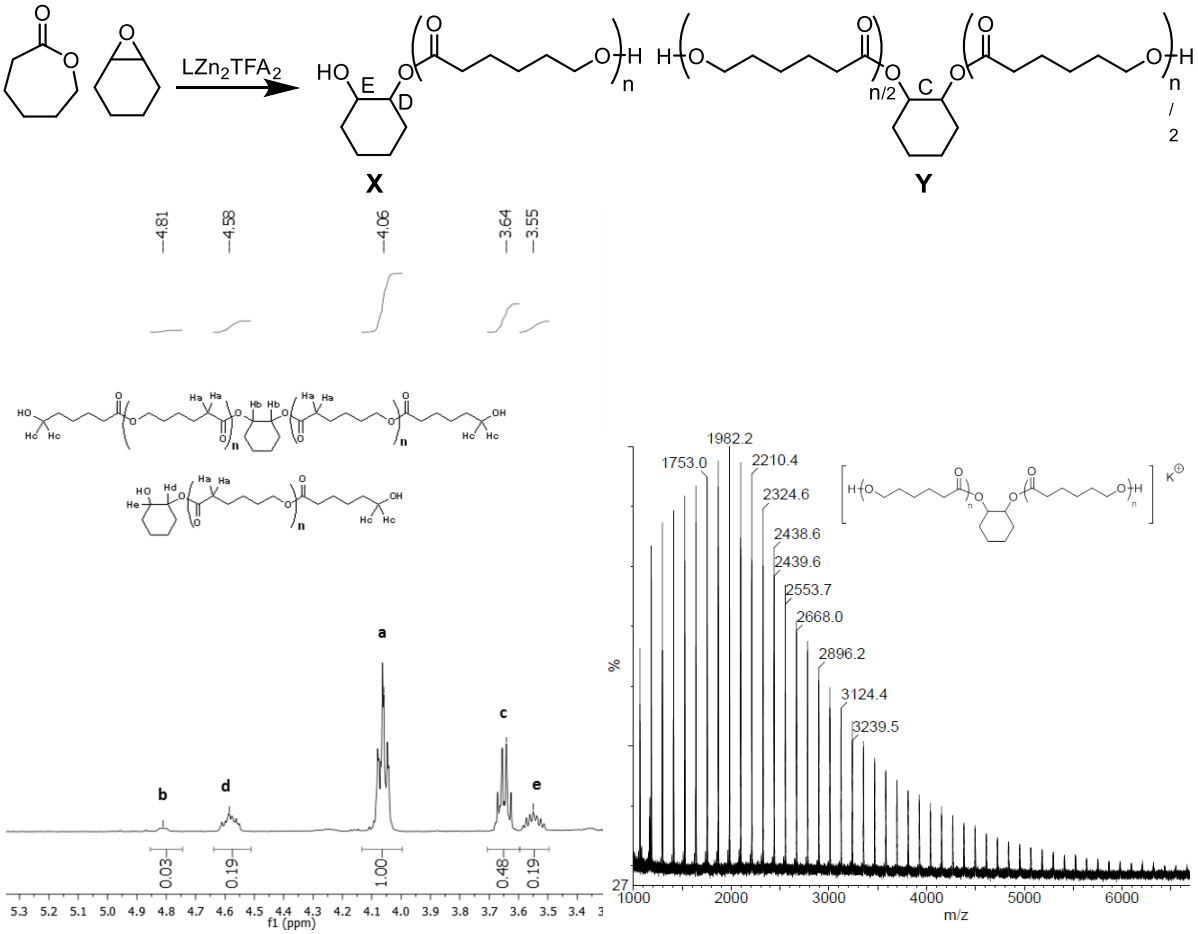

Figure: 2.5.3: Scheme showing the structure of PCL when synthesised by $[LZn_2(OCOCF_3)_2]$/CHO. Excerpt of the ^{1}H NMR spectrum of PCL, showing the different end group signals. MALDI-ToF Spectrum of PCL.

Series calculated for $[(C_6H_{10}O_2)_n+C_6H_{12}O_2+K]^+ = [(114.07)_n+116.16+39.1]^+$.

The presence of the two different structures can be confirmed by use of the ^{31}P NMR end group analysis (Figure 2.5.4).[14] The difference between a primary and secondary hydroxide in the ^{31}P NMR spectrum was shown to be up to 5 ppm, with primary hydroxides giving the higher chemical shifts. The ^{31}P NMR end group analysis was also carried out on control species and PCL. The spectrum of PCL showed two peaks in the hydroxyl region (142-148 ppm) at 146.47 and 147.90 ppm. The signal at 147.9 ppm has previously been reported as the primary hydroxyl end group of PCL.

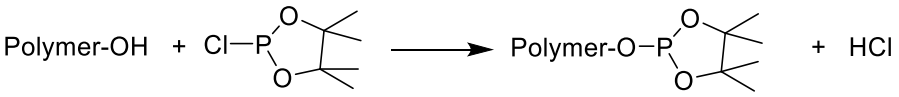

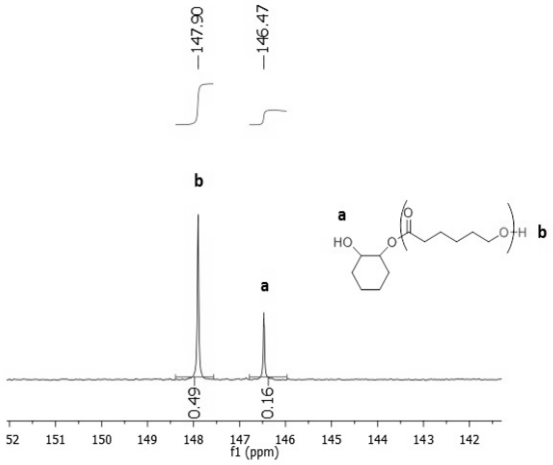

Sample	δ ppm
Poly(ε-caprolactone) [a]	147.83
Cyclohexene diol [b]	146. 26
Ethylene Glycol [b] [d]	147.75
Bisphenol A [c]	138.57
Methanol [d]	148.93

a) δ reported by Marchessault (14) b) δ reported by S. Paul c) used as an internal standard d) δ reported by Wroblewski (25)

Figure 2.5.4: ^{31}P NMR endgroup analysis of PCL, synthesised according to Table 2.2, Run 4. The Table shows the ^{31}P NMR shifts of reference compounds.

The [$LZn_2(OCOCF_3)_2$]/CHO system was shown to be active for the immortal ROP of ε-CL, where the addition of 10 and 20 equivalents of chain transfer agent reduces the molar mass of the PCL. Experiments conducted with the [$LZn_2(OCOCF_3)_2$]/CHO and isopropanol, as the chain transfer agent, led to the formation of PCL with predictable molar masses (Table 2.3, Runs 8-9). The MALDI-ToF spectra show series attributable to both PCL polyols and PCL end-capped by iso-propyl ester groups (Figure 2.5.5).

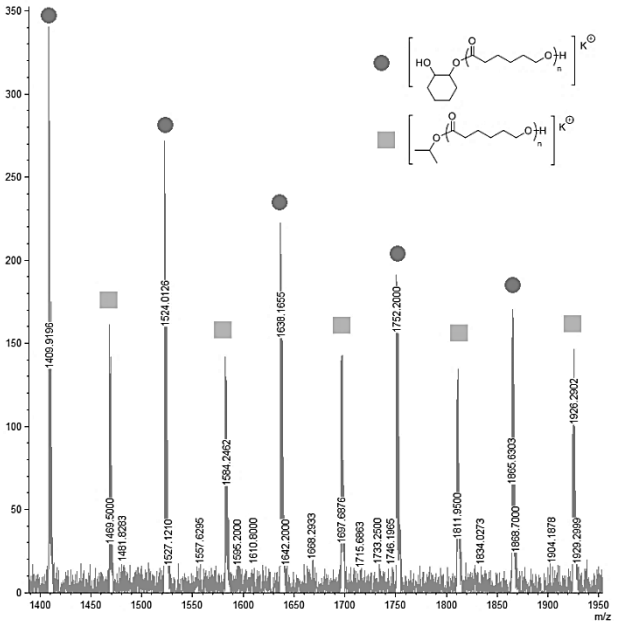

Figure 2.5.5: MALDI-ToF spectrum of PCL synthesised according to Table 2.2, Run 8.

The circles show the polyester polyol series including one cyclohexane diol unit. They are represented by $[(C_6H_{10}O_2)n+C_6H_{12}O_2+K]+ = [(114.07)n+116.16+39.1]+$. The squares mark the polycaprolactone series, including an isopropyl alcohol unit. They are represented by $[(C_6H_{10}O_2)n+C_3H_8O+K]+ = [(114.07)n+60.05+39.1]+$.

The ROP of ε-CL with $[LZn_2(OAc)_2]$ is known to be switched off by the addition of carbon dioxide. This is proposed to be due to the very fast insertion of CO_2 into the zinc alkoxide bond. The resulting zinc-carbonate species is completely inactive for the ROP of ε-CL. During the formation of a block copolymer, carbon dioxide will be removed from the system *via* the application of vacuum/nitrogen cycles. However, there may be some residual carbon dioxide dissolved in the system even after the vacuum/nitrogen cycles. In order to determine if the ring opening polymerisation is affected by the presence of residual carbon dioxide, a mixture of $[LZn_2(OCOCF_3)_2]$, CHO and ε-CL was saturated with carbon dioxide for 1 h at room temperature. The carbon dioxide was then removed using 6 short vacuum/nitrogen cycles, before the reaction mixture was heated to 80 °C. The saturation experiment cannot be carried out at 80 °C as this would result in the formation of PCHC. Although, the ROP took longer (2 h) to reach full conversion (TOF = 100 h^{-1}) it led to the exclusive production of PCL and showed a reasonable agreement between experimental and calculated values for the

molar mass. This experiment shows that 6 vacuum/nitrogen cycles are sufficient to allow the ROP of ε-CL to proceed successfully.

In conclusion, the $[LZn_2(OCOCF_3)_2]$/CHO catalyst system is effective for the ROP of ε-caprolactone. In the absence of any epoxide, no polymerization occurs. However, in the presence of epoxide, efficient and controlled ring opening polymerization results. With the discovery that $[LZn_2(OCOCF_3)_2]$ was an efficient catalyst for both ROCOP and ROP, the next step was to investigate its application as a catalyst to different mixtures of these monomers and in particular to investigate whether the catalyst exerts any block sequence selectivity.

2.6 Combining Ring Opening Copolymerisation and Ring Opening Polymerisation

2.6.1 Catalyst Selectivity

As previously shown, a mixture of $[LZn_2(OCOCF_3)_2]$/CHO/CO_2 /ε-CL resulted in the selective formation of dihydroxyl terminated PCHC. Whereas a similar mixture, which has had the CO_2 removed, resulted only in the formation of PCL. This selectivity was exploited to produce ABA poly(ester-b-carbonate-b-ester) materials.

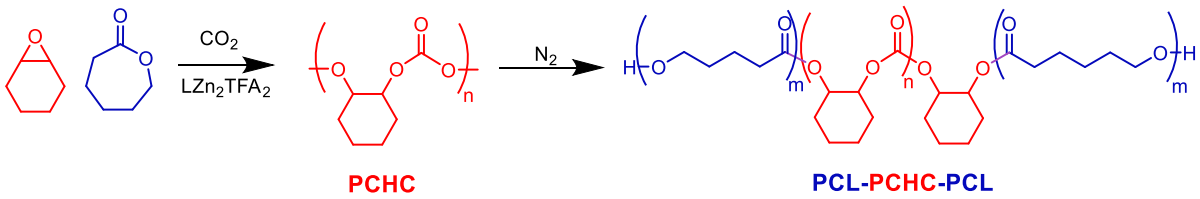

Figure 2.6.1: Scheme showing the formation of PCL-PCHC-PCL block copolymer.

The terpolymerisation of $[LZn_2(OCOCF_3)_2]$/CHO/ε-CL (1:2000:200) and CO_2, was monitored by *in-situ* ATR IR spectroscopy and ^1H NMR spectroscopy (Figure 2.6.2).

Initially, the absorption at 1010 cm^{-1}, which is assigned to poly(cyclohexene carbonate), increased in intensity. The assignment was made from a control experiment on CHO/CO_2 ROCOP. During the first 16 h when carbon dioxide is present, the absorption assigned to PCHC increased (1010 cm^{-1}), while that assigned to PCL remained unchanged (1190 cm^{-1}). Once again, the signals for ε-Cl/PCL were unambiguously assigned from control experiments on ε-caprolactone ROP. The selective formation of PCHC was also observed in the ^{1}H NMR spectrum, whereby the presence of PCHC is observed (4.65 ppm) but there is no signal at 4.05 ppm, indicating no PCL has formed.

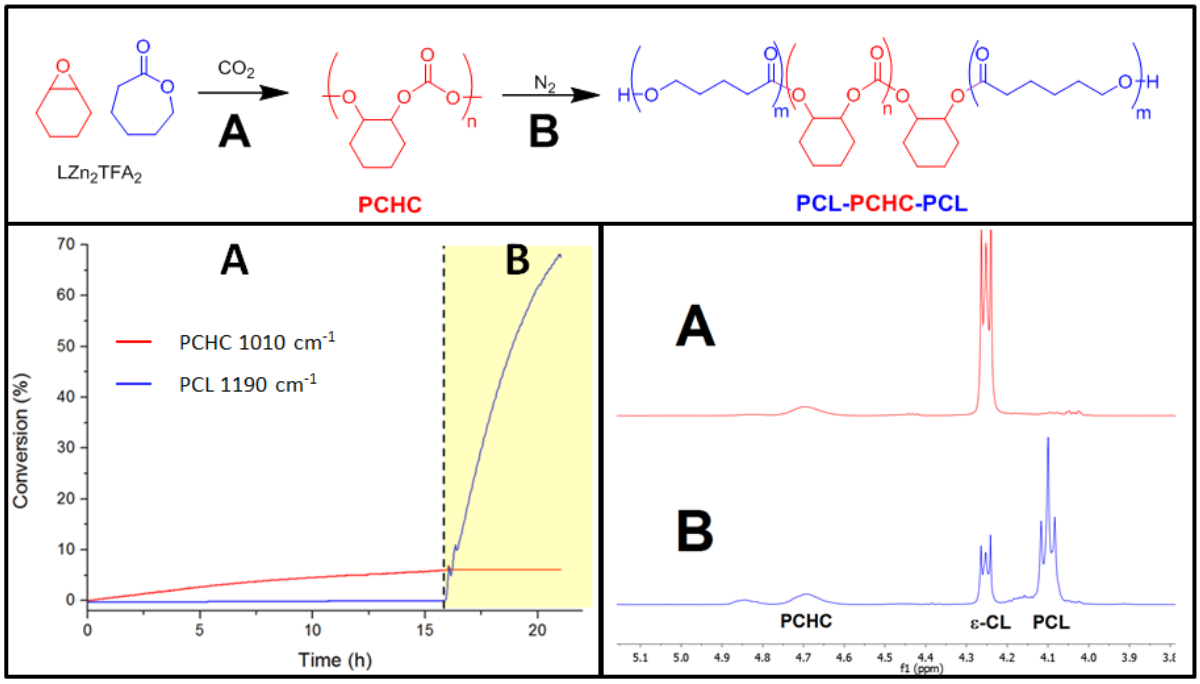

Figure 2.6.2: Scheme showing the formation of copoly(ester-*b*-carbonate-*b*-ester) and monitoring the reaction *via in-situ*-ATR and ^{1}H NMR spectroscopy (Table 2.4, Run 1).

Plot showing the change in intensity of specific IR resonances during the copolymerisation of CHO/ε-CL/CO_2. The absorptions at 1010 cm^{-1} is assigned to PCHC, that at 1190 cm^{-1} is assigned to PCL. Excerpt of the ^{1}H NMR spectrum of the polymer aliquots removed during the polymerization. The top spectrum (A) corresponds to the first aliquot taken after 16 h, and shows only polycarbonate (PCHC). The bottom spectrum (B) shows the aliquot taken after 21 h and corresponds to the copoly(ester-*b*-carbonate-*b*-ester). The proposed structure for the triblock copolymer is illustrated above.

After 16 h the carbon dioxide was removed by 6 short vacuum/nitrogen cycles, which was sufficient to remove it as evidenced by the sharp drop in the intensity of the signal at 2340 cm^{-1} (Section 2.3.5). These conditions only caused minimal loss of residual monomers or solvent, (Section 2.3.5). The removal of the carbon dioxide also caused an instant increase in the absorption for PCL (1190 cm^{-1}). The formation of PCL was also observed in the ^{1}H NMR spectrum, with the appearance of a signal at 4.05 ppm. The intensity of the signal at 1010 cm^{-1} (PCHC) no longer increased after the carbon dioxide is removed. Thus the ^{1}H NMR spectroscopy and *in-situ* IR spectroscopy showed that [$LZn_2(OCOCF_3)_2$] exhibits chemoselective control, whereby the formation of PCHC occurs exclusively when carbon dioxide was present and PCL will only form when the CO_2 was removed. The same selectivity was observed when the terpolymerisation was run using different molecular equivalents of monomers over the range [$LZn_2(OCOCF_3)_2$]:xx, (xx = 200-600 equivalents of ε-CL). This allowed a series of different molar masses and compositions to be targeted.

A range of different copoly(ester carbonates) were prepared with controllable compositions over a range of different molar masses (~4000-14,000 g mol^{-1}), and all showed moderate/narrow dispersities (Đ = 1.10-1.50) (Table 2.4). Independent of the relative ratio of the mixture of monomers, the terpolymerisations followed the same selectivity: ROCOP occured first and when CO_2 was removed ROP occured. The polycarbonate blocks were generally of low molar mass, with narrow dispersity. The slower overall rate was due to the comparatively high dilution of the catalyst in the terpolymerisations, over 16 h the typical conversions were 10 - 20 %, corresponding to a molar mass of 900 - 4,500 g mol^{-1}. After removal of the carbon dioxide, the ROP of ε-CL occurred leading to copolymers with higher molar masses and, in some cases, a slight broadening of dispersity. This increase in dispersity was proposed to arise due to a relatively slower rate of initiation of ε-caprolactone by the polymer end-capped cyclohexene alkoxide (a secondary alkoxide) compared to propagation from the ε-caproyl alkoxide (a primary alkoxide) leading to more complex polymerization kinetics (as discussed in Section 2.1 and Section 2.5). The broadening of the dispersity is not proposed to result from contamination of the polymers by PCHC homopolymer. The block copolymer was purified by precipitation of the polymer from THF by MeOH. This would fractionate any shorter chains, and because the PCHC block was significantly shorter than the block copolymer, it would be expected that the homopolymer would remain in the filtrate.

The purification of the crude polymer, by fractionation using THF and MeOH, resulted in a slight increase in the sample M_n (6000 g mol^{-1}, Đ = 1.20 from 4000 g mol^{-1} Đ = 1.30). ^{1}H NMR spectroscopy including DOSY analysis (see Appendix) of the filtrate from the precipitation of the polymer showed that it contained no homopolymers but rather very short PCL-PCHC-PCL chains. As only block copolymers were being fractionated, this indicated there is no contamination from the homopolymers but rather that the block copolymers being produced show a range of chain lengths.

Table 2.4: Shows the data for polymerizations conducted using [LZn$_2$(OCOCF$_3$)$_2$], ε-CL, CHO and CO$_2$ leading to the formation of ABA type PCL-PCHC-PCL triblock copolymers.

#	Cat:CHO:ε-CL	% CHO convn.[a] (time)	M_n[b] PCHC / g mol^{-1} Đ)	% ε-CL convn.[a] (time)	M_n[b] PCL-PCHC-PCL / g mol^{-1} (Đ)	Molar Ratio carbonate: ester linkages[c]
1	1:2000:200	6 (16 h)	1,880 (1.08)	68 (5 h)	4,000 (1.33)	1:1
2	1:1000:400[d]	9 (18 h)	900 (1.07)	81 (2h)	3,300 (1.41)	1:6
3	1:500:200[e]	15 (18 h)	2,600 (1.16)	69 (1.5 h)	6,500 (1.48)	1:2
4	1:500:400[f]	15 (18 h)	2,200 (1.12)	78 (1.5 h)	12,800 (1.49)	1:6
5	1:500:400[e]	15 (25 h)	2,200 (1.08)	70 (1.5 h)	13,800 (1.43)	1:4
6	1:500:100	17 (18 h)	4,500 (1.08)	53 (1.5 h)	6,600 (1.35)	1:0.5
7	1:500:600	6 (18 h)	2,900 (1.19)	51 (1.5 h)	12,500 (1.29)	1:10

Polymerization conditions: 80 °C, under 1 atm CO_2 pressure for a fixed time period, after which the carbon dioxide was removed by six cycles of vacuum-nitrogen and the polymerization allowed to progress for a further time period. a) Determined by ^{1}H NMR spectroscopy, the CHO conversion was determined from the normalised integrals for the CH signals at 3.05 ppm (CHO) and 4.58 ppm (PCHC). The ε-CL conversion was determined from the normalised integrals for the signals at 4.05 ppm (PCL) *vs*. 4.15 ppm (ε-CL). b) Determined by SEC, with THF as the eluent, using polystyrene standards to calibrate the instrument. c) Determined by ^{1}H NMR spectroscopy by comparison of the normalised integrals for the PCHC CH signals at 4.58 ppm and the PCL CH_2 signals at 4.05 ppm. Reactions conducted with added toluene: d) 3.5 mL e) 4.45 mL. f) 2.2 mL.

The relative ratio of carbonate: ester linkages in the copolymers can be deduced by comparing the integrals for the main chain ester *vs*. carbonate resonances in the ^{1}H NMR spectra (e.g. at 4.05 ppm for the PCL *vs*. 4.65 ppm for the PCHC). Thus, the ratio can be controlled over the range 1:1 through to 1:15, with a reasonable agreement between the experimental results and those expected on the basis of polymerization conversion and corresponding to weight fractions of PCL from 26 to 72 %. This ratio does not change after the fractionation of the copolymer providing further evidence for block formation. The molar masses all show clear increases from the polycarbonate to the copoly(ester-carbonate), consistent with block copolymer formation. The M_n values obtained by SEC are calibrated against narrow molar mass polystyrene standards, and as such are relative rather than absolute values. Despite this estimation, it is apparent that the molar masses obtained for both the polycarbonate and copoly(ester carbonates) are lower than would be expected on the basis of reagent stoichiometry and conversion. Typically the copolymer molar masses are 3-4 times lower than would be expected, consistent with the presence of chain transfer agents. It has previously been observed, using a range of different catalysts and processes for ROCOP of CO_2/CHO, that the polymer molar masses are frequently lower than would be expected.[9,26-41] As discussed in Sections 2.1 and 1.2.1, it is proposed that 1,2-cyclohexanediol, formed by side-reactions between the epoxide and any residual water, functions as a telechelic chain transfer agent leading to the formation of polyols.[13,31]

2.6.2 Polymer Characterisation

While [$LZn_2(OCOCF_3)_2$] has shown to be able to utilise switch catalysis to form block copolymers, the structure of the blocks needs to be examined. One of the goals of forming ABA type block copolymers is to have complete control of not only the sequence of the blocks but also the structure (ABA *vs* AB), and for all chains to be homogeneous (i.e. have the same composition). Analysis of the copoly(ester-carbonate) by SEC showed a monomodal signal which was significantly shifted from the SEC trace of the polycarbonate species (Figure 2.6.3). An aliquot taken during the first phase of polymerization, when only PCHC was produced, was analysed by SEC and showed an M_n of 1800 g mol^{-1} (Đ= 1.08). An aliquot removed from the polymerization after the formation of PCL showed the M_n

increasing to 4000 g mol^{-1} (Đ= 1.30). This gives confidence a single species has been formed (as opposed to a bimodal trace or overlapping traces indicating two species present).

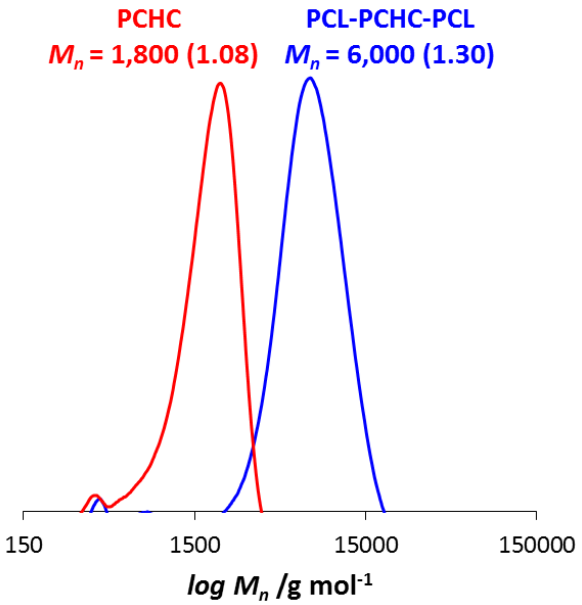

Figure 2.6.3: The evolution of the molar mass (M_n) as the copolymerisation proceeds (Table 2.3, Run 1).

The PCHC has a M_n of 1800 g mol^{-1}. After the carbon dioxide is removed, the ring opening polymerisation of ε-Cl occurs which leads to the formation of PCL-PCHC-PCL. The molar mass increased to 4000 g mol^{-1}. The molar mass is determined by SEC, with THF as the eluent, using narrow polystyrene standards to calibrate the instrument.

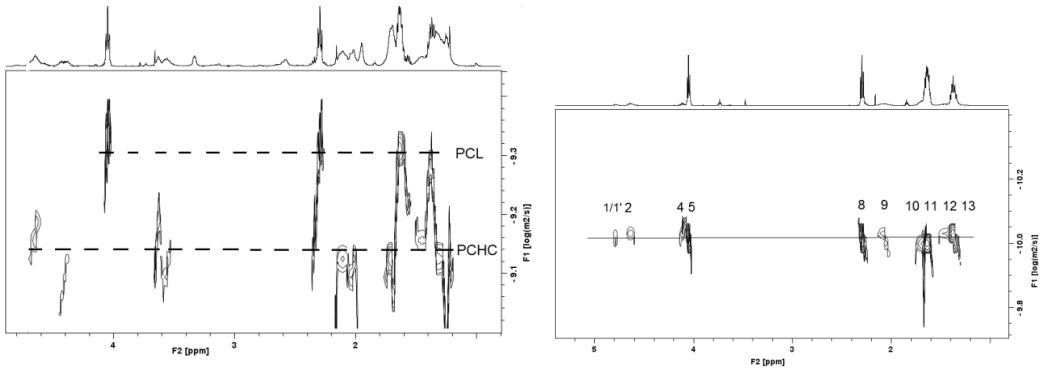

Figure 2.6.4: ^{1}H DOSY spectra. Left: A mixture of PCL and PCHC samples. Right PCL-PCHC-PCL.

While the mixture of polymers shows two species diffusing at different rates, the block copolymer shows a single diffusion co-efficient.

^{1}H DOSY NMR was also used to determine whether or not multiple species are present in the polymeric sample (Figure 2.6.4).[17-19] It was shown that a sample of PCHC and PCL of similar molar masses (1586 and 1348 g mol^{-1} respectively) gave two distinct diffusion co-efficients, one correlating to PCL and the other to PCHC. The ^{1}H DOSY NMR of the copolymer showed only a single diffusion co-efficient which is the same for both the PCHC and PCL signals, confirming that only a single species was present in the copoly(ester-carbonate).

^{1}H NMR spectroscopy of the copoly(ester-carbonate) was carried out on the aliquots taken during the polymerisation (Figure 2.6.5). From the comparison of the integrals of the main chain resonances to the end group signals and any new signals which may appear, information on the composition of the copolymer can be obtained. The first aliquot was taken at 25 h, just before the carbon dioxide was removed. At this stage only ROCOP has occurred and only PCHC was present. The relative integrals of the signals assigned to the PCHC main chain methine resonances [4.65 ppm, assigned to H^{1})] against those assigned to the end

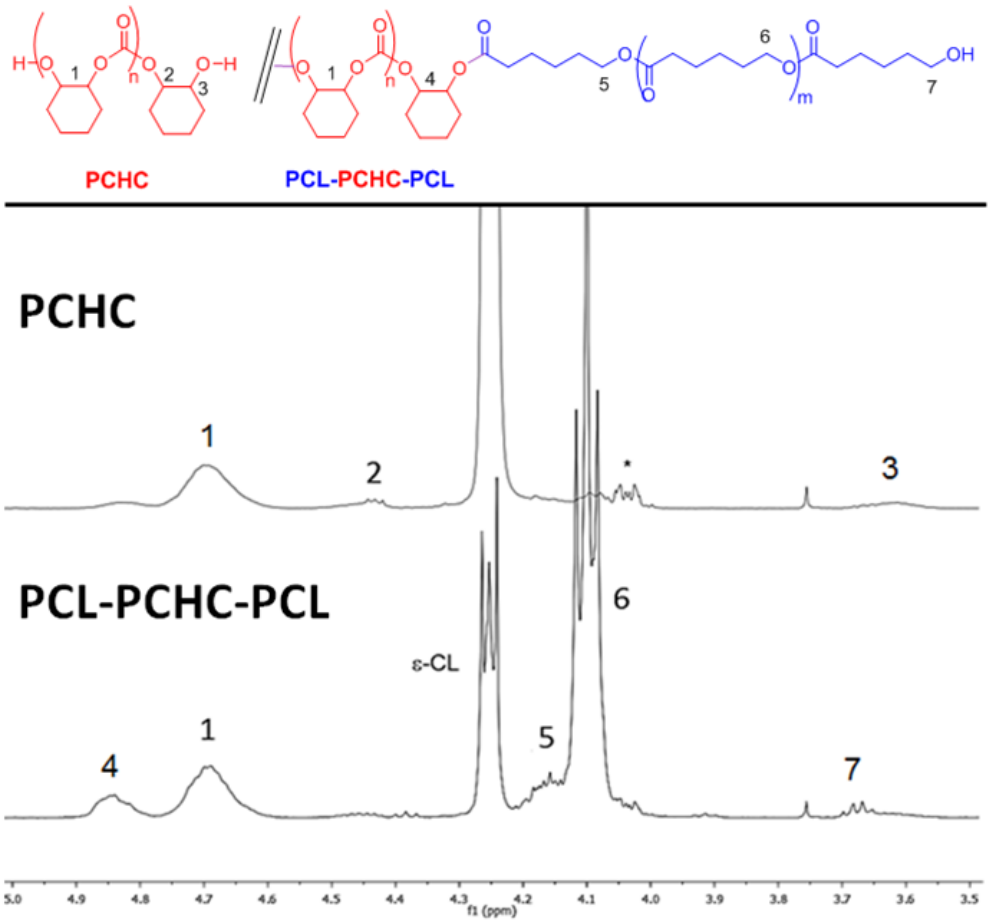

Figure: 2.6.5: Excerpts from the ^{1}H NMR spectra of aliquots taken from the terpolymerisation (Table 2.3, Run 5).

The top spectrum corresponds to the first aliquot taken after 25 h, and shows only polycarbonate (PCHC). The bottom spectrum shows the aliquot taken after 26.5 h and corresponds to the copoly(ester - carbonate). The proposed structure for the triblock copolymer is illustrated above.

groups [at 4.41 (H^2) and 3.57 (H^3) ppm] can be used to estimate the molar mass, resulting in a value of 1420 g mol^{-1}, which corresponded well with that obtained by SEC and indicating that approximately 5 chains grow per catalyst due to the presence of chain transfer agents (1,2 cyclohexane diol). The number of chains was determined by calculating the molar mass if only 1 chain was formed (Number of chains = $\overline{DP}$ x molar mass of the PCHC repeat unit = 75 x 142) and dividing that by the molar mass observed by SEC (2,200). The finding that approximately 5 chains grow per catalyst is similar to previous work using this catalyst and

others.[1,23] The second aliquot was taken at 26.5 h and showed resonances corresponding to both PCHC and PCL (4.65 ppm and 4.05 ppm). The relative ratio of carbonate:ester was calculated by the comparison of the normalised relative integrals, providing an estimate of the relative quantities of each block present in the copolymer. The carbonate: ester integral ratio is 1:4, determined from ^{1}H NMR spectrum, which corresponded well with the expected ratio on the basis of monomer conversions and loadings (predicted ratio = 1:4).

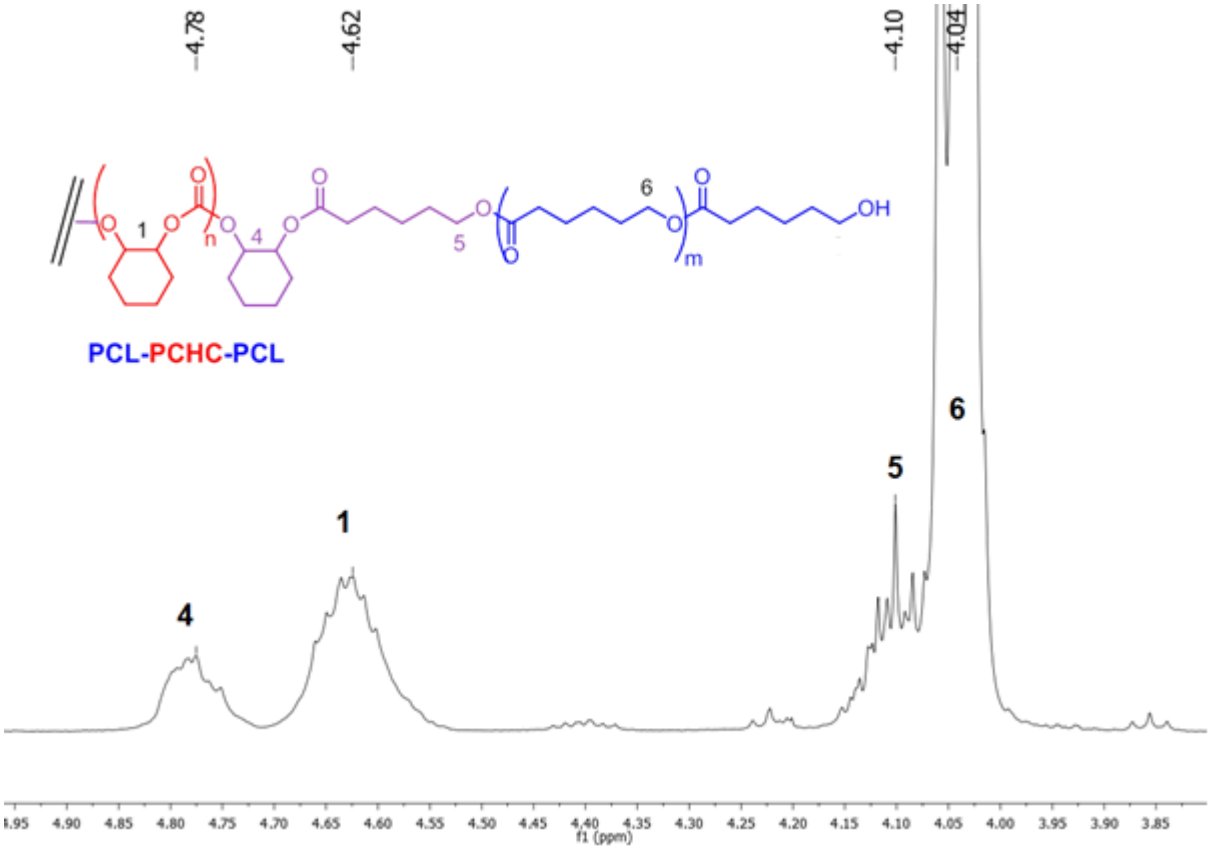

Figure 2.6.6: Excerpt from the ^{1}H NMR spectrum of PCL-PCHC-PCL (Table 2.3, Run 5).

The structure is shown above along with assignments.

After the formation of PCL, as well as the signal for the PCL at 4.05 ppm, three new signals appeared in the ^{1}H NMR spectrum at 4.78, 4.11 and 3.64 ppm. These signals were also

present in the ^{1}H NMR spectrum of the purified copolymer (Figure 2.6.6), indicating that they are truly being caused by protons from the copolymer, rather than impurities or monomers. The signal at 3.64 ppm was assigned to the methylene unit of terminal caproyl units (labelled H^{7}), and has been previously reported. The signals at 4.78 and 4.11 ppm were not observed in the ^{1}H NMR spectra of either PCHC or PCL alone. They were proposed to be the carbonate and ester linkage unit signals on the basis of their $^{13}C\{^{1}H\}$, DEPT 135 and HSQC/HMBC NMR spectra (vide infra).

The new signal at 4.78 ppm was assigned to the cyclohexene methine protons (labelled H^{4}) of the carbonate junction unit – the cyclohexene ring attached to the polycaprolactone block. DEPT 135, showed that the correlating ^{13}C resonance (73.4 ppm in $^{13}C\{^{1}H\}$ spectrum) corresponds to a methine group (CH). 2D HMBC NMR spectroscopy detects heteronuclear correlations over the range of 2-4 bonds. In the HMBC spectrum of the copolymer the signals for the carbonate junction unit correlated with the methylene protons of the cyclohexene ring (1.3-2.0 ppm) from the polycarbonate block. The ^{1}H NMR spectrum of PCL formed using the LZn_2TFA_2/CHO catalyst system has a signal at 4.85 ppm, which has previously been reported to be the cyclohexene methine protons that are present in the chain extender motif (Section 2.4).[11] These cyclohexene methine protons were in a very similar environment to the cyclohexene methine protons of the carbonate junction unit, and therefore it was expected for them to result in similar chemical shifts. The combined evidence suggests the signal at 4.78 ppm was due to methine protons on a cyclohexene ring next to a polyester group. The new signal at 4.11 ppm was assigned to the first caproyl methylene group (labelled H^{5}) – the ester junction unit. DEPT 135 shows that the correlating ^{13}C resonance (67.8 ppm in $^{13}C\{^{1}H\}$ spectrum) corresponds to a methylene group (CH_2). In the HMBC spectrum of the copolymer, the signals for the ester junction unit, correlated with the polycaprolactone main chain methylene protons (1.25 – 1.8 ppm).

One curious finding was that the relative intensity of the junction unit for the carbonate block was greater than would be expected on the basis of reagent conversions and polymer molar masses. The ratio of the carbonate junction unit: carbonate main chain peaks (integrals of H_4:H_1) was observed to be 1:3, against a calculated value of 1:8, regardless of the solvent applied or the relaxation time (from t_1 2.2-25 s). The ratio of 1:8 was calculated by

determining the chain length of the polycarbonate or degree of polymerisation (DP) which is achieved by comparing the number of moles of CHO consumed by the number of chains have formed. Fromthe conversion of CHO, the degree of polymerisation ($\overline{DP}$) is 75 units ($\overline{DP}$ = conversion x moles of CHO = 0.15 x 500). However it has been established from the molar mass that multiple chains are being formed per catalyst, in this case ~ 5 chains. Thus, the average PCHC block length was ~15 units long.
As there are two linking units per block of PCHC so the expected ratio was 1:8. The ratio of ester junction units:ester main chain peaks (the integrals of H_4:H_5) was 1:29, which is in line with the value expected (1:28, calculcated from the degree of polymerisation and considering the presence of 5 chains per catalyst). Again this remains constant with longer relaxation times. The calculated ratio takes into account the 5 chains of PCHC being formed during the ROCOP.

The ratio of the carbonate junctions:ester junctions (the integrals of peaks H_4:H_5) was expected to be 1:1 for an ABA type block copolymer, however a value of 2:1 was consistently obtained. Contamination by AB type polymer would shift the integrals in the opposite direction; if such contaminants were present the ratio of carbonate:ester junctions would be expected to be 1:2. This fact combined with the finding that the caproyl linking unit:ester block ratio matches the calculated ratio so well, suggests there is minimal AB type polymer present. The higher than expected intensity of the carbonate junction signal implied that for the carbonate blocks, the 'junction unit' resonances in the ^{1}H NMR spectra actually corresponded to two cyclohexene carbonate repeat units at each of the junctions, in contrast for the ester blocks the junction corresponds to the expected single caproyl repeat unit which is directly connected to the carbonate block.

The $^{13}C\{^{1}H\}$ NMR spectrum provided further support for the formation of a block copolymer: there were only two peaks observed in the carbonyl region of the spectrum, assigned to carbonate and ester blocks, respectively. This finding implied there was little to no chain scrambling, i.e. there was limited transesterification / carbonylation between the blocks.

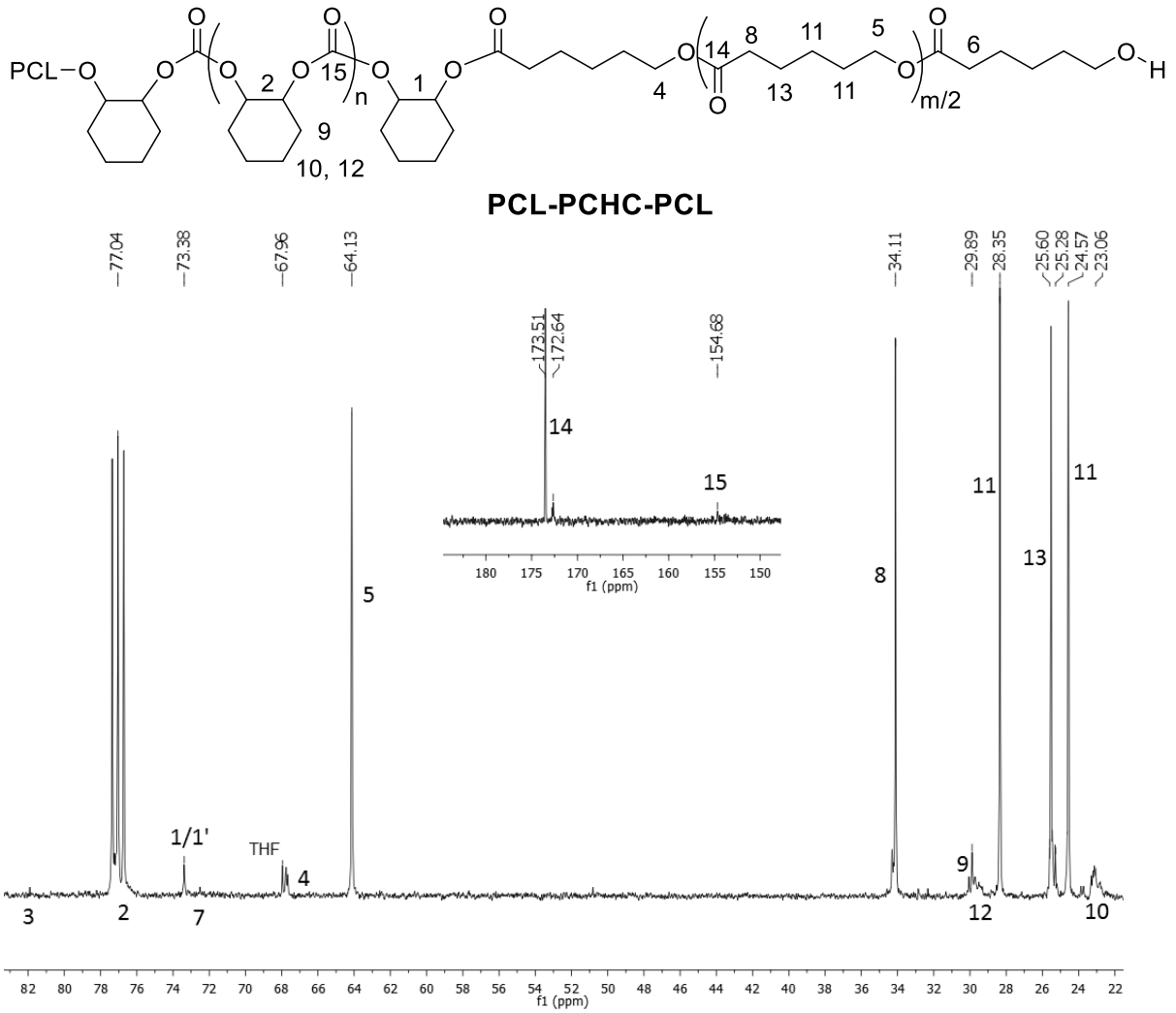

Figure 2.6.7: {^{1}H}^{13}C NMR spectrum of PCL-PCHC-PCL, (Table 2.3, Run 5).

The excerpt shows the carbonyl region.

Considering all of the above information the major products of the terpolymerisation of CHO/ε-CL/CO_2/[$LZn_2(OCOCF_3)_2$] had an ABA composition. The use of [$LZn_2(OCOCF_3)_2$] as a catalyst allows the formation of the copoly(ester-*b*-carbonates-*b*-ester)s in a truly one-pot method.

All previous reports of terpolymerisation of epoxide/lactone/CO_2, from other researchers, have resulted in the formation of random copolymers rather than polymers with a defined structure. A heterogeneous catalyst, zinc glutarate, has been applied to the terpolymerisation of PO/ε-CL/CO_2, and the resulting polymer was mostly comprised of polycarbonate blocks with random incorporation of short polyester blocks or even single ester linkages.[42,43,42,44]

Increasing the molar ratio of ε-CL in the feed ratio led to slightly greater ester block lengths but the copolymers remained rather ill-defined (Đ = 1.5-4.0). The homogeneous β-diketiminate zinc catalysts were also investigated for the terpolymerisation of LA/CHO/CO_2.[45] The structures of the copolymers were not discussed, although both carbonate and ester linkages were present. Curiously, using excess epoxide (CHO), the ratio of carbonate:ester linkages remains rather similar, despite decreasing the quantity of lactide in the monomer feed. Using a Schiff base tri-zinc catalyst with ε-CL/CHO/CO_2, resulted in a tapered block terpolymer, although it should be noted that significant quantities of cyclic carbonate was also formed.[46] Increasing the quantity of ε-CL in the feedstock, increased the proportion of ether linkages and cyclic carbonate formed, both of which are by-products of ROCOP. A detailed study was carried out into the polymerisation and it was discovered that these trizinc catalysts showed faster caprolactone polymerisation, with the first blocks being mostly polyester in composition, followed by tapered incorporation of carbonate units; this is interesting as it is quite different to the findings using the current di-zinc catalyst.[47] Another recent report used cross chain exchange to form a PCHC-PCL copolymer.[48] Cross chain exchange occurs when two polymerisations, in this case ε-Cl ROP and CHO/CO_2 ROCOP were occurring simultaneously and the presence of chain transfer reactions means that the polymer chains could 'swap' catalysts. The catalysts used were tin octanoate for the ROP and a Zn/Co DMC for ROCOP. This resulted in a block copolymer, albeit with a significant polyether contamination. The size of the blocks was controlled by the relative rates of chain transfer, which was controlled by the amount of alcohol added. The multi block copolymer had longer polycarbonate blocks compared to the ester blocks. The ^{1}H NMR signals of the carbonate and ester junction signals as described above were also reported for this block copolymer.

Compared to these previous catalysts and processes, the di-zinc catalyst leads to the selective preparation of ABA block copolymers of well-defined structures. By varying the amount of ε-CL in the monomer feed, it is possible to control the molar ratio of carbonate to ester linkages in the resulting polymer.

2.6.3 Properties

The thermal properties of the triblock copolymers were characterized using DSC and TGA and were compared against the homopolymers and blends (Table 2.5).

Table 2.5: The thermal properties of the triblock copolymers compared to mixtures of the polymers.

#	Polymer	M_n / g mol^{-1} a)	Molar ratio carbonate: ester linkages c)	T_g / °C b)	T_m / °C	T_c / °C
1	PCHC	920	1:0	108	-	-
2	PCL	1350	0:1	-	53*	-
3	Blend of PCL and PCHC	1350 920	1:1	-41 100	12	-
4	PCL-PCHC-PCL (Table 2.4, Run 6)	6,600	1:0.5	34	-	-
5	PCL-PCHC-PCL (Table 2.4, Run 1)	4,000	1:1	-13	-	-
6	PCL-PCHC-PCL (Table 2.4, Run 3)	6,500	1:2	-37	-	-
7	PCL-PCHC-PCL (Table 2.4, Run 2)	3,300	1:6	-54	27 (χ_c = 22%)	-4
8	PCL-PCHC-PCL (Table 2.4, Run 5)	13,800	1:4	-53	38 (χ_c = 28%)	-8
9	PCL-PCHC-PCL (Table 2.4, Run 4)	12,800	1:6	-54	40 (χ_c = 30%)	-10
10	PCL-PCHC-PCL (Table 2.4, Run 7)	12,500	1:10	-51	43 (χ_c = 48%)	23

* The crystallinity of this sample was too high for the glass transition to be observed. a) Determined by SEC with THF as the eluent, using polystyrene standards to calibrate the instrument b) The T_g was calculated from the third heating cycle of the DSC measurement and was heated at 10 °C/minute from -100 to 130 °C (# 1-3, 5-8) or 40 °C/minute from -80 to 100 °C(# 4, 9-10) c) Determined by ^{1}H NMR spectroscopy by comparison of the normalised integrals for the PCHC CH signals at 4.58 ppm and the PCL CH_2 signals at 4.05 ppm .

The values for the glass transition temperatures observed for the independent control samples of polycarbonate and polyester were slightly lower than those reported previously in the literature (PCHC: 117 and PCL: -60 °C).[49,50] This was due to the lower molar masses of the polymers studied here. A 1:1 blend of the two homopolymers showed the expected T_g for the PCHC portion but suppression of the crystallinity of PCL, as observed by a significant reduction in the T_m. The ABA copolymers showed controllable glass transition and melting temperatures, dependent on the composition and molar mass of the polymers. At 1:1 compositions of ester: carbonate, a single T_g was observed at -13 °C. For a 1:0.5 composition, a single T_g was also observed but at a higher temperature 34 °C. This suggests that the PCHC inhibits the crystallinity of the PCL, a finding which has previously been observed by Xaio and Meng in a series of rather less well defined terpoly(caprolactone-cyclohexene carbonates) and by Li *et al* with a series of blocky terpoly(caprolactone-cyclohexene carbonates).[46,48]As the proportion of ester blocks increases beyond 1:2, the glass transition temperature decreased, consistent with the increased content of PCL. Once the composition of ester exceeded 1:4, then crystallization of the PCL block was observed, resulting in both melting and crystallization peaks (Table 2.5, Runs 7-10). The temperatures at which these processes occurred are lower than for pure PCL, indicative of smaller crystalline domains due to the block copolymer structure. The χ_c (% crystallinity) of the samples was determined for those materials exhibiting a T_m (Section 2.3.7);[20] overall, the χ_c increases quite significantly and values in the range 22-48 % are observed (Table 2.5, Runs 7-10). In comparison, the terpolymers prepared by Xiao and Meng showed higher crystallinities (χ_c 80-90 %), which may relate to the different chain repeat unit structures as the materials were not ABA type block copolymers.[46] For the polymers prepared in this study, glass transition temperatures were also observed in all cases.

The Fox-Flory equation can be used to predict the T_g values for miscible polymers, however for these copolymers the calculated values were in poor agreement with the experimental values, particularly at higher ester contents, indicative of poor miscibility between the blocks. A similar finding was also observed for the blend (Table 2.5, Run 3), however the fact that the T_g of the block copolymer with a low ester content is so highly moderated by the composition of the block copolymer (T_g varies from 34 to -37 °C with compositions between 1:0.5-1:2), suggested that the blocks were at least partially miscible. It could be that just the

regions in closest proximity to the junction are miscible, but when the ester content is low this may include the majority of the chain. Once the polyester block is longer, and becomes semicrystalline, the T_g is reasonably constant regardless of the composition (1:6 – 1:10). This suggests that once the polyester block is semicrystalline, it is no longer miscible with the amorphous polycarbonate block. One potential reason for the lack of T_g for the carbonate block of the immiscible polymers, is its low proportion making it undetectable. The degree of crystallinity of the PCL block was reduced by the presence of polycarbonate.

Both the undefined copoly (caprolactone-cyclohexene carbonate) produced by Meng *et al* and the multiblock poly (caprolactone-cyclohexene carbonate) produced by Fan *et al* (described in Section 2.6.2) have similar thermal properties.[46,48] At low caprolactone content, a single T_g was observed, for the undefined copolymer this appears around 46 °C, but for the multiblock copolymer it occured at 71-79 °C. As the caprolactone content increases the T_g was no longer observed, rather a T_m was observed at 45-58 °C with the value increasing with PCL content for both polymers. The experiments were not conducted at temperatures below -30 °C which is a limitation as the T_g of PCL is -60 °C. In any case, the high PCL content terpolymers may have a T_g around -55 °C that is not being measured. In all cases the presence of the PCHC inhibits the crystallisation of the PCL and despite the immiscibility only a single T_g is observed. The immiscibility was tested by the examination of blends of PCHC and PCL, which displayed two T_g values, one from each polymer block.

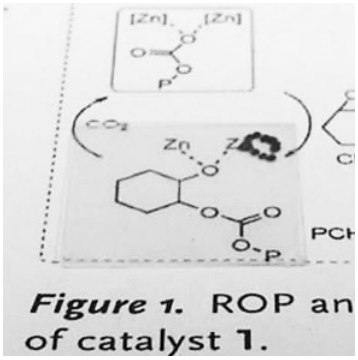

Figure 2.6.8: A spin coated PCL-PCHC-PCL film sitting on a picture from reference [4].
Picture reproduced with permission. The polymer was synthesised according to Table 2.3, Run 5. The film is completely transparent.

It is common that block copolymer containing a crystalline block results in the formation of semicrystalline copolymers. These semicrystalline copolymers typically display a single T_g value and a T_m. The most commonly reported example is poly(propylene carbonate-b-lactide) where the PPC and PLA blocks have been shown to be immiscible. Blends of the polymers showed two glass transition temperatures at 32 °C (PPC) and 57 °C (PLA). Terpolymers, prepared using a rare earth ternary catalyst, displayed a single T_g (34 °C), and with high PLA content polymers also displaying a T_m (158 °C).[51] Poly(propylene-b-caprolactone) displayed similar results, with the T_g of the PPC block being observed, along with the melting temperature of the PCL.[42,43]

As part of a preliminary evaluation of the copolymers, thin films were spin coated from tetrahydrofuran solutions onto glass slides. Figure 2.6.8 shows photographs of the glass slides (with images/text behind) which demonstrate the transparency of the films. In order to probe the mechanical properties of the PCL-PCHC-PCL copolymers, they were used as polyols in the formation of polyurethanes. The copolymers were coupled with methylene diphenyl isocyanate (MDI), using tin octanoate as a catalyst. The molar mass was sufficient for tensile mechanical data to be collected.

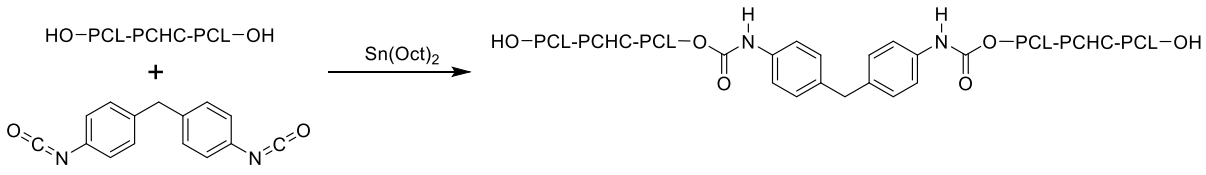

Figure 2.6.9: Scheme showing the formation of polyurethanes.

Reaction carried out using a 1:1 ratio of Isocyanate to polymer, with 1 wt% of $Sn(Oct)_2$, in toluene, at 60 °C for 2 h.

Films of the polyurethanes were made by solvent casting the polymers from dichloromethane solution. Dog bones were cut of the poly(caprolactone) and poly(caprolactone-cyclohexene carbonate-caprolactone) polyurethanes. It was not possible to cut dog bones of the poly(cyclohexene carbonate) polyurethane as the film was too brittle. The mechanical

properties of PCHC have been reported in the literature and it is a strong polymer (high Young's modulus) with a relatively high yield point but which is very inflexible.[52] The poly(caprolactone) polyurethane (PCL PU) behaved as a plastic, it was reasonably strong (E = 151 MPa) at low strain, and had a low yield point (10.6 MPa). After the yield point it stretched. The instrument used to measure the stress strain curves can only stretch the materials to 450 %, and at this point the PCL PU was still intact. The poly(caprolactone-cyclohexene carbonate-caprolactone) polyurethane (PCHC/PCL PU) behaves as a ductile plastic. The Young's modulus was considerably lower than for PCL PU. The yield point is 53 MPa, but the distinction between the elastic and plastic regions is not clear. The elongation at break of the PCHC/PCL PU was greater than 450 %. The copolymer has combined the higher yield point of PCHC with the flexibility of PCL but has a considerably lower Young's modulus than either of the homopolymers.

Table 2.6: Mechanical properties of the triblock copolymers and homopolymers.

Polymer	*PCHC:PCL* [a)]	M_n [b)]	M_n *(PU)* [b)]	E /MPa	Elongation at break /%	Yield point /MPa
PCHC	1:0	7,100 (1.11)	52,700 (1.24)	3600-3700 *	1-2*	40-44*
PCL	0:1	5,400 (1.24)	85,000 (1.41)	151	>450	10.6
PCL-PCHC-PCL	1:7	13,800 (1.50)	74,800 (1.11)	9.9	>450	53

a) Determined by ^{1}H NMR spectroscopy by comparison of the normalised integrals for the PCHC CH signals at 4.58 ppm and the PCL CH_2 signals at 4.05 ppm b) determined by SEC with THF as the eluent, using polystyrene standards to calibrate the instrument. *[52]

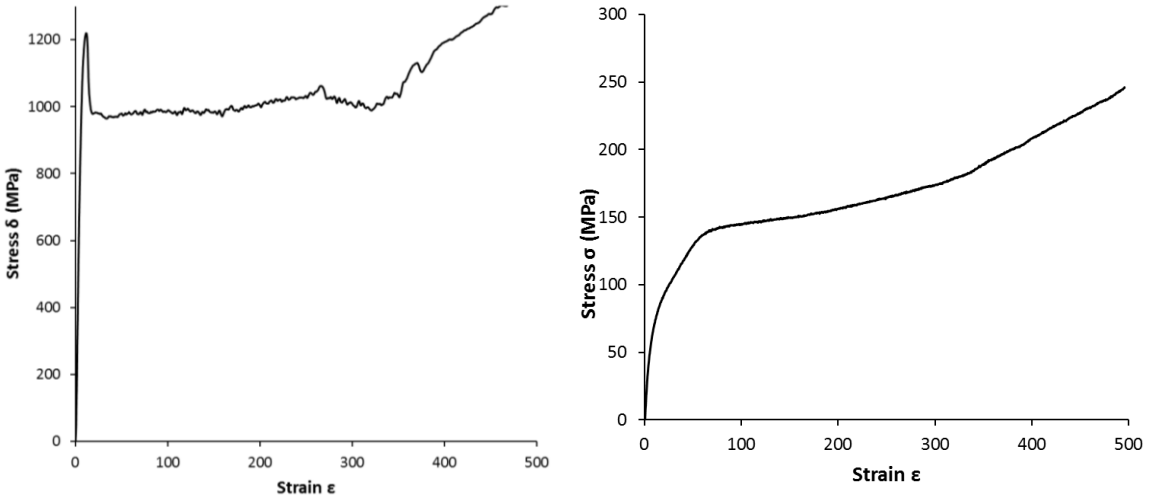

Figure 2.6.10: Plots of stress-strain curves for PCL (Left) and PCL-PCHC-PCL (Right).

2.7 Conclusions and Outlook

A di-zinc catalyst undergoes switchable catalysis and delivers polymers with dihydroxyl endgroups. It produced dihydroxyl terminated polycarbonate, even under the dilute conditions suitable for block copolymer formation. The combination of the di-zinc catalyst and cyclohexene oxide formed an active catalytic system for the ring opening polymerisation of ε-caprolactone. It was also used for the terpolymerisation of cyclohexene oxide, carbon dioxide and ε-caprolactone, whereby initially the formation of poly(cyclohexene carbonate) occurs. Once the carbon dioxide was removed, the ring opening polymerisation of ε-caprolactone occurred. The terpolymerisation method was sufficiently robust, that altering the ratio of monomers did not affect the observed selectivity. Altering the monomer feed ratio, resulted in a predictable change to the carbonate: ester ratio of the block copolymers and the composition of the polymer can be accurately predicted from the conversions of monomers. Thus, materials with tuneable compositions of ester (33 – 90 %) and molar masses (3,000 -14,000 $gmol^{-1}$) were formed. The copolymers were found to have a predominately ABA type block structure as established using NMR spectroscopy, ^{1}H DOSY spectroscopy; SEC analysis and DSC. All data indicates ABA triblock copolymer formation. The relative difference in the rates of initiation from primary *versus* secondary alkoxides results in more polydisperse samples and some variation in the chain length of the triblock copolymers.

The thermal properties of the polymers were very strongly dependent on the quantity of ester present. The presence of the carbonate block (more than 20 %) disrupted the crystallinity of the polyester, forming semi-crystalline block copolymers.

Overall the findings in this chapter demonstrate the potential to apply the switchable catalysis using [$LZn_2(OCOCF_3)_2$]. The catalyst was highly selective for polyol formation and this was exploited to prepare ABA type block copolymers. The proof of concept studies were applied only to cyclohexene oxide as the epoxide and ε-caprolactone as the lactone. It is of interest to establish whether the same selectivity occurs using a wider range of monomers and these findings are presented in Chapter 3.

References

(1) Kember, M. R.; Knight, P. D.; Reung, P. T. R.; Williams, C. K. *Angew. Chem. Int. Ed.* **2009**, *48*, 931.
(2) Jutz, F.; Buchard, A.; Kember, M. R.; Fredriksen, S. B.; Williams, C. K. *J. Am. Chem. Soc.* **2011**, *133*, 17395.
(3) Kember, M. R.; Buchard, A.; Williams, C. K. *Chem. Commun.* **2011**, *47*, 141.
(4) Romain, C.; Williams, C. K. *Angew. Chem. Int. Ed.* **2014**, *53*, 1607.
(5) Ajellal, N.; Carpentier, J.-F.; Guillaume, C.; Guillaume, S. M.; Helou, M.; Poirier, V.; Sarazin, Y.; Trifonov, A. *Dalton Trans.* **2010**, *39*, 8363.
(6) Aida, T.; Inoue, S. *Acc. Chem. Res.* **1996**, *29*, 39.
(7) Ikpo, N.; Barbon, S. M.; Drover, M. W.; Dawe, L. N.; Kerton, F. M. *Organometallics* **2012**, *31*, 8145.
(8) Chang, C.-H.; Chuang, H.-J.; Chen, T.-Y.; Li, C.-Y.; Lin, C.-H.; Lee, T.-Y.; Ko, B.-T.; Huang, H.-Y. *J. Polym. Sci., Part A: Polym. Chem.* **2016**, *54*, 714.
(9) Cheng, M.; Moore, D. R.; Reczek, J. J.; Chamberlain, B. M.; Lobkovsky, E. B.; Coates, G. W. *J. Am. Chem. Soc.* **2001**, *123*, 8738.
(10) Chamberlain, B. M.; Cheng, M.; Moore, D. R.; Ovitt, T. M.; Lobkovsky, E. B.; Coates, G. W. *J. Am. Chem. Soc.* **2001**, *123*, 3229.
(11) Zhu, Y.; Romain, C.; Poirier, V.; Williams, C. K. *Macromolecules* **2015**, *48*, 2407.
(12) Romain, C.; Zhu, Y.; Dingwall, P.; Paul, S.; Rzepa, H. S.; Buchard, A.; Williams, C. K. *J. Am. Chem. Soc.* **2016**, *138*, 4120.
(13) Buchard, A.; Jutz, F.; Kember, M. R.; White, A. J. P.; Rzepa, H. S.; Williams, C. K. *Macromolecules* **2012**, *45*, 6781.
(14) Spyros, A.; Argyropoulos, D. S.; Marchessault, R. H. *Macromolecules* **1997**, *30*, 327.
(15) Wagner, H. L. *J. Phys. Chem. Ref. Data* **1985**, *14*, 611.

(16) Kim, J. G.; Cowman, C. D.; LaPointe, A. M.; Wiesner, U.; Coates, G. W. *Macromolecules* **2011**, *44*, 1110.
(17) Meduri, A.; Fuoco, T.; Lamberti, M.; Pellecchia, C.; Pappalardo, D. *Macromolecules* **2014**, *47*, 534.
(18) Viéville, J.; Tanty, M.; Delsuc, M.-A. *Journal of Magnetic Resonance* **2011**, *212*, 169.
(19) Zawaneh, P. N.; Doody, A. M.; Zelikin, A. N.; Putnam, D. *Biomacromolecules* **2006**, *7*, 3245.
(20) Crescenzi, V.; Manzini, G.; Calzolari, G.; Borri, C. *Eur. Polym. J.* **1972**, *8*, 449.
(21) Kember, M. R.; White, A. J. P.; Williams, C. K. *Inorg. Chem.* **2009**, *48*, 9535.
(22) Kember, M. R.; Copley, J.; Buchard, A.; Williams, C. K. *Polym. Chem.* **2012**, *3*, 1196.
(23) Kember, M. R.; Williams, C. K. *J. Am. Chem. Soc.* **2012**, *134*, 15676.
(24) Kowalski, A.; Duda, A.; Penczek, S. *Macromolecules* **1998**, *31*, 2114.
(25) Wroblewski, A. E.; Lensink, C.; Markuszewski, R.; Verkade, J. G. *Energy & Fuels* **1988**, *2*, 765.
(26) Klaus, S.; Lehenmeier, M. W.; Anderson, C. E.; Rieger, B. *Coord. Chem. Rev.* **2011**, *255*, 1460.
(27) Coates, G. W.; Moore, D. R. *Angew. Chem. Int. Ed.* **2004**, *43*, 6618.
(28) Nakano, K.; Kamada, T.; Nozaki, K. *Angew. Chem. Int. Ed.* **2006**, *45*, 7274.
(29) Darensbourg, D. J. In *Synthetic Biodegradable Polymers*; Rieger, B., Künkel, A., Coates, W. G., Reichardt, R., Dinjus, E., Zevaco, A. T., Eds.; Springer Berlin Heidelberg: Berlin, Heidelberg, 2012, p 1.
(30) Nakano, K.; Nakamura, M.; Nozaki, K. *Macromolecules* **2009**, *42*, 6972.
(31) Wu, G.-P.; Darensbourg, D. J.; Lu, X.-B. *J. Am. Chem. Soc.* **2012**, *134*, 17739.
(32) Lu, X.-B.; Ren, W.-M.; Wu, G.-P. *Acc. Chem. Res.* **2012**, *45*, 1721.
(33) Ren, W.-M.; Zhang, X.; Liu, Y.; Li, J.-F.; Wang, H.; Lu, X.-B. *Macromolecules* **2010**, *43*, 1396.
(34) Sugimoto, H.; Kuroda, K. *Macromolecules* **2008**, *41*, 312.
(35) Darensbourg, D. J.; Mackiewicz, R. M.; Rodgers, J. L.; Phelps, A. L. *Inorg. Chem.* **2004**, *43*, 1831.
(36) Darensbourg, D. J.; Mackiewicz, R. M. *J. Am. Chem. Soc.* **2005**, *127*, 14026.
(37) Darensbourg, D. J.; Mackiewicz, R. M.; Billodeaux, D. R. *Organometallics* **2005**, *24*, 144.
(38) Bok, T.; Yun, H.; Lee, B. Y. *Inorg. Chem.* **2006**, *45*, 4228.
(39) Xiao, Y.; Wang, Z.; Ding, K. *Chem. Eur. J.* **2005**, *11*, 3668.
(40) Dean, R. K.; Dawe, L. N.; Kozak, C. M. *Inorg. Chem.* **2012**, *51*, 9095.
(41) van Meerendonk, W. J.; Duchateau, R.; Koning, C. E.; Gruter, G.-J. M. *Macromolecules* **2005**, *38*, 7306.
(42) Hwang, Y.; Jung, J.; Ree, M.; Kim, H. *Macromolecules* **2003**, *36*, 8210.
(43) Hwang, Y.; Kim, H.; Ree, M. *Macromolecular Symposia* **2005**, *224*, 227.
(44) Hwang, Y.; Kim, H.; Ree, M. *Mac. Symp.* **2005**, *224*, 227.
(45) Kröger, M.; Folli, C.; Walter, O.; Döring, M. *Adv. Synth. Catal.* **2006**, *348*, 1908.
(46) Xu, Y.; Wang, S.; Lin, L.; Xiao, M.; Meng, Y. *Polym. Chem.* **2015**, *6*, 1533.
(47) Xu, Y.; Wang, S.; Lin, L.; Xiao, M.; Meng, Y. *Polym. Chem.* **2015**, *6*, 1533.

(48) Li, Y.; Hong, J.; Wei, R.; Zhang, Y.; Tong, Z.; Zhang, X.; Du, B.; Xu, J.; Fan, Z. *Chem. Sci.* **2015**, *6*, 1530.
(49) Tang, M.; Purcell, M.; Steele, J. A. M.; Lee, K.-Y.; McCullen, S.; Shakesheff, K. M.; Bismarck, A.; Stevens, M. M.; Howdle, S. M.; Williams, C. K. *Macromolecules* **2013**, *46*, 8136.
(50) Mang, S.; Cooper, A. I.; Colclough, M. E.; Chauhan, N.; Holmes, A. B. *Macromolecules* **2000**, *33*, 303.
(51) Gu, L.; Qin, Y.; Gao, Y.; Wang, X.; Wang, F. *Chin. J. Chem* . **2012**, *30*, 2121.
(52) Koning, C.; Wildeson, J.; Parton, R.; Plum, B.; Steeman, P.; Darensbourg, D. J. *Polymer* **2001**, *42*, 3995.

Chapter 3 : ABA Triblocks prepared from Other Lactones

3.1 Introduction

While the use of [$LZn_2(OCOCF_3)_2$] and switch chemistry to form poly(ester-*b*-carbonates), was a successful method, the poly(caprolactone-*b*-cyclohexene-*b*-caprolactone) produced has a broad dispersity and lacked a homogeneous structure. The ring opening polymerisation of ε-caprolactone was not fully controlled due to the difference in the rate of insertion of primary and secondary alkoxides into [$LM_2(X)_2$].[1] After the initial insertion of a ε-CL unit, the two chain ends differ in reactivity, which causes faster propagation from the primary alkoxide chain end resulting in non-homogeneous chain structures. The chemoselective control displayed by [$LZn_2(OCOCF_3)_2$] depended on the ring opening of the lactone being slower than the insertion of carbon dioxide. It was of interest to verify whether the use of alternative lactones would change the selectivity displayed by [$LZn_2(OCOCF_3)_2$], and whether or not ABA triblock copolymers could be formed. The use of alternative lactones also provides the opportunity to access different thermal and mechanical properties compared to the PCL-PCHC-PCL block copolymer. The two lactones selected were δ-valerolactone (δ-VL) and ε-decalactone (ε-DL).

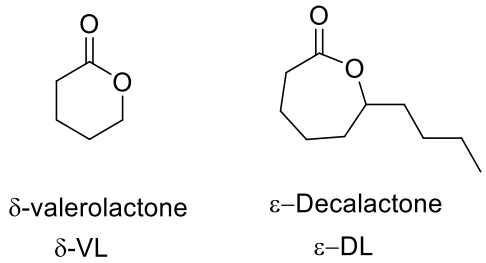

Figure 3.1.1: Scheme showing the structures of δ-valerolactone and ε-decalactone.

δ-Valerolactone is a six membered lactone and can be considered a model for various bio derived lactones.[2,3] An important consideration is that the low ring strain of 6-membered rings means that their ring opening polymerisation is less thermodynamically favoured and results in a lower ceiling temperature compared to PCL.[2,4-16] This prevents full monomer

conversion, limiting the molar masses that are accessible and complicating its use in block copolymer formation.

ε-Decalactone can be derived from castor oil.[17,18] It can also be considered a model for other substituted lactones, such as menthone, many of which can be easily bioderived.[19] Poly(ε-decalactone) is an amorphous polymer and has only received attention in recent years.[3,17,18,20-22] There are also several studies of PDL copolymers with lactide, as PLA and PDL are immiscible. The PDL acts as a soft segment to the PLA's hard segment forming a thermoplastic elastomer.[17,18,21] The ROP of PDL is often reported as significantly slower than that of ε-Cl due to steric hindrance.[9,23] The ring opening of ε-decalactone has been reported by Williams and co-workers using both [$LZn_2(OAc)_2$] and [$LZn_2(Ph)_2$].[24] The ROP of ε-DL was noted to be significantly slower than that of ε-CL using [$LZn_2(Ph)_2$] (TOF = 7.2 h^{-1} *vs* 154 h^{-1} respectively). An important benefit of using ε-DL compared to ε-CL is that the propagating species is a secondary alkoxide (compared to the primary alkoxide formed during ε-CL propagation, section 2.1). This is expected to be important in improving chain homogeneity when using CHO as the switch agent.

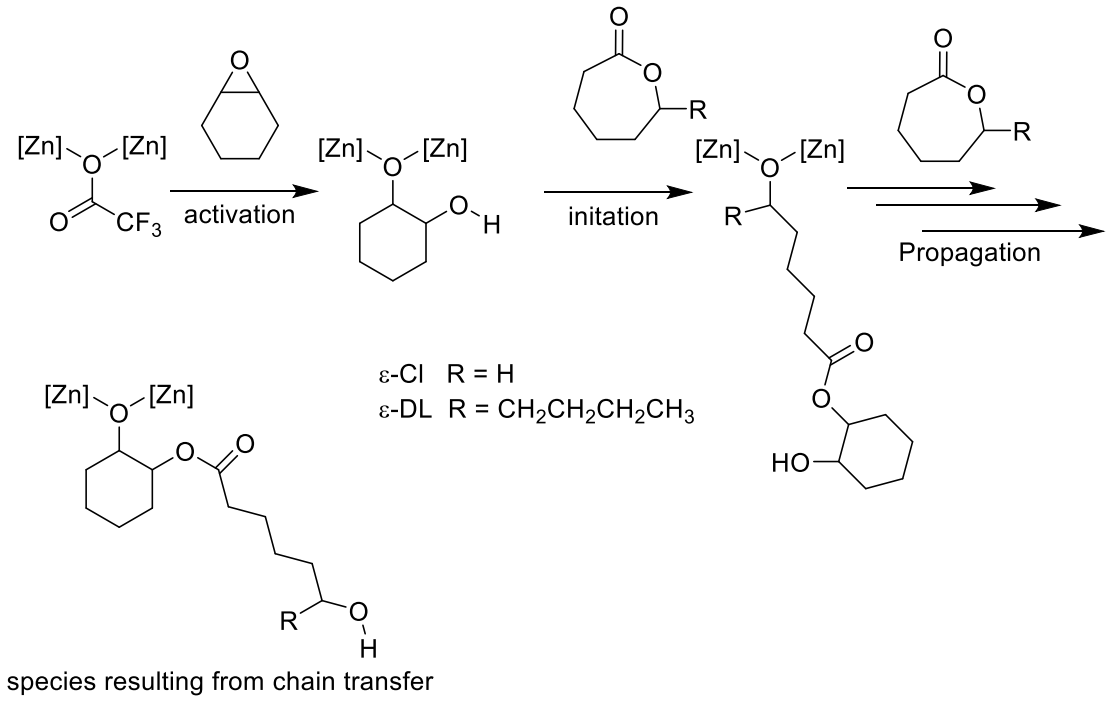

Figure 3.1.3: Scheme showing the proposed mechanism for the ROP of ε-DL.

The properties of PCL-PCHC-PCL were mostly dominated by the ester component of the block copolymer. This is because the ester block (PCL) is a larger proportion of the block copolymer. By changing the polyester in the poly(ester-carbonate-ester), the properties of the block copolymer should be altered. PVL has a very similar structure to PCL and therefore there are many similarities in their physical behaviour. PVL is slightly less crystalline than PCL, indicated by its lower melting temperature (T_m = 58 °C), the lower crystallinity may also be responsible for PVL having a marginally higher Young's modulus than PCL.[4,25] None the less, PVL is significantly less flexible than PCL, and has a much shorter elongation at break (200 % for PVL *versus* 1000 % for PCL).[4,25] The physical properties of PDL are much less reported than PCL as it is an amorphous polymer with a low T_g (-53 °C) and so, at low molar masses, it is a gel/fluid at room temperature. This makes it difficult to form films to test for the physical properties. The amorphous nature of PDL is completely different to PCL, so it should provide a completely different set of properties to the triblock copolymer.

Table 3.1: Comparison of the thermal and physical properties of polylactones.

	T_g / °C	T_m / °C	Tensile strength σ /MPa	Young's Modulus (E) /GPa	Elongation at break / %
PCL[25]	-60 - -65	58-65	20-42	0.2-0.44	300-1000
PVL[4]	-67	59	-	0.57	150-200
PDL[18]	-53	-	-	-	-

3.2 Aims

While the switch catalysis of [$LZn_2(OCOCF_3)_2$] has been fully explored with the CHO/ε-CL system, it is interesting to know whether or not alternative lactones will follow the same selectivity: with ROCOP occurring exclusively when carbon dioxide is present and ROP occurring only once the carbon dioxide has been removed. δ-Valerolactone and ε-decalactone were chosen because they have different properties to ε-caprolactone and are good representative monomers for broader classes of 6- and 7- membered rings.

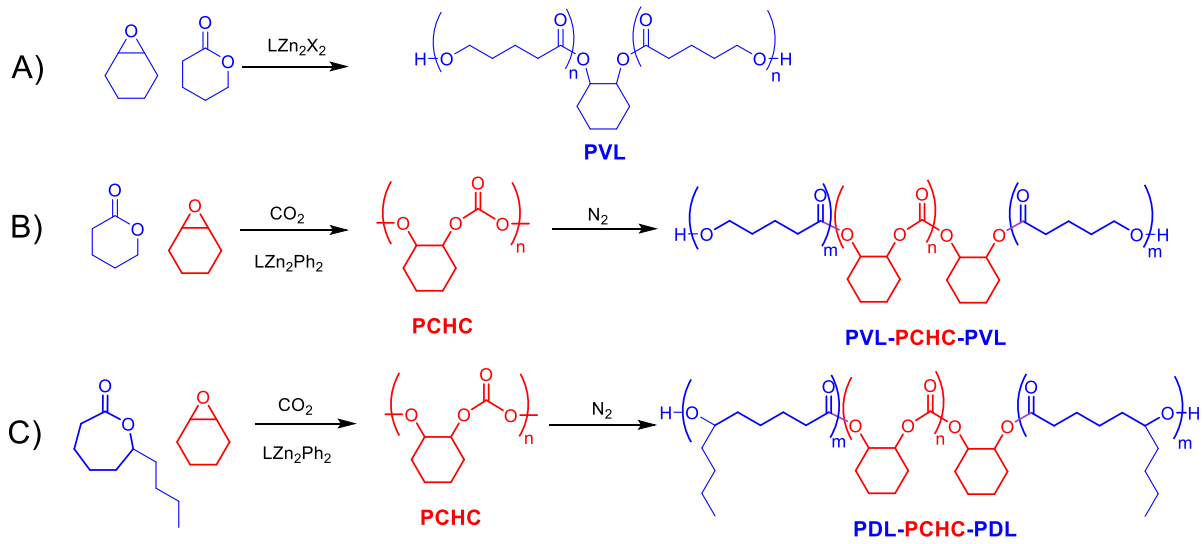

Figure 3.2.1: Scheme showing the targeted reactions and copolymer structures.

The method of forming ABA type block copolymers, developed in the previous chapter will be used with the lactones: δ-VL and ε-DL. The selectivity of the system will be confirmed using ^{1}H NMR spectroscopy. The structure of the resulting copolymers will be investigated using SEC analysis, ^{1}H NMR spectroscopy and DOSY NMR spectroscopy. The properties of the copolymers with be determined and compared with the parent polymers and the equivalent PCL-PCHC-PCL copolymers.

3.3 Ring Opening Polymerisation of δ-valerolactone

3.3.1 Theoretical Calculations

δ-Valerolactone is a cyclic lactone which can undergo ring opening polymerisation to form an aliphatic polyester.[4] The ring opening of δ-valerolactone is not as thermodynamically favoured as the ring opening of ε-CL.[26] This means in most cases the polymerisations reach equilibrium prior to all the monomer being consumed and it results in an equilibrium monomer concentration.[26] During ring opening polymerisation, the entropy decreases due to the loss of translational degrees of freedom. For small ring sizes (3-4) this loss is compensated for by the release of ring strain. With higher ring sizes (>6), although there is

little ring strain, the resulting polymer chain is very flexible and this means the loss of entropy is not so great and the polymerisations often proceed at higher temperatures.[26] With intermediate ring sizes, the ring strain is low and the loss of entropy can be a limitation. When polymerisation does occur, the equilibrium position depends on the conditions.[26]

The enthalpy and entropy of the ring opening polymerisation δ-valerolactone are ΔH_p^0 = -27.4 kJ·mol^{-1} and ΔS_p^0 = -65.0 J·mol^{-1}K^{-1} respectively. As the entropy is negative, at higher temperatures the equilibrium is shifted completely to the monomers and the polymerisation no longer occurs. This temperature is the ceiling temperature (T_c) and is defined in equation 1.

$$T_c = \frac{\Delta H_P^\circ}{\Delta S_P^\circ + R ln[M]_0} \quad \text{equation 1)}^{26}$$

[T_c = Ceiling temperature, ΔH_p^0 = enthalpy change, ΔS_p^0 = entropy change, R = gas constant, [M] = concentration of monomer]

Under the standard conditions used for ROP with [$LZn_2(OCOCF_3)_2$] (1:1000:100 Catalyst:CHO:lactone with 0.02 g catalyst) the initial concentration of lactone wa 0.84 M. At this concentration the ceiling temperature was predicted to be 139 °C. It was also possible to calculate the maximum conversion under these conditions, at the reaction temperature (80 °C) (equation 3).

$$[M_{eq}] = \exp\left(\frac{\Delta H_p^\circ}{RT} - \frac{\Delta S_p^\circ}{R}\right). \quad \text{(equation 2)}^{26}$$

[T = Temperature, $[M]_{eq}$ = concentration of monomer at equilibrium]

$$\text{Conversion} = \frac{1-[M_{eq}]}{1}. \quad \text{(equation 3)}^{26}$$

Using the conditions described above, the $[M_{eq}]$ was 0.22 M and therefore, the maximum conversion should be 79 %.

3.3.2 Polymerisations

The catalytic system derived from [$LZn_2(OCOCF_3)_2$] and CHO was tested for the ROP of δ-VL. The reaction between [$LZn_2(OCOCF_3)_2$], CHO and δ-VL resulted in the selective formation of polyester. The polymerisation was rapid (TOF = 100 h^{-1}) but there was a significant lag time (~20 minutes). The lag time can be observed by *in-situ* ATR-IR spectroscopy and also by ^{1}H NMR analysis (Figure 3.3.2). The IR absorption at 1058 cm^{-1}, which has been assigned to δ-VL, can be observed to decrease only after 20 minutes and then reached a constant value after 60 minutes (Figure 3.3.1). The IR absorption at 1186 cm^{-1}, which has been assigned to PVL, underwent a concurrent increase in intensity. The ^{1}H NMR spectroscopy showed there was very little conversion of δ-VL to PVL before 20 minutes (<5 %) and after this point the conversion increased rapidly until it reached ~79 % at around 60 minutes. The conversion was calculated by the comparison of the integrals of the peaks at 4.29 ppm (methylene protons of δ-VL) and 4.07 ppm (methylene protons of PVL). The maximum conversion the polymerisation reaches was 79 %, which is in exact agreement with the theoretical maximum conversion under these conditions as calculated in section 3.3.1.

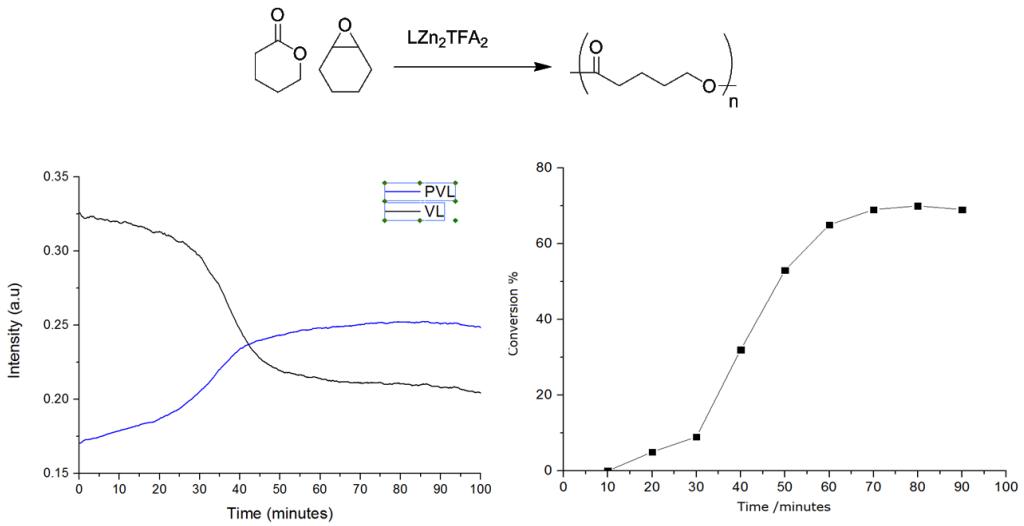

Figure 3.3.1: The ROP of δ-VL using [$LZn_2(OCOCF_3)_2$]/CHO.

Left: Intensity changes of selected IR resonances. The absorption at 1085 cm^{-1} is assigned to δ-valerolactone, whilst that at 1186 cm^{-1} is assigned to polyvalerolactone. Right: Plot showing the conversion of δ-VL with time.

The polymerisation was observed to be well controlled, with the molar mass increasing linearly with the conversion and the dispersity values remaining narrow throughout the polymerisation (Đ < 1.35).

The structure of the PVL was analysed by NMR spectroscopy and MALDI-ToF spectrometry. MALDI-ToF analysis showed two PVL series, one featured a single ring opened cyclohexene unit as the end group, and the other was cyclic polyvalerolactone.

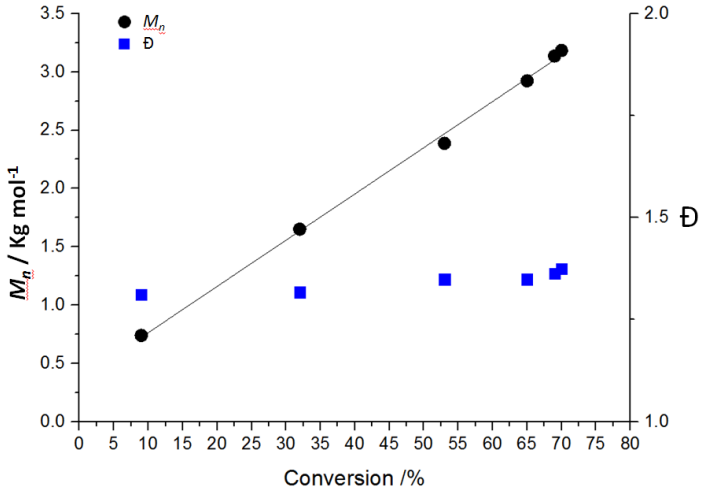

Figure 3.3.2: Graph showing the linear correlation between the % conversion of δ-VL and the molar mass of PVL.

M_n determined by SEC with THF as the eluent, using polystyrene standards to calibrate the instrument.

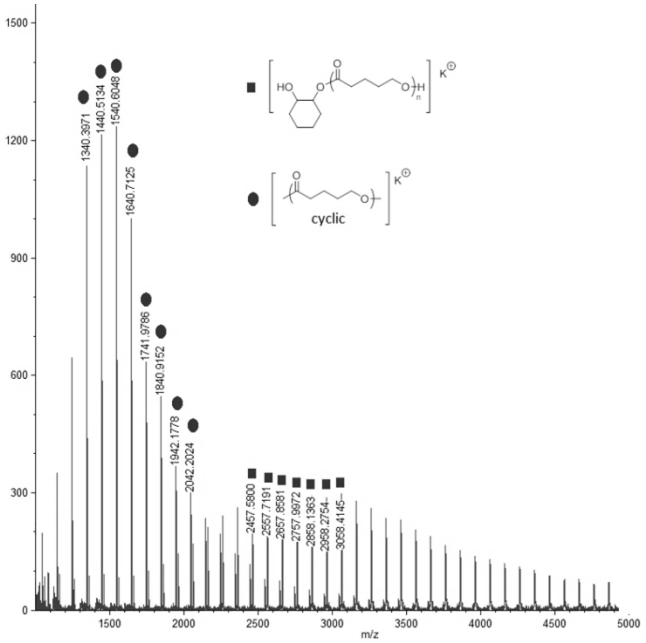

Figure 3.3.3: MALDI-ToF spectrum of PVL, (Table 3.2, Run 1).

The polyester polyol series are represented by: $[(C_5H_8O_2)_m+C_6H_{12}O_2+K]^+ = [(110.05)_m+116.16+39.1]^+$ and $[(C_5H_8O_2)_m+K]^+ = [(110.05)_m+39.1]^+$

The ^{1}H NMR spectrum of polyvalerolactone, showed the characteristic main chain signals for PVL at 3.66 and 4.83ppm. There were also multiple end group signals in both the ^{1}H NMR and 2D NMR spectra. Such findings are comparable with PCL formed using $[LZn_2(OCOCF_3)_2]$/CHO, whereby the cyclohexene unit can either be an end group or a chain extender. Indeed, when the ^{31}P NMR end group analysis was carried out on PVL, signals for both primary and secondary hydroxyls were observed (Figure 3.3.5). The presence of two species was due to the difference in the rate of insertion of a primary and secondary hydroxide into the zinc carboxylate (/carbonate) bond. The rate of polymerisation of δ-VL was slightly slower than that of ε-CL, so the disparity between the rate of insertion and propagation was not as great and therefore slightly less of the asymmetric species wasproduced. It was not possible to differentiate the cyclic species from the linear species by NMR spectroscopy.

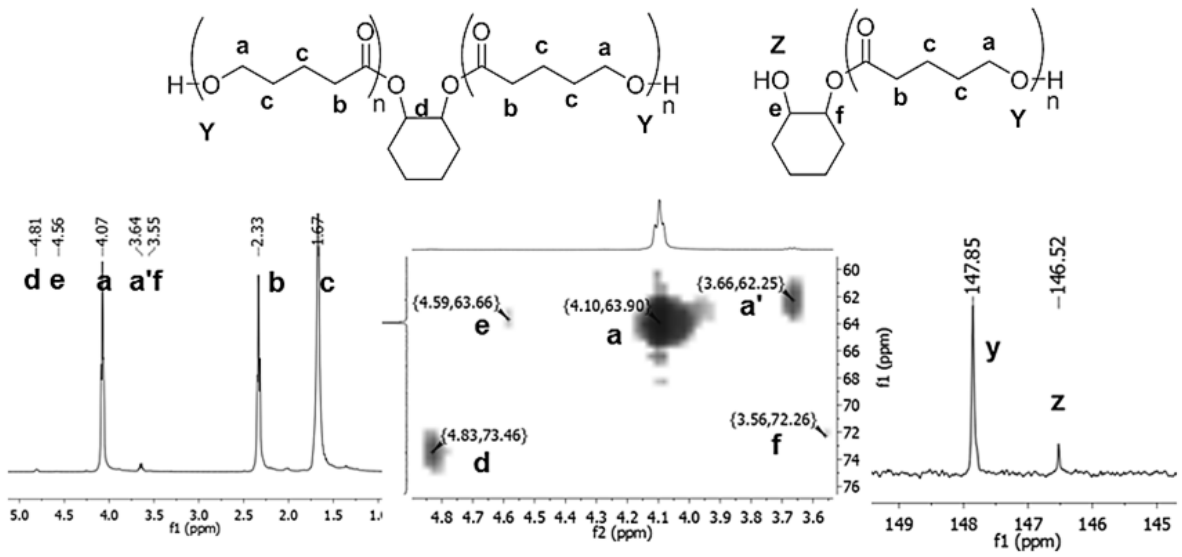

Figure 3.3.5: Scheme showing the structures of the symmetrical and unsymmetrical PVL chains.

Left: ^{1}H NMR spectrum of PVL, with assignments. Middle: HSQC spectrum showing the end groups of both species. Right: ^{31}P end group analysis of PVL, It shows that both 1° and 2° hydroxyl groups are present.

One significant difference compared to ROP using ε-CL was that the reaction between $[LZn_2(OCOCF_3)_2]$ and δ-VL without any CHO being present resulted in polyester formation. The reaction of a loading of 1:400 equivalents of $[LZn_2(OCOCF_3)_2]$:δ-VL resulted in 45 % PVL formation after 24 hours. This may be due to δ-VL being rather more susceptible to ionic ROP where any traces of H^+ may function as catalysts. It is known that $[LZn_2(OCOCF_3)_2]$ contains additional water (~5 equiv.) due to the use of hydrated zinc trifluoroacetate in the synthesis. In a control experiment between 2 equivalents of water and δ-VL (no catalyst present), a reaction occured leading to a new signal appearing in the ^{1}H NMR spectrum at 3.90 ppm. No reaction was observed between ε-CL and water under the same conditions. It is observed that even low quantities of water reacted with δ-VL to set up an equilibrium to form 5-hydroxypentanoic acid. The signal at 3.90 ppm resulted from the formation of this species. It is proposed that the free acid can react with δ-VL *via* an activated monomer mechanism to generate PVL and also react directly with the catalyst *via* acid

exchange. When the reaction between $[LZn_2(OCOCF_3)_2]$ and δ-VL was carried out under a CO_2 atmosphere (1 bar), the formation of polyester was reduced (TOF = 2 h^{-1} *vs* 7.5 h^{-1}). It may be that carbon dioxide can insert into the propagating species and switch off catalysis.

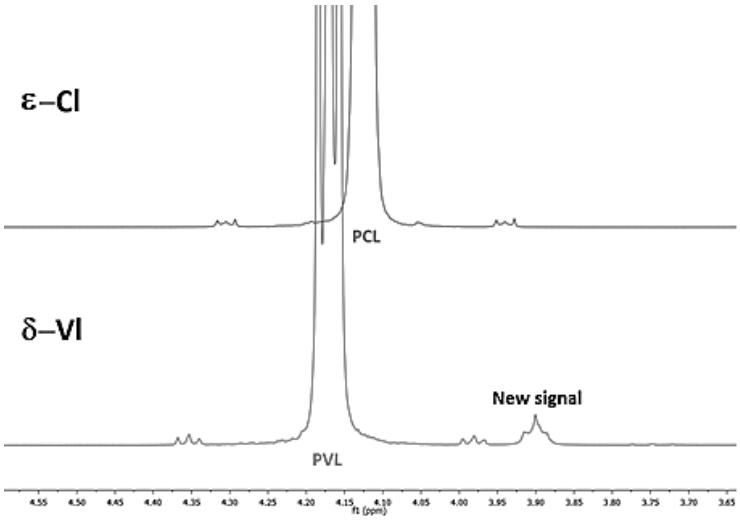

Figure 3.3.6: Excerpts from the ^{1}H NMR spectrum of the reaction between ε-CL and δ-VL with water.

Reaction conditions: 200:2 loading of lactone:water, 80 °C, 24h. The bottom spectrum from the reaction with δ-VL, has a new signal at 3.90 ppm, indicating a reaction has occurred.

Table 3.2: The ROP of δ-VL using $[LZn_2(OCOCF_3)_2]$

#	$[LZn_2(OCOCF_3)_2]$:CHO:δ-VL	Conversion δ-VL / % [a]	TOF /h^{-1} [b]	M_n (Đ) $gmol^{-1}$ [c]
1	1:1000:100	79	79	3278 (1.32)
2	1:0:400	45	7.5	2151 (1.18)
3	1:0:400*	12	2	-

Polymerisations carried out at 2.5 M δ-VL, at 80 °C under nitrogen, 24 h. * under 1 atm carbon dioxide a) Determined from the normalised relative integrals in the ^{1}H NMR spectrum. PVL at 4.08 ppm and δ-VL at 4.15 ppm b) TOF = (mol of monomer/mol of catalyst)/h. Monomer conversions determined from ^{1}H NMR spectroscopy. c) determined by SEC with THF as the eluent, using polystyrene standards to calibrate the instrument. A correction factor of 0.57 is applied.[27]

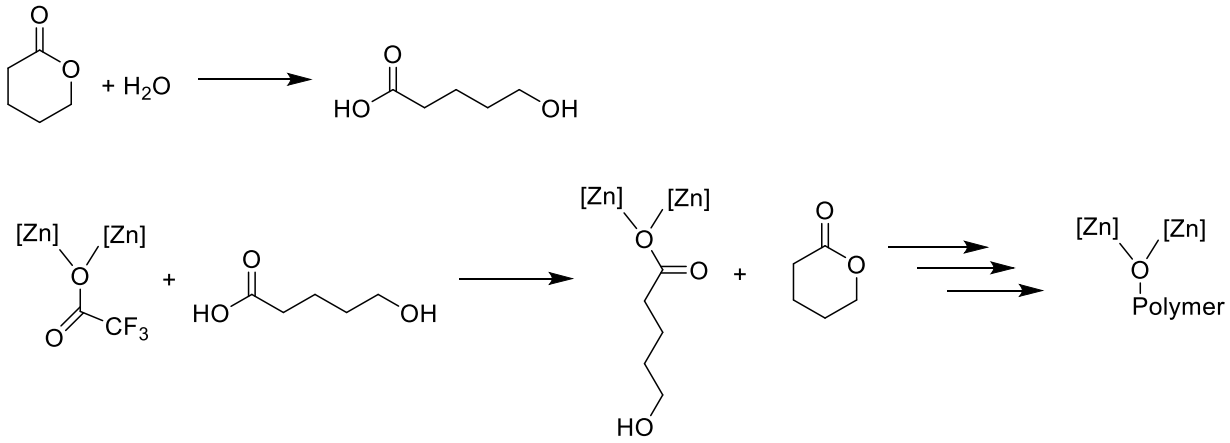

Figure 3.3.7: Scheme showing the ring opening of δ-VL by water and the use of 5-hydroxypentanoic acid as a chain transfer agent.

It is clear that the ROP of δ-VL occurs quicker using $[LZn_2(OCOCF_3)_2]$/CHO compared to $[LZn_2(OCOCF_3)_2]$ alone. However the fact that the catalyst allows ROP to occur without any epoxide present means that this system will not be fully selective when presented with monomer mixtures. Moreover it is likely that given the long timescales of ROCOP, the ROP of δ-VL may occur. This means the use of $[LZn_2(OCOCF_3)_2]$ as a catalyst for δ-VL ROP appears unsuited to selective catalysis.

An alternative catalyst $[LZn_2(Ph)_2]$ has been found to be active for the ROCOP of CHO/CO_2 and formed exclusively polycarbonate polyols. This finding is important as it would allow exclusive formation of ABA type block copolymers. For the ROCOP of CHO/CO_2, the polymerisation was initiated by the zinc alkoxide resulting from $[LZn_2(Ph)_2]$ and 1,2-cyclohexene diol. The presence of 1,2-cyclohexene diol is due to the presence of protic impurities in the reaction system which can ring open the epoxide. The catalyst formed is a zinc alkoxide species and it is proposed that it undergoes rapid insertion of carbon dioxide, in an analogous manner to the propagating species formed from $[LZn_2(OAc)_2]$. $[LZn_2(Ph)_2]$ was also shown to be an active catalyst for the ROP of ε-DL in the presence of a diol. $[LZn_2(Ph)_2]$ was synthesised according to the literature procedure.[24] The reaction between $[LZn_2(Ph)_2]$ and δ-VL did not result in polyester formation. However the addition of two equivalents of isopropanol (iPrOH) to the catalyst solution resulted in the rapid and exclusive formation of poly(valerolactone) (TOF = 1226 h^{-1}). When the reaction was conducted under

an atmosphere of carbon dioxide (1 atm), it resulted in no polymerisation. In order to confirm the chemoselectivity of the [$LZn_2(Ph)_2$]/ROH catalyst system, the ROP of δ-VL was carried out under a carbon dioxide atmosphere. Using a loading of 1:2:400 [$LZn_2(Ph)_2$]/iPrOH/δ-VL in the presence of carbon dioxide, no polyester was observed after 24 h. This confirmed the suitability of [$LZn_2(Ph)_2$] towards selective catalysis.

Table 3.3: The ROP of δ-VL using [$LZn_2(Ph)_2$].

#	[$LZn_2(Ph)_2$]:δ-VL:iPrOH	Time /h	Conversion δ-VL /% [a]	TOF /h^{-1} [b]	M_n (Đ) $gmol^{-1}$ [c]
1	1:400:0	24	-	-	-
2	1:400:2	0.33	92	1226	19710 (1.39)
3	1:400:2*	24	-	-	-

Polymerisations carried out at 2.5 M δ-VL, at 80 °C under nitrogen.* carried out under carbon dioxide a) Determined from the normalised relative integrals in the ^{1}H NMR spectrum. PVL at 4.08 ppm and δ-VL at 4.15 ppm b) TOF = (mol of monomer/mol of catalyst)/h. Monomer conversions determined from ^{1}H NMR spectroscopy. c) determined by SEC with THF as the eluent, using polystyrene standards to calibrate the instrument. A correction factor of 0.57 is applied.[27]

The ability of [$LZn_2(Ph)_2$]/ROH to form exclusively polycarbonate polyols from the ROCOP of CHO/CO_2, its ability to catalyse the ROP of δ-DL and the finding that CO_2 was a switch agent for ROP are important signals of its potential to function as a switchable catalyst.

3.4 ABA Block Copolymers

3.4.1 Catalyst Selectivity and Polymer Structure

δ-Valerolactone

Polymerisations were initially investigated using a molar loading of 1:400:2000 equivalents of [$LZn_2(Ph)_2$]:δ-VL:CHO, under 1 atm CO_2 pressure. The reaction was monitored using ^{1}H NMR spectroscopy. During the first 18 h, only PCHC formed, and a signal, corresponding to

the methine protons of the PCHC, appeared at 4.65 ppm. During this time period, there was no indication of PVL formation, as there was complete retention of the signal from the methylene protons of δ-VL at 4.25 ppm and no sign of a signal for the methylene protons of PVL at 4.08 ppm. After 18 h, the carbon dioxide atmosphere was removed from the system using 6 short vacuum/nitrogen cycles. Once the carbon dioxide was removed, the ROP of δ-VL occured. The ROP was demonstrated by the appearance of the signal at 4.08 ppm, corresponding to the methylene protons on PVL. There was no further ROCOP, as evidenced by the intensity of the signal corresponding to the methine protons on PCHC at 4.65 ppm remaining unchanged. The terpolymerisation of δ-VL/CHO/CO_2 using [$LZn_2(Ph)_2$] occured by the same selectivity rules as the terpolymerisation of ε-CL/CHO/CO_2 with [$LZn_2(OCOCF_3)_2$]. The system was highly selective, showing ROCOP occurring only when carbon dioxide is present and ROP occurring only after the CO_2 has been removed.

A series of block copolymers, with different molar masses and block compositions, were targeted. In each instance, the same monomer selectivity was observed, with exclusive PCHC formation while carbon dioxide was present, and then polyvalerolactone formation after the carbon dioxide was removed. The molar mass increased after the formation of the polyvalerolactone block, and all showed narrow to moderate dispersities (Đ =1.3-1.5). The ratio of carbonate:ester in the copolymer was determined from comparison of the normalised integrals of the main chain signals for the two blocks. For PCHC, the main chain methine resonance appeared at 4.65 ppm, and for PVL, the main chain methylene protons adjacent to the ester appeared at 4.08 ppm. By comparison of the integrals of the peaks at 4.65 ppm and 4.08 ppm, the carbonate:ester ratio was obtained. In all cases, the experimentally determined ratio was in close agreement with the theoretical ratio calculated on the basis of monomer conversion. This indicates that the majority of each polymer being formed was included in the block copolymer and not as a homopolymer, which would be removed during purification.

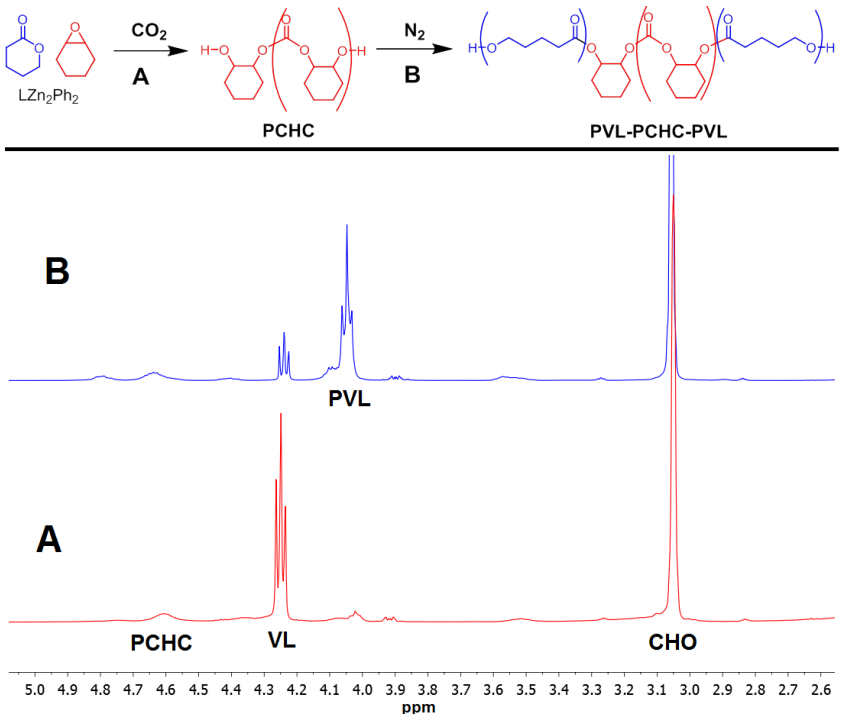

Figure 3.4.1: Scheme showing the formation of PVL-PHC-PVL (above) and the ^{1}H NMR spectra of the aliquots taken from the terpolymerisation (below) (Table 34, Run 2).

The bottom spectrum (A), 17 h, shows the formation of PCHC with the signal at 4.65 ppm but no formation of the PVL signal at 4.08 ppm. The top spectrum (B), 23 h, shows the appearance of the signal for PVL at 4.08 ppm alongside the signal for PCHC at 4.65 ppm.

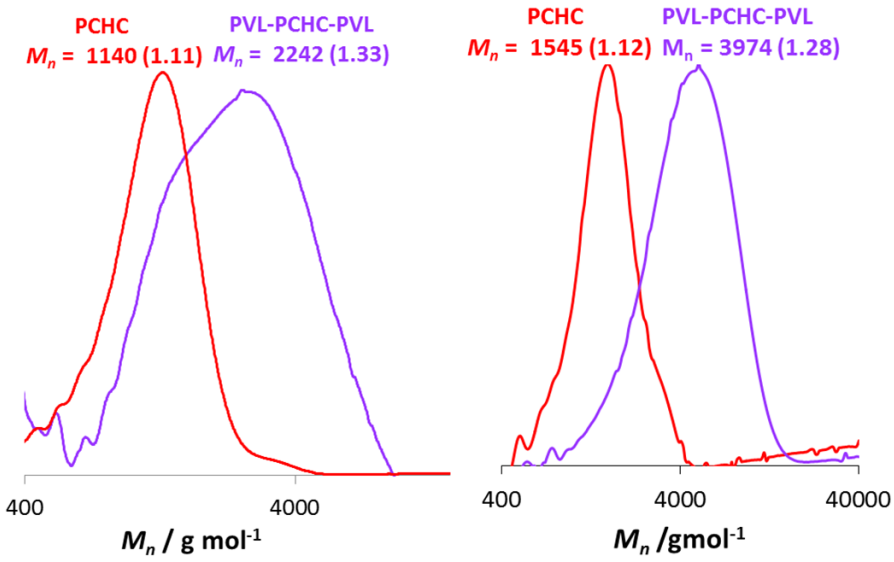

Figure 3.4.2: SEC analysis of PCHC and PVL-PCHC-PVL synthesised using CHO as solvent (Table 3.4, Run 1) [left] and using toluene as a solvent (Table 3.4, Run 4) [right].

Table 3.4: The formation of Poly(valerolactone-cyclohexene carbonate-valerolactone) [A = PCHC, ABA =PVL-PCHC-PVL].

#	$[LZn_2(Ph)_2]$:CHO:δ-VL	TOF A / h^{-1} a)	M_n (Đ) A / g mol^{-1} b)	TOF ABA / h^{-1} a)	M_n (Đ) ABA / g mol^{-1} b)	Molar ratio of carbonate:ester linkages NMR c)	Molar ratio of carbonate:ester linkages Experimental d)
1	1:2000:400	16.5	1140 (1.10)	49	2242 (1.33)	1:1.2	1:1.1
2	1:1000:400*	5.3	1454 (1.12)	54	4031 (1.50)	1:1.3	1:3.6
3	1:1000:200*	6.3	1285 (1.09)	26	2243 (1.46)	1:1.7	1:1.6
4	1:1000:600*	2.7	1545 (1.12)	11	3974 (1.28)	1:5.5	1:1.1

Polymerisations carried out at 80 °C, under 1 atm of carbon dioxide. * 1.1mL toluene used as a solvent. a) TOF = (mol of monomer/mol of catalyst)/h. Determined by ^{1}H NMR spectroscopy, the CHO conversion was determined from the normalised integrals for the CH signals at 3.05 ppm (CHO) and 4.58 ppm (PCHC). The δ-VL conversion was determined from the normalised integrals for the signals at 4.08 ppm (PvL) *vs*. 4.25 ppm (δ-VL). b) Determined by SEC with THF as the eluent, using polystyrene standards to calibrate the instrument. c) Determined from the normalised relative integrals at 4.65ppm (PCHC) and 4.908 ppm (PVL) in the ^{1}H NMR spectrum. d) Determined from the calculated monomer conversion (see above).

SEC analysis of the terpolymerisation reactions showed a significant increase in molar mass after the polymerisation of δ-VL. The copolymer was slightly broader after the ROP. Initially, the terpolymerisations were carried out using excess cyclohexene oxide as the solvent (Table 3.4, Run 1). As the cyclohexene oxide may be a source of diol (CHD), the use of excess CHO as solvent seems to result in the SEC trace of the ABA block copolymer being unsymmetrical (Figure 3.4.2, left). As it was quite polydisperse, there was not a clear shift between the signal for PCHC and PVL-PCHC-PVL. Furthermore, there was a shoulder on the SEC trace of the copolymer. The bimodality suggests that not all chains have an ABA structure, and there may be some PCHC chains remaining in the copolymer. To overcome

this limitation, toluene was used as the solvent, thereby reducing diol formation. This allowed the formation of ABA copolymers without any residual PCHC contaminant. The SEC trace of the block copolymer, formed with toluene as a solvent, was symmetrical and showed a clear increase in molar mass compared to the PCHC block, indicating that a homogeneous structure has formed (Figure 3.4.2, right).

^{1}H DOSY NMR spectroscopy was used to distinguish the formation of a block copolymer *versus* the formation of homopolymers. A block copolymer should result in a single diffusion co-efficient which corresponds to the ^{1}H NMR signals for both PCHC and PVL. The ^{1}H DOSY NMR spectrum of the triblock copolymers showed that all the signals have the same diffusion co-efficient ($D = 1.07 \times 10^{-10}$ m^2/s, $R_H = 3.79 \times 10^{-9}$). This was indicative of the PCHC and PVL blocks belonging to the same species.

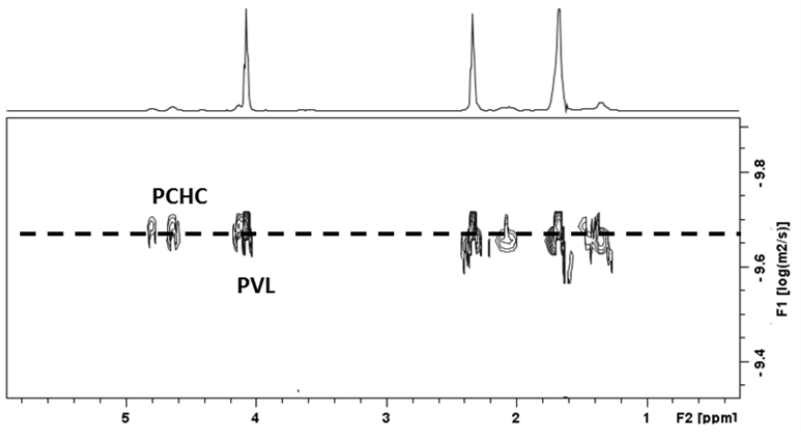

Figure 3.4.3: ^{1}H DOSY NMR spectrum of PVL-PCHC-PVL, (Table 3.4, Run 2).

Detailed NMR analysis was carried out on the triblock copolymer in the same manner as described in section 2.6.2. During ROCOP of CHO/CO_2, 8 chains of PCHC were formed per catalyst. This was calculated by the comparison of the $\overline{DP}$ and the molar mass recorded for the block. This is similar to the quantity of PCHC chains formed during the formation of PCL-PCHC-PCL block copolymers. The formation of multiple chains is due to presence of 1,2-cyclohexene diol as discussed in section 1.2.1. After the polymerisation of δ-VL, two

new peaks appeared in the ^{1}H NMR spectrum at 4.79 ppm and 4.13 ppm. These peaks were also present in the ^{1}H NMR spectrum for the purified copolymer (by precipitation from THF with MeOH). Given that very similar peaks were seen for PCL-PCHC-PCL, it is logical to assign the peaks at 4.79 ppm and 4.13 ppm as the junction units between the PCHC and PVL blocks. The peak at 4.79 ppm was assigned to the methine protons on the cyclohexene ring next to the polyvalerolactone block (H^{1}). The peak at 4.13 ppm was assigned to the methylene protons on the valerolactone unit next to the PCHC block (H^{3}). All peaks were identified by 2D NMR spectroscopy. Comparison of the ratios of the normalised integrals of the main chain units and junction units gave an insight into the structure of the copolymer. The ratio of the integrals of carbonate main chain units to carbonate junction unit is 4:1, this is considerably lower than the expected value of 9:1. The same phenomenon was observed in the ^{1}H NMR spectrum of PCL-PCHC-PCL, and was proposed to be due to the two carbonate units adjacent to the ester blocks contributing to the junction signal rather than just a single unit. The ratio of ester junction units to ester main chain units was 1:47, which is close to the calculated value of 1:40. The ratio of ester junction unit:carbonate junction unit was 1:2, which is in line with the ABA type structure.

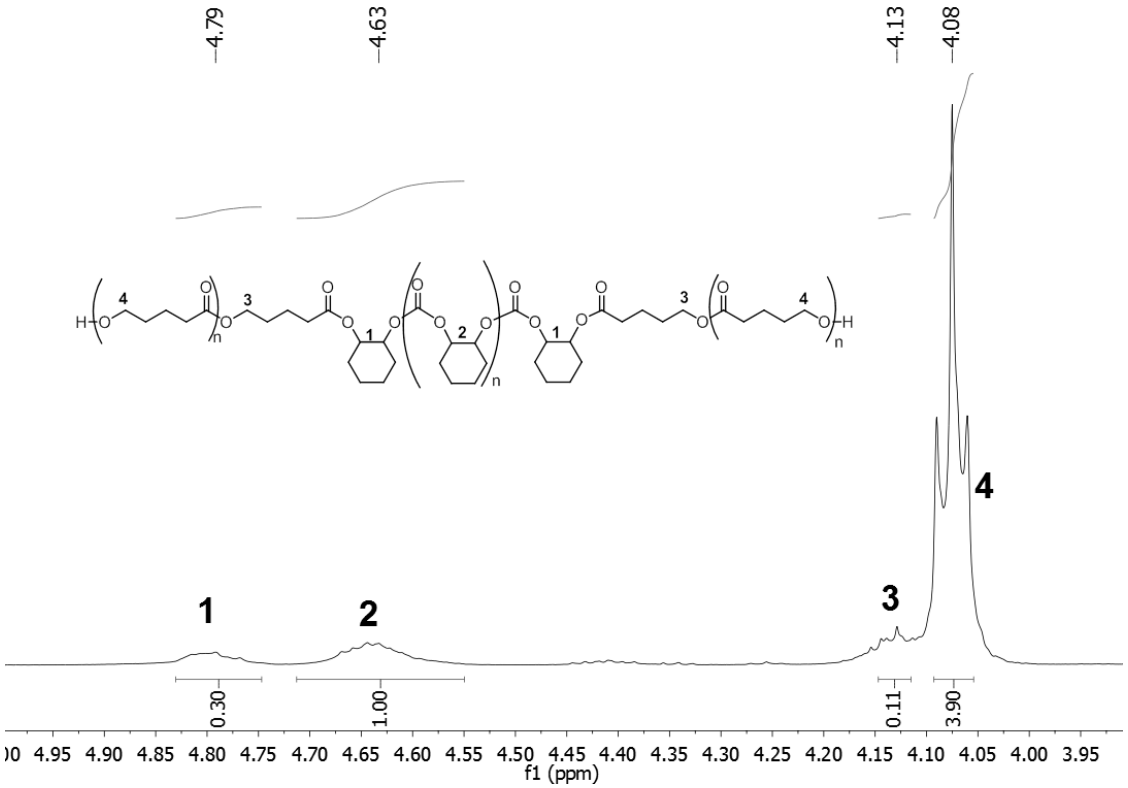

Figure 3.4.4: Excerpt from the ^{1}H NMR spectrum of PVL-PCHC-PVL, (Table 3.3, Run 2).

It shows the signals for carbonate and ester linkage units and the junction signals, alongside the structural assignment.

ε-Decalactone

The ROP of ε-DL has previously been reported using [$LZn_2(Ph)_2$] and alcohols.[24] The ROP of ε-DL was considerably slower than that of ε-CL (TOF = 7 h^{-1} *vs* 154 h^{-1} respectively). Thus, it is expected that the rate of initiation would be equivalent or faster than the rate of propagation and the majority of chains will have the chain extended structure (Section 3.1). The monomer should be well suited to block copolymer formation and it was expected that selective ABA block structures would form.

The terpolymerisation of ε-DL/CHO/CO_2 (1:200:2000 loading [$LZn_2(Ph)_2$]:ε-DL:CHO, 80 °C) was carried out under the same conditions as the previous terpolymerisations with ε-CL and δ-VL. During the first 16 h, exclusively PCHC was formed, indicated by the appearance

of a signal at 4.65 ppm in the ^{1}H NMR spectrum, corresponding to the polymer methine signals. No ROP of ε-DL was observed during this period, as there was no change in the intensity of the signal corresponding to the methylene protons of ε-DL at 2.6 ppm and no signal at 2.25 ppm corresponding to the methylene protons of PDL. However, once the carbon dioxide was removed, only minimal PDL was formed (2 %) during the next 24 h. The terpolymerisations were carried out under high dilutions in order to manage the overall viscosity. However, the high dilution was expected to considerably reduce the rate of ε-DL ROP. The long reaction times, were proposed to lead to catalyst degradation. In order to increase the rate of ε-DL ROP, the terpolymerisations were carried out at 100 °C. This was slightly detrimental to the ROCOP, as carbon dioxide is less soluble in CHO at these temperatures and therefore more cyclic carbonate is formed. The cyclic carbonate can be easily removed by precipitation after the polymerisation. During the terpolymerisation of ε-DL/CHO/CO_2, (1:200:2000 loading [$LZn_2(Ph)_2$]:ε-DL:CHO, 100 °C) only PCHC formed while carbon dioxide was present. The reaction was monitored by ^{1}H NMR spectroscopy and during the first 17 h, when carbon dioxide was present, the signal for the methine protons of PCHC appeared at 4.65 ppm. There are no resonances corresponding to PDL in the ^{1}H NMR spectrum (methylene protons at 2.25 ppm). It is only after the removal of carbon dioxide, that the ROP of ε-DL occured and a resonance corresponding to the polymer methylene protons appeared at 2.25 ppm. This confirmed that ε-DL followed the same selectivity rules observed with both ε-CL and δ-VL.

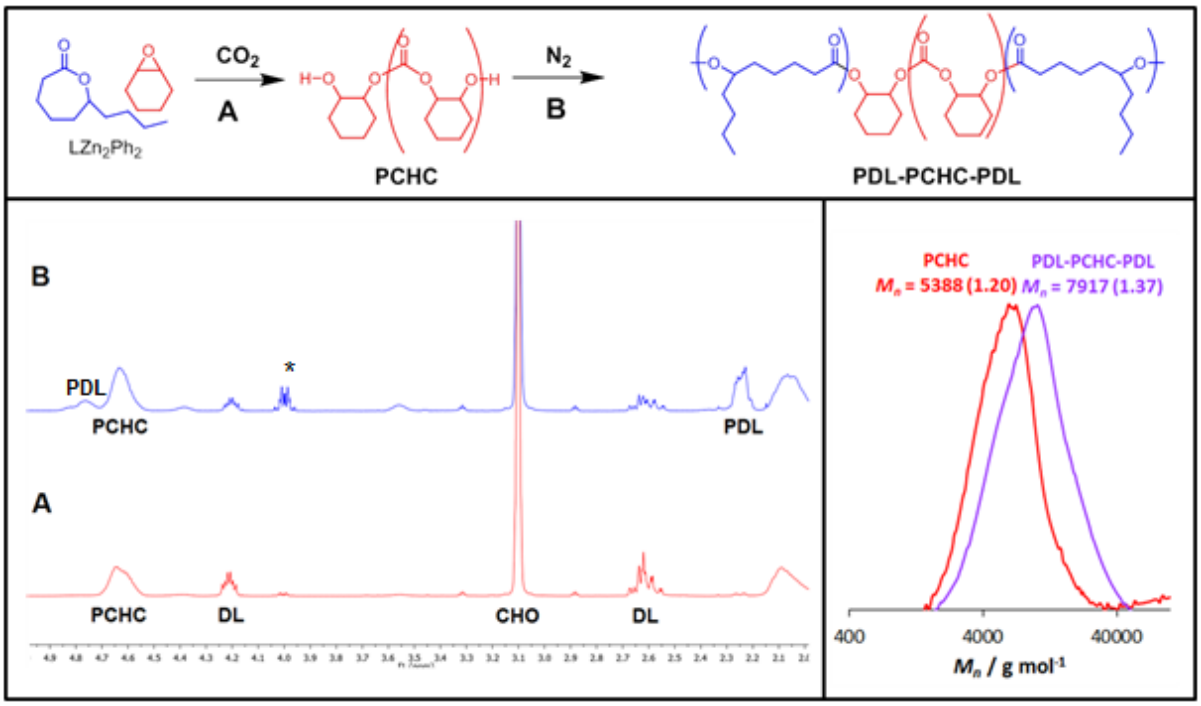

Figure 3.4.5: Scheme showing the formation of poly(decalactone-cyclohexene carbonate-decalactone) and monitoring the reaction *via in-situ*-ATR and 1H NMR spectroscopy. (Table 3.5, Run 3).

Bottom left: Excerpt of the ^{1}H NMR spectra of the aliquots taken at 17 h (bottom) and 24.5 h (top). The bottom spectrum (A), taken at 17 h, shows the formation of PCHC at 4.65 ppm but no formation of PDL at 2.25 ppm. The top spectrum (B), taken at 24.5 h, shows the appearance of a signal for PDL at 2.25 ppm. * cyclic carbonate Bottom right: SEC analysis of the aliquots, showing an increase in molar mass.

Table 3.5: Synthesis of Poly(decalactone-cyclohexene carbonate-decalactone).

#	TOF /h^{-1} a) PCHC	M_n (Đ) /g mol^{-1} b) PCHC	TOF /h^{-1} a) PDL	M_n (Đ) /g mol^{-1} b) PDL-PCHC-PDL	Molar ratio of ester:carbonate linkages c) NMR	Molar ratio of ester:carbonate linkages d) theoretical
1	25	5827 (1.18)	10	6829 (1.45)	1:2.6	1:2.7
2	9.4	5388 (1.20)	5.8	7917 (1.37)	1:1	1:1

Polymerisation carried out at a 1:200:2000 loading of $[LZn_2(Ph)_2]$:ε-DL:CHO and 100 °C and under 1 atm of carbon dioxide. a) TOF = (mol of monomer/mol of catalyst)/h. Monomer conversions determined by ^{1}H NMR spectroscopy, the CHO conversion was determined from the normalised integrals for the CH signals at 3.05 ppm (CHO) and 4.58 ppm (PCHC). The ε-DL conversion was determined from the normalised integrals for the signals at 2.22 ppm (PDL) *vs*. 2.65ppm (δ-VL) b) Determined by SEC with THF as the eluent, using polystyrene standards to calibrate the instrument. c) Determined from the normalised relative integrals of the signals at 4.65ppm (PCHC) and 2.22 (PDL) in the ^{1}H NMR spectrum . d) determined from the calculated monomer conversions, see above.

A series of block copolymers were synthesised by quenching the reaction at different time points during the ROP of ε-DL. In each instance, ROCOP of CHO/CO_2 was followed by the ROP of ε-DL only after the carbon dioxide was removed. In all cases, the formation of a triblock copolymer caused an increase in molar mass. The higher molar masses for the PCHC blocks compared with the PCL/PVL triblock copolymers (~5000 v ~2000 g mol^{-1} comparatively) was due to the higher temperature of the polymerisation (100 °C) and the use of CHO as the solvent *versus* toluene, increasing the degree of polymerisation. In all cases, the ratio of carbonate:ester units, as determined by the relative ratios of the signals at 4.65 ppm for PCHC and 2.25 ppm for PDL in the ^{1}H NMR spectrum, was in good agreement with the ratio calculated from the degrees of polymerisation. The ratio of carbonate:ester units was not altered by purification of the polymer (by precipitation from THF with MeOH), suggesting that only fractionation occurred and the starting materials or cyclic contaminants were removed.

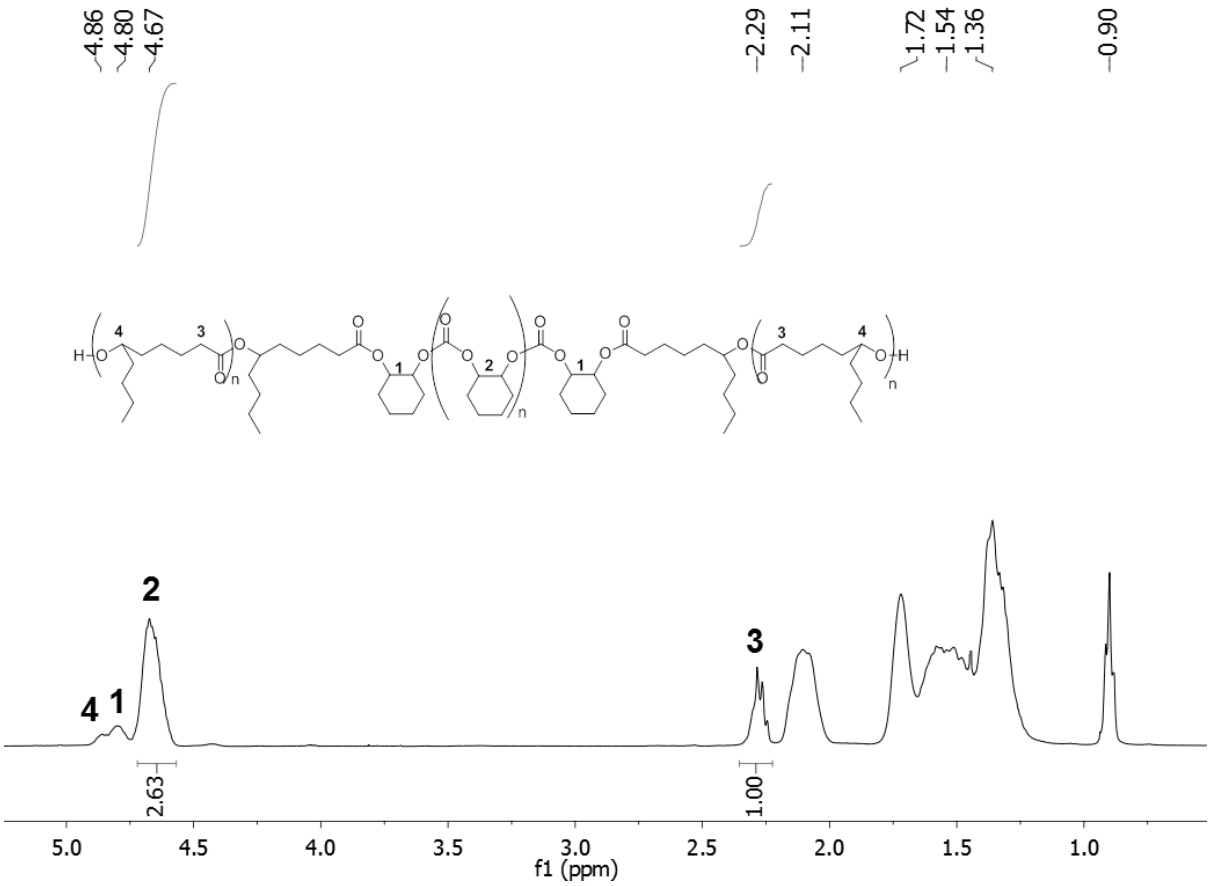

Figure 3.4.6: ^{1}H NMR spectrum of PDL-PCHC-PDL.

The ^{1}H NMR spectrum of PDL contained a resonance at 4.85 ppm, corresponding to the methine proton adjacent to the ester oxygen (H_4), and a signal at 2.22 ppm, corresponding to methylene protons adjacent the carbonyl group (H_3). In the block copolymers containing PCL and PVL, the resonances corresponding to the methylene protons nearest the ester oxygen (at 4.05 and 4.08 ppm respectively), were used to calculate polyester content of the block copolymer. In PDL, the proton nearest the ester oxygen was a methine proton and had a signal at 4.85 ppm (H_4). During the formation of PDL-PCHC-PDL, a new signal appeared at 4.80 ppm. This signal was assigned to the methine protons of the carbonate junction unit (H_1), as it appeared during the formation of PDL, but only in the terpolymerisation and not the homopolymerisation of ε-DL. There was a significant overlap between the signal for PDL at 4.85 ppm (H_4) and the carbonate junction unit at 4.80 ppm (H_1), which was why an alternative signal (methylene protons at 2.22 ppm, H_3) is used to quantify the proportion of

PDL in the terpolymers. Unfortunately, it was also impossible to isolate a signal corresponding to the ester junction unit. It was therefore not possible to compare the ratio of end groups to main chain protons for the PCHC/PDL system.

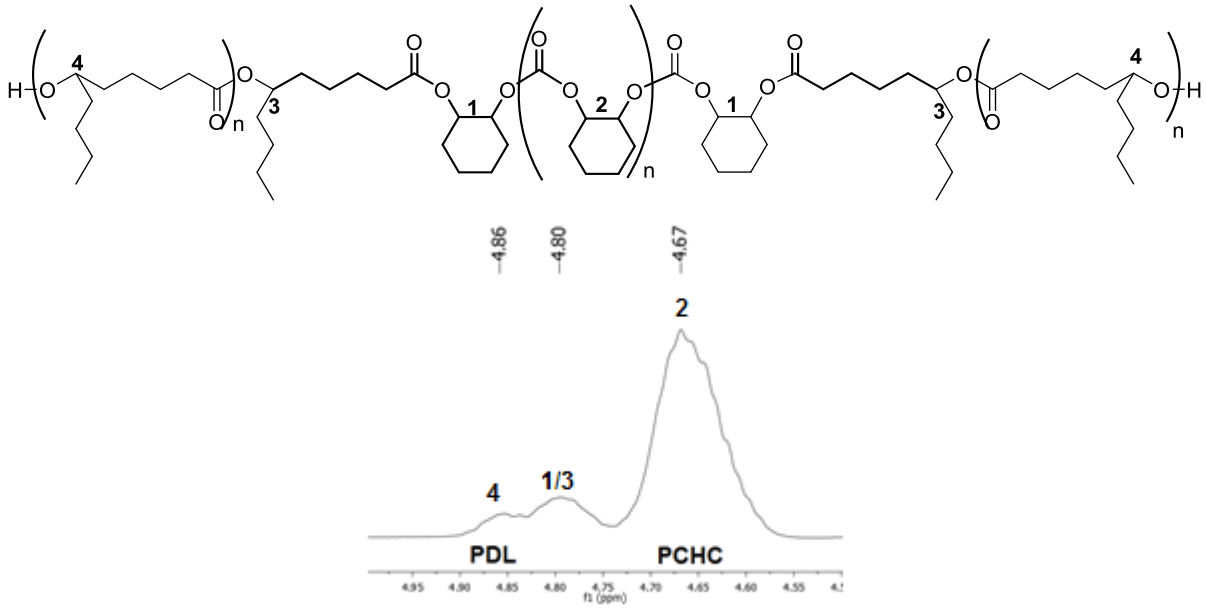

Figure 3.4.7: Excerpt of PDL-PCHC-PDL (Table 3.5, Run 1).

Note the overlap between the signals at 4.86 and 4.80 ppm, which correspond to the methine proton of PDL and the methine protons of the carbonate junction unit respectively.

The ^{1}H DOSY NMR spectrum of PDL-PCHC-PDL showed a single species with a diffusion co-efficient of 2.21 x 10^{-10} s^{-1} confirming the block structure. The combined data support the formation an ABA type block copolymer.

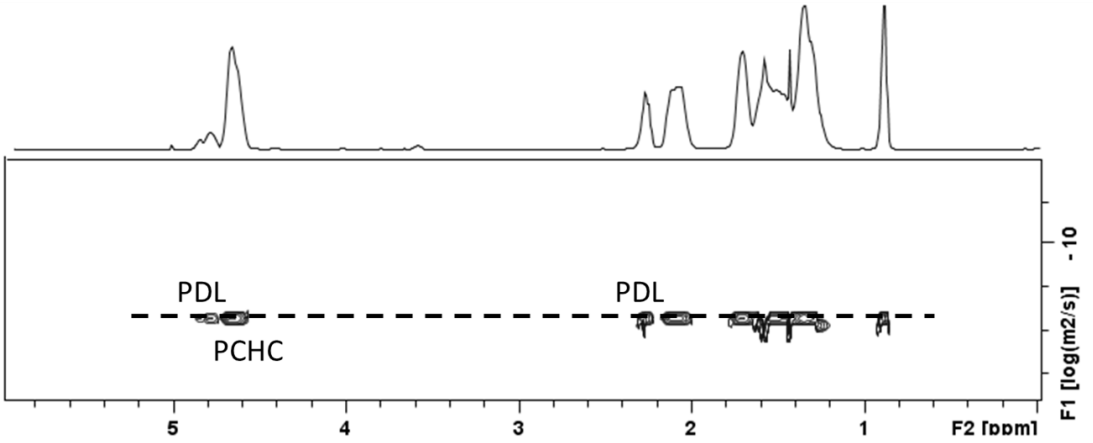

Figure 3.4.8: ^{1}H DOSY NMR spectrum of PDL-PCHC-PDL (Table 3.5, Run 2).

3.5.2 Properties

Table 3.6: Thermal properties of PDL-PCHC-PDL and PVL-PCHC-PVL.

#		Molar ratio of Carbonate:Ester [a)]	% Carbonate	M_n / gmol^{-1} [b)]	T_g / °C [c)]	T_m (T_c) / °C
1	PCHC	0:1	100		108	
2	PVL	1:0	0	4791		43
3	PDL[24]	1:0	0		-58	
4	PVL-PCHC-PVL	1:2.2	31	2242	-19	
5	PVL-PCHC-PVL	1:1.7	37	2243	-14, 109	
6	PVL-PCHC-PVL	1:5.5	15	3974	-46	-2.6 (36)
7	PDL-PCHC-PDL	1: 0.45	68	6829	48	

a) Determined by ^{1}H NMR spectroscopy by comparison of the normalised integrals for the PCHC CH signals at 4.65 ppm and the PVL CH_2 signals at 4.08 ppm or PDL CH_2 signals at 2.22 ppm b) Determined by SEC with THF as the eluent, using polystyrene standards to calibrate the instrument c) The T_g was calculated from the third heating cycle of the DSC measurement and was heated at 10 °C/minute from -100 to 130 °C (# 1-3, 5-8) or 40 °C/minute from -80 to 100 °C(# 4, 9-10).

The thermal properties of the PDL and PVL triblock copolymers were analysed by DSC. PVL is a semi-crystalline copolymer with a melting temperature (T_m) of 43 °C. The value obtained (43 °C, Table 3.5) is lower than the reported value (52 °C) [4] which is probably due to the low molar mass of the sample. PVL may also show a T_g of -67 °C for the amorphous region but this is rarely observed due to the high crystallinity of many samples. The PVL-PCHC-PVL triblock copolymers have controllable glass transition and melting temperatures, which are dependent on the copolymer's molar mass and composition. At a 1:1.7 carbonate:ester composition, two T_g's were observed at -14 and 109 °C. The transition at 109 °C corresponds to the PCHC block. The transition at -14°C must therefore be due to amorphous PVL. This value was higher than the T_g for pure PVL due to the suppression of the crystallinity. At a 1:2.2 carbonate:ester composition a single T_g is observed at -19 °C. It seems likely that the T_g of the PCHC block is being obscured. As the ester content increased, the crystallinity of the PVL block begins to be observable, and both T_m and T_c transitions become apparent. The temperatures of the melting transition are reduced compared to those of pure PVL, which is indicative of smaller crystalline domains. The χ_c (% crystallinity) was determined to be 36 %, so the block copolymer was significantly less crystalline than pure PVL. These thermal properties were similar to those of PCL-PCHC-PCL. In both cases a ester content of greater than 1:4 (carbonate:ester) was required before any crystallinity is observed. PDL was an amorphous polymer with a T_g at -58 °C. The PDL-PCHC-PDL triblock copolymer was an amorphous polymer with a single T_g around 43 °C. The Flory-Fox equation was used to predict the T_g's of completely miscible polymers (section 2.3.6). The predicted T_g of PDL and PCHC was determined to be 2 °C. This was not close to the experimentally observed value, indicating the polymers may only be partially miscible. Partially miscibility moderates the thermal properties of the terpolymer but was dependent on the precise composition of the copolymer.

As discussed in Chapter 2, in order to probe the mechanical properties of the triblock copolymers, the molar masses were increased by polyurethane formation. Films of the polyurethanes were made by solvent casting the polymers from dichloromethane.

Table 3.7: Mechanical properties of the polyurethanes.

	Polymer	*PCHC:PL* [a)]	M_n [b)]	M_n *(PU)* [b)]	E /MPa	Elongation at break /%	Yield point
1	PCHC	1:0			3600-3700 *	1-2*	40-44*
2	PVL	0:1			0.57 **	150-200 **	
3	PDL						
4	PVL-PCHC-PVL	1:7	3,300 (1.35)	12,00 (1.69)	25.4	15.3	8.6
5	PDL-PCHC-PDL	1:1	7.900 (1.37)	15,200 (1.89)	46.5	400	7
6	PCL	0:1	5,400 (1.24)	85,000 (1.41)	151	>450	10.6
7	PCL-PCHC-PCL	1:7	13,800 (1.50)	74,800 (1.11)	9.9	>450	53

a) Determined by ^{1}H NMR spectroscopy by comparison of the normalised integrals for the PCHC CH signals at 4.58 ppm and the PVL CH_2 signals at 4.08 ppm or PDL CH_2 signals at 2.22 ppm b) determined by SEC with THF as the eluent, using polystyrene standards to calibrate the instrument.

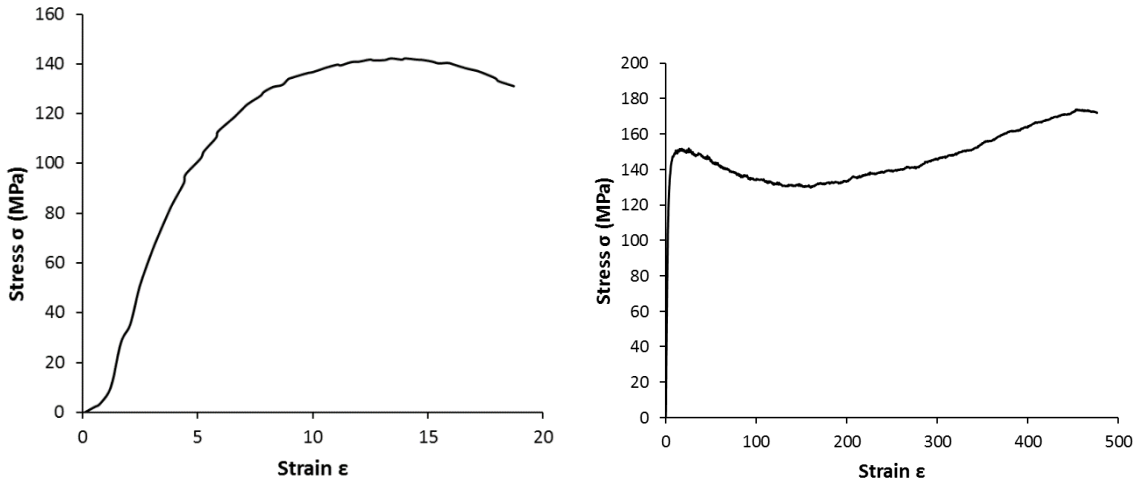

Figure 3.5.1: Plots of strain *vs* stress curves for PVL/PCHC PU (Left) and PDL/PCHC PU (right).

The polyurethane made from Poly(valerolactone-cyclohexene carbonate-valerolactone) (PVL/PCHC PU) has a Young's modulus of 25.4 MPa with a low yield point and a low elongation at break. It was a soft inflexible plastic whereas the polyurethane made from poly(decalactone-cyclohexene carbonate-decalactone) (PDL/PCHC PU) behaved as a traditional flexible plastic. Due to the amorphous nature of PDL/PCHC PU and the miscibility of PCHC and PDL, the polyurethane film was transparent. It has a Young's modulus of 46.5 MPa and a yield point of 7 MPa. It's elongation at break is greater than 450 %. The PDL/PCHC PU behaved in a similar way to the PCL/PCHC PU although it had a higher Young's modulus (46.5 *vs* 9.9 MPa). The PVL/PCHC PU was different to the other two triblock copolymers in that it was an inflexible polymer and this was likely to be because PVL has a smaller chain length than PCL and PDL.

3.6 Conclusions and Outlook

The chapter has continued the investigation of switchable catalysis using monomer mixtures. A new di zinc catalyst [$LZn_2(Ph)_2$] has been investigated for epoxide/CO_2/lactone terpolymerisation. The di zinc catalyst was known to produce dihydroxyl terminated polycarbonate, a requirement for the block copolymer formation.[24] The monomer selectivity displayed in the formation of poly(caprolactone-b-cyclohexene carbonate-b-caprolactone) was shown to be applicable to alternative monomers, specifically δ-valerolactone and ε-decalactone. Using either lactone, the terpolymerisation with cyclohexene oxide and carbon dioxide resulted in the selective formation of polycarbonate while the carbon dioxide was present. It was only once the carbon dioxide was removed that the ring opening polymerisation occurred and the polyester formed. The terpolymerisation method was sufficiently robust, that altering the ratio of monomers does not affect the observed selectivity. Altering the monomer feed ratio, resulted in a predictable change to the carbonate:ester ratio of the block copolymers and the composition of the polymer could be accurately predicted from the conversions of monomers. The copolymers were found to have a predominately ABA type block structure as established using NMR spectroscopy, size exclusion chromatography analysis and differential scanning calorimetry. All data indicates ABA triblock copolymer formation.

The thermal properties of poly(valerolactone-b-cyclohexene carbonate-b-valerolactone) were very similar to that of poly(caprolactone-b-cyclohexene carbonate-b-caprolactone). At high carbonate contents (> 40 %), the polycarbonate and poly(valerolactone) blocks were partially miscible. The presence of the carbonate block disrupts the crystallinity of the polyester, forming amorphous or semi-crystalline block copolymers (ester content > 60 %). Poly(decalactone-b-cyclohexene carbonate-b-decalactone) was a completely amorphous material with a T_g around 48 °C, indicating that the polycarbonate and poly(decalactone) blocks were miscible. The lack of agreement between the observed glass transition temperature and the calculated value from the Flory-Fox equation, indicated that the blocks were only partially miscible. The copolymer wass transparent once films had been formed.

Overall the findings in the chapter demonstrate the ability to apply the switchable catalysis with $[LZn_2(X)_2]$, to a range of lactones and exclusively for ABA block copolymers. The use of different lactones shows that the selectivity is not influenced by the reactivity of the lactones. The next chapter will continue to investigate the switch chemistry of the di zinc catalysts. In particular, their ability to switch not just from ring opening copolymerisation to ring opening polymerisation but also in the reverse direction and the feasibility of forming multiblock copolymers will be explored.

References

(1) Zhu, Y.; Romain, C.; Poirier, V.; Williams, C. K. *Macromolecules* **2015**, *48*, 2407.
(2) Xiong, M.; Schneiderman, D. K.; Bates, F. S.; Hillmyer, M. A.; Zhang, K. *Proc. Natl. Acad. Sci. USA* **2014**, *111*, 8357.
(3) Martello, M. T.; Burns, A.; Hillmyer, M. *ACS Macro Lett.* **2012**, *1*, 131.
(4) Aubin, M.; Prud'homme, R. E. *Polymer* **1981**, *22*, 1223.
(5) Kurcok, P.; Penczek, J.; Franek, J.; Jedlinski, Z. *Macromolecules* **1992**, *25*, 2285.
(6) Osaki, M.; Takashima, Y.; Yamaguchi, H.; Harada, A. *Organic & Biomolecular Chemistry* **2009**, *7*, 1646.
(7) Chang, Y. A.; Waymouth, R. M. *Polym. Chem.* **2015**, *6*, 5212.
(8) Misaka, H.; Kakuchi, R.; Zhang, C.; Sakai, R.; Satoh, T.; Kakuchi, T. *Macromolecules* **2009**, *42*, 5091.
(9) Gowda, R. R.; Chakraborty, D. *J. Mol. Catal. A: Chem.* **2009**, *301*, 84.
(10) Toncheva, N. V.; Mateva, R. P. *Adv. Polym. Tech.* **2007**, *26*, 121.

(11) Price, G. J.; Lenz, E. J.; Ansell, C. W. G. *Eur. Polym. J.* **2002**, *38*, 1753.
(12) Lou, X.; Detrembleur, C.; Jérôme, R. *Macromolecules* **2002**, *35*, 1190.
(13) Furuhashi, Y.; Sikorski, P.; Atkins, E.; Iwata, T.; Doi, Y. *J. Polym. Sci., Part B: Polym. Phys.* **2001**, *39*, 2622.
(14) Ihara, E.; Tanabe, M.; Nakayama, Y.; Nakamura, A.; Yasuda, H. *Macromol. Chem. Phys.* **1999**, *200*, 758.
(15) Storey, R. F.; Herring, K. R.; Hoffman, D. C. *J. Polym. Sci., Part A: Polym. Chem.* **1991**, *29*, 1759.
(16) Aubin, M.; Bédard, Y.; Morrissette, M.-F.; Prud'homme, R. E. *J. Polym. Sci., Part B: Polym. Phys* **1983**, *21*, 233.
(17) Lin, J.-O.; Chen, W.; Shen, Z.; Ling, J. *Macromolecules* **2013**, *46*, 7769.
(18) Olsén, P.; Borke, T.; Odelius, K.; Albertsson, A.-C. *Biomacromolecules* **2013**, *14*, 2883.
(19) Wanamaker, C. L.; O'Leary, L. E.; Lynd, N. A.; Hillmyer, M. A.; Tolman, W. B. *Biomacromolecules* **2007**, *8*, 3634.
(20) Tang, D.; Macosko, C. W.; Hillmyer, M. A. *Polym. Chem.* **2014**, *5*, 3231.
(21) Schneiderman, D. K.; Hill, E. M.; Martello, M. T.; Hillmyer, M. A. *Polym. Chem.* **2015**, *6*, 3641.
(22) Schneiderman, D. K.; Hillmyer, M. A. *Macromolecules* **2016**, *49*, 2419.
(23) Song, C. X.; Feng, X. D. *Macromolecules* **1984**, *17*, 2764.
(24) Zhu, Y.; Romain, C.; Williams, C. K. *J. Am. Chem. Soc.* **2015**, *137*, 12179.
(25) Van de Velde, K.; Kiekens, P. *Polym. Test.* **2002**, *21*, 433.
(26) Duda, A.; Kowalski, A. In *Handbook of Ring-Opening Polymerization*; Wiley-VCH Verlag GmbH & Co. KGaA: 2009, p 1.
(27) Save, M.; Schappacher, M.; Soum, A. *Macromol. Chem. Phys.* **2002**, *203*, 889.

Chapter 4 : Multiblock Copolymers using Switch Catalysis

4.1 Introduction

Nature has the ability to form perfectly controlled polymers from mixtures of monomers, such as DNA, RNA and proteins.[1] In contrast, synthetic chemistry is still in its infancy with respect to the formation of such controlled polymers.[2] As a general rule, when forming polymers a compromise between precision and synthetic ease is usually made. The most controlled method of making sequence controlled polymers is a classical step by step synthesis. This works well to prepare new polypeptides and other polyamides but is less developed for other polymer backbones.[3] This method is often hampered by multiple purification steps and can only produce small quantities of polymer. The alternative would be to form highly controlled multiblock structures using chain growth polymerisation mechanisms but this is usually very challenging. Even under ideal conditions chain growth polymerisations result in a distribution of chains. This complicates the block sequence control[4] and there are not yet a sufficient range methods which can select monomers from mixtures. The most common techniques to form multiblock copolymers are sequential addition of monomers, coupling of preformed polymers, or *in-situ* chain shuttling.

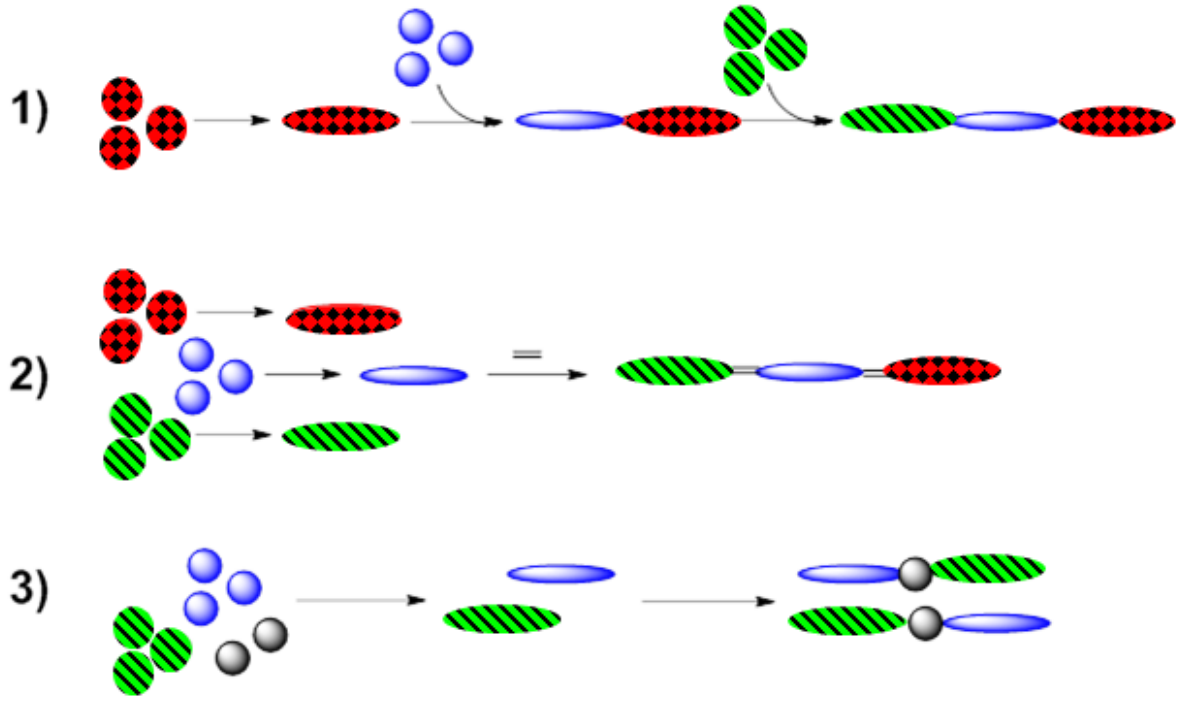

Figure 4.1.1: Scheme depicting the methods used to make multiblock copolymers.

1) Sequential addition of monomers to a living polymerisation 2) Coupling of preformed polymers can be done after purification or *in-situ*. 3) Chain shuttling, using a chain transfer agent.

Sequential Addition

In controlled or living polymerisations sequential addition of monomers can be an effective route to block copolymers.[5] Sequential addition of monomer requires the polymerisation to be living – the catalysts must fully consume the monomer and must not undergo termination reactions. Sequential addition to form multiblock copolymers has been used with RAFT polymerisation to form an icosablock copolymer (20).[4,6] Perrier and co-workers used a combination of 3 monomers to form the icosablock copolymers;[6] the initial conditions required up to 24 h for the enchainment of each block and had very short block lengths.[7] Optimisation of the initiator improved conditions considerably, allowing block lengths to increase above 100 units, and the time was reduced to 2 h.[6] The optimised conditions meant that no purification was required however, despite the formation of up to 20 blocks, only 3 distinct monomers were used all of which were acryl amides. The structure of the multiblock copolymer was confirmed by ^{1}H NMR spectroscopy and MALDI-ToF analysis, and SEC

analysis showed a clear increase in molar mass after each block formation. Due to the very shortblock length of the initial block copolymer it is likely that the majority of chains are defective and don't contain all 20 blocks. Once the block length was increased to above 100 units the likelihood of defective chains was significantly reduced.[4] In most reports of sequential addition to form a multiblock copolymer, the monomers are functionalised variations of a common structure, most commonly acrylates/methacrylates.[5] This is because the catalyst must fully consume the monomer and the majority of catalysts are tuned to be highly active for a particular class of monomer.

Sequential addition to form a multiblock has been used in the field of ROCOP to form diblocks and triblocks (Section 1.4.1).[8,9] The [ZnBDI] catalysts, developed by Coates and co-workers, have been used to form multiblock copolycarbonates by the sequential addition of 6 different functionalised cyclohexene oxides.[10] The catalyst was sufficiently robust to tolerate various functional groups attached to the cyclohexene ring, including vinyl, ketal, triethylsiloxyl, PEG, and fluorophilic groups. All monomers were polymerised in similar reaction times, allowing the formation of the hexablock copolymer regardless of the order of monomers. When the catalyst had a norbornene based initiating group the multiblock copolymer contained a functional end group. The double bond of the norbornene can be used in a ring opening metathesis polymerisation, resulting in a graft copolymer.[11] Sequential addition has been combined with selective catalysis by our research group to form heptablock copolymers.[12] [$LZn_2(Ph)_2$] selectively forms triblock copolyesters from a mixture of lactone, anhydride and epoxide. The selectivity arises from the chemoselectivity displayed by the [$LZn_2(X_2)$] catalysts, whereby the nature of the catalysts zinc oxygen bond controls monomer enchainment. The reaction is a controlled polymerisation and therefore the addition of more equivalents of the monomer results in further selective polymerisation. Thus, by adding more anhydride and lactone, a heptablock copolymer was formed.

Post Polymerisation Chain Coupling

The coupling of preformed polymers requires the formation of polymers with functional end groups and an efficient method to react them (typically a Click reaction). For oxygenated

polymers the most common functional end group is a hydroxyl group. These can be directly used for the coupling reaction or post modified to another functional group. The formation of multiblocks is most often achieved by the coupling of diblock or triblock copolymers.[13,14] The coupling method can be done in one of two ways a) using an additional linking unit, often an isocyanate; or b) direct coupling of carefully designed functional end groups. The use of isocyanates to couple di or triblock copolymers to form multiblock polymers is a common technique, especially for dihydroxyl end groups.[15-26] However the isocyanate group is toxic and may cause problems in biomedical application especially if the polymers are degradable.[16 17,18] The direct coupling of functional end groups requires the synthesis of block copolymers with complimentary end groups. One common tactic is to couple polymers with hydroxyl end groups and carboxylic end groups in order to achieve condensation, although ensuring the complete reaction can be challenging.[13,14] Yamamoto and co-workers designed PLLA-PCL block copolymers whereby the PLA block was terminated by a hydroxyl group but the PCL block was terminated by a carboxylic group.[13] The condensation was conducted in the presence of N,N'-diisopropylcarbodiimide, 4-(dimethylamino)pyridine and 4-dimethylaminopyridine 4-toluenesulfonate and resulted in multiblock copolymers. Li *et al* developed a system whereby the ROP of a cyclic ogliomeric ester was initiated by a polyether polyol to form a triblock copolymer which self-condensed to form a multiblock copolymer.[14] The multiblock copolymers were found to be much more thermally stable ($T_{d\ 5\%}$ = 350 °C) than either of the homopolymers ($T_{d\ 5\%}$ = 250 °C).

Chain Shuttling Processes

Some multiblock copolymers are formed by chain shuttling, whereby the polymer chains can switch from one polymerisation site to another. It typically requires two catalysts which are orthogonal (can not polymerise the other monomer), but where the polymers can be exchanged by a common chain transfer species.[27] It was used to form a multiblock PCHC-PCL copolymer using a DMC catalyst to form PCHC and tin octanoate to form PCL. Control of the block length was achieved by control of the amount of alcohol added as an initiator but in all polymerisations the block length was short and chains were highly polydisperse. The resulting structure was random although regions containing blocks were expected. The

depolymerisation and exchange of acyclic diene metathesis (ADMET) polymerization was used to make copolyolefines.[28] These methods result in short block lengths which are controlled by the amount of the chain transfer agent and the composition is usually random.

Summary of the Literature

There are several methods for the formation of multiblock copolymers, however there are restrictions and limitations for each method. The most controlled method is the sequential addition of monomers, but this is limited by the number of catalysts and monomers that can adhere to the stringent conditions required for the multiblock copolymer synthesis. Other methods such as coupling of polymers or chain shuttling can not provide the same level of control but do allow a diverse range of components to be combined. Switch catalysis could be a useful method to form multiblock copolymers, as it should allow a one-pot polymerisation using a mixture of monomers. Control over the block lengths can be achieved by controlling the catalyst chain end chemistry. Catalysts which can switch between different polymerisation mechanisms would allow the formation of multiblock copolymers where the blocks are particularly and benefically diverse in structure.

4.2 Aims

In this chapter the performance of $[LZn_2(OCOCF_3)_2]$ in switch catalysis, especially over multiple cycles of switches, will be investigated. The catalyst $[LZn_2(OCOCF_3)_2]$ must be able to switch successfully from ROP to ROCOP and from ROCOP to ROP. It also needs to be able to switch multiple times without loss of selectivity. It is important to ensure that that only polycarbonate forms while CO_2 is present and that polyester formation only occurs once the CO_2 is removed. The effect of the multiple switches on the catalytic activity will be determined by analysis of the rates of reactions.

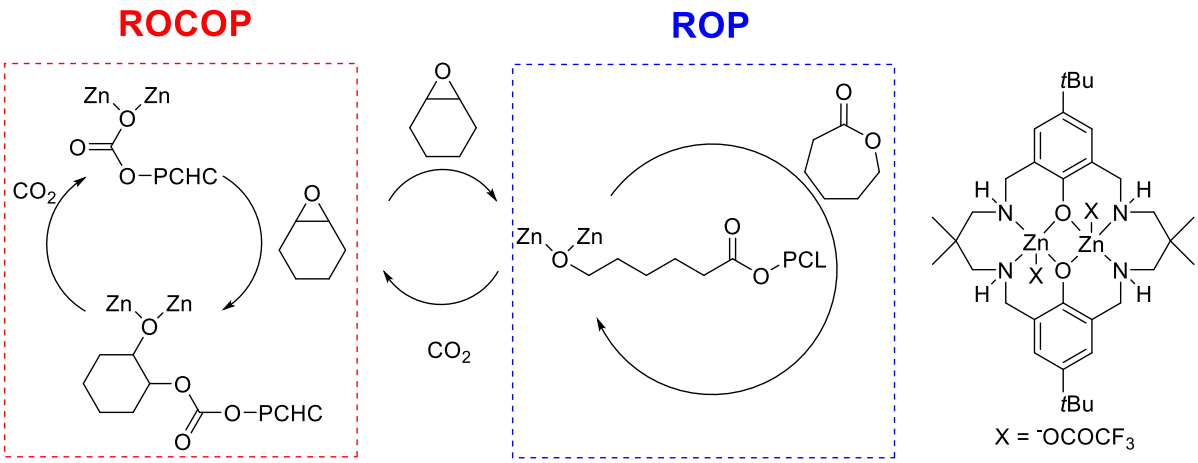

Figure 4.2.1: Mechanism of ROCOP of CHO/CO_2 and the ROP of ε-CL and the method of switching between the two. Right: Structure of [$LZn_2(OCOCF_3)_2$].

Another key consideration will be to establish that the multiblock copolymer structure is obtained. The copolymer structure will be analysed and the properties compared to the parent polymers and the triblock copolymers.

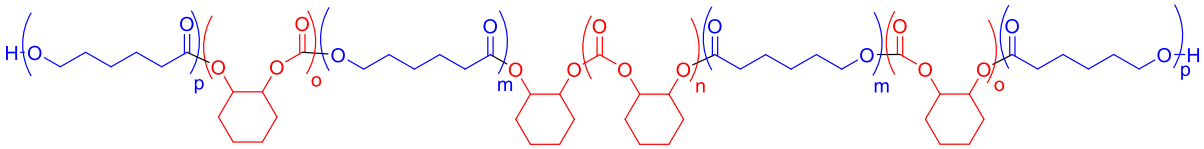

PCL - PCHC - PCL - PCHC - PCL - PCHC - PCL

Figure 4.2.2: Proposed structure of a multi (hepta) block copolymer synthesised using switch catalysis.

4.3 Catalyst Selectivity

4.3.1 Polymerisation Selectivity

[$LZn_2(OCOCF_3)_2$] was used to synthesise multiblock copolymers from a mixture of CHO/ε-CL/CO_2. The terpolymerisation was carried out at 80 °C with a loading of 1:800:400

Cat:CHO:ε-CL. Toluene was used as the solvent to limit the solution viscosity. The relatively low loading of CHO was used to prevent excess chain transfer agents being carried forward (section 1.2.1).

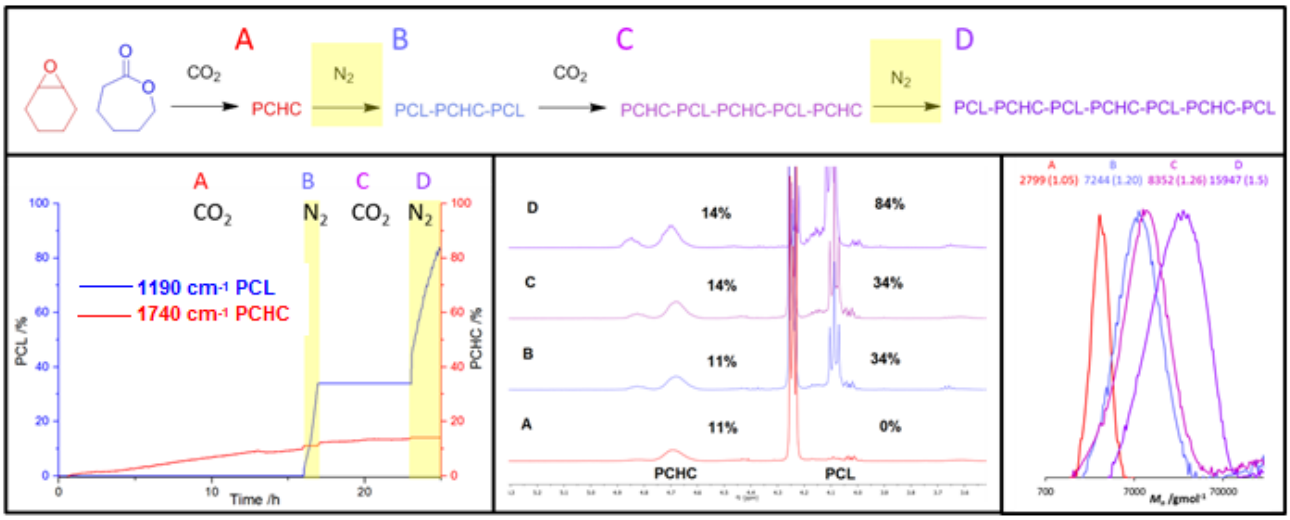

Figure 4.3.1: Scheme showing the formation of a multiblock copolymer by the terpolymerisation of CHO/ε-CL/CO_2 when subjected to repeated CO_2/N_2 cycles.

Left: The terpolymerisation can be monitored by *in-situ* ATR-IR infrared spectroscopy. The absorption at 1190 cm^{-1} corresponds to PCL. The absorption at 1740 cm^{-1} corresponds to PCHC. The absorptions were assigned from control reactions and have been correlated against the known conversions determined from ^{1}H NMR spectroscopy. Middle: ^{1}H NMR spectroscopy. The conversions were determined from the comparison of the normalised integrals of the methine protons of PCHC at 4.65 ppm, the methine protons of CHO at 3.10 ppm and the methylene protons of ε-caprolactone at 4.20 ppm and the methylene protons of PCL at 4.05 ppm. Right: SEC traces of aliquots taken throughout the terpolymerisation.

The terpolymerisation was followed by *in-situ* IR spectroscopy and ^{1}H NMR spectroscopy of aliquots taken from the reaction. During stage A (1-16 h), exclusively PCHC was formed as monitored *via* the increase of the intensity of the IR absorption at 1740 cm^{-1} and the appearance of the signal at 4.65 ppm in the ^{1}H NMR spectrum. It is only once the carbon dioxide was removed (Stage B, 16 - 17 h) that the formation of PCL occurs. The carbon

dioxide was removed by six brief vacuum/nitrogen cycles. The formation of PCL was confirmed by the increase in intensity of the absorption at 1190 cm^{-1} and the appearance of a signal at 4.05 ppm in the ^{1}H NMR spectrum. During Stage B there was little change in the absorption at 1740 cm^{-1} and ^{1}H NMR spectroscopy shows there was no further formation of PCHC (normalised integral of signal at 4.65 ppm remains constant). Carbon dioxide was reintroduced to the system at 17 h, (Stage C, 17 - 23 h). The IR absorption at 1190 cm^{-1} no longer changed in intensity, whereas the absorption at 1740 cm^{-1} increased in intensity. ^{1}H NMR spectroscopy shows that only PCHC was being formed during this stage, with the signal at 4.65 ppm increasing in intensity and the signal at 4.11 ppm not changing. Stage D began at 23 h (23 - 25 h) with the removal of the carbon dioxide. Again an increase in the absorption of 1190 cm^{-1} was observed with concurrent flat lining of the absorption of 1740 cm^{-1}. The signal at 4.11 ppm in the ^{1}H NMR spectroscopy increased in intensity and there was no more formation of PCHC. The data is consistent with the ability to form multiblock copolymers using alternating switch periods.

Table 4.1: Synthesis of a multiblock copolymer from the terpolymerisation of ε-CL/CHO/CO_2.

Stage	Time /h	Conversion CHO [a]	Conversion ε-CL [b]	TOF [c]	M_n (Đ) [d]
A	16	11	0	5.5	2800 (1.05)
B	1	0	34	136	7240 (1.20)
C	6	14	0	4	8350 (1.26)
D	2	0	84	66	15900 (1.50)

Conversion refers to the particular monomer conversion during the specific stage, so a value of 0 % means the conversion is unchanged from the previous stage a) Determined by ^{1}H NMR spectroscopy, the CHO conversion was determined from the normalised integrals for the CH signals at 3.05 ppm (CHO) and 4.58 ppm (PCHC). b) The ε-CL conversion was determined from the normalised integrals for the signals at 4.05 ppm (PCL) *vs*. 4.15 ppm (ε-CL). c) TOF = (mol of monomer/mol of catalyst)/h. d) Determined by SEC, with THF as the eluent, using polystyrene standards to calibrate the instrument.

4.3.2 Polymerisations Conducted in Solution

It is known from the molar mass values that during the formation of PCHC, multiple polymer chains are formed *via* chain transfer reactions. The chain transfer agent is proposed to be 1,2-cyclohexene diol, likely formed from the ring opening of CHO by water (section 1.2.1). When 1,2-cyclohexene diol was used as chain transfer agent during the ROP of ε-CL, with $[LZn_2(OCOCF_3)_2]$ as the catalyst, the rate of initiation from secondary hydroxyl groups was slower than that from primary hydroxyls, leading to a mixture of chain architectures (section 2.1). In the formation of the multiblock copolymer, the end groups formed during stages A and C are secondary hydroxyls, therefore subsequent PCL formation (in stage B and D) may also be hampered by the difference in the relative rates as initiation from primary *versus* secondary hydroxyl groups. One option to improve the initiation from secondary hydroxyl groups is to control and maximise the ratio of initiator: monomer (ε-CL) during ROP. The use of toluene as a solvent, limits the amount of excess CHO, required which in turn limits the amount of 1,2-cyclohexene diol formed and the number of chains being formed during stage A.

Another benefit of using a solvent is to reduce the viscosity of the system, as this allows efficient mixing and diffusion of the monomer to the initiating end groups. The amount of solvent used must be carefully controlled, as reducing the overall catalyst concentration, directly reduces the rate of polymerisation and may also increase degradation of the catalyst. The use of toluene has been shown not to alter the selectivity of ring opening copolymerisation (no ether linkages formed) (section 2.4.1) however, there is increased cyclic carbonate formation. The cyclic carbonate can easily be removed during the purification of the multiblock copolymer. A series of experiments were run at variable epoxide concentrations and the optimum value was found to be 3.5 M of CHO (0.0042 M of catalyst), as it allowed the balancing of the various factors mentioned above. The overall volume of the system was also important and in this work, the polymerisations were carried out at a volume of ~8 mL (in a 100 mL Schlenk). It was noted that even minor increases (0.5 mL) to the volume resulted in problems, even if the concentration remained the same. The volume restriction is imposed by the specific instrumentation (*in-situ* ATR –IR probe) whereby the reaction vessel size is fixed. It seems likely that designing a system with a larger reaction

surface area and/or optimized mixing would also overcome limitations of viscosity, thereby increasing the rate of polymerisation and facilitating efficient carbon dioxide removal.

4.3.3 Rate of Ring Opening Polymerisation

While the monomer selectivity remained the same even after multiple switches, the rate of polymerisation was affected. The TOF value of later ROCOP stage (stage C) has a very similar value to the first ROCOP stage (TOF = 4 h^{-1} and 5 h^{-1} respectively). However, for the ROP stages, there was a big difference in the TOF values. During the 1st stage (B), the TOF value is 136 h^{-1}. But during the 2nd stage (D) the TOF value was reduced to 66 h^{-1}. This significant decrease in the rate was likely to be due to the reduction in overall monomer concentration.

Table 4.2: The rate of polymerisation compared for each stage of the multiswitch copolymerisation.

Stage	Time	Conversion CHO [a)]	Conversion ε-CL [b)]	TOF [c)]
A	16	11	0	5.5
B	1	0	34	136
C	6	14	0	4
D	2	0	84	66

a) Determined by ^{1}H NMR spectroscopy, the CHO conversion was determined from the normalised integrals for the CH signals at 3.05 ppm (CHO) and 4.58 ppm (PCHC). b) The ε-CL conversion was determined from the normalised integrals for the signals at 4.05 ppm (PCL) *vs*. 4.15 ppm (ε-CL). c) TOF = (mol of monomer/mol of catalyst)/h. Monomer conversions determined from ^{1}H NMR spectroscopy.

The rate of polymerisation can be calculated from the absorption data collected by the ATR-IR spectroscopy. The equation for the ROP of ε-CL can be written as:

$$Rate = k_p\ [\varepsilon - CL]^x[Cat]^y$$

Because the ROP of ε-CL is first order in ε-CL, the rate can be expressed as:

$$Rate = k_{obs}\ [\varepsilon - CL] \qquad k_{obs} = k_p\,[Cat]^y$$

The rate is the change in ε-CL with respect to time, so the equation can be rearranged as follows:

$$\ln\frac{[\varepsilon - Cl]}{[\varepsilon - Cl]_0} = -kt$$

The concentration of ε-CL and the absorption are directly correlated (Beers law – Section 2.3.5) so the absorption can be directly substituted for concentration.

$$\ln\frac{A_t}{A_0} = -kt$$

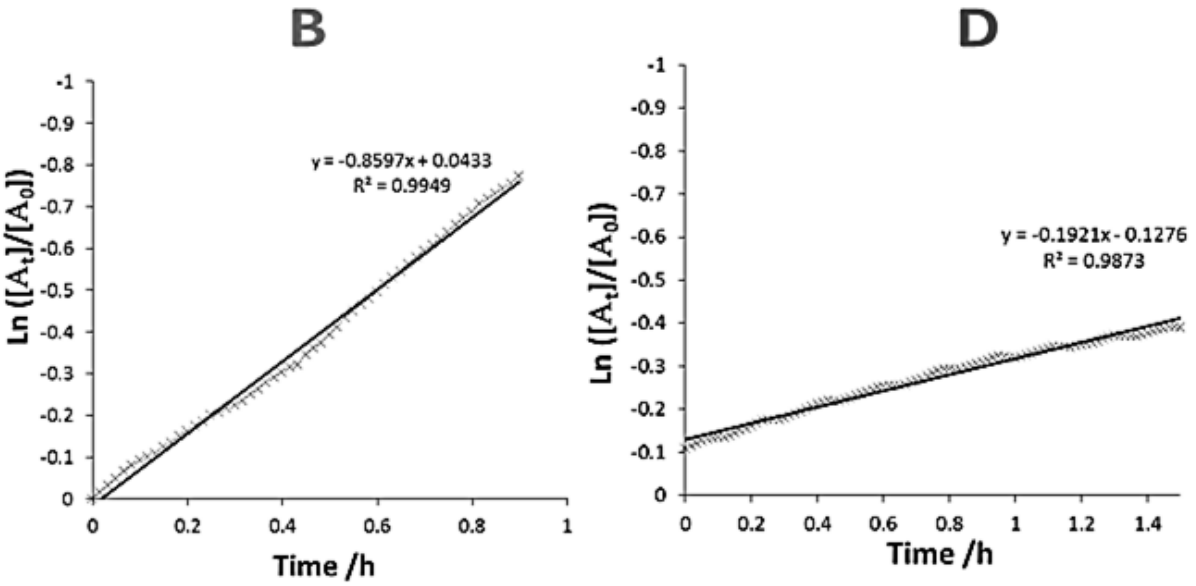

Figure 4.3.2: Plots of $\ln\frac{A_t}{A_0}$ versus time for stage B (Left) and stage D (Right).

When $\ln\frac{A_t}{A_0}$ $versus$ time is plotted for each ROP stage the k_{obs} can be determined. During stage D of the multiblock formation the conversion of ε-CL reaches 84 %. At these levels of conversion the rate of the ROP decreases, due to the reduction in caprolactone concentration. Therefore in the calculation of the k_{obs} value for stage D, the last half hour has not been included (24.5 - 25 h). The k_{obs} calculated for stage B was 0.85 s^{-1} and for stage D was 0.19 s^{-1}. The reduction in rate was mainly due to the decrease in overall ε-CL concentration, along with the increase in viscosity of the system. The concentration of ε-CL was calculated at 1.62 M [ε-CL] at the beginning of stage B and ~ 1M [ε-CL] (by conversion) at the beginning of stage D. A k_{obs} has not been calculated for the ROCOP stages (A and C) because the conversion of CHO is low (< 14 %), and the reaction is still in its initiation period. There is little decrease in the turnover frequency of stage A and C.

4.3.4 Discussion

While there are no other reports of multiblock copolymers synthesised by switch catalysis, there are several reports of catalysts for ROP which can be switched on and off (section 1.5). The closest report detailing the formation of a multiblock copolymer involving a related method is the use of $[LZn_2(Ph)_2]$ and alcohol to form a poly(PCHPE-PDL) multiblock copolymer.[12] From a mixture of PA and ε-DL, PCHPE is selectively formed, followed by PDL formation. The multiblock copolymer can only be formed by the sequential addition of more of the mixture of monomers. There is the potential for the introduction of impurities during such additions. In contrast, the system using $[LZn_2(OCOCF_3)_2]$ shows controlled and reversible selectivity over several switches. The ability of $[LZn_2(OCOCF_3)_2]$ to switch is not affected by previous switches. The catalyst activity appears reasonably stable under the reaction conditions and the observed decrease in activity as the polymerisation progresses can be attributed to the reduced overall monomer concentration and is exacerbated by the increase in solution viscosity. Therefore, there is good evidence that $[LZn_2(OCOCF_3)_2]$ is able to selectively polymerise ε-CL and CHO/CO_2. Further analysis of the polymer formed using this method is required in order to determine whether or not a pure multiblock copolymer has formed.

4.4 Polymer Characterisation

The structure of the copolymer resulting from the multiple switches was investigated by SEC analysis, NMR spectroscopy and thermal analysis. The multiblock copolymer is expected to have the structure BABABAB, where B is PCL and A is PCHC. The heptablock structure results from the telechelic structure of the initial PCHC block.

4.4.1 NMR Spectroscopy

The proposed structure of the copolymer formed during the multi switch catalysis is drawn in Figure 4.4.1.

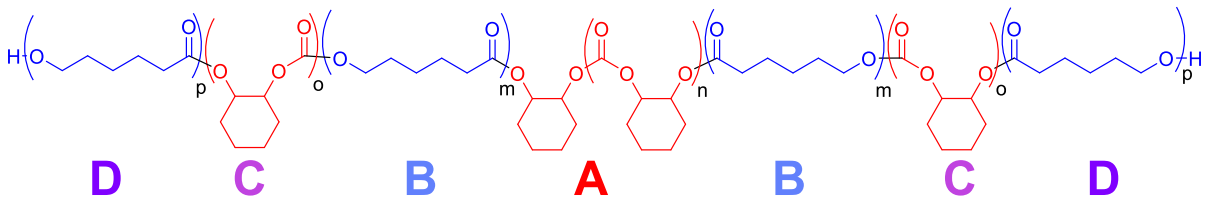

Figure 4.4.1: Proposed structure of a multi (hepta) block copolymer synthesised using switch catalysis. A-D refers to the stages of polymerisation according to Figure 4.3.1.

Table 4.3: Multiblock Characterisation by ^{1}H NMR .

	Time	Conversion CHO [a)]	Conversion ε-CL [b)]	$\overline{DP}$ PCHC [c)]	$\overline{DP}$ PCL [c)]	Ratio carbonate:ester theoretical [d)]	Ratio carbonate:ester ^{1}H NMR [e)]
A	16	11	0	88	0	1:0	1:0
B	1	0	34	88	136	1:1.5	1:1.6
C	6	14	0	112	136	1:1.2	1:1.3
D	2	0	84	112	336	1:3	1:3

a) Determined by ^{1}H NMR spectroscopy, the CHO conversion was determined from the normalised integrals for the CH signals at 3.05 ppm (CHO) and 4.65 ppm (PCHC). b) The ε-CL conversion was determined from the normalised integrals for the signals at 4.05 ppm (PCL) *vs*. 4.15 ppm (ε-CL). c) $\overline{DP}$ = relative molar equivalents of monomer x conversion d) ratio of carbonate:ester = ratio $\overline{DP}$ PCHC: $\overline{DP}$ PCL. e) Calculated from the comparison of the normalised integrals for 4.65 ppm for PCHC and 4.05 ppm for PCL

During the synthesis of the multiblock copolymer, aliquots were taken at the end of each stage (A-D). ^{1}H NMR analysis was carried out on these aliquots. PCHC formation is indicated by the signal at 4.65 ppm, assigned to the methine protons on the cyclohexene ring. PCL formation was indicated by the signal at 4.05 ppm, assigned to the methylene protons nearest the ether linkage. The ratio of carbonate: ester in the block copolymer was calculated from the normalised integrals of the aforementioned two signals. At each stage of the polymerisation, the ratio of carbonate: ester was in good agreement with the calculated values. The final multiblock copolymer was purified by precipitation from THF by MeOH. The ratio of PCHC: PCL in the final purified copolymer was 1:3.1, which is also in good agreement with the calculated value, indicating that neither PCHC nor PCL was being removed in large quantities by the precipitation of the copolymer. This suggests that the majority of the PCHC and PCL formed are attached to each other, rather than as separate chains. As mentioned in section 4.3 measures were taken to limit the extent of chain transfer occurring during ROCOP, stage A. The number of chains formed can be calculated by comparison of the ^{1}H NMR signals of the main chain methine resonances (4.65 ppm) and the end group methine resonances (4.40 ppm and 3.60 ppm). The ratio was observed to be 16:1, which corresponds to a molar mass of 2,400 g mol^{-1}. This is in reasonable agreement with the

molar mass determined by SEC (2799 g mol^{-1}). The theoretical molar mass, calculated from a conversion of 11% CHO (2000 equiv.) is 12,500 g mol^{-1}. By comparing the theoretical and experimental molar mass, the number of chains being formed is ~ 5 chains per catalyst. This value is in line with previously determined values using the dinuclear catalysts and others in the literature.[29-34]

The ^{1}H NMR spectrum of the multiblock copolymer showed both the characteristic signals of the main chain PCHC and PCL units (4.65 and 4.05 ppm) and signals assigned to the junction units between the ester and carbonate blocks (4.78 and 4.11 ppm respectively). Thus given that there are an average of 5 chains per equivalent of catalyst, the $\overline{DP}$ for each block will correspond to the monomer conversion /5.

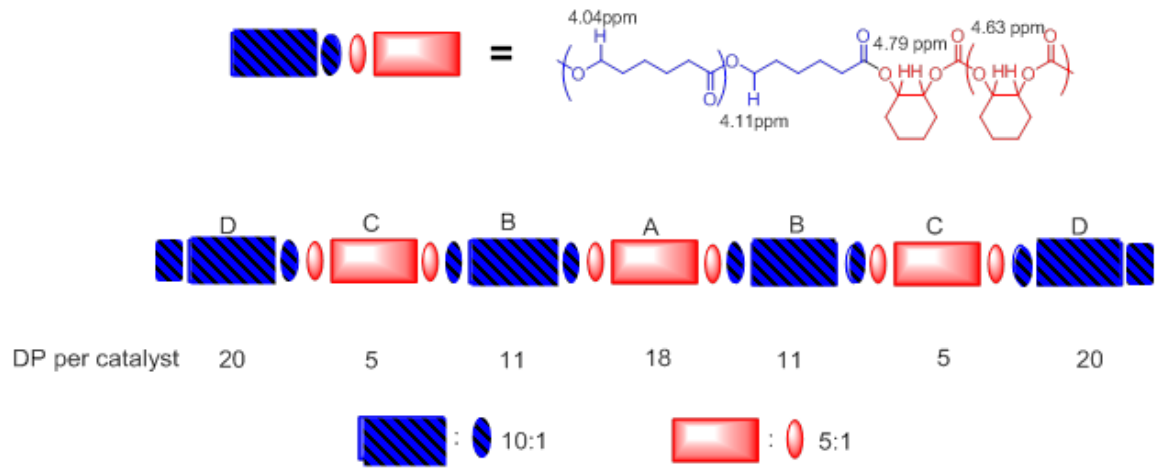

Figure 4.4.2: **Scheme showing the $\overline{DP}$ of each block and the ratio of junction unit: main chain unit.**

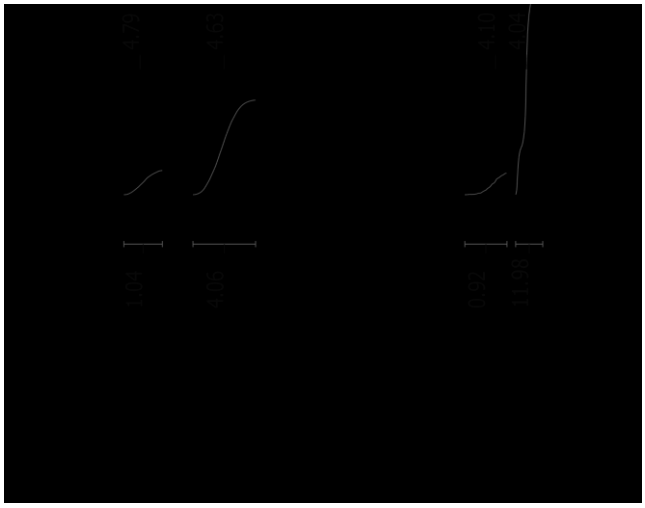

Figure 4.4.3: Excerpt of the ^{1}H NMR spectrum of the multiblock copolymer, showing the relative ratios of main chain PCHC (4.63 ppm), PCL (4.04 ppm) and the ester (4.10 ppm) and carbonate (4.79 ppm) junction units.

The peak at 4.11 ppm corresponds to the ester junction unit, resulting from the methylene protons of the PCL unit directly attached to the carbonate block. The ratio of the integrals of the main chain ester signal (4.05 ppm) to the junction unit signal (4.11 ppm) is 13:1. The calculated ratio was 10:1 which was in reasonable agreement with the observed ratio. The peak at 4.78 ppm corresponds to the methine protons of a PCHC unit attached to the ester block. The ratio of the main chain carbonate signal (4.65 ppm) to the junction unit signal (4.78 ppm) was 4:1, which was close to the calculated ratio is 5:1. For the ABA triblock copolymer (Chapter 2), the ratio of ester: carbonate junction units (4.11 ppm: 4.78 ppm) was 1:2, this was proposed to be due to the signal for the carbonate junction unit resulting from PCHC unit. However the multiblock copolymer showed a ratio of ester: carbonate junction units of 1:1. This is what would be expected from the calculated ratio if only one unit of each polymer (ester and carbonate) contributes to the signals. This could potentially be due to the fact the multiblock copolymer was longer than the majority of the ABA block copolymers. Therefore the intensity of the junction signals was smaller so the integration was not as accurate. The good agreement between the calculated values and observed values for the various ratios provided good support for the clean formation of the multiblock copolymer, rather than the formation of discrete homo/copolymers.

Since the $\overline{DP}$ of each block varies from 5-20 units, it was relevant to consider the probability of all chains having the same structure e.g. a BABABAB copolymer. As there was always a distribution of chain lengths formed, even when the dispersity was narrow. At low $\overline{DP}$'s there may be a proportion of chains that do not incorporate the block. The longer the block length, the more likely that all chains will contain that block. In a theoretical example, Perrier and co-workers showed that for an 18 block copolymer, if each block has a length of 3 units, then the majority of chains formed will be defective.[4] Lengthening the block, results in an exponential decrease in the likelihood of defects. When the block length is 6 units, for a 20 block copolymer, only 5 % of chains will be defective.[4] In this study, the lowest $\overline{DP}$ was ~5 units, (PCHC, stage C). Therefore, it is possible that a low proportion of chains may not contain polycarbonate in this section of the polymer. The number of defective chains is likely to be low, as the block length of 5 is still considered long in this type of calculation.

4.4.2 DOSY NMR Spectroscopy

^{1}H DOSY NMR spectroscopy allows the determination of the diffusion co-efficient of a species. ^{1}H DOSY NMR spectroscopy can be used to distinguish between copolymers and homopolymers (section 2.3.6). ^{1}H DOSY NMR spectra of the aliquots taken from the end of each stage of the multiblock copolymer synthesis were analysed. As each new block was formed, a clear decrease in the diffusion co-efficient was observed which corresponds to an increase in the hydrodynamic radius, as expected with increasing chain length and molar masses of the species. In all cases, only a single species was observed with all signals for PCHC and PCL having the same diffusion coefficient. This indicated that a block copolymer had formed rather than the a mixture of homopolymers.

Table 4.4: ^{1}H DOSY NMR analysis of the aliquots taken during the multiblock copolymer synthesis.

Stage	M_n of copolymer [a)]	D / x 10^{-10} m^2/s	R_h / x 10^{-9} m [b)]
A	2800	3.95	1.03
B	7240	2.22	1.83
C	8350	1.76	2.31
D	15900	1.08	3.76

a) determined by SEC with THF as the eluent, using polystyrene standards to calibrate the instrument b) $R_h = (k_B T)/6\pi\eta D$ [k_B is the Boltzmann constant, T is the temperature, and η is the solvent viscosity at the measured temperature, D is the diffusion coefficient, R_H is the hydrodynamic radius].

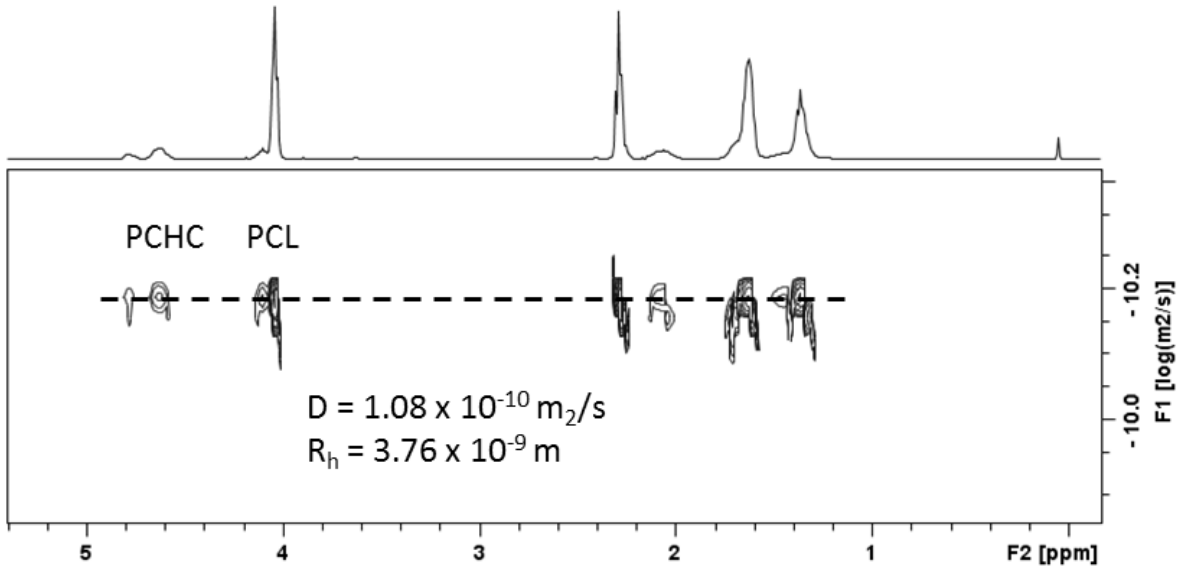

Figure 4.4.4: ^{1}H DOSY NMR spectrum of the multiblock copolymer.

4.4.3 SEC Analysis

The aliquots were also analysed by SEC in THF, using PS standards. During the formation of the multiblock copolymer, the molar mass increased after each stage. The increase was

considerably greater after the formation of PCL (stage B and D), due to the much faster rate of polymerisation (and consequently higher $\overline{DP}$). It is particularly relevant that the first and final aliquots do not overlap. The molar masses values are in reasonable agreement with the calculated values considering ~5 chains form per catalyst. By comparing the increase in molar mass values it is possible to make correlations about the proportion of ester and carbonate blocks. This is achieved by comparing the molar mass of the blocks at each stage with the overall molar mass. In most cases, the comparison was in good agreement with the ratio of carbonate: ester units as calculated by ^{1}H NMR spectroscopy providing an independent verification of the multiblock copolymer structure.

Table 4.5: SEC analysis of the Multiblock copolymer.

#	M_n of copolymer [a]	M_n of block [b]	Ratio carbonate:ester (SEC) [c]	Ratio carbonate:ester (^{1}H NMR) [d]	M_n Calculated (Block) [e]
A	2800	2800	1:0	1:0	2500
B	7240	4450	1:1.6	1:1.6	(3100) 5600
C	8350	1080	1:1.1	1:1.3	(680) 6280
D	15900	7600	1:3.0	1:3.0	(4560) 10800

a) determined by SEC with THF as the eluent, using polystyrene standards to calibrate the instrument. b) Increase in molar mass. So for M_n for B block = M_nB -M_nA. c) ratio of the total M_n of all carbonate blocks : total M_n of all ester blocks formed at that stage. d) Calculated from the comparison of the normalised integrals for 4.65 ppm for PCHC and 4.05 ppm for PCL e) M_n calculated = $\overline{DP}$ x Molar mass of repeat unit /5. 142 g mol^{-1} for PCHC and 114 g mol^{-1} for PCL.

4.4.4 DSC Analysis

Thermal analysis of block copolymers provides information of the interactions between the blocks (Section 2.3.7). DSC analysis of the multiblock copolymer showed three glass transition temperatures (T_g) at -68, -5 and 64 °C. The T_g at -68 °C was assigned to PCL blocks and was close to the values previously reported values for the pure PCL (T_g = -60

°C).[35] There was no indication of a melting transition, so it seems the crystallinity of the PCL has been completely suppressed. The T_g at 64 °C has been assigned to the PCHC block, although the value was considerably lower than values for pure PCHC, (T_g = 115 °C).[36] The multiblock copolymer only contained very short PCHC blocks (1000 -3000 g mol^{-1}), which was likely to be the reason for the lowered T_g value. The T_g value at -5 °C was assigned to regions in which the blocks are miscible. For perfectly miscible block copolymers the Fox-Flory relationship can be used to calculate the T_g. In this case, a calculated value of -1 °C was obtained. This was in reasonable agreement with the observed transition, indicating that there were regions of complete block miscibility. The suppression of the crystallinity of PCL by the presence of PCHC, was also observed for the ABA triblock copolymers, where the ester content was less than 80 %. In the multiblock copolymer the overall content of ester was determined to be ~75 %. Therefore the suppression of crystallinity was in line with the previous findings.

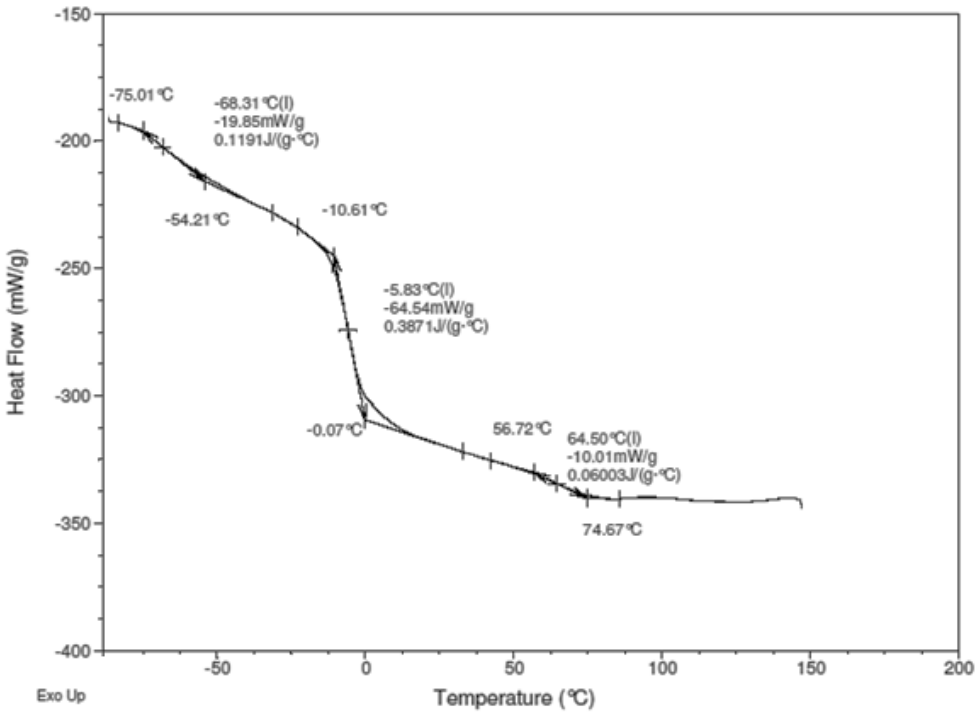

Figure 4.4.5: DSC of the multiblock copolymer.

The T_g was calculated from the third heating cycle of the DSC measurement and was heated at 10 °C/min from −100 to 150 °C.

4.5 Conclusions and Outlook

Switchable catalysis using [$LZn_2(OCOCF_3)_2$] has previously been exploited from ABA triblock copolymers. Here it was exploited multiple times to prepare multiblock copolyester carbonates compromising short blocks of polycaprolactone and poly(cyclohexene carbonate). The catalyst can be switched between either ring opening copolymerisation to form poly(cyclohexene carbonate) or ring opening polymerisation to form polycaprolactone with excellent selectivity and reversibility. However, there was a disparity in the relative rates of polymerisation which means that increasing the degree of polymerisation of the poly(cyclohexene carbonate) block was slow. Another factor was the issue of chain transfer, which results in the formation of multiple chains per equivalent of catalyst. The chain transfer reaction must be efficient and also there must be a balance between the relative rates of the polymerisation from primary and secondary alkoxide groups. It was feasible to develop a catalyst system that allowed the formation of a heptablock copolymer. The structure of the copolymer was confirmed by SEC analysis and ^{1}H NMR spectroscopy and ^{1}H DOSY NMR spectroscopy. This is a rare example of a one-pot system to form a multiblock copolymer and represents a straightforward method to combine different polymerisation mechanisms. It is also the first example of a catalyst which can switch between two different polymerisations in both directions and result in a multiblock copolymer.

In terms of future improvements to the system it would be beneficial to develop a catalyst where the rates of the two polymerisations (ROCOP/ROP), are comparable and fast. Such an increase in rate would allow more blocks to be included in the multiblock copolymer and also reduce the polymerisation time, preventing any catalyst degradation. In a system where both the polymerisations are rapid, it would be considerably easier to tune block length by controlling the length of time the system is exposed to particular conditions, as opposed to having to account for the slow ROCOP stages. Another future development would be to develop a catalyst where chain transfer occurs equally rapidly between the primary and secondary hydroxyls. Another option, would be to test a lactone which propagates *via* secondary hydroxyl groups such as ε-DL. None the less for optimised performance the rates of propagation from the cyclohexenyl and lactone hydroxyl should be comparable.

In the next chapter, the switch chemistry of $[LZn_2(X)_2]$ will be developed and the effect of additional monomers will be investigated. The ring opening copolymerisation of anhydride and epoxides will be combined with the ring opening of copolymerisation of epoxides and carbon dioxide and ring opening polymerisation of lactones in an attempt to make multiblock copolymers containing three distinct blocks.

References

(1) Bates, F. S.; Fredrickson, G. H. *Physics Today* **1999**, *52*, 32.
(2) Bates, F. S.; Hillmyer, M. A.; Lodge, T. P.; Bates, C. M.; Delaney, K. T.; Fredrickson, G. H. *Science* **2012**, *336*, 434.
(3) Badi, N.; Lutz, J.-F. *Chem. Soc. Rev.* **2009**, *38*, 3383.
(4) Gody, G.; Zetterlund, P. B.; Perrier, S.; Harrisson, S. *Nat Commun* **2016**, *7*.
(5) Lodge, T. P. *Macromol. Chem. Phys.* **2003**, *204*, 265.
(6) Gody, G.; Maschmeyer, T.; Zetterlund, P. B.; Perrier, S. *Nat Commun* **2013**, *4*.
(7) Semsarilar, M.; Perrier, S. *Nat Chem* **2010**, *2*, 811.
(8) Nakano, K.; Kamada, T.; Nozaki, K. *Angew. Chem. Int. Ed.* **2006**, *45*, 7274.
(9) Darensbourg, D. J.; Ulusoy, M.; Karroonnirum, O.; Poland, R. R.; Reibenspies, J. H.; Çetinkaya, B. *Macromolecules* **2009**, *42*, 6992.
(10) Kim, J. G.; Cowman, C. D.; LaPointe, A. M.; Wiesner, U.; Coates, G. W. *Macromolecules* **2011**, *44*, 1110.
(11) Kim, J. G.; Coates, G. W. *Macromolecules* **2012**, *45*, 7878.
(12) Zhu, Y.; Romain, C.; Williams, C. K. *J. Am. Chem. Soc.* **2015**, *137*, 12179.
(13) Jikei, M.; Takeyama, Y.; Yamadoi, Y.; Shinbo, N.; Matsumoto, K.; Motokawa, M.; Ishibashi, K.; Yamamoto, F. *Polym. J.* **2015**, *47*, 657.
(14) Huang, W.; Wan, Y.; Chen, J.; Xu, Q.; Li, X.; Yang, X.; Li, Y.; Tu, Y. *Polym. Chem.* **2014**, *5*, 945.
(15) Guillaume, S. M. *Eur. Polym. J.* **2013**, *49*, 768.
(16) Nakayama, Y.; Okuda, S.; Yasuda, H.; Shiono, T. *React. Funct. Polym.* **2007**, *67*, 798.
(17) Nagata, M.; Sato, Y. *J. Polym. Sci., Part A: Polym. Chem.* **2005**, *43*, 2426.
(18) Zhang, J.; Xu, J.; Wang, H.; Jin, W.; Li, J. *Mater. Sci. Eng., C* **2009**, *29*, 889.
(19) Eceiza, A.; de la Caba, K.; Gascón, V.; Corcuera, M. A.; Mondragon, I. *Eur. Polym. J.* **2001**, *37*, 1685.
(20) Kricheldorf, H. R.; Meier-Haack, J. *J. Polym. Sci., Part A: Polym. Chem.* **1993**, *31*, 1327.
(21) Bachari, A.; Bélorgey, G.; Hélary, G.; Sauvet, G. *Macromol. Chem. Phys.* **1995**, *196*, 411.
(22) Zaschke, B.; Kennedy, J. P. *Macromolecules* **1995**, *28*, 4426.
(23) You, J. H.; Choi, S.-W.; Kim, J.-H.; Kwak, Y. T. *Macromol Res* **2008**, *16*, 609.
(24) Ho, C.-H.; Wang, C.-H.; Lin, C.-I.; Lee, Y.-D. *Eur. Polym. J.* **2009**, *45*, 2455.

(25) Simula, A.; Nikolaou, V.; Anastasaki, A.; Alsubaie, F.; Nurumbetov, G.; Wilson, P.; Kempe, K.; Haddleton, D. M. *Polym. Chem.* **2015**, *6*, 2226.
(26) Chang, R.; Shan, G.; Bao, Y.; Pan, P. *Macromolecules* **2015**, *48*, 7872.
(27) Li, Y.; Hong, J.; Wei, R.; Zhang, Y.; Tong, Z.; Zhang, X.; Du, B.; Xu, J.; Fan, Z. *Chem. Sci.* **2015**, *6*, 1530.
(28) Hu, N.; Mai, C.-K.; Fredrickson, G. H.; Bazan, G. C. *Chem. Commun.* **2016**, *52*, 2237.
(29) Kember, M. R.; Knight, P. D.; Reung, P. T. R.; Williams, C. K. *Angew. Chem. Int. Ed.* **2009**, *48*, 931.
(30) Kember, M. R.; Copley, J.; Buchard, A.; Williams, C. K. *Polym. Chem.* **2012**, *3*, 1196.
(31) Kember, M. R.; Williams, C. K. *J. Am. Chem. Soc.* **2012**, *134*, 15676.
(32) Nakano, K.; Hashimoto, S.; Nozaki, K. *Chem. Sci.* **2010**, *1*, 369.
(33) Darensbourg, D. J.; Moncada, A. I.; Choi, W.; Reibenspies, J. H. *J. Am. Chem. Soc.* **2008**, *130*, 6523.
(34) Moore, D. R.; Cheng, M.; Lobkovsky, E. B.; Coates, G. W. *J. Am. Chem. Soc.* **2003**, *125*, 11911.
(35) Tang, M.; Purcell, M.; Steele, J. A. M.; Lee, K.-Y.; McCullen, S.; Shakesheff, K. M.; Bismarck, A.; Stevens, M. M.; Howdle, S. M.; Williams, C. K. *Macromolecules* **2013**, *46*, 8136.
(36) Mang, S.; Cooper, A. I.; Colclough, M. E.; Chauhan, N.; Holmes, A. B. *Macromolecules* **2000**, *33*, 303.

Chapter 5 : Pentablock Copolymers: Introducing New Monomers

5.1 Introduction

Polyesters are commercially synthesized by condensation methods, which although successful do not allow control of molar mass, end groups or monomer enchainment. Aliphatic polyesters can be synthesised by the ROP of cyclic esters or the ROCOP of epoxides and anhydrides, both of which are controlled polymerisation methods.[1] The ROP of cyclic esters is well-studied but is somewhat limited by the range of cyclic esters which are commercially available or which can be prepared on a large scale.[2] In contrast, ROCOP of anhydrides and epoxides to produce polyesters is much less explored but could be attractive due to the wide availability of varied anhydrides and epoxides, which allows manipulation of the structures and properties. For example, the glass transition temperatures (T_g) of polyesters can be moderated from 33-123 °C simply by switching from propylene oxide to cyclohexene oxide while still containing Phthalic Anhydride (PA) as the anhydride.[1,3]

Block copolymers which have an AB or ABA structure are predicted to adopt 4 microphase structures (lamellae, double gyroid, cylinders, and spheres), whereas the introduction of a third distinct (C) block dramatically increases the number of phases that have been reported and leads to a wealth of new microstructures and potential applications.[4] The introduction of branching or cyclisation further increases the number of potential microstructures. Increasing the complexity of the block copolymer, even by a small amount, may eventually lead to multifunctional plastics or other products, such as drug delivery platforms or patterning scaffolds for micro engineering.[4] There are very few examples of block copolymers which contain three distinct blocks, where at least one is synthesised by ROCOP. Coates and co-workers, used a [ZnBDI] catalyst and sequential addition of functionalised epoxides to form a hexablock copoly(carbonate).[5] The same group also reported the synthesis of poly(isoprene-styrene-propylene carbonate), an ABC block copolymer that self-assembled into several different morphologies.[6]

As mentioned in Section 1.4.2 the terpolymerisation of anhydrides/epoxides/carbon dioxide is now well precedented as a route to make poly(ester-b-carbonates).[1] Many ROCOP catalysts successfully enchain both epoxides and carbon dioxide and epoxides and anhydrides.[1] Thereby offering the chance to select the catalyst of choice to make a particular block copolymer. The catalyst [$LZn_2(OAc)_2$] has been shown to form block copolymers from

PA/CHO/CO_2 even at 1 bar of CO_2 pressure, which is a lower pressure than many other catalysts and this significantly simplifies the process.[7] The selectivity results from the insertion of anhydride into the alkoxide species occurring faster than the insertion of carbon dioxide.[8] Therefore, the formation of polycarbonate only occurs after anhydride is fully consumed. It has also been shown that the di zinc catalysts are effective for both anhydride/epoxide copolymerisation and ε-CL ROP, operating by a switch catalysis method.[9] Indeed, a detailed DFT study carried out alongside experimental work has shown that the insertion of anhydride into the zinc alkoxide intermediate bond leads to the most stable product, with the insertion of CO_2 yielding the next most stable product.[10] It is proposed that both kinetic and thermodynamic factors govern the selective insertion of anhydride over carbon dioxide and the formation of poly(ester-b-carbonate). The insertion of ε-CL into the zinc alkoxide intermediate not only leads to a less stable product but also has a higher energy barrier than alternative monomers. Therefore, the formation of any polylactone block only occurs, after the consumption or removal of anhydride or carbon dioxide.[10] So far all experiments have been conducted using mixtures of up to 3 different monomers. An important next step is to discover whether it is possible to selectively polymerise a mixture of 4 monomers.

5.2 Aims

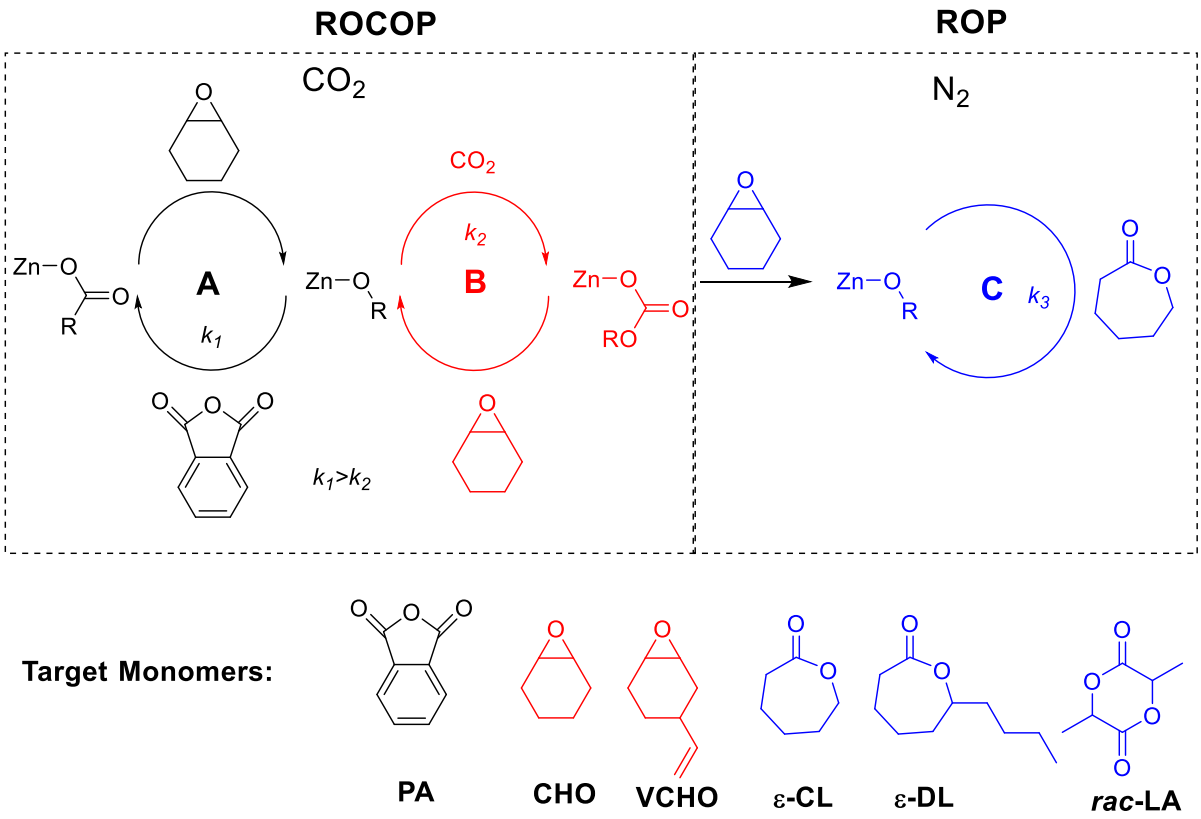

Figure 5.2.1: Scheme showing the proposed mechanism switch catalysis and the target monomers.

The aim is to investigate the polymerisations of anhydrides/CO_2/epoxides/lactones. In particular, the goal is to determine whether the switch catalysis, which enables the combination of ROCOP and ROP, will also operate with a mixture of 4 different monomers. The rules uncovered in previous investigations suggest that the ROCOP of PA/CHO should occur first, followed by the ROCOP of CO_2/CHO and finally ROP should initiate only when the CO_2 is removed. The selectivity of the system will be investigated using *in-situ* ATR IR spectroscopy and ^{1}H NMR spectroscopy, which allows the monitoring of discrete signals for particular monomers and polymers blocks. The structure of the resulting copolymers will be analysed using the methods outlined in section 2.3 and it remains important to discover whether pure block copolymers result, or if there is contamination or the production of a mixture of products.

5.3 Ring Opening Copolymerisation of PA/CHO/CO_2

While the catalyst [$LZn_2(OAc)_2$] has been shown to be active for the copolymerisation of PA/CHO, it results in a mixture of acetate and hydroxyl end capped polymers being produced.[7] There is a bimodal molar mass distribution and the formation of a mixture of AB and ABA block copolymers. In order to improve the control of the ROCOP, a catalyst system is required that only cleanly produces a single series of chains and in this work α,ω-dihydroxyl terminated chains are targeted. Previous research by the Williams research group has discovered that the catalyst [$LZn_2(OCOCF_3)_2$] is able to copolymerise CO_2/CHO to afford only dihydroxyl end capped PCHC.[11] Thus it was a sensible catalyst to investigate for PA/CHO ROCOP.

The catalyst [$LZn_2(OCOCF_3)_2$] was tested using a loading of 1:2:100:500 Catalyst:CHD:PA:CHO, where CHD was used as a chain transfer agent to control the polymerisation. The polymerisation resulted in the selective formation of only perfectly alternating polyester, however the SEC trace was bimodal. The MALDI-ToF spectrum showed two series of chains: one has α,ω-dihydroxyl end groups and the other has both trifluoroacetate and hydroxyl end groups. This finding is in contrast to the copolymerisation of CHO/CO_2 using the [$LZn_2(OCOCF_3)_2$], which selectively forms only the α,ω-dihydroxyl terminated series.[11] One reason may be that the copolymerisation for PA/CHO takes an hour to reach complete conversion (in anhydride) and it has already been shown (Section 2.4.1) that the complete hydrolysis of the trifluoroacetate end groups is not complete until 6 hours into the reaction. Therefore, the presence of trifluoroacetate end groups on some polyester chains may result from the significantly greater rates of polymerisation compared to the CHO/CO_2 ROCOP. The presence of a series of chains with trifluoroacetate end groups means that the [$LZn_2(OCOCF_3)_2$] catalyst is not suitable for the formation of a single type of block copolymers.

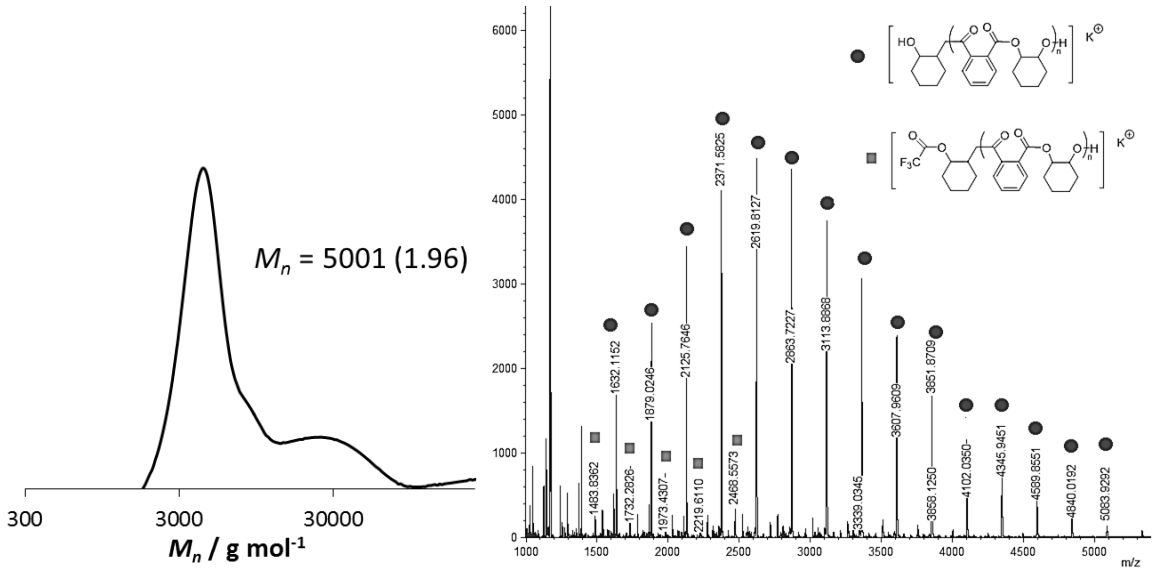

Figure 5.3.1: SEC trace and MALDI-ToF spectrum obtained for the PCHPE, synthesised using [$LZn_2(OCOCF_3)_2$].

The polyester polyol series are represented by circles and calculated for $[(C_{14}H_{14}O_4)_n+C_6H_{12}O_2+K]^+ = [(246.09)_n+116.16+39.1]^+$. The trifluoroacetate terminated series is represented by squares and calculated for $[(C_{14}H_{14}O_4)_n+C_8H_{11}FO_3+K]^+ = [(246.09)_n+212.06+39.1]^+$.

An alternative catalyst system, [$LZn_2(Ph)_2$] combined with a diol (CHD), has been shown to be an effective catalyst for the ROCOP of PA/CHO.[9] The catalyst is proposed to form by the *in-situ* reaction between [$LZn_2(Ph)_2$] and diol (CHD). It produces exclusively α,ω-dihydroxyl terminated chains, and is therefore a much better candidate for the formation of block copolymers. The PCHPE produced by this catalyst system features a monomodal molar mass distribution.[9]

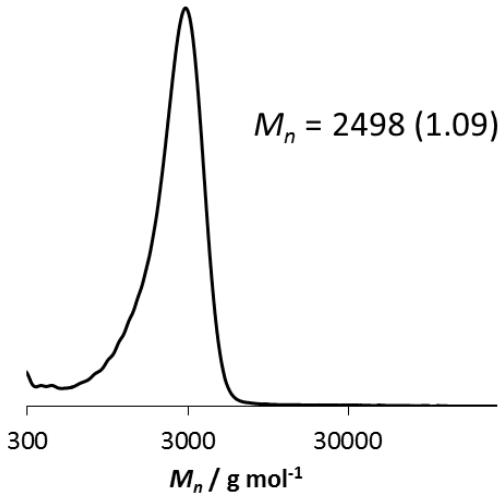

Figure 5.3.2: SEC analysis of poly (cyclohexene phthalate).

Synthesised using a 1:2:50:500 loading of [$LZn_2(Ph)_2$]:CHD:PA:CHO. Polymerisation carried out at 100 °C for 1 hour.

The catalyst system [$LZn_2(Ph)_2$]/CHD afforded well-defined poly(ester-b-carbonate) from a reaction conducted at 1:2:2000:50 [$LZn_2(Ph)_2$]:CHD:CHO:PA, under 1 bar of CO_2 at 100 °C. The polymerisation was monitored using an ATR-IR spectroscopic probe (Figure 5.3.3). Initially the formation of only polyester (1070 cm^{-1}) was observed. During this period the signals for polycarbonate (1240 cm^{-1}) remained unchanged and have no appreciable intensity. All IR signals were assigned from control experiments using pure monomers or polymers

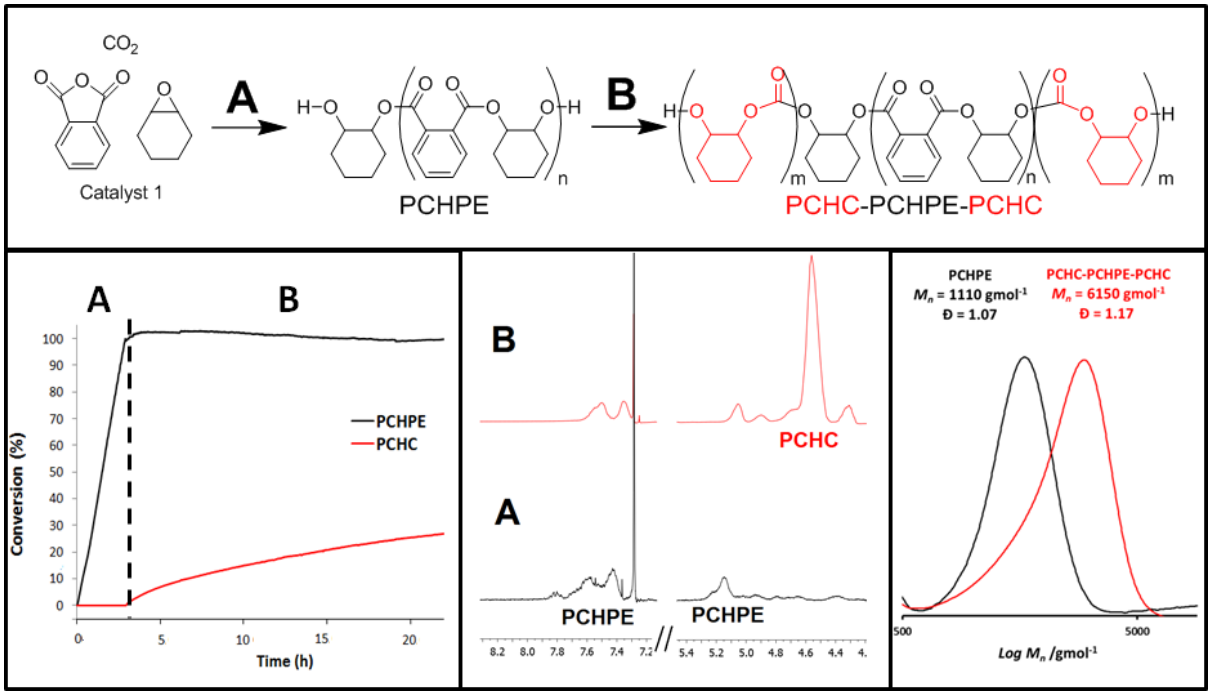

Figure 5.3.3: Scheme showing the formation of poly(PCHC-PCHPE-PCHC) and spectroscopic analysis of the reaction.

Conditions in section 5.3. Left: Plot showing the percent conversion of various polymer blocks *versus* time. The intensity of the assigned resonances was normalised and calibrated against the percent conversions determined from ^{1}H NMR spectroscopy of aliquots withdrawn periodically. The absorption at 1240 cm^{-1} is assigned to PCHC, that at 1070 cm^{-1} to PCHPE.[7] Middle: Selected region of the ^{1}H NMR spectra of aliquots taken during the reaction. Spectrum A) was taken at 2.55 h, B) at 22 h. Spectrum A shows signals due to of PCHPE (7.30-7.83 and 5.05 ppm) but the signal for PCHC (4.65 ppm) is absent. Spectrum B shows signals due to PCHC (4.65 ppm). Right: SEC traces of the same polymer aliquots showing an increase in molar mass as the ABA type block copolymer forms.

^{1}H NMR spectroscopy was also used to confirm the different species present during different phrases of reaction (Figure 5.3.3). An aliquot taken after the first 2.55 h showed signals assigned to PCHPE (7.30-7.83 ppm), but no signals were observed for PCHC (4.65 ppm). Once the phthalic anhydride was fully consumed (after 2.55 h), the formation of PCHC was observed by the appearance of signals at 4.65 ppm assigned to the PCHC block.

The block copolymer structure was confirmed by SEC analysis of the same aliquots taken from the terpolymerisation (Figure 5.3.3). There was a clear increase in molar mass after the

formation of the PCHC blocks and in both cases the molar mass distribution (Đ)) remains monomodal and narrow. The ^{1}H DOSY NMR spectrum of the copolymer showed that all the ^{1}H NMR signals have the same diffusion coefficient (Figure 5.3.4), and therefore should belong to a single polymer species in solution. The diffusion coefficient for the copolymer is determined to be D = 2.89 x 10^{-10} m^2/s, which corresponds to a hydrodynamic radius R_h = 1.41 x 10^{-9} m.

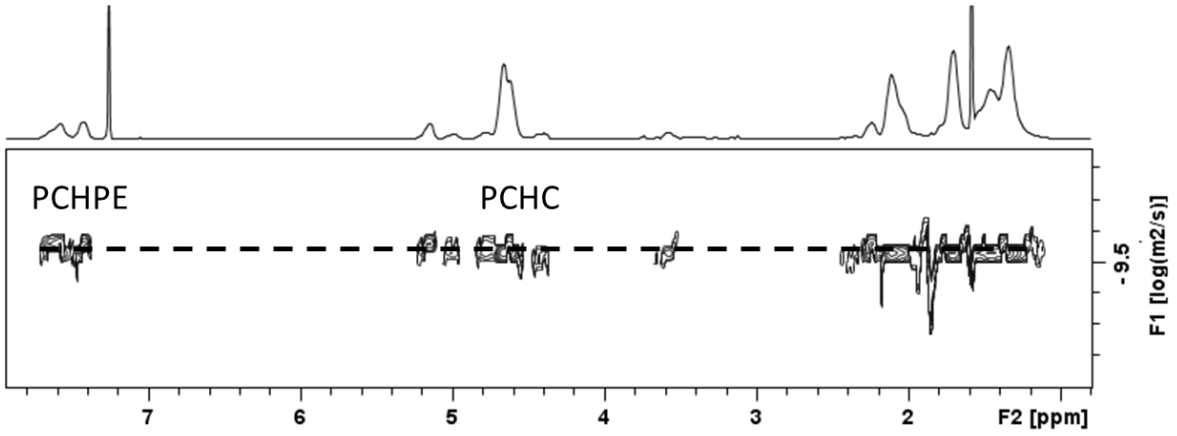

Figure 5.3.4: ^{1}H DOSY NMR spectrum for poly(PCHC-PCHPE-PCHC).

Reaction conditions in section 5.3.

5.4 Pentablock Formation - Lactones

5.4.1 Catalyst Selectivity

Given that the terpolymerisation of PA/CHO/CO_2 using the catalyst system [$LZn_2(Ph)_2$]/CHD, was able to selectively form ABA block copolymers, the next step was to investigate the effect of the addition of a lactone monomer (ε-CL). The reaction of the catalyst system [$LZn_2(Ph)_2$]/CHD with PA/CHO/CO_2/ε-CL (1:2:50:1550:200 loading, 100 °C, 1 atm) was monitored using *in-situ* ATR-IR spectroscopy (Figure 5.4.1). The analysis showed that initially epoxide/anhydride ROCOP occurred, as shown by the increase in the absorption at 1070 cm^{-1}, assigned to PCHPE. The signals assigned to PCHC (1334 cm^{-1}) and

PCL (1190 cm^{-1}) showed no appreciable intensity change over the time period. Furthermore, no conversion was detected in the ^{1}H NMR spectra of aliquots withdrawn during this time period (Figure 5.4.1). The ^{1}H NMR spectra showed only the signals for PCHPE (5.15 ppm) and the monomers CHO (3.10 ppm) and ε-CL (4.20 ppm). Once the PA was fully consumed 4.5h, the ROCOP of CHO/CO_2 occurred as observed by the increase of the absorption at 1334 cm^{-1} (PCHC) and the formation of a signal at 4.65 ppm (PCHC) in the ^{1}H NMR spectrum.

The carbon dioxide was removed from the reaction at 23 h, by a series of short vacuum/nitrogen cycles. There was minimal loss of unreacted monomers due to this process but the carbon dioxide was efficiently removed (examples given in Section 2.3.5). Once the carbon dioxide was removed, the ROP of ε-CL occurred, as evidenced by the increase in the intensity of the IR absorption at 1190 cm^{-1} and the appearance of a signal at 4.05 ppm in the ^{1}H NMR spectrum. The IR spectroscopic data showed the sequential selective formation of various different polymers: PCHPE (A), PCHC (B) and PCL (C). There was a very clear polymerisation selectivity and it seems that the catalyst system does operate by a switch catalysis route. None the less, it is also important to characterise the final copolymer to determine its microstructure.

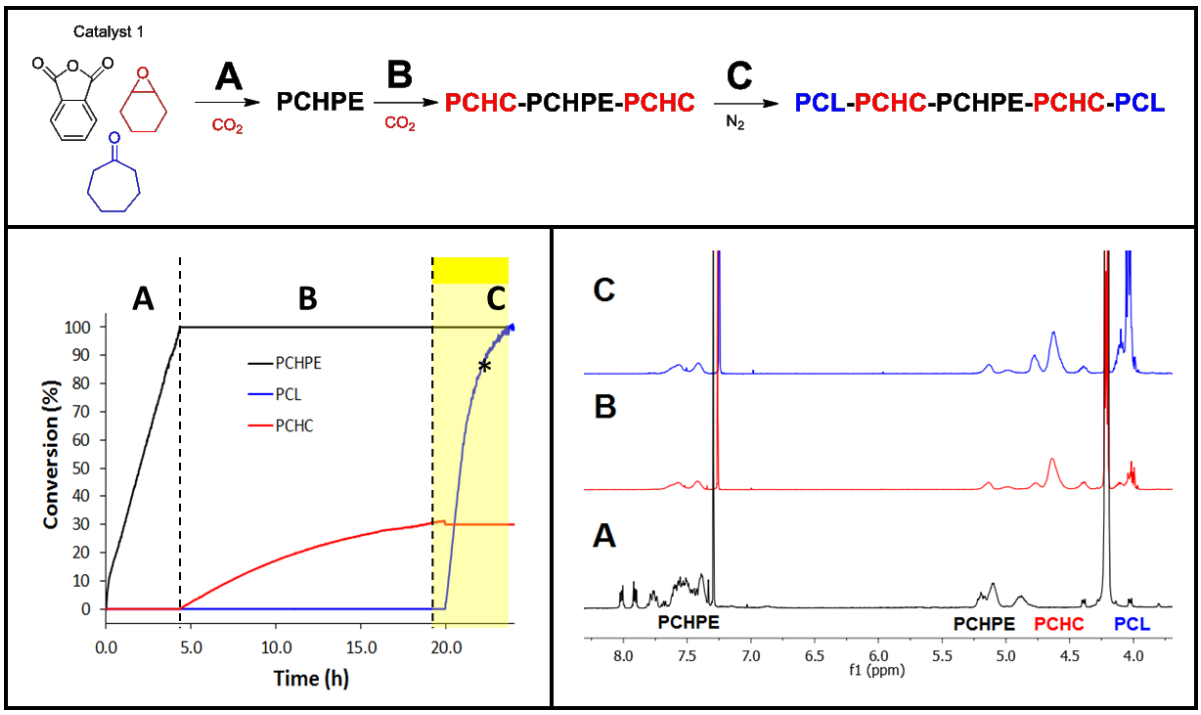

Figure 5.4.1: Scheme showing the formation of pentablock copolymer and monitoring the reaction *via in-situ*-ATR and ^{1}H NMR spectroscopy. (Table 5.2, Run 1).

Left: Plot showing the percent conversion of various polymer blocks *versus* time. The intensity of the assigned resonances was normalised and calibrated against the percent conversions determined from ^{1}H NMR spectroscopy of aliquots withdrawn periodically. The absorption at 1334 cm^{-1} is assigned to PCHC, that at 1070 cm^{-1} to PCHPE and that at 1190 cm^{-1} to PCL. The small blip at 20 h is due to loss of material as described in Section 2.3.5. Right: Selected region of the ^{1}H NMR spectra of aliquots taken during the reaction. Spectrum A) was taken at 4.45 h B) at 19 h C) at 25 h. A shows signals due to PCHPE (7.30-7.83 and 5.05 ppm) but the signals for PCHC (4.65 ppm) and PCL (4.05 ppm) are absent. B shows signals due to PCHC (4.65 ppm) but the signal for PCL (4.05 ppm) is still absent. C shows the signal due PCL (4.05 ppm) after the carbon dioxide has been removed. All analysis on the purified polymer was run on a sample, where the polymerisation was only taken to ~75 % conversion. This is to prevent viscosity building up.

5.4.2 Pentablock Copolymer Structure

While it was already shown that the terpolymerisation of PA/CHO/CO_2 produced an ABA type block copolymer, the effect of the addition of ε-CL was previously unknown. Although each polymerisation occurs independently and sequentially, this is in itself not an indication

of block copolymer formation. The polymer was separated from residual epoxide by precipitation from a THF solution by the addition of MeOH. ^{1}H DOSY NMR spectroscopy showed that all the ^{1}H NMR resonances (for PCHPE, PCHC and PCL) have the same diffusion co-efficient, (D = 2.38 x 10^{-10} m^2/s, R_H of 1.7 x 10^{-9} m) (Figure 5.4.2). This finding indicated that the blocks were part of a single species, rather than there being a mixture of the discrete polymers. The ^{1}H DOSY NMR spectrum of a mixture of the same polymers showed separate diffusion coefficients for each polymer (PCHPE, PCHC and PCL).

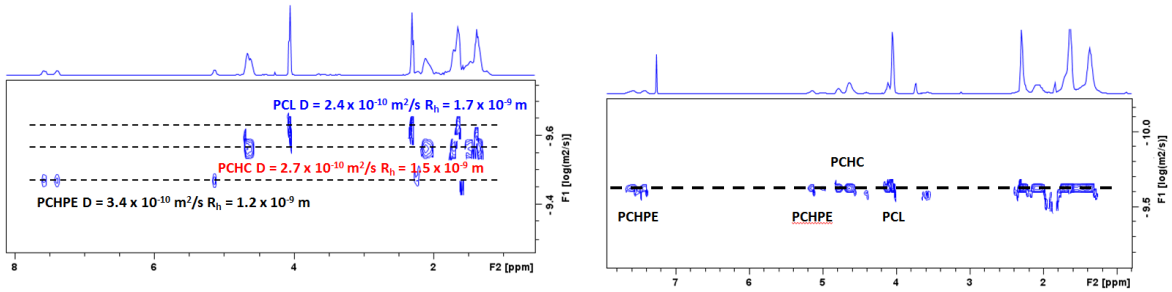

Figure 5.4.2: ^{1}H DOSY NMR spectra of Left: a mixture of PCHPE/PCHC/PCL and Right: the pentablock copolymer (Table 5.2, Run 1).

The ^{1}H NMR spectrum of the pentablock copolymer can be used to determine the relative amounts of each block and the values can be compared to the reaction stoichiometry and monomer conversions. The ^{1}H NMR spectrum of the pentablock copolymer showed discrete signals for PCHPE (5.20 ppm, Hc), PCHC (4.65 ppm, Hd) and PCL (4.05 ppm, He) blocks. The relative ratio of the normalised integrals of these signals gives the proportions of each block within the polymer. In the sample studied (Table 5.2, Run 1) the values were 1:5:7 for PCHPE:PCHC:PCL (Figure 5.4.3). The calculated ratio for the sample was 1:6:7 PCHPE:PCHC:PCL. The close agreement between the experimental and calculated values suggested that the material was a block copolymer. If discrete or contaminating polymers were present, the integrals would be expected to change upon polymer precipitation.

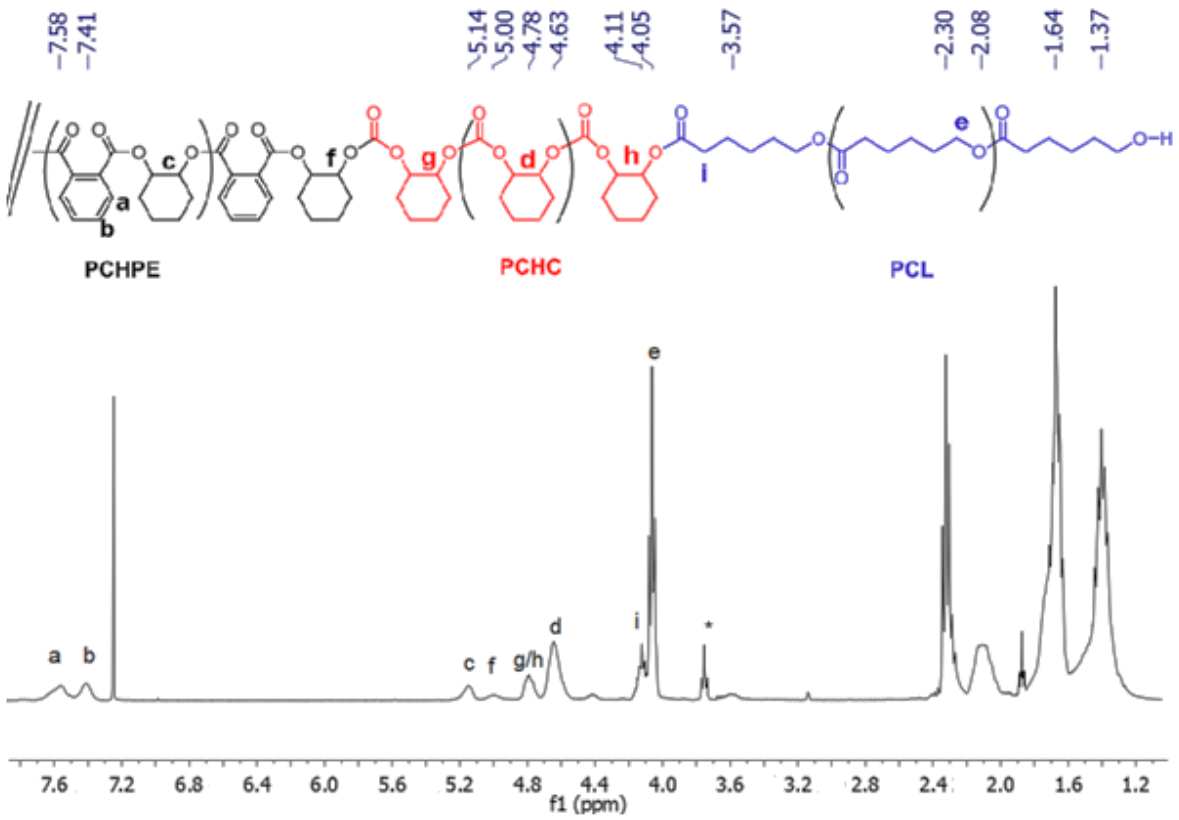

Figure 5.4.3: ^{1}H NMR spectrum of the pentablock copolymer synthesised according to Table 5.2, Run 1.

Another indicator of block formation was to examine the signals corresponding to junction units in the ^{1}H NMR spectrum. The comparison of the ^{1}H NMR spectra of the aliquots taken at 4.45 h, 23 h and 25 h with the spectrum of the final polymer showed that certain signals (f, g/h, i) appeared with the formation of specific polymer blocks (Figure 5.4.2). The ^{1}H NMR spectrum of the aliquot taken at 4.45 h included signals at 5.10 and 4.88 ppm as well as the signals for the main chain methine protons (Hc) of PCHPE at 5.14 ppm. The higher chemical shift signals have previously been assigned as the end groups of PCHPE.[7] The ratio of the end group resonance to the main chain methine resonances (Hc) is 1:1:3. This ratio was used to determine that the $\overline{DP}$ is 4, which corresponds to a molar mass of 980 g mol^{-1}, which is similar to the molar mass value obtained by SEC (880 g mol^{-1}). The finding indicated that ~12 polymer chains had formed per catalyst which was in line with the presence of CHD as a chain transfer agent (Section 1.2.1).

Analysis of the aliquot taken at 23 h, showed the disappearance of the peaks at 5.10 ppm and 4.88 ppm accompanied by the appearance of a signal for the main chain methine protons of PCHC at 4.65 ppm (Hd), and new signals at 5.00 (Hf) and 4.78 (Hg) ppm. These new signals were assigned to the methine protons of the junction units and corresponded to the last PCHPE and first PCHC unit at the block junction (Hf and Hg respectively). The ratio of the relative integrals of the PCHPE junction unit (Hf; 5.00ppm) to the main chain PCHPE signal (Hc, 5.14 ppm) was 1:3. This corresponded to the $\overline{DP}$ as was calculated before the formation of PCHC, indicating that all PCHPE chains should have reacted to form PCHPE-PCHC blocks. Comparison of the relative integrals of the junction units, Hf (4.78 ppm) and Hg (5.00 ppm) showed that the ratio was 1:2. This was quite different to the expected ratio of 1:1. However, a similar phenomenon was previously observed for the relative integrals of the junction units between PCHC and PCL in the ^{1}H NMR spectrum of a PCL-PCHC-PCL triblock copolymer. It was hypothesised that 2 PCHC units contribute to the junction signal at 4.78 ppm (Hg). The signal for the PCHC-PCL junction unit occurred at the same chemical shift (4.78 ppm) as that for the PCHPE-PCHC junction unit. This was to be expected as the signal corresponds to carbonate groups attached to an ester group in both cases. In the case of the current copolymer, the ratio of the relative integrals of the peaks at 4.78 and 5.00 ppm (Hf, Hg) did not change using different NMR solvents, or by altering the NMR relaxation times or rates. It suggested that the higher than expected intensity of the peak at 4.78 ppm (Hf) has a real physical basis, rather than being a spectroscopic artefact.

The peaks at 4.41 ppm and 3.6 ppm were assigned to the end group signals of PCHC. The ratio of main chain methine protons of PCHC (Hc, 4.65 ppm) to the end group methine protons (4.41 ppm), taken from the ^{1}H NMR spectrum of the aliquot at 23 h, is 1:7. This value was used to determine a $\overline{DP}$ of 192, (considering that 12 chains are formed initially). The value was a little lower than the $\overline{DP}$ calculated from the conversion of the monomers, 295. The difference may be due to the limits of integral accuracy. The intensity of the peak at 4.78 ppm (Hg) increased after the PCL block has formed. Before the formation of PCL (spectrum from aliquot taken at 23 h) the ratio of signals d to g/h was 1:7.2; whereas afterwards it increased to 1:3. The doubling of the intensity for signal g, suggests that all of the PCHC chains have reacted to form PCL blocks. Another new peak also appeared during the formation of PCL (after 25 h), signal i (4.11 ppm). The peak is already known and

corresponds to the caprolactone junction unit attached to the PCHC chain.[12] The ratio of peaks Hi:He was 1:9, corresponding to a $\overline{DP}$ of 240 (taking into account the 12 chains), was again slightly lower than the $\overline{DP}$ of 336 calculated from the conversion of the monomers, potentially due to the limits of accuracy in integration.

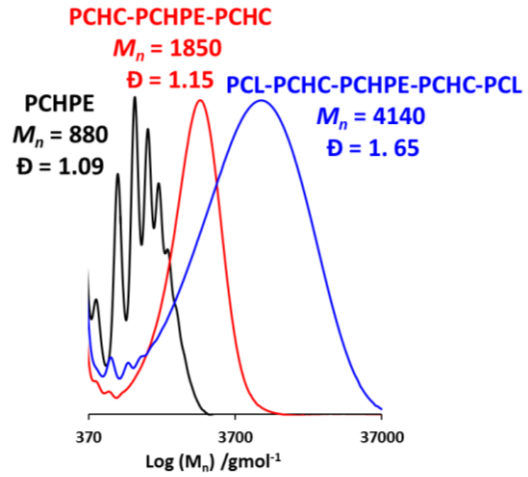

Figure 5.4.4: SEC analysis of the aliquots taken from the terpolymerisation of PA/CHO/ε-CL/CO_2 (Table 5.2, Run 1).

To confirm the block nature of the copolymer, the aliquots taken during the different phases of the terpolymerisation were analysed by SEC (Figure 5.4.4). A typical block copolymer would show a clear increase in the molar mass with the formation of each block and the dispersity should remain narrow. The aliquot taken at 4.45 h had a molar mass of 880 g mol^{-1} (Đ = 1.09). The low molar mass corresponds to oligomers, which can be separated by the SEC column, causing the distinctive pattern observed in Figure 5.4.4. The formation of the PCHC block resulted in an increase in the molar mass (1850 g mol^{-1}, Đ=1.15), and the molar mass distribution was monomodal with a narrow dispersity (Đ =1.15). The molar mass also increased after the formation of the PCL block, and the distribution remained monomodal but broader (Đ = 1.65). The slight broadening likely resulted from an increase in complexity of the system. As with the formation of ABA type PCL-PCHC-PCL copolymers, the ROP of ε-CL caused an increase in the dispersity. This is due to disparity in the relative rates of

propagation and initiation from primary and secondary alkoxides during the ROP of ε-CL as discussed in section 2.5. It is nonetheless clear that the chains have pentablock structures (from NMR junction analysis, DOSY spectroscopy) but it is likely that the PCL blocks have a broader distribution of chain lengths ($\overline{DP}$). This phenomenon appears to affect all PCL containing block copolymers and becomes increasingly apparent with greater numbers of blocks, presumably due to the potential for the 2° alkoxide polymer end group to become less accessible with increasing block complexity.

As with the formation of ABA type copolymers, the phenomenon can be mitigated by the use of a lactone featuring a 2° propagating alkoxide group. The ring opening of ε-DL, results in a 2° alkoxide and is expected to show initiation from the cyclohexene species. It is proposed that using ε-DL may result in a more controlled polymerisation and the formation of symmetrical block copolymers with narrow dispersities.

5.4.3 Block Copolymers using Other Combinations

In order to try and form other pentablock copolymers especially those that have a well-defined structure, indicated by a narrow dispersity, the ROP of ε-DL was investigated. The polymerisation of PA/CHO/CO_2/ε-DL was investigated using the catalyst system [$LZn_2(Ph)_2$]/CHD. However, while the ROCOP of PA/CHO and CHO/CO_2 occurred successfully, minimal polymerisation of ε-DL was observed. The extended time required for the ROP process, (TOF = 7.2 h^{-1} for ε-DL *vs* 154 h^{-1} for ε-CL) required significantly longer time for the reaction (48 h with ε-DL *vs* 24 h with ε-CL). It is proposed that the increase in reaction time resulted in some catalyst degradation and that polymerisation from polymeric chain ends may further decrease rates to impractical levels. In order to decrease the overall reaction time, an alternative epoxide was investigated. The ROCOP of vinyl cyclohexene oxide (VCHO) occurred considerably faster than that of CHO, both with anhydrides and carbon dioxide (Table 5.1). The increase in the rate of ROCOP is attributed to the increased rate of ring opening polymerisation of VCHO compared to CHO. The ring opening is the rate determining step of the polymerisation.

Table 5.1: comparison of the ROCOP of CHO and VCHO with CO_2 and PA.

#	Epoxide	catalyst:epoxide:anhydride:CO_2	TON [a)]	TOF /h^{-1} [b)]
1	VCHO	1:1000:0:1 atm	210	60
2	CHO	1:1000:0:1atm	630	31.5
3	VCHO	1:1550:50	50	50
4	CHO	1:1550:50	50	11

1 carried out at 80°C for 3.5 h, 2 carried out at 80 °C for 20 h, 3 carried out at 100 °C for 1 h, 4 carried out at 100°C for 4.55 h. *Carried out under 1 atm carbon dioxide a) TON = mol of epoxide consumed/mol of catalyst b) TOF = TON/ h.

The ROCOP of PA/VCHO followed by VCHO/CO_2 took 4 h to reach a similar block length in the copolymer as when using CHO as the epoxide. The ROP of ε-DL occurred after the carbon dioxide had been removed and the molar mass increased with the formation of each block. In line with the previous results, the dispersity of the block copolymer remains narrow after the ROP of ε-DL, due to the phenomenon of alkoxide structure affecting rate. The reaction shows that using VCHO as the epoxide can dramatically reduce the reaction time without affecting the block selectivity.

Table 5.2: Polymerisation of epoxide/anhydride/CO_2/lactone using the [$LZn_2(Ph)_2$]/CHD catalyst system.

#	Monomers	TOF [a] PE	TOF [a] PC	TOF [a] PL	M_n [b] PE	M_n [b] PC	M_n [b] PL	PE:PC:PL calc. [c]	PE:PC:PL NMR [d]
1	PA:CO_2:CHO:ε-CL	11.2	15.5	168	880 (1.09)	1850 (1.15)	4140 (1.65)	1:6:7	1:5:7
2	PA:CO_2:VCHO:ε-CL	33.3	62	154	800 (1.16)	1630 (1.24)	3820 (2.04)	1:2:6	1:2:7
3	V PA:CO_2:CHO:ε-DL	38.5	51.6	7.2	804 (1.06)	1490 (1.15)	1950 (1.19)	1:3:3	1:3:5

PE = polyester from PA/epoxide, PC = polycarbonate from CO_2/epoxide, PL = polyester from lactone. Polymerisation carried out at loadings of 1:2:50:1550:200 [$LZn_2(Ph)_2$]:CHD:PA:epoxide:lactone, at 100 °C, and 1 atm of CO_2. a) TOF = (mol of epoxide consumed/mol of catalyst) / h b) determined by SEC with THF as the eluent, using polystyrene standards to calibrate the instrument c) calculated from the normalised relative integrals in the 1H NMR spectrum. 4.65 ppm for the methine protons of PCHC. 4.05 ppm for the methylene protons of PCL. 5.05 ppm for the methine protons of PCHPE. 7.58 ppm for the aromatic methine protons of PVCHPE. 2.48 ppm for the methine proton of PVCHC. 2.31 ppm for methylene protons of PDL. d) Calculated from the conversion of monomer and starting stoichiometry.

The polymerisation of PA/CO_2/VCHO/ε-DL showed exactly the same selectivity as those observed for PA/CO_2/CHO/ε-CL. The selectivity was observed both in the IR spectroscopy and ^{1}H NMR spectroscopy, with the formation of PVCHPE occurring initially, followed by the formation of PVCHC once the PA had been fully consumed. The formation of PDL only occurred once the carbon dioxide was fully removed.

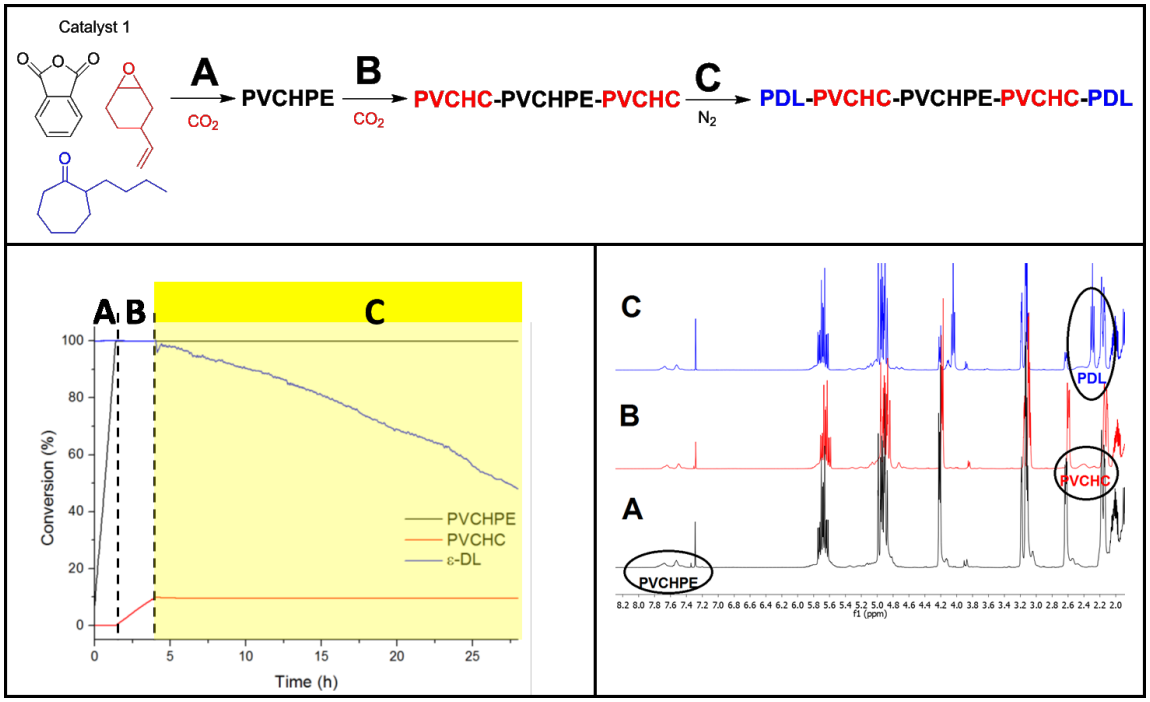

Figure 5.4.5: **Scheme showing the formation of pentablock copolymer and monitoring the reaction *via in-situ*-ATR and 1H NMR spectroscopy. (Table 5.2, Run 3).**

Left: Plot showing the percent conversion of various polymer blocks *versus* time. The intensity of the assigned resonances was normalised and calibrated against the percent conversions determined from ^{1}H NMR spectroscopy of aliquots withdrawn periodically. The absorption at 1767 cm^{-1} is assigned to PVCHC, that at 1070 cm^{-1} to PVCHPE and that absorption at 1015 cm^{-1} to ε-DL (a monomer, hence decrease in absorption). Right: Selected region of the ^{1}H NMR spectra of aliquots taken during the reaction. Spectrum A) was taken at 1.5 h B) at 5 h C) at 26 h. A shows signals due to PVCHPE (7.30-7.83 ppm), but the signals for PVCHC (2.58 ppm) and PDL (2.31 ppm) are absent. Spectrum B shows the signals for PVCHC (2.58 ppm) but the signal for PDL (2.31ppm) is still absent. Spectrum C shows the appearance of the signal for PDL (2.31 ppm) after the carbon dioxide has been removed.

The purified pentablock copolymer showed a single diffusion co-efficient (D = 3.03 x 10^{-10} m^{2}/s, Rh = 1.23 x 10^{-9} m) in the ^{1}H DOSY NMR spectrum which indicated that the three polymer blocks are attached in a single chain.

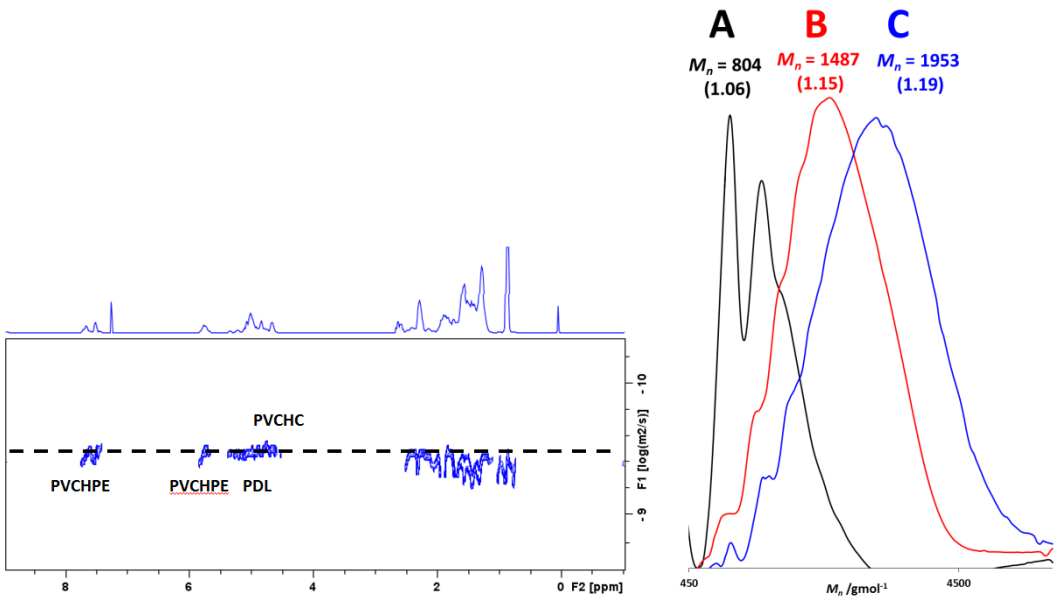

Figure 5.4.6: ^{1}H DOSY spectrum (left) and SEC analysis of the aliquots taken from the polymerisation (right) of the pentablock copolymer (Table 5.2, Run 3).

SEC analysis of the aliquots taken throughout the polymerisation showed that the molar mass increased after the formation of each block. There was a clear increase in molar mass and the dispersity remained narrow throughout the reaction. The slower rate of propagation of ε-DL resulted in the rate of initiation being faster than the rate of propagation, which allowed the formation of PDL to occur symmetrically from both sides of the polymer. From the ^{1}H NMR spectrum, the composition of the pentablock copolymer was determined. The ^{1}H NMR spectrum of PDL-PVCHC-PVCHPE-PVCHC-PDL was somewhat complicated because the vinyl protons of PVCHC overlap with the methine protons of PVCHC and PDL. The relevant signals were deconvoluted before the normalised integrals were calculated. The ratio of PVCHPE:PVCHC:PDL calculated from the ^{1}H NMR spectrum was 1:3:5, which is close to the calculated ratio of 1:3:3. The overlapping signals in the ^{1}H NMR spectrum means it is not possible to carry out any analysis of signals that correspond to junction units. Overall the combined data strongly suggests that the polymerisation of PA/CHO/CO_2/ε-DL results in a pentablock copolymer.

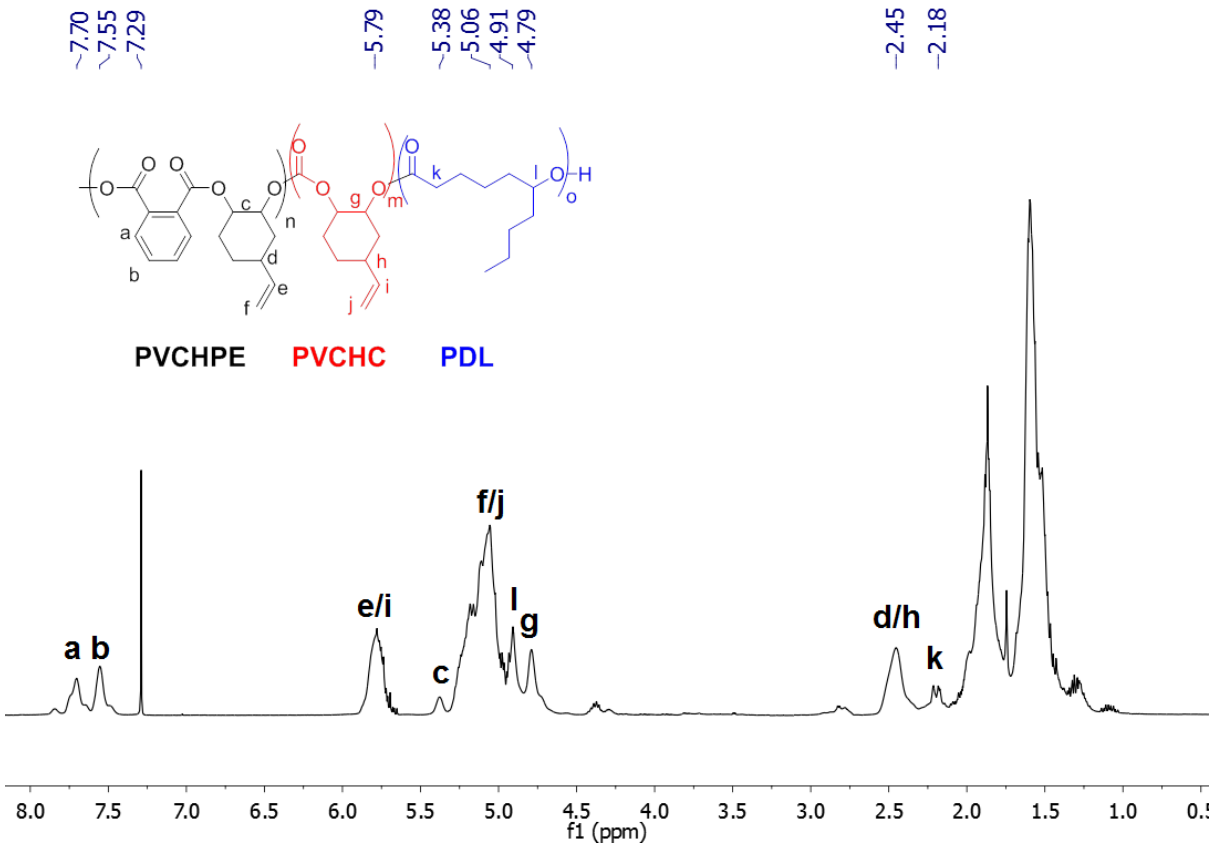

Figure 5.4.8: ^{1}H NMR spectrum of the pentablock copolymer resulting from the terpolymerisation of PA/VCHO/ε-Dl/CO_2 (Table 5.2, Run 3).

Peak at 7.26 ppm is $CDCl_3$.

5.4.4 Properties

Table 5.3: Thermal properties of the pentablock copolymers.

	#	A	B	C	A:B:C a)	T_g /°C b)
			PCHPE		1:0:0	107 [7]
			PVCHPE		1:0:0	13
			PCHC		0:1:0	115 [13]
			PVCHC		0:1:0	65
			PCL		0:0:1	-60 [14]
			PDL		0:0:1	-58 [9]
246	1	PCHPE	PCHC	PCL	1:5:7	-10, 7
297	2	PVCHPE	PVCHC	PCL	1:2:7	-35
306	3	PVCHPE	PVCHC	PDL	1:3:5	-51

a) Determined by ^{1}H NMR spectroscopy by comparison of the normalised integrals: 4.65 ppm for the methine protons of PCHC. 4.05 ppm for the methylene protons of PCL. 5.05 ppm for the methine protons of PCHPE. 7.58 ppm for the aromatic methine protons of PVCHPE. 2.48 ppm for the methine proton of PVCHC. 2.31 ppm for methylene protons of PDL. b) The T_g was calculated from the third heating cycle of the DSC measurement. Experiments were conducted with heating at 10 °C/minute from -100 to 130 °C (# 1-3, 5-8) or at 40 °C/minute from -80 to 100 °C(# 4, 9-10) c).

The thermal properties for the pentablock copolymers were characterised using DSC and compared against the various homopolymers. The PCL-PCHC-PCHPE-PCHC-PCL block copolymer showed two glass transitions at -10 and 7 °C. It is known that PCHPE and PCHC are miscible and the T_g for PCHPE-PCHC block copolymers has been reported at 97-104 °C.[7] PCHC and PCL are also known to be miscible.[12] Therefore the two glass transitions seem to be an indication that there is some miscibility between all three blocks. It is difficult to clearly assign particular block structures to the T_g values. For the VCHO containing pentablock copolymers, only one glass transition was observed again indicating block miscibility. For the PDL containing pentablock copolymer the T_g was at -51 °C, which is close to the glass transition of PDL homopolymer and indicates that the PDL block may not

be miscible with the other blocks. It has been previously reported that PCHPE and PDL are not miscible.[9] For the PCL containing pentablock copolymer, a single glass transition was observed at -35 °C, which indicates there is some miscibility between the PCL and PVCHPE/PVCHC blocks, consistent with previous results.[12]

5.4.5 Conclusion

The selective polymerisation of mixtures of four monomers: anhydride, carbon dioxide, epoxide and lactone, has been used to form block copolymers. In all cases, the terpolymerisation of anhydride/epoxide/carbon dioxide/lactone showed the same block sequence selectivity. ROCOP of epoxide/anhydride is followed by ROCOP of epoxide/carbon dioxide and the ROP of lactone only occurs after the carbon dioxide is removed. The selectivity was confirmed by monitoring the reactions by ^{1}H NMR spectroscopy and by *in-situ* ATR IR spectroscopy. The block structures were confirmed in all cases using SEC analysis, ^{1}H DOSY NMR and ^{13}C NMR spectroscopy.

5.5 Pentablock Formation using Lactide

Rac-lactide is a cyclic diester which readily undergoes ring-opening polymerisation to give a biodegradable polyester.[15] *Rac*-lactide can be derived from starch, thus offering a green route to the polyester. PLA is a semi-crystalline polymer with a T_g of 60 °C and at T_m of 170 °C.[16] Williams and co-workers have previously reported the synthesis of PLA-PCHC-PLA triblock copolymers in a two-step method by the formation of polycarbonate polyols that were subsequently used as the macroinitators during the ROP of lactide (Section 1.4.3.1).[11] The resulting copolymer showed two glass transitions at 60 °C and 90 °C corresponding to the PLA and PCHC portions respectively and suggested block immiscibility. When *L*-LA was used to form isotactic PLA blocks, no melting temperature for the copolymers was observed, regardless of the composition of the triblock copolymers (1:10 -1:2.5), indicating that the crystallinity of the lactide was suppressed. In contrast, the PCL-PCHC-PCL block copolymers showed that the crystallinity of PCL was only suppressed at high PCHC block

contents and there was some degree of miscibility between the PCHC and PCL blocks (determined by moderation of T_g values). Therefore, it was of interest to investigate the use of LA in the formation of the pentablock copolymer.

5.5.1 Catalyst Selectivity with *rac*-LA

The polymerisation of PA/CHO/*rac*-LA/CO_2 using catalyst system [$LZn_2(Ph)_2$]/CHD (loading of 1:2:50:2000:200 [$LZn_2(Ph)_2$]:CHD:PA:CHO:*rac*-LA) was monitored using *in-situ* ATR-IR spectroscopy (Figure 5.5.1). Initially the absorption at 1727 cm^{-1}, assigned to PCHPE, increased in intensity, indicating that epoxide/anhydride ROCOP occurred first. The signals assigned to PCHC (1823 cm^{-1}) and PLA (1191 cm^{-1}) showed no increase in intensity. The reaction was also monitored using ^{1}H NMR spectroscopy of aliquots withdrawn periodically from the reaction (Figure 5.5.1). The aliquot taken at 4.45 h showed only the signals for PCHPE (7.3-7.8 and 5.15 ppm) and the monomers CHO (3.10 ppm) and LA (5.05 ppm). After 4.45 h the PA was fully consumed and the signal at 1191 cm^{-1} (PLA) rapidly increased in intensity. There was no change in the signal corresponding to PCHC (1823 cm^{-1}). ^{1}H NMR spectra of aliquots taken during this period confirmed that the formation of PLA was occurring, with a key signal for LA (5.05 ppm) decreasing in intensity and a new signal appearing corresponding to PLA (5.10 ppm). The new signal overlaps slightly with the signal for PCHPE, but its overall intensity increased during this period whereas the signals at 7.30-7.85 ppm, for PCHPE only, remained constant. There was no peak at 4.65 ppm, indicating that no PCHC was formed during this period. The consumption of LA took 45 minutes, after which time there was no further increase in the absorption at 1191 cm^{-1}. After 5.30 h, the absorption corresponding to PCHC (1823 cm^{-1}) began to increase and ^{1}H NMR spectroscopy confirmed the formation of PCHC by the appearance of a signal at 4.65 ppm (PCHC). The entire reaction was carried out under a carbon dioxide atmosphere.

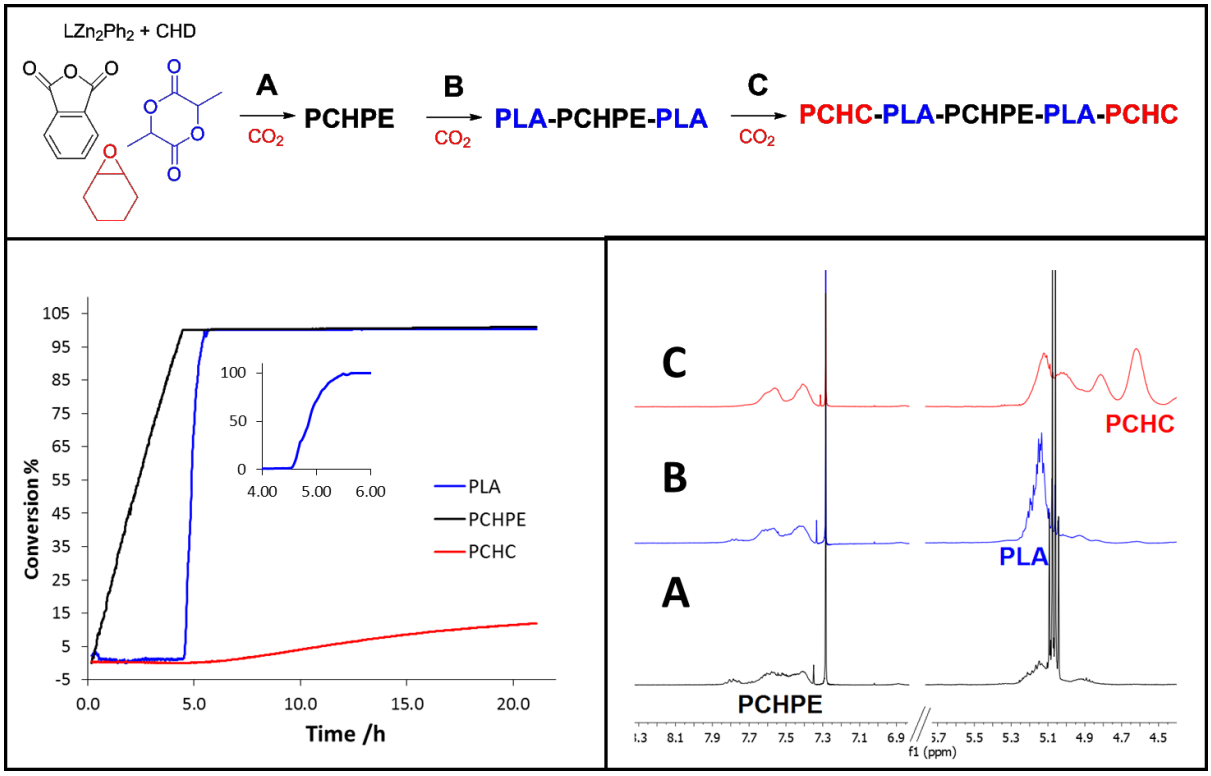

Figure 5.5.1: **Scheme showing the formation of pentablock copolymer and monitoring the reaction *via in-situ*-ATR and ^{1}H NMR spectroscopy (Table 5.4, Run 1).**

Left: Plot showing the percent conversion of various polymer blocks *versus* time. The intensity of the assigned resonances was normalised and calibrated against the percent conversions determined from ^{1}H NMR spectroscopy of aliquots withdrawn periodically. The absorption at 1727 cm^{-1} is assigned to PCHPE, that at 1823 cm^{-1} to PCHC and that at 1191 cm^{-1} to PLA. Right: Selected region of the ^{1}H NMR spectra of aliquots taken during the reaction. Spectrum A) was taken at 4.75 h B) at 5.5 h C) at 21 h. A shows signals due to PCHPE (7.30-7.83 ppm), but the signals for PCHC (4.65ppm) and PLA (5.15 ppm) are absent. Spectrum B shows the signals for PLA (5.15 ppm) but the signal for PCHC (4.65 ppm) is still absent. Spectrum C shows the appearance of the signal for PCHC (4.65ppm).

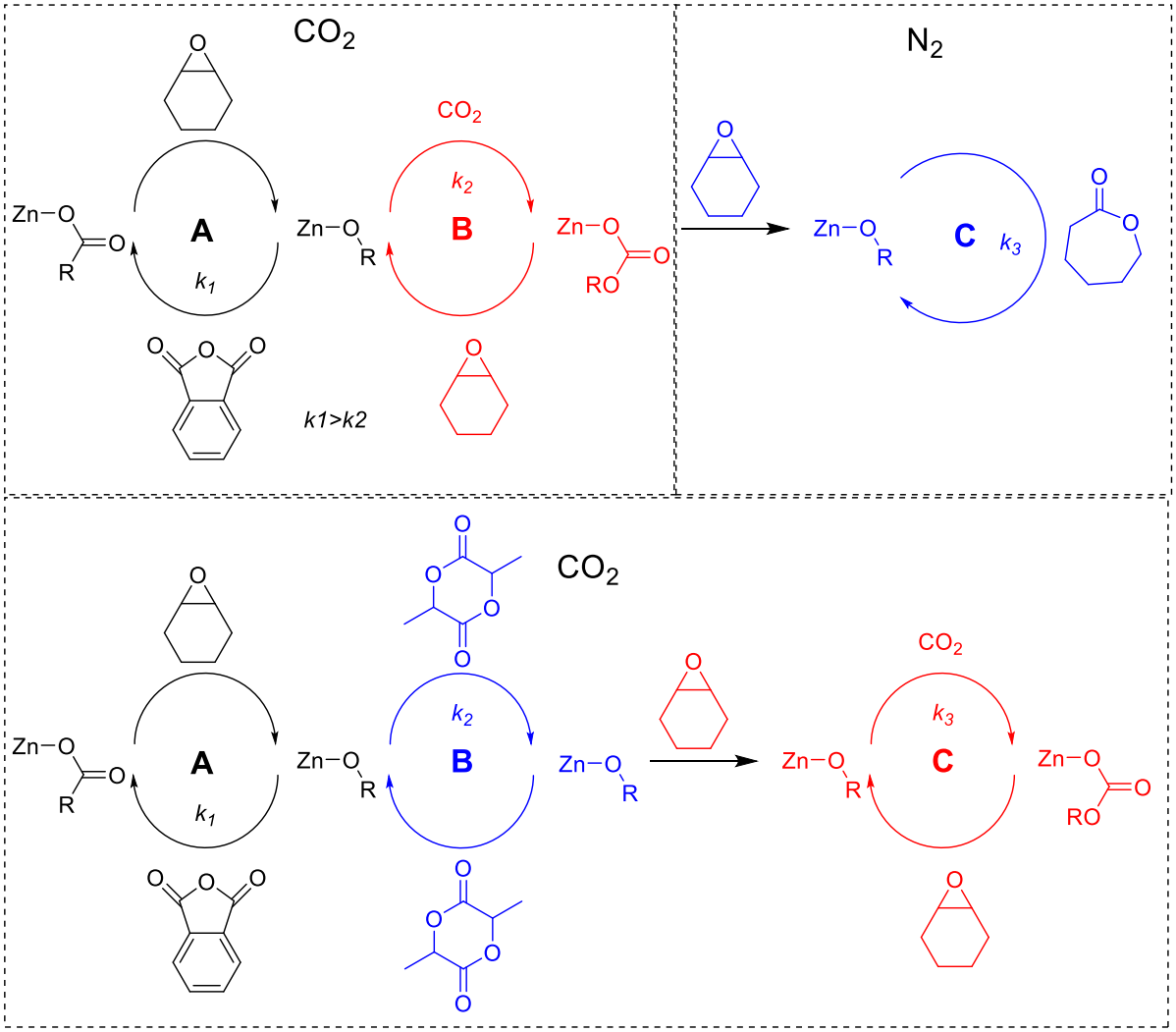

Figure 5.5.2: Scheme showing the selectivity and possible pathways during the polymerisation of PA/CHO/CO_2/ε-CL (top), compared with those for PA/CHO/CO_2/LA (bottom).

The reaction selectivity using *rac*-LA was quite distinct compared to that observed using ε-CL or ε-DL. The selectivity was repeatable and remained the same regardless of the loading of lactide (Table 5.4, runs 1, 2). The hypothesis to rationalise the selectivity using lactones proposed that ROP only occurs when PA or CO_2 have been removed from the system. The selectivity is determined by the relative rates of insertion of the various monomers into the zinc alkoxide intermediate formed by the ring opening of CHO. For the polymerisations of PA/CHO/CO_2/ε-CL, the reactivity order is the insertion of PA>CO_2>ε-CL and the same

selectivity was observed using ε-DL. However, using *rac*-LA the observed order was the insertion of PA>LA> CO_2. Therefore in the case of *rac*-LA, it seems the relative rates of insertion into the zinc alkoxide intermediates are: PA>*rac*-LA>CO_2 (Figure 5.5.2).

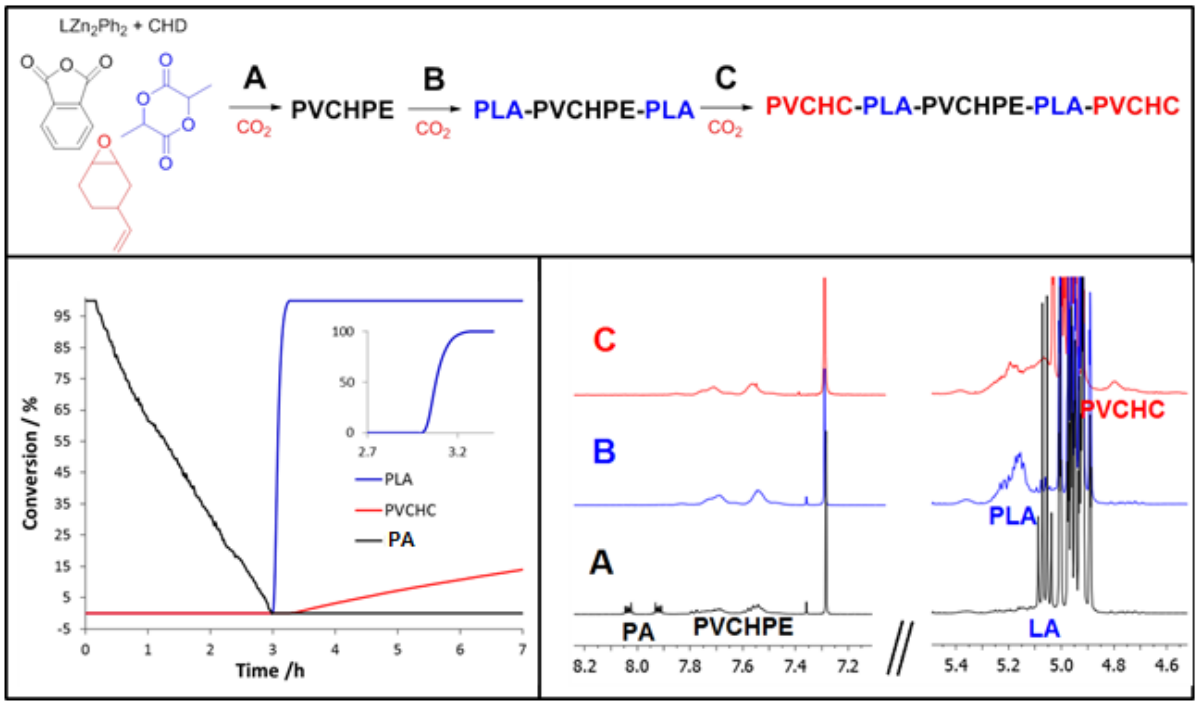

Figure 5.5.3: Scheme showing the formation of pentablock copolymer and monitoring the reaction *via in-situ*-ATR and ^{1}H NMR spectroscopy (Table 5.4, Run 3).

Left: Plot showing the percent conversion of various polymer blocks *versus* time. The intensity of the assigned resonances was normalised and calibrated against the percent conversions determined from ^{1}H NMR spectroscopy of aliquots withdrawn periodically. The absorption at 1857 cm^{-1} is assigned to PA (a monomer), that at 1264 cm^{-1} to PVCHC and that at 1180 cm^{-1} to PLA.. Right: Selected region of the ^{1}H NMR spectra of aliquots taken during the reaction. Spectrum A) was taken at 3 h B) at 3.5 h C) at 7 h. Spectrum A shows the signals or PVCHPE (7.30-7.83 ppm) but the signals for PVCHC (4.85ppm) and PLA (5.15 ppm) are absent. Spectrum B shows the signals for PLA (5.15 ppm) but the signal for PVCHC (4.85 ppm) is still absent. Spectrum C shows the signal for PVCHC (4.85ppm).

In order to further investigate the selectivity observed using *rac*-LA, the reaction was also carried out using VCHO instead of CHO. The reaction of PA/VCHO/*rac*-LA/CO_2 with the

catalyst system [$LZn_2(Ph)_2$]/CHD (loading of 1:2:50:2000:200 [$LZn_2(Ph)_2$] :CHD:PA:VCHO:*rac*-LA) was monitored using *in-situ* ATR-IR and ^{1}H NMR spectroscopy (Figure 5.5.3, Table 5.4, Run 3). The reaction showed the same selectivity order as with CHO. The PA was consumed first forming PCHPE and once the PA was fully consumed, the ROP of lactide occurred. The ROP of lactide took approximately 15 minutes and when the lactide was fully consumed the insertion of carbon dioxide occurred, forming polycarbonate.

Table 5.4: Polymerisations of PA:CO_2:Epoxide:*rac*-LA.

#	PA:CHO:LA	Time A /h	M_n (Đ) [a] PE /g mol^{-1}	Time B /h	M_n (Đ) [a] PE-PLA /g mol^{-1}	Time C /h	Conversion [b] CHO /%	M_n (Đ) [a] PE-PLA-PC /g mol^{-1}
1	50:2000:200	4.5	1280 (1.18)	0.75	2280 (1.38)	15.5	12	2090 (1.24)
2	50:2000:100	4.75	1260 (1.13)	0.5	2270 (1.21)	16.75	10	1930 (1.22)
3	50:2000:200 *	3	774 (1.05)	0.25	2850 (1.23)	3.75	14	2840 (1.48)

*VCHO. Polymerisations carried out at 100°C, under 1 atm of carbon dioxide. a) Determined by SEC with THF as the eluent, using polystyrene standards to calibrate the instrument. b) Determined from the normalised relative integrals in the ^{1}H NMR spectrum at 3.10 ppm for CHO and 4.65 ppm for PCHC.

5.5.2 Control Reactions

In order to ensure that the selectivity observed was not caused by the specific conditions of the reaction, a series of control experiments were carried out.

Ring Opening Polymerisation of Lactide

The reaction between the catalyst system [$LZn_2(Ph)_2$]/CHO and LA resulted in efficient formation of PLA. The polymerisation was rapid with a TOF > 200 h^{-1}. The molar mass of PLA was 1550 g mol^{-1} (Đ = 1.42), which was considerably lower than the theoretical molar mass (28,800 g mol^{-1}). The reduction in molar mass was proposed to be due to the presence of 1,2-cyclohexene diol, which acts as a chain transfer agent causing the reduction in molar mass. The molar mass values suggested that 8 chains form per catalyst, which is similar to other experiments using CHO.

Table 5.5: Ring opening polymerisation of *rac*-Lactide.

#	[$LZn_2(Ph)_2$]:CHO:LA	conversion /% [a]	TOF / h^{-1} [b]	M_n (Đ) [c] / g mol^{-1}	$M_{n\ theo.}$ [d] / g mol^{-1}
1	1:2000:200	>99%	>200	1,550 (1.42)	28,800
2	1:0:200	87	174	28,400 (1.19)	19,800
3	0:2000:200	-	-	-	-

Polymerisations carried out at 1M δ LA, at 100°C under nitrogen, for 1h. a) Determined from the normalised relative integrals in the ^{1}H NMR spectrum. PLA at 5.15 ppm and LA at 5.05 ppm b) TOF = (mol of monomer/mol of catalyst)/h. Monomer conversions determined from ^{1}H NMR spectroscopy. c) Determined by SEC with THF as the eluent, using polystyrene standards to calibrate the instrument. A correction factor of 0.53 is applied. d) M_n theo = $\overline{DP}$ x molar mass of repeat unit. The molar mass of the repeat unit of PLA is 144 g mol^{-1}, assuming 1 chain per catalyst.

There was no reaction between CHO and LA on their own, indicating the need for a catalyst. The catalyst [$LZn_2(Ph)_2$] does react with LA (in the absence of CHO) but the reaction was very slow and uncontrolled. The molar mass of the PLA was higher than the theoretical mass (28,400 g mol^{-1} *vs* 19,800 g mol^{-1}), suggesting that there was incomplete initiation from all sites. As the [$LZn_2(Ph)_2$]/CHO system was more active than [$LZn_2(Ph)_2$] alone, the most

likely pathway for the ROP of LA with $[LZn_2(Ph)_2]$/CHO was *via* the formation of a zinc alkoxide species.

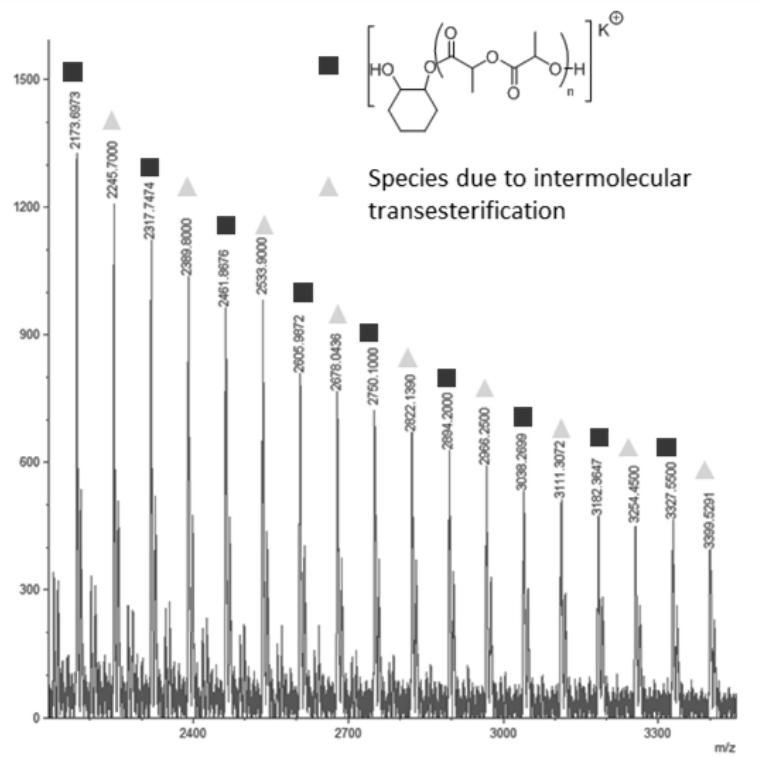

Figure 5.5.4: MALDI-ToF spectrum of PLA synthesised by $[LZn_2(Ph)_2]$/CHO.

The polyester polyol series are represented by squares and calculated for $[(C_6H_8O_4)_n+C_6H_{12}O_2+K]^+ = [(144.04)_n+116.16+39.1]^+$. The series represented by triangles is due to intermolecular transesterification and calculated for $[(C_6H_8O_4)_n+C_3H_4O_2+C_6H_{12}O_2+K]^+ = [(144.04)_n+72+116.16+39.1]^+$.

MALDI-ToF analysis of the PLA formed by $[LZn_2(Ph)_2]$/CHO showed a single cyclohexene unit is incorporated, likely as a chain extender. The series were separated by 72 m/z due to intermolecular transesterification reactions. The cyclohexene unit must result from initiation by 1,2-cyclohexene diol, which is proposed to contaminate CHO despite repeat purifications. The significant quantity of transesterification was likely responsible for the broader dispersity

values. Further evidence for transesterification was observed in the $^{13}C\{^{1}H\}$ NMR spectrum where there are signals in the carbonyl region at 169.59 and 169.34 ppm.

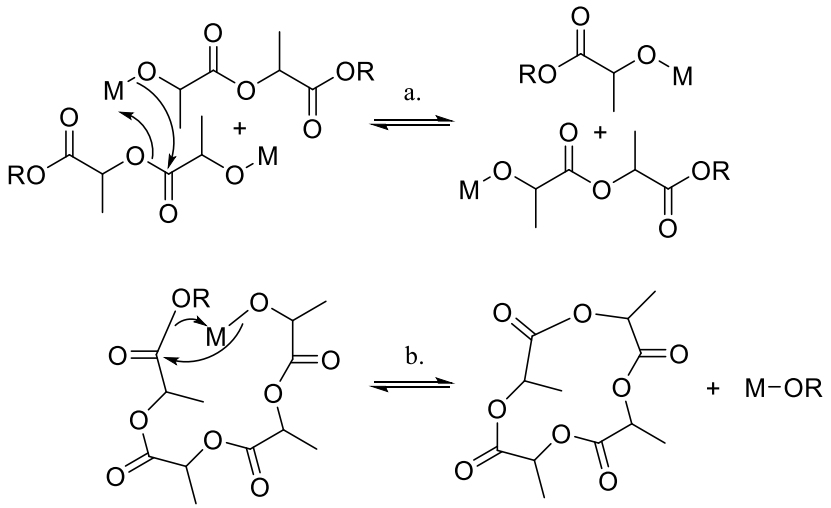

Figure 5.5.5: Mechanism of transesterification in PLA Top) intermolecular Bottom) intramolecular.

Analysis of the molar mass by ^{1}H NMR spectroscopy gave a value of 2160 g mol^{-1}, which was in reasonable agreement with the molar mass determined by SEC (1550 g mol^{-1}). The ^{1}H NMR spectrum of PLA formed by $[LZn_2(Ph)_2]$/CHO showed two peaks from the main chain of the polymer. The methine protons appearred at 5.15 ppm and the methyl protons at 1.58 ppm. There is also a small peak at 4.37 ppm, which has been assigned to the methine proton closest to the hydroxyl end groups of the PLA chain and at 1.48 for the methyl protons closest to the hydroxyl group.[17] There are very small peaks at 4.86, 4.60 and 3.56 ppm; these have been assigned to the methine protons on the cyclohexene ring. While these peaks are not of a strong intensity in the ^{1}H NMR spectrum they are clearly visible in the 2D HSQC spectrum. The peak at 4.86 ppm arises from the methine protons of a cyclohexene ring as chain extender and the peaks at 4.60 and 3.56 ppm from the methine protons of a cyclohexene ring end group. The end groups are similar to those observed in the formation of PCL with $[LZn_2(X)_2]$/CHO (X= OAc, $OCOCF_3$, Ph).[18]

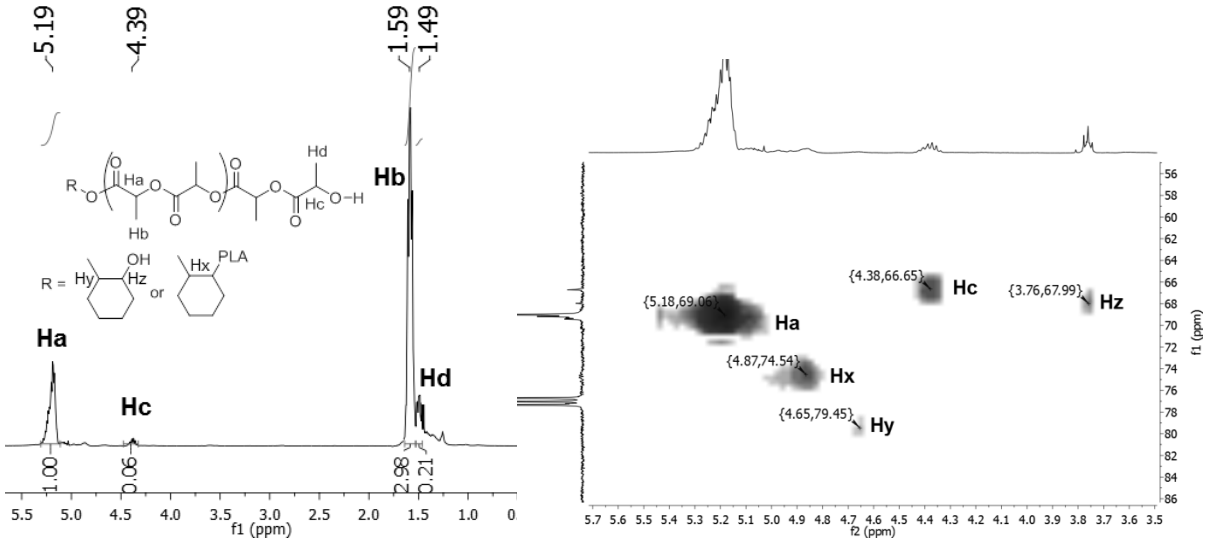

Figure 5.5.6: NMR spectrum of PLA synthesised according to Table 5.1, Run 4.

The spectra show the presence of the end capped and chain extended species. Right: ^{1}H NMR spectrum Left: HSQC spectrum.

For the ROP of ε-CL, it has been reported that the presence of the cyclohexene end capped chains was due to the slower rate of initiation the secondary alkoxide species *versus* the primary alkoxide species (section 2.5)[18]. The ROP of ε-DL does not result in the formation of any end capped chains. The zinc alkoxide species from the ring opening of lactide is a secondary alkoxide. However the rate of ROP for LA appears to be considerably faster than that of ε-DL (TOF > 100 h^{-1} *vs* 25 h^{-1}, 1:100:1000 [$LZn_2(Ph)_2$]:cyclic ester:CHO at 100 °C). The observation of the chain end capped signals at 4.60 and 3.56 ppm, while of low intensity, indicated that the chain transfer reaction is not competing effectively with propagation and therefore the unsymmetrical end capped structures can form.

Polymerisation of PA/CHO/LA

The terpolymerisation of PA/CHO/LA using the catalyst system [$LZn_2(Ph)_2$]/CHD was carried out under a nitrogen atmosphere, with a loading of 1:2:100:200:2000 ([$LZn_2(Ph)_2$]:CHD:PA: LA:CHO). These quantities retained the same catalyst and lactide concentration as during the pentablock formation. The reaction was monitored by ^{1}H NMR

spectroscopy. During the first 3 h, the ROCOP of CHO/PA occurred. The consumption of PA was observed by the disappearance of the aromatic signals at 8.00 and 7.88 ppm and the evolution of signals at 7.54 and 7.37 ppm. There was no change in the signal for lactide at 5.05 ppm. After 3 hours the complete consumption of PA had occurred, and then the ROP of lactide began. The signals for lactide at 5.05 and 1.62 ppm disappeared and the signals for PLA evolved at 5.11 and 1.49 ppm.

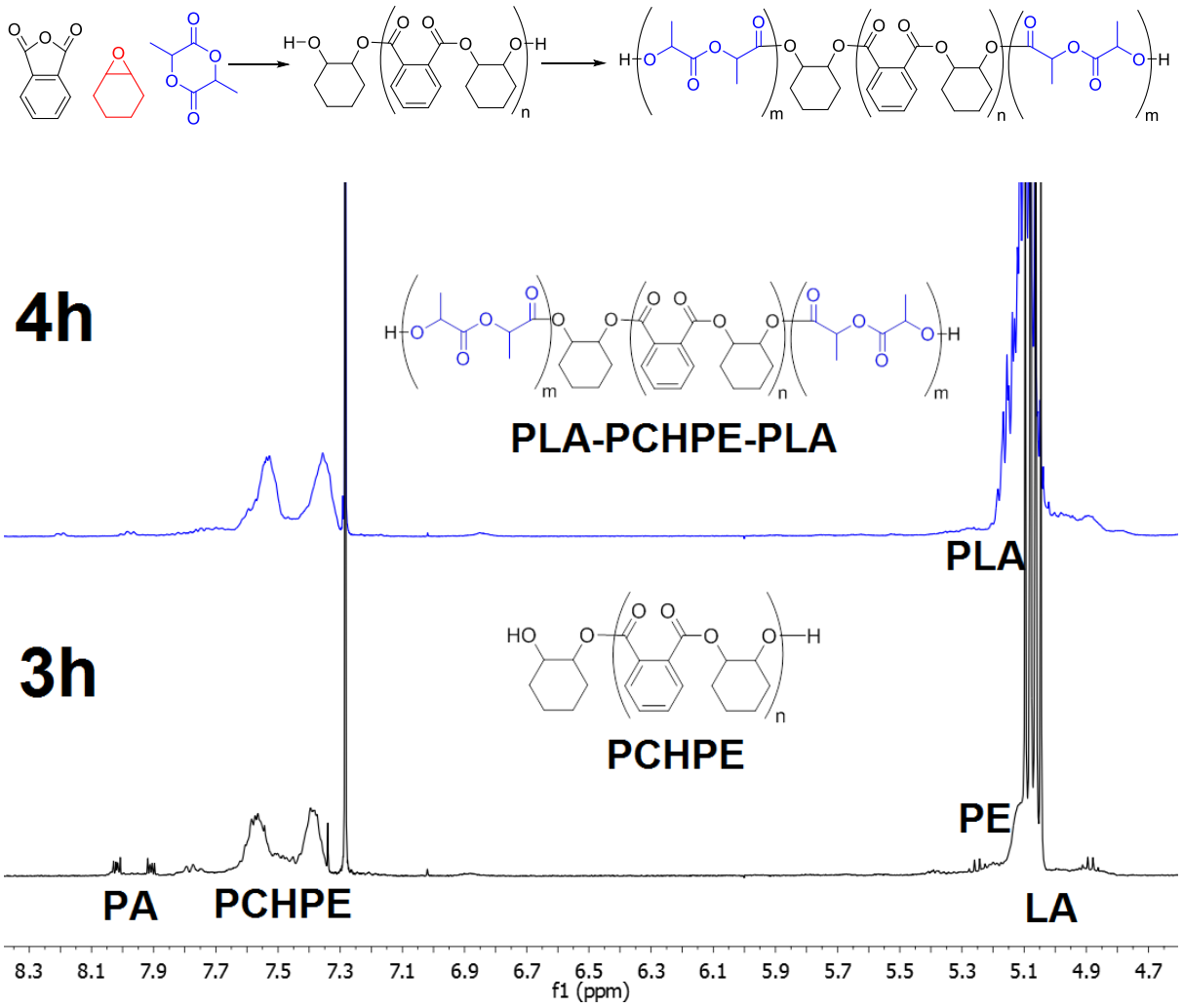

Figure 5.5.7: ^{1}H NMR spectra of the aliquots taken from the polymerisation of PA/CHO/LA.

Bottom: Spectrum taken at 3 h, shows the formation of PCHPE at 7.3-7.7 ppm but no sign of PLA at 5.15 ppm. Top: Spectrum taken at 4 h shows the formation of PLA at 5.15 ppm.

Table 5.6: Terpolymerisation of PA/CHO/LA.

#	[$LZn_2(Ph)_2$]:CHD:CHO:PA:LA	TOF /h^{-1} a) ROCOP	M_n / g mol^{-1} b)	TOF /h^{-1} a) ROP	M_n / g mol^{-1} b)	PE:PLA exp c)	PE:PLA theo d)
1	1:2:2000:100:200	33	5061 (1.23)	200	3260 (1.32)	1:3	1:2

Polymerisations carried out at 1M LA, at 100°C under nitrogen. a) TOF = (mol of monomer/mol of catalyst)/h. Monomer conversions determined from the normalised relative integrals in the ^{1}H NMR spectrum. PA at 8.50 - 7.95 and PCHPE at 7.55 -7.35. PLA at 5.15 ppm and LA at 5.05 ppm b) determined by SEC with THF as the eluent, using polystyrene standards to calibrate the instrument. c) calculated from the normalised relative integrals in the 1H NMR spectrum at 5.20 ppm for the methine protons of PCHPE and 5.1 for the methine protons of PLA d) Calculated from the conversion of monomer.

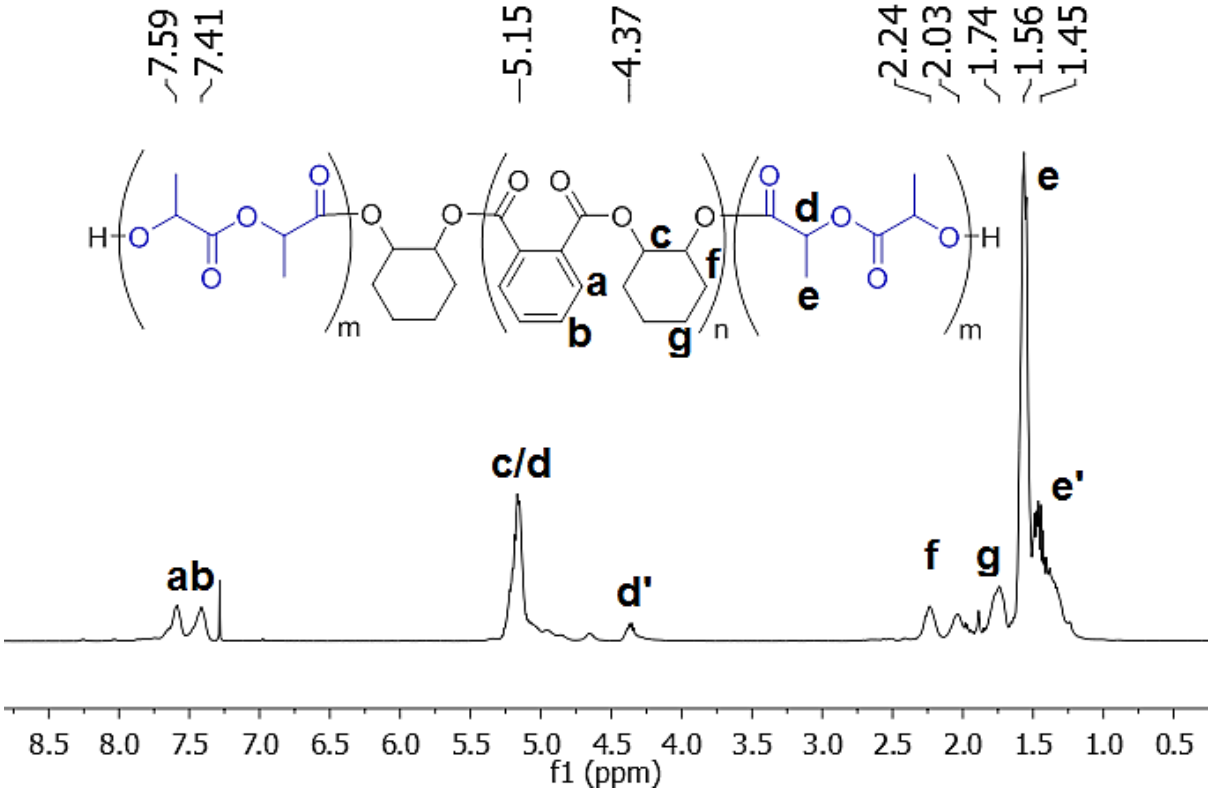

Figure 5.5.8: **^{1}H NMR spectrum of poly (lactide-cyclohexene phthalate-lactide), synthesised according to Table 5.6.**

The block copolyester was purified by precipitation from THF using pentane and the sample dried *in vacuo*. The ^{1}H NMR spectrum showed signals for the aromatic protons of the main chain unit of PCHPE at 7.59 (Ha) and 7.42 (Hb) ppm. The signals for the main chain methine protons of PCHPE (Hc) and PLA (Hd) were both at 5.15 ppm. In order to calculate the ratio of PCHPE to PLA, the integral of the signal at 7.59 ppm (Ha) was used to determine the proportion of PCHPE. The normalised value given for the PCHPE integral was deducted from the integral of the signal at 5.15 ppm (Hc/d) to give the integral of PLA. The ratio of PCHPE:PLA was determined to be 1:3 which was in reasonable agreement with the calculated value of 1:2. The ^{1}H NMR spectrum also showed signals for the end groups of PLA at 4.37 ppm and 1.45 ppm. There were signals for the junction unit at 5.02 and 4.66 ppm. Based on 2D NMR spectroscopy they have been assigned to two methine protons from the cyclohexene ring on the junction unit between the PCHPE and PLA blocks. This was slightly different to other junction units which have been reported (e.g. PCHC-PCL) where both methine protons result in a single resonance. In both PCHPE and PCHC, the methine protons of the endgroup cyclohexene unit have separate resonances, so it was not unreasonable that the methine protons in the junction unit may also show inequivalence as in this case. The ratio of junction units to main chain units for PCHPE is 1:20. Due to the endgroups of PCHPE being obsucured in the ^{1}H NMR spectrum the number of chains can not be calculated. The ratio of the integral of the resonce at 4.66 ppm (corresponding to a methine proton from the junction unit) to the signal at 4.37 ppm (PLA endgrouo) is 1:2, which was as expected, as there are two methine protons in the final PLA unit.

The ^{13}C{^{1}H} NMR of the block copolyester shows two signals in the carbonyl region. The characteristic signal for PCHPE was present at 166.6 ppm and the PLA signal was at 169.3 ppm. The PLA signal showed a second peak at 169.59 ppm. The two signals arise due to transesterification within the PLA block. Transesterification between the PCHPE and PLA block would result in the formation of many other new peaks, typically with a resonance between those of the homopolymers. No such signals are observed, indicating that no detectable cross-transesterification has occurred.

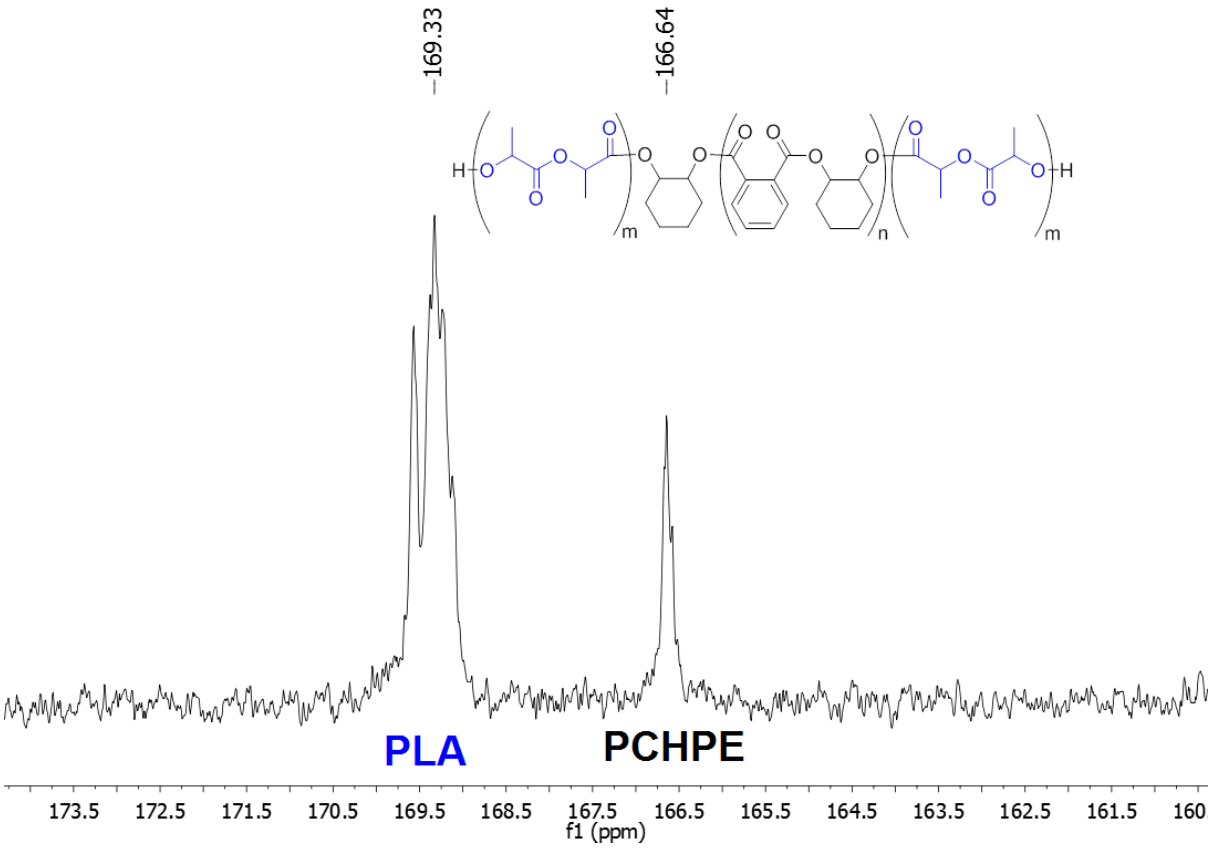

Figure 5.5.9: $^{13}C\{^{1}H\}$ NMR spectrum of poly (lactide-cyclohexene phthalic ester-lactide), synthesised according to Table 5.6.

Terpolymerisation of LA/CHO/CO_2

The terpolymerisation of CHO/CO_2/LA using [$LZn_2(Ph)_2$] was monitored using ^{1}H NMR spectroscopy (loading 1:2000:200 [$LZn_2(Ph)_2$]:CHO:LA at 100 °C, 1 atm CO_2) (Table 5.7, Run 1). During the first hour only the ROP of LA was observed and the signal for PLA appeared at 5.15 ppm and the resonance of LA at 5.05 ppm decreased in intensity. There was no sign of PCHC formation (4.65 ppm) during this period. After 1 h, the lactide was fully consumed, and the signal at 5.15 ppm remained at a constant intensity and the peak at 5.05 ppm had disappeared. At this time, the ROCOP of CHO/CO_2 occurred as observed by the appearance of the signal at 4.65 ppm, corresponding to PCHC. The polymerisation was also carried out at 80 °C using the same reaction conditions (Table 5.7, Run 2). Again, the first

reaction was the ROP of LA; however at 80 °C the reaction was considerably slower and the full consumption of LA took 4 h. Despite the increase in time taken to fully consume the lactide, the ROCOP only occured when the lactide was fully consumed.

Table 5.7: Polymerisation of LA/CHO/CO_2.

#	$[LZn_2(Ph)_2]$:CHO:LA	Temp /°C	TOF PLA /h^{-1} a)	M_n /g mol^{-1} b)	TOF PCHC /h^{-1} a)	M_n /g mol^{-1} b)	PLA:PCHC exp c)	PLA:PCHC theo d)
1	1:2000:200	100	200	3346 (1.23)	10	1950 (1.27)	1:1.3	1:1.1
2	1:2000:200	80	50	3325 (1.28)	16	2037 (1.32)	1:1.6	1:1.5

Polymerisations carried out at under 1 atm of carbon dioxide. a) TOF = (mol of monomer/mol of catalyst)/h. Monomer conversions determined from ^{1}H NMR spectroscopy PCHC at 4.65 ppm and CHO at 3.10 ppm. PLA at 5.15 ppm and LA at 5.05 ppm b) Determined by SEC with THF as the eluent, using polystyrene standards to calibrate the instrument. c) Determined from the normalised relative integrals in the ^{1}H NMR spectrum. PCHC at 4.65 ppm and PLA at 5.15 ppm d) Determined from monomer conversions.

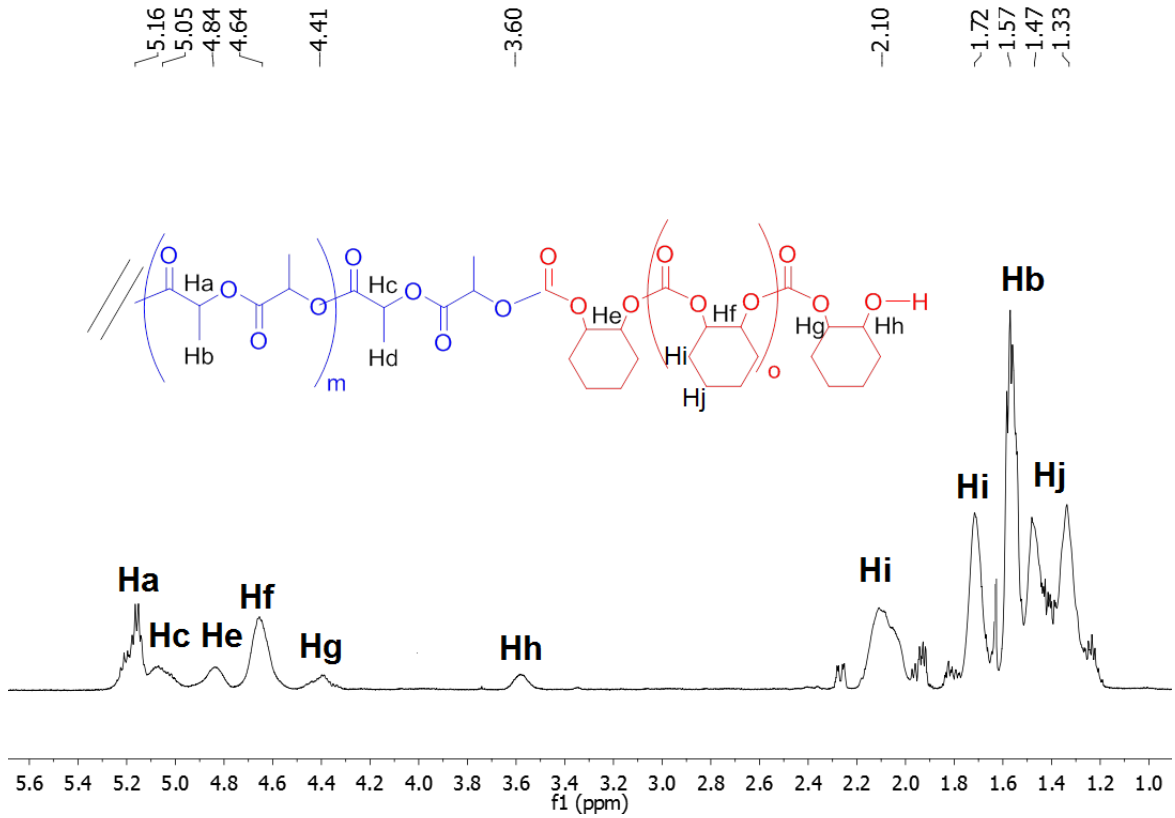

Figure 5.5.10: ^{1}H NMR spectrum of poly(cyclohexene carbonate-lactide-cyclohexene carbonate) synthesised according to Table 5.7, Run 1.

The triblock copolymer was purified by precipitation from THF using pentane. The ^{1}H NMR spectrum of the copolymer showed the characteristic peaks for the main chain methine protons in PLA at 5.15 ppm and the main chain methine protons of PCHC at 4.65 ppm. The ratio of PLA:PCHC signals was 1:1.3, which is in good agreement with the theoretical value of 1:1.1. The end group signals for PCHC were present at 4.40 and 3.60 ppm. There are also new peaks at 5.05 ppm and 4.85 ppm, which correspond to the junction units. The peak at 5.05 ppm was assigned to the methine proton of the PLA junction unit, and the peak at 4.85 ppm to the methine protons of the PCHC junction unit on the basis of 2D NMR experiments.

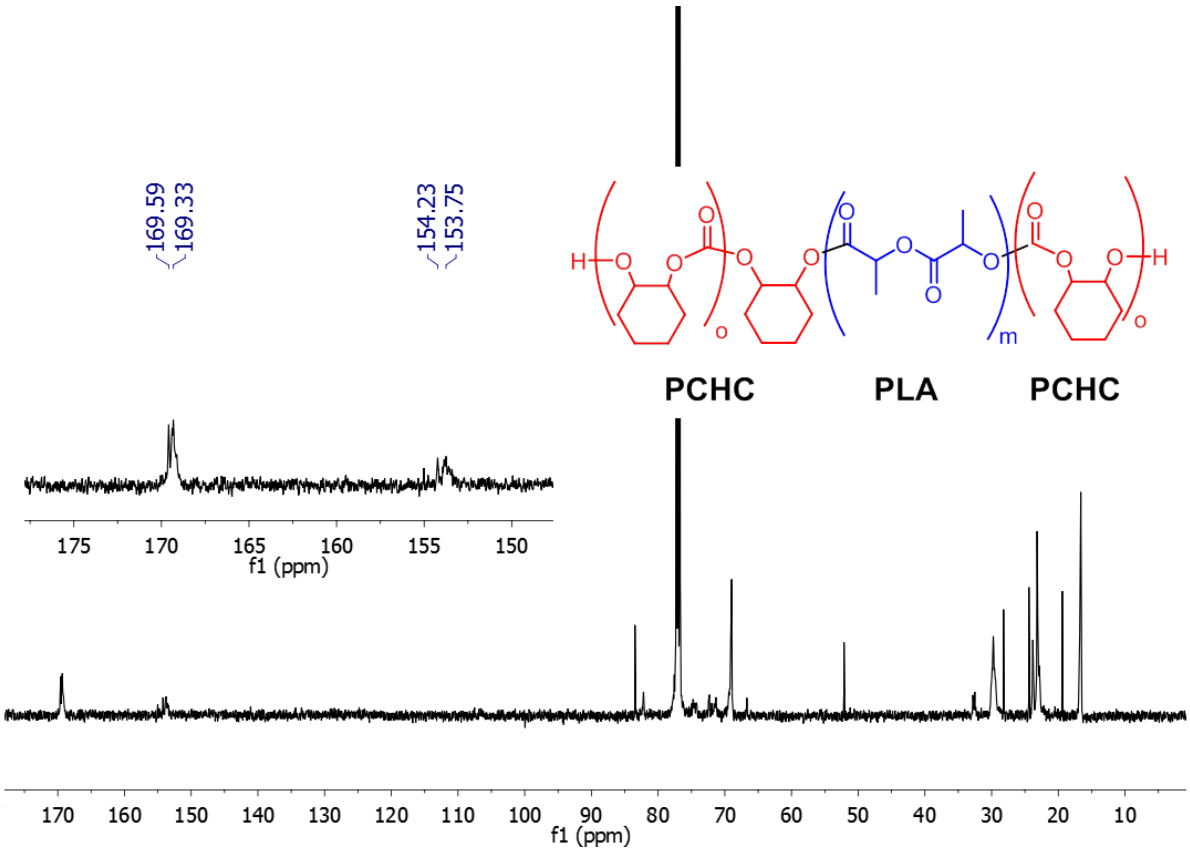

Figure 5.5.11: $^{13}C\{^{1}H\}$ NMR spectrum of of poly (cyclohexene carbonate-lactide-cyclohexene carbonate) synthesised according to Table 5.7, Run 1.

The $^{13}C\{^{1}H\}$ NMR spectrum of the block copolymer showed two main peaks in the carbonyl region. The peaks at 154 and 153 ppm correspond to PCHC and those at 169.3 and 169.5 ppm are from the PLA. Transesterification between the two blocks would result in additional carbonyl signals, typically at chemical shifts between the resonances from the polymer blocks.

The selectivity observed during the polymerisation of CHO/CO_2/LA means that the insertion of lactide into the zinc alkoxide intermediate is occurring faster than the insertion of carbon dioxide. Changing the concentration of lactide or temperature, which both decrease the rate of lactide ring opening, does not influence the selectivity. Another consideration is whether the selectivity remains the same at higher pressures of carbon dioxide, which should increase the rate of carbon dioxide insertion by increasing its concentration. The polymerisation of

LA/CHO/CO_2 with [$LZn_2(Ph)_2$] was carried out at 20 bar. Two equivalent reactions were carried out with one terminated after 1 hr and the other at 17 h. After 1 h, the conversion of LA was 12 %, whereas the conversion of CHO was 2 %. At 17 h, the conversion of LA was 100 % and the conversion of CHO was 31 %. This suggested that at 20 bar of carbon dioxide, the formation of PLA and PCHC occurred at the same time. It is likely that the higher pressure, and therefore concentration of carbon dioxide means that insertion of carbon dioxide into a zinc alkoxide bond is faster. Therefore, the insertion of carbon dioxide has become competitive with the insertion of lactide.

Table 5.8: Terpolymerisation of LA/CHO/CO_2 at 20 bar.

#	[$LZn_2(Ph)_2$]:CHO:LA	Time	conversion PLA /% [a]	Conversion PCHC / % [b]	TOF PLA/PCHC [c]	M_n (Đ) /g mol^{-1} [d]
1	1:2000:200	17	100	31	11/36.5	3054 (1.32)
2	1:2000:200	1	12	2	24/40	355 (1.32)

Polymerisations carried out at 100 °C, 20 atm of carbon dioxide at 1M *rac* LA. a) Determined from the normalised relative integrals in the ^{1}H NMR spectrum. PCHC at 4.65 ppm and CHO at 3.10 ppm. b) Determined from the normalised relative integrals in the ^{1}H NMR spectrum. PLA at 5.15 ppm and LA at 5.05 ppm c)TOF = (mol of monomer/mol of catalyst)/h. Monomer conversions determined from ^{1}H NMR spectroscopy d) Determined by SEC with THF as the eluent, using polystyrene standards to calibrate the instrument.

5.5.3 Polymer Structure of the Pentablock Copolymers

The proposed structure of the pentablock copolymer resulting from the polymerisation of PA/CHO/CO_2/LA is drawn in Figure 5.5.14. The majority of the discussion refers to the analysis of the pentablock copolymer formed according to Table 5.9, Run 1, but related data was obtained for all of the pentablock copolymers formed. The ^{1}H NMR spectrum of the pentablock copolymer formed with VCHO (Table 5.9, Run 3), is more complicated due to the additional vinyl signals as mentioned in section 5.4.3, which prevents any rigorous integration of its composition.

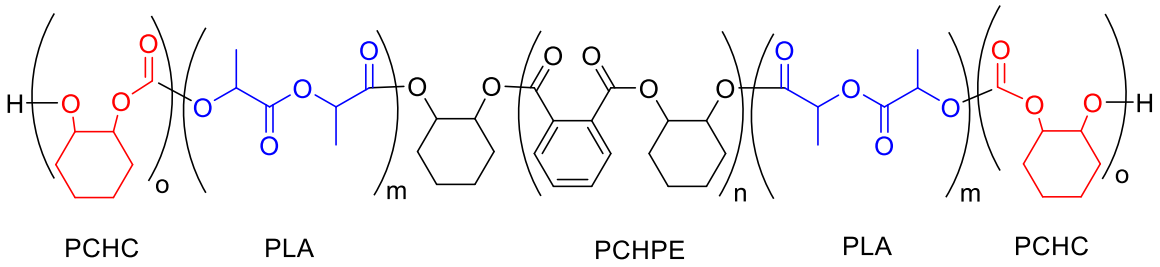

Figure 5.5.12: Structure of pentablock copolymer formed from the terpolymerisation of PA/CHO/CO_2/LA.

Table 5.9: Polymerisation of PA/CHO/CO_2/LA.

#	PA:CHO:LA	M_n (Đ) [a] PE /g mol^{-1}	M_n (Đ) [a] PE-PLA /g mol^{-1}	Conversion [b] CHO /%	M_n (Đ) [a] PE-PLA-PC /g mol^{-1}	PE:PLA:PC NMR [c]	calculated PE:PLA:PC [d]
1	50:2000:200	1280 (1.18)	2280 (1.38)	12	2090 (1.24)	1:4:6	1:4:5
2	50:2000:100	1260 (1.13)	2270 (1.21)	10	1930 (1.22)	1:2:5	1:2:4
3	50:2000*:200	774 (1.05)	2850 (1.23)	14	2860 (1.48)	-	1:4:6

*VHCO. Polymerisations carried out at 100°C, under 1 atm of carbon dioxide. a) Determined by SEC with THF as the eluent, using polystyrene standards to calibrate the instrument. b) Determined from the normalised relative integrals in the ^{1}H NMR spectrum at 3.10 ppm for CHO and 4.65 ppm for PCHC. c) Determined from the normalised relative integrals in the ^{1}H NMR spectrum at 7.35 ppm for PE and 4.65 ppm for PCHC and 1.71 for PLA. d) Calculated from the conversion of monomer.

SEC analysis was carried out on the aliquots taken at each stage of the reaction. The molar mass of the polyester (PCHPE/PVCHPE) block formed during stage A, was typically between 800-1300 g mol^{-1}. The low molar mass was due to the presence of 1,2-cyclohexene diol (Section 1.2.1).

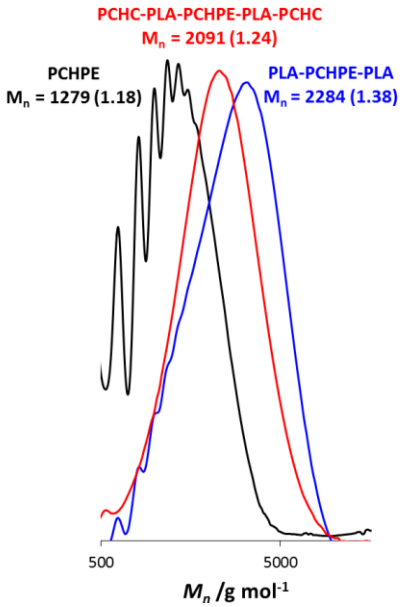

Figure 5.5.13: SEC analysis of the aliquots from the terpolymerisation of PA/CHO/CO_2/LA, Table 5.9, Run 1.

After the formation of the PLA block the molar mass increased and the dispersity remained narrow. There was a clear shift of the molar mass to higher values, which suggests that the PLA block was attached to the polyester. However, after the formation of PCHC the molar mass of the copolymer appearred to slightly decrease. The reduction in molar mass occurred in every case where PCHC was attached to a PLA block, regardless of the conditions of synthesis, length of the blocks or presence of other blocks in the copolymer. All SEC analysis was conducted using a refractive index (RI) detector, which uses polystyrene standards for calibration (Section 2.3.4). The apparent decrease in molar mass is assumed to be due to different chain conformations (hydrodynamic radii) and is not an indication of chain degradation. The conformation of a polymer is affected by the solvent; therefore, carrying out the SEC analysis in an alternative solvent may be of interest. When SEC analysis was carried out in chloroform the molecular weights were considerably different to those detected using THF. The molar mass of the PCHPE block was too low to be measured (a different set of columns was employed, which are less sensitive to oligomers). The molar mass of the PLA-PCHPE-PLA triblock copolymer was 1430 g mol^{-1} (Đ=1.46) and the molar mass of the PCHC-PLA-PCHPE-PLA-PCHPE pentablock copolymer was 1670 g mol^{-1} (Đ=1.29). The

difference in molar mass values with the different solvent provides some indication of differences in solution conformations. The NMR spectroscopy provides good evidence for the formation of a pentablock copolymer: signals for all three polymers (PCHPE, PLA, PCHC) were observed and the ratio of the block was in good agreement with the calculated values. Therefore, with the increase in molar mass observed by SEC in chloroform for the pentablock copolymer, and the NMR data it is assumed the apparent decrease in molar mass is due to more complex polymer – solvent interactions. A related phenomenon was observed by Byers and co-workers, in the formation of a triblock copoly(ether-ester) (PCHO-PLA-PCHO).[19] The formation of the ether block (PCHO) resulted in an apparent decrease in molar mass values, when analysed by SEC with an RI detector. The use of a light scattering (LS) detector resulted in the expected increase in molar mass being observed for the triblock copoly (ether-ester).

The pentablock copolymer was also analysed by ^{1}H DOSY NMR, which showed a single diffusion coefficient corresponding to all of the polymers (Figure 5.5.17). The diffusion coefficient is 3.16 x 10^{-10} m^2/s, which corresponds to a hydrodynamic radius of 1.29 x 10^{-9} m. It seems that a copolymer has been formed rather than a blend of homopolymers.

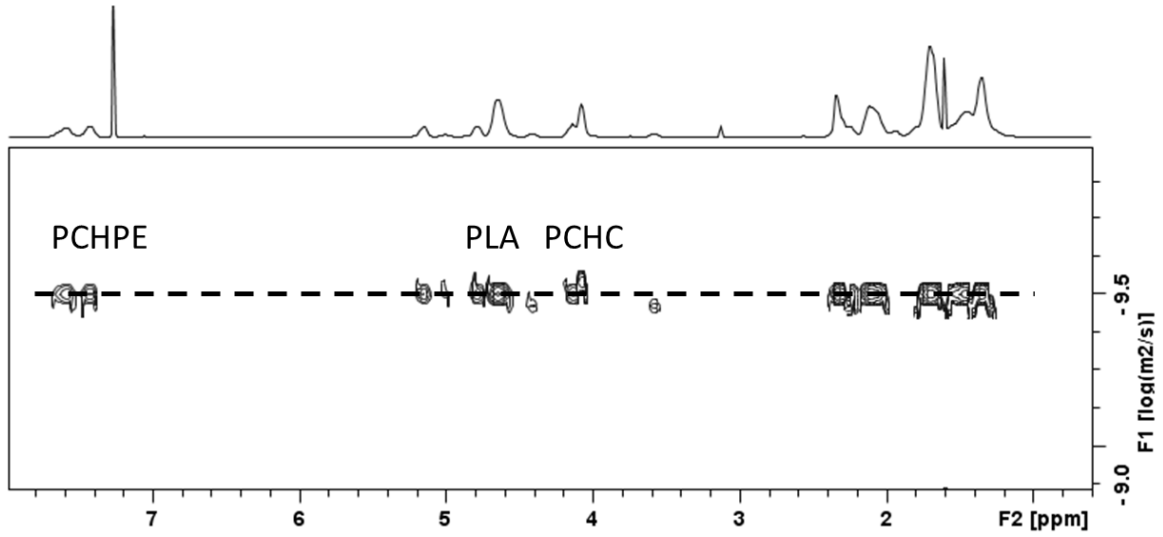

Figure 5.5.14: ^{1}H DOSY NMR spectrum of the pentablock copolymer from the polymerisation of PA/CHO/CO_2/LA, Table 5.99, Run 1.

The copolymers were purified by precipitation from THF using pentane. The ^{1}H NMR spectrum of the purified copolymer showed peaks for PCHPE at 7.58 and 7.43 ppm (Ha, Hb) and PCHC at 4.65 ppm (Hh). The methine protons of PLA resulted in a signal at 5.15 ppm (Hf), however this was directly overlapping with the methine protons from PCHPE (5.15 ppm) (Hc). This is perhaps unsurprising as both protons are methine protons next to an ester group. The ratio of PCHPE:PLA:PCHC was calculated using the signals at 7.43 ppm for PCHPE (Ha), 4.65 ppm for PCHC (Hh) and 1.72 ppm for PLA (Hg). All signals are deconvoluted and normalised before integration. In all cases the ratio of PCHPE:PLA:PCHC from the ^{1}H NMR spectrum was close to the theoretical ratio (calculated from the degree of polymerisation).

As well as peaks assigned to the main chain units of the three blocks, there were several other peaks in the spectrum of the pentablock copolymer. The two peaks at 4.41(Hn) and 3.58 (Ho) ppm are known as the end group signals of PCHC (Hn, Ho).[13] These signals were only present in the ^{1}H NMR spectrum of the pentablock copolymer, after the formation of the PCHC block has occurred. The other new peaks in the spectrum are at 4.84 (Hm) and 5.02 (Hk) ppm. The peak at 5.02 ppm (Hm) appeared after the formation of PLA block, whereas that at 4.84 ppm, appeared after the formation of the PCHC block. Both signals remained in the spectrum of the purified copolymer, indicating they arise from junction units. Both peaks correlated with the methylene protons of the cyclohexene ring (by COSY NMR spectroscopy) suggesting they are part of either a PCHPE or PCHC unit. The peak at 5.02 ppm (Hk) is assigned to the methine protons of the PCHPE junction unit, adjacent to the PLA block and the peak at 4.85 ppm (Hm) is assigned to the methine protons of the PCHC junction unit adjacent to the PLA block. Due to the overlap of the junction units, any integration of the peaks, even when deconvoluted, would likely be inaccurate and the ratio of junction units to main chain units was not determined.

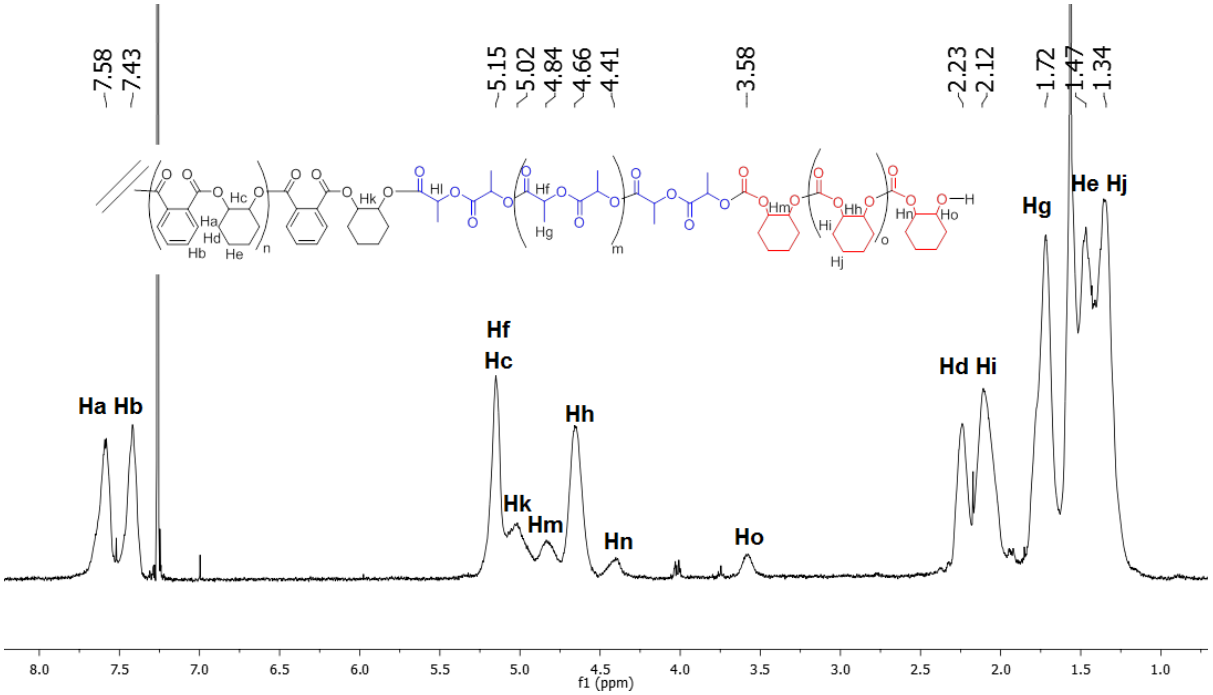

Figure 5.5.15: ^{1}H NMR spectrum of the pentablock copolymer from the polymerisation of PA/CHO/CO_2/LA, Table 5.9, Run 1.

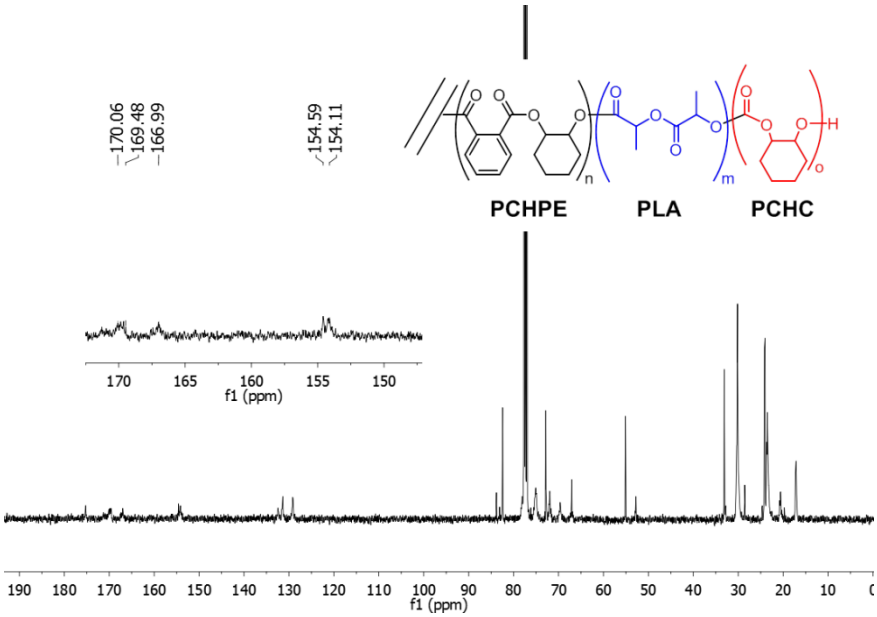

Figure 5.5.16: ^{13}C{^{1}H} NMR spectrum pentablock copolymer synthesised according to Table 5.99, Run 1.

^{13}C NMR spectrum of the pentablock copolymer showed several peaks in the carbonyl region. The carbonyl peaks of PCHPE and PCHC were present at 166.9 ppm and 154.6-153.1 ppm. The characteristic signal for PLA was present at 169.3 and at 169.6 ppm. There is no evidence that any cross transesterification has occurred between the PLA and the PCHPE blocks, as there were no new signals in the carbonyl region.

5.6 Conclusion

Switchable Catalysis using [$LZn_2(Ph)_2$] with 1,2 cyclohexene diol has previously been used to successfully prepare triblock and multiblock copolymers by combing ring opening copolymerisation of epoxides and carbon dioxide and ring opening polymerisation of lactones. Here the combination of the ring opening copolymerisation of anhydride/epoxide and carbon dioxide/epoxide with the ring opening polymerisation of lactones or lactide was used to form pentablock copolymers. Using mixtures of four monomers still allows highly selective enchainment but the order of selectivity changes from lactones to lactide.

The combination of anhydride, carbon dioxide, epoxide and lactone results in the selective sequential formation of alternating polyester, polycarbonate and finally aliphatic polyester blocks. The used of ε-decalactone improves the polymerisation control, but all the characterisation data is highly indicative of pentablock formation in all cases.

The combination of anhydride, carbon dioxide, epoxide and lactide results in the selective sequential formation of alternating polyester, polylactide and then polycarbonate blocks. The selectivity is reproducible under a range of conditions at 1 atm of carbon dioxide. Experiments carried out at higher pressures of carbon dioxide showed that the insertion of carbon dioxide becomes competitive with the insertion of lactide and this area should be investigated further in the future. The insertion of lactide into the zinc alkoxide species has not yet been studied computationally, but it is known that the zinc lactate intermediates can be strongly stabilised by forming a five-membered metallochelate.[20-22] Such a species may contribute thermodynamically to the altered selectivity observed using lactide. The structures

of all the pentablock copolymers were confirmed by SEC analysis, ^{1}H NMR spectroscopy and ^{1}H DOSY NMR spectroscopy.

The findings of this chapter represent a significant advance as there are very few other examples of catalysts which are able to selectively enchain mixture of 4 monomers.[4] The formation of a multiblock copolymer containing three distinct blocks is unusual and provides the possibility to access unusual self-assembled structures. The formation of pentablock copolymers which contain vinyl groups also allows further modification of the structure and the introduction of functionality. The detailed study of block microstructure, self-assembly and functionalization could be a fruitful future research area.

References

(1) Paul, S.; Zhu, Y.; Romain, C.; Brooks, R.; Saini, P. K.; Williams, C. K. *Chem. Commun.* **2015**, *51*, 6459.
(2) Williams, C. K. *Chem. Soc. Rev.* **2007**, *36*, 1573.
(3) Kember, M. R.; Buchard, A.; Williams, C. K. *Chem. Commun.* **2011**, *47*, 141.
(4) Bates, F. S.; Hillmyer, M. A.; Lodge, T. P.; Bates, C. M.; Delaney, K. T.; Fredrickson, G. H. *Science* **2012**, *336*, 434.
(5) Kim, J. G.; Cowman, C. D.; LaPointe, A. M.; Wiesner, U.; Coates, G. W. *Macromolecules* **2011**, *44*, 1110.
(6) Cowman, C. D.; Padgett, E.; Tan, K. W.; Hovden, R.; Gu, Y.; Andrejevic, N.; Muller, D.; Coates, G. W.; Wiesner, U. *J. Am. Chem. Soc.* **2015**, *137*, 6026.
(7) Saini, P. K.; Romain, C.; Zhu, Y.; Williams, C. K. *Polym. Chem.* **2014**, *5*, 6068.
(8) Jeske, R. C.; Rowley, J. M.; Coates, G. W. *Angew. Chem. Int. Ed.* **2008**, *47*, 6041.
(9) Zhu, Y.; Romain, C.; Williams, C. K. *J. Am. Chem. Soc.* **2015**, *137*, 12179.
(10) Romain, C.; Zhu, Y.; Dingwall, P.; Paul, S.; Rzepa, H. S.; Buchard, A.; Williams, C. K. *J. Am. Chem. Soc.* **2016**, *138*, 4120.
(11) Kember, M. R.; Copley, J.; Buchard, A.; Williams, C. K. *Polym. Chem.* **2012**, *3*, 1196.
(12) Paul, S.; Romain, C.; Shaw, J.; Williams, C. K. *Macromolecules* **2015**, *48*, 6047.
(13) Koning, C.; Wildeson, J.; Parton, R.; Plum, B.; Steeman, P.; Darensbourg, D. J. *Polymer* **2001**, *42*, 3995.
(14) Tang, M.; Purcell, M.; Steele, J. A. M.; Lee, K.-Y.; McCullen, S.; Shakesheff, K. M.; Bismarck, A.; Stevens, M. M.; Howdle, S. M.; Williams, C. K. *Macromolecules* **2013**, *46*, 8136.

(15) Buchard, A.; Bakewell, C. M.; Weiner, J.; Williams, C. K. In *Organometallics and Renewables*; Meier, A. R. M., Weckhuysen, M. B., Bruijnincx, A. P. C., Eds.; Springer Berlin Heidelberg: Berlin, Heidelberg, 2012, p 175.
(16) Albertsson, A.-C.; Varma, I. K. *Biomacromolecules* **2003**, *4*, 1466.
(17) Espartero, J. L.; Rashkov, I.; Li, S. M.; Manolova, N.; Vert, M. *Macromolecules* **1996**, *29*, 3535.
(18) Zhu, Y.; Romain, C.; Poirier, V.; Williams, C. K. *Macromolecules* **2015**, *48*, 2407.
(19) Biernesser, A. B.; Delle Chiaie, K. R.; Curley, J. B.; Byers, J. A. *Angew. Chem. Int. Ed.* **2016**, n/a.
(20) Wheaton, C. A.; Hayes, P. G. *Chem. Commun.* **2010**, *46*, 8404.
(21) Stanford, M. J.; Dove, A. P. *Chem. Soc. Rev.* **2010**, *39*, 486.
(22) Williams, C. K.; Breyfogle, L. E.; Choi, S. K.; Nam, W.; Young, V. G.; Hillmyer, M. A.; Tolman, W. B. *J. Am. Chem. Soc.* **2003**, *125*, 11350.

Chapter 6 : Overall Conclusion

The thesis has investigated the chemoselectivity of $[LZn_2(X)_2]$ catalysts in order to form complex block copolymers using monomer mixtures. The combination of carbon dioxide/ epoxide and lactone was selectively polymerised to form an ABA triblock copolymer. The result is a rare example of truly selective polymerisation catalysis and exemplifies the switchable catalysis concept. The selectivity of $[LZn_2(X)_2]$ was then tested to determine its reversibility and a well-defined heptablock poly(ester – carbonate) was prepared and characterised. There are currently no other known catalysts or polymerisation methods that are fully selective, reversible and where the switch can be performed multiple times to form multiblock copolymers. The selectivity of the dizinc catalysts $[LZn_2(X)_2]$ is sufficiently robust that multiple polymerisations can be combined without the loss of any selectivity. From a mixture of four monomers, well defined pentablock copolymers were formed. The precise structure of the pentablock structure depends on the combination of monomers used.

Overall these studies have allowed a greater understanding of the possible pathways and factors controlling the selectivity of the di-zinc catalysts. Figure 6.1 shows an overview of the hypothesised key intermediates and the processes controlling the selectivity. Considering that all the reactions share a common zinc alkoxide intermediate, selectivity is proposed to arise from control of which monomers react with it. It is proposed that the insertion of anhydride occurs most favourably, due to both faster rates and the product being the most thermodynamically stable linkage as established by DFT calculations.[1] Once all the anhydride has been consumed the ring opening of an epoxide molecule returns the system to the zinc alkoxide intermediate. The insertion of lactide seems to be the next most favourable process, again probably governed by a combination of kinetic and thermodynamic considerations although this is yet to be confirmed by DFT calculations. The insertion of carbon dioxide is next most favourable reaction with the zinc alkoxide intermediate. The insertion of lactone has been shown to form the least stable linkage and also has a high activation barrier.[1] The combination of these effects means that the insertion of lactone only occurring after complete consumption or removal of anhydride and carbon dioxide. The new selective switch catalysis allows monomers to be combined in multiple variations and the switches can be performed reversibly. This is powerful and allows new and interesting copolymer microstructures to be easily produced.

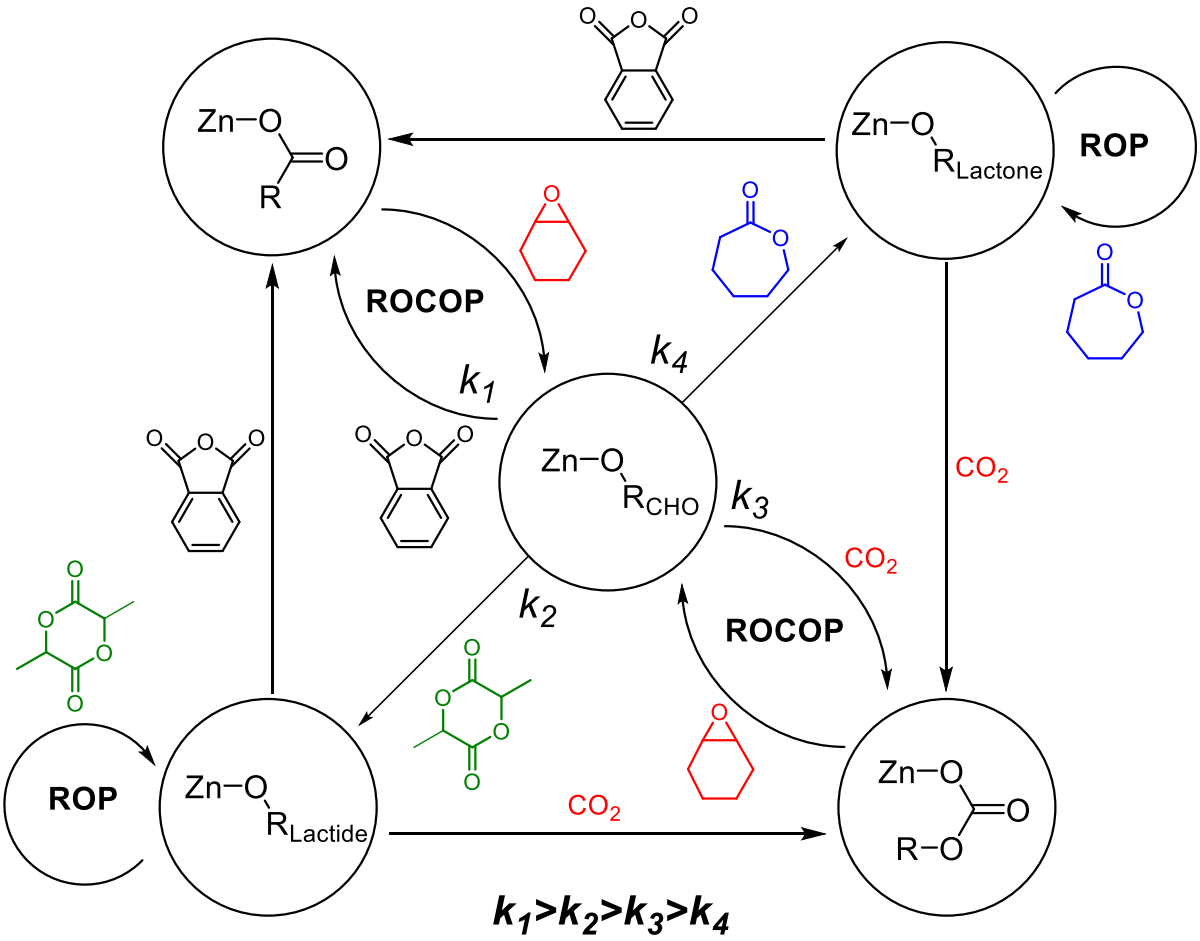

Figure 6.1: Scheme showing how the monomers interact with the zinc alkoxide species.

Future Work

One area requiring development is to expand the range of catalysts and monomers able to exhibit this reactivity. It is especially interesting to target monomers such as propylene oxide or maleic anhydride, because there is considerable interest in aliphatic copolymers, due to their potential for biomedical applications. Some examples of catalyst classes which could be investigated include metal salens, porphyrins and [ZnBDI] complexes (Figure 6.2)

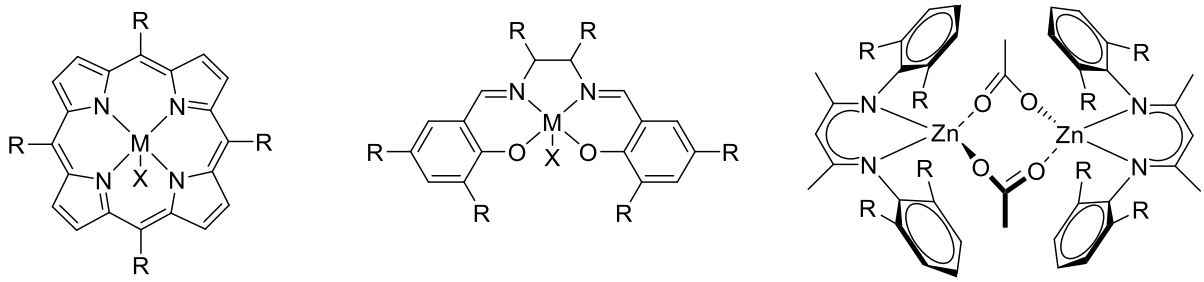

Figure 6.2: Structure of potential catalyst targets for investigating switch chemistry.

These catalysts show good activity in carbon dioxide/ epoxide ring opening copolymerisation and in some cases are also known as suitable ligands for ROP.[2-5] For example [ZnBDI] alkoxide complexes are highly active for lactide ring opening polymerisation.[2] Very recently Chisolm and co-workers reported that when using a chromium tetraphenylporphyrin with a mixture of propylene oxide and lactide exclusively forms polylactide. At low temperatures, a single propylene oxide unit is enchained as an endgroup, and the polylactide formed is highly isotactic. At higher temperatures the propylene oxide becomes enchained but is quickly removed *via* a back biting reaction, resulting in 3,6-dimethyl-1,4-dioxan-2-one.[3] Given this result and the success of porphyrin catalysts as ring opening copolymerisation catalyst, it is relevant to explore switch methods analogous to those developed in this thesis.

There is significant interest in multiblock copolymers and a more detailed study of the material properties, rheology and application is warranted. Multiblock copolymers are of interest due to the potential for complex self-assembly.[6] Block copolymers with A and B blocks are interesting and have been well studied; the addition of a third C block, increases the complexity as there are more potential self-assembly structures.[7] ABC block copolymers are less well studied both in terms of synthesis and properties.[6,8] The switchable catalysis described in this thesis provides a facile method to produce multiblock copolymers, and should continue to be explored to tune the composition of the materials.

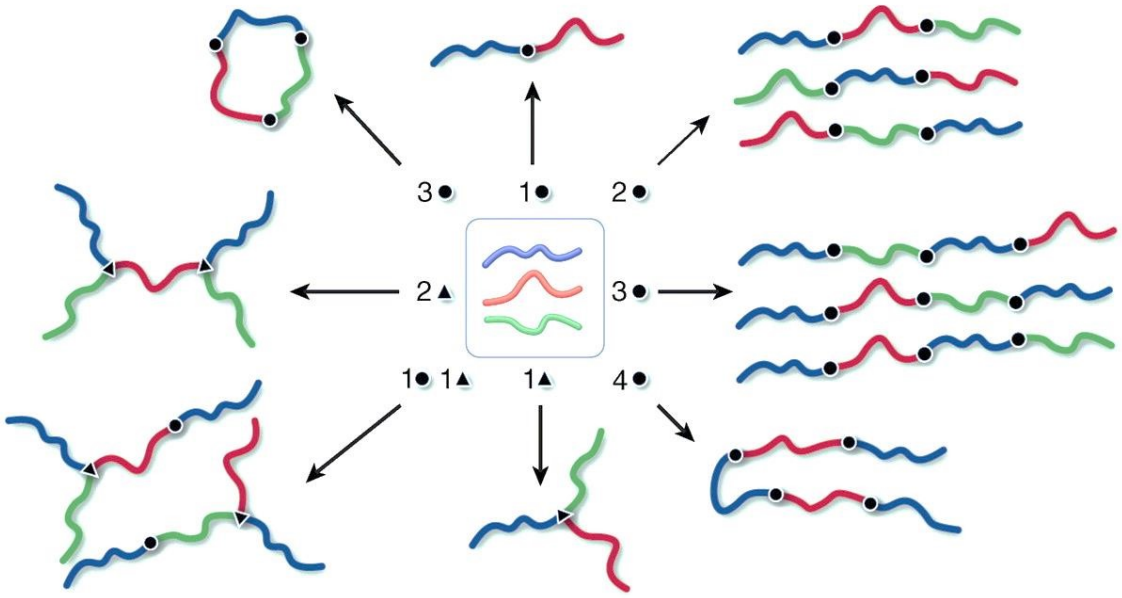

Figure 6.3: **A subset of the structures available with two (*k* = 2) or three (*k* = 3) block types produced by varying the number of blocks (*n*) and the functionality of the connector at each block-block juncture (difunctional, circles; trifunctional, triangles).**

Figure reproduced from Science 2012, 336, 434-440, with permission.[9]

The addition of degradable sections within the multiblock copolymer, such as the polylactide and polylactone sections used within this work, open up the potential applications for multiblock copolymers even further.[9] Multiblock copolymers containing biodegradable section could have applications within the controlled release of drugs and the formation of scaffolds.[10] There is an added advantage to having blocks which can be removed using orthogonal conditions as this allows, allows the formation of complex nanostructures.

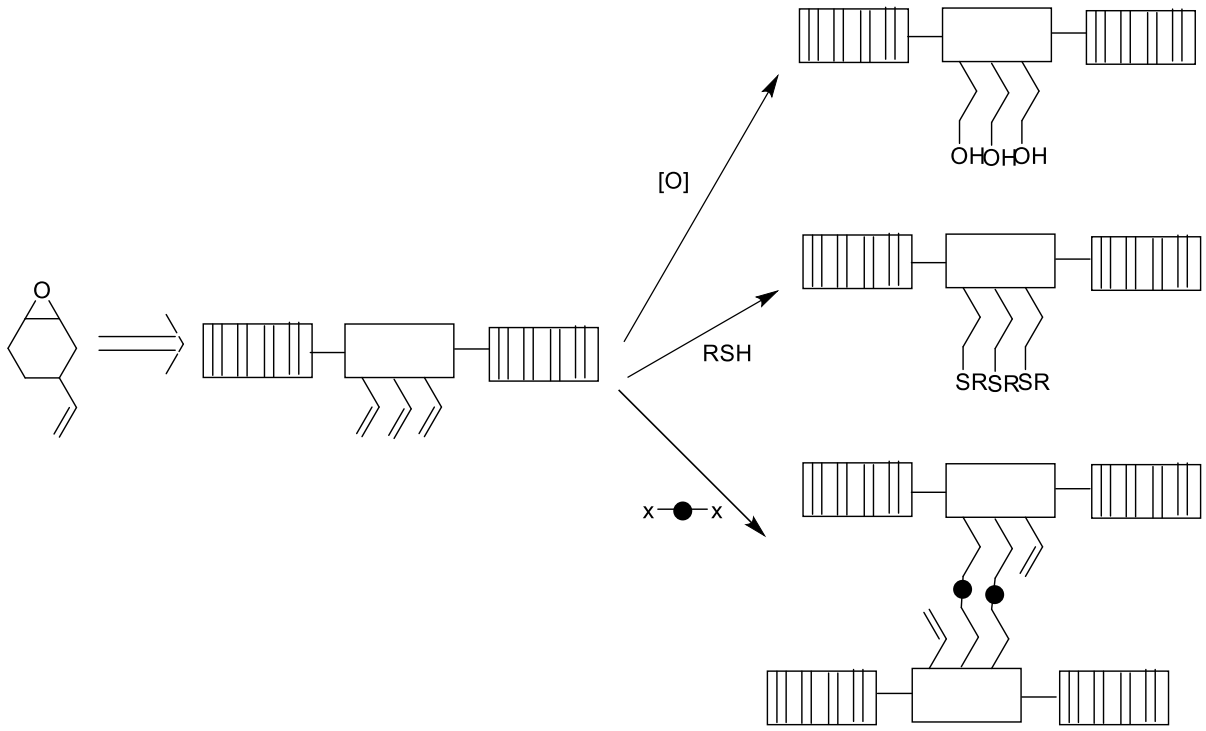

Figure 6.4: **Scheme showing potential functionalisations of multiblock copolymers.**

There is significant scope for further functionalization of the multiblock copolymers, for example by the introduction of vinyl groups which is easily achieved using vinyl cyclohexene oxide and which can be post-functionalised to produce other new block copolymers (Figure 6.4). Potential routes for functionalization include oxidation to give hydroxyl groups, which results in the formation of an amphiphilic polymer. This would allow self-assembly in aqueous media and access to polymersomes and micelles. The thiolene reaction is a very versatile Click reaction and could allow substitution of vinyl functionalised polymers with drugs, proteins and other bioactive molecules.

References

(1) Romain, C.; Zhu, Y.; Dingwall, P.; Paul, S.; Rzepa, H. S.; Buchard, A.; Williams, C. K. *J. Am. Chem. Soc.* **2016**, *138*, 4120.
(2) Brulé, E.; Robert, C.; Thomas, C. M. In *Sequence-Controlled Polymers: Synthesis, Self-Assembly, and Properties*; American Chemical Society: 2014; Vol. 1170, p 349.

(3) Balasanthiran, V.; Chatterjee, C.; Chisholm, M. H.; Harrold, N. D.; RajanBabu, T. V.; Warren, G. A. *J. Am. Chem. Soc.* **2015**, *137*, 1786.
(4) Paul, S.; Zhu, Y.; Romain, C.; Brooks, R.; Saini, P. K.; Williams, C. K. *Chem. Commun.* **2015**, *51*, 6459.
(5) Trott, G.; Saini, P. K.; Williams, C. K. *Phil. Trans. R. Soc. A* **2016**, *374*.
(6) Bates, F. S.; Fredrickson, G. H. *Physics Today* **1999**, *52*, 32.
(7) Zheng, W.; Wang, Z.-G. *Macromolecules* **1995**, *28*, 7215.
(8) Lodge, T. P. *Macromol. Chem. Phys.* **2003**, *204*, 265.
(9) Bates, F. S.; Hillmyer, M. A.; Lodge, T. P.; Bates, C. M.; Delaney, K. T.; Fredrickson, G. H. *Science* **2012**, *336*, 434.
(10) Hillmyer, M. A.; Tolman, W. B. *Acc. Chem. Res.* **2014**.

Chapter 7 : Experimental

7.1 General Procedures:

7.1.1 Materials and Methods

Unless stated all reactions were carried out in air. Anaerobic reactions were conducted using a nitrogen filled glovebox or standard anaerobic techniques (i.e. Schlenk lines). All solvents and reagents were purchased from commercial sources (Alfa Aesar, Sigma Aldrich, Strem, VWR) and used as received unless otherwise stated.

Dry THF and hexane, were prepared by distilling them from sodium and benzophenone. They were subsequently stored under nitrogen. Toluene was dried by distilling from sodium and subsequently stored under nitrogen. Deuterated solvents were distilled from CaH_2 and stored under nitrogen. All solvents were degassed by performing at least three several freeze-thaw cycles.

Cyclohexene Oxide (CHO) (Alfa Aesar), was dried by stirring it over CaH_2 for 48 h and it was then filtered and fractionally distilled, under nitrogen, before being stored under nitrogen. Vinyl cyclohexene oxide, ε-caprolactone, ε-decalactone, δ-valerolactone, methoxy ethylene glycol were dried over CaH_2 for 18 h and distilled, under reduced pressure, before being stored under nitrogen. Phthalic anhydride (Sigma Aldrich, 98%) was purified by dissolving it in hot benzene, filtering impurities and crystallisation from chloroform. It was purified by sublimation. *Racemic*-lactide was purified by repeat (x3) crystallization from toluene, followed by sublimation. The purified lactide was then dried under vacuum for 72h.

High pressure copolymerisation reactions were carried out in a Parr 5513 25 mL bench reactor using CP grade (99.99%) carbon dioxide (BOC) which had been passed through a VIVI P600-1 CO_2 gas purifying column before the polymerisation. Low pressure copolymerisation reactions used Research grade (99.99%) carbon dioxide (BOC), which had been passed through a drierite column.

7.1.2 Measurements

NMR

Nuclear magnetic resonance (NMR) spectra were recorded on a Bruker Av400 spectrometer operating at 400 MHz for ^{1}H and 100 MHz $^{13}C\{^{1}H\}$ spectra. Solvent peaks were used as internal references for ^{1}H and ^{13}C chemical shifts (ppm). Additional NMR experiments were performed by Mr. P. Haycock: when needed; higher resolution $^{31}P\{^{1}H\}$ NMR, $^{13}C\{^{1}H\}$ NMR and ^{1}H NMR experiments were performed on a Bruker Av500 spectrometer. Spectra were processed and analysed using Mestrenova v8 software.

DOSY experiments were performed at a steady temperature of 298 K with at least 32 gradient increments using the ledbpgp2s sequence. Complete diffusion was ensured using the T1/T2 module of Topspin and DOSY transformations using either mono, bis- or tri-exponential fitting were performed using the same software after zero filling. Further processing was achieved using the topspin software; DOSY data collection and analysis carried out by Mr P. Haycock, Imperial College London.

SEC

The molecular weights and dispersities were characterized using a Shimadzu LC-20AD instrument, with SEC grade THF as the eluent at a flow rate of 1.0 $mL \cdot min^{-1}$ at 40 °C. Two Mixed Bed PSS SDV linear S columns were used in series. Near monodispersed polystyrene standards were used to calibrate the instrument. The polyesters were dissolved in SEC grade THF and filtered prior to analysis. Crude polymers were used for SEC characterization unless stated otherwise. The following conversion factors were applied:

Table 7.1: Correction factors used to determine M_n values by SEC analysis

$$M_{n(corrected)} = X \cdot M_{n(SEC)}$$

Polymer	X	Ref.
PCL	0.56	[1]
PVL	0.57	[1]
PDL	0.054	[2]
PLA	0.58	[3]

Mass spectrometry and MALDI-ToF

All MALDI–ToF measurements were performed using a MALDI micro MX micromass instrument. The matrix was dithranol, the ionising agent was KOAc and the solvent THF. Solutions of 10 mg/mL concentrations were made of the matrix, salt and polymer and combined in a 2:1:2 ratio. The spectra were analysed using mmass software. Other mass spectrometry, ESI, LC and GC, were performed by Lisa Haigh, Imperial College London.

IR Spectroscopy

In-situ ATR-IR Spectroscopy: The polymerizations were monitored using a Mettler-Toledo ReactIR 4000 spectrometer, equipped with a mercuric cadmium telluride (MCT)Schlenk detector and a silver halide DiComp probe. The absorptions were processed by normalising the signals against the baseline. The data was calibrated by independent determination of the conversion of the monomer, using ^{1}H NMR spectroscopy.

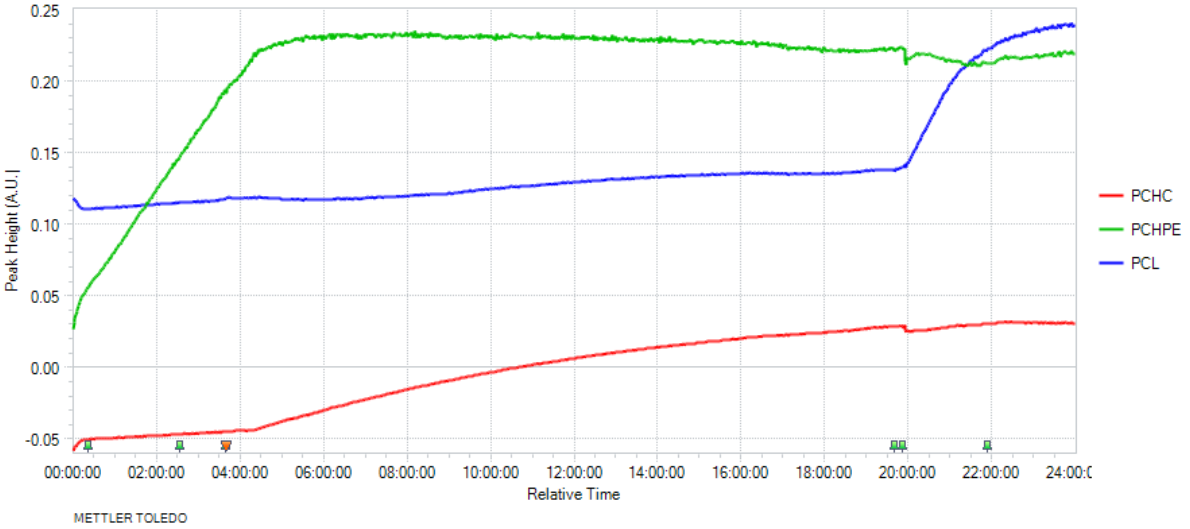

Figure: Plot showing an example of the raw data obtained by *in-situ* ATR spectroscopy. before normalisation against known conversions of monomers. The reaction is the terpolymerisation of PA/CHO/CO_2. The absorption at 1334 cm^{-1} is assigned to PCHC, the absorption at 1070 cm^{-1} is assigned to PCHPE and the absorption at 1190 cm^{-1} assigned to PCL. These assignments are based on control reactions.

Differential Scanning Calorimetry

The polymers thermal properties were measured using a DSC Q2000 instrument (TA Instruments, UK). A sealed empty crucible was used as a reference, and the DSC was calibrated using indium. Samples were heated from 25 °C to 125 °C, at a rate of 10 °C·min^{-1}, under a helium flow, and were kept at 125 °C for 2 min to erase the thermal history. Subsequently, the samples were cooled to -100 °C, at a rate of 10 °C·min^{-1}, and kept at -100 °C·min^{-1} for further 2 mins, followed by a heating procedure from -100 °C to 130° C, at a rate of 10 °C·min^{-1}. Each sample was measured over three heating–cooling cycles. The glass transition temperatures (T_g) reported are taken from the third cycle.

Tensile Testing

Solvent-cast polyester sheets were prepared by pouring DCM solutions of the polymers into a Teflon mold. The solvent was slowly evaporated, in the fume hood, at room temperature over

2 weeks. Dumbbell-shaped sample bars were then cut out from the polyester sheet (35 mm in length, 2.1 mm in width and 0.4 mm in thickness) using a Zwick Punch (Zwick D-7900, Ulm-Einsingen Type 7102, Werk-Nr. 85688) with cutting blades. The mechanical performance (strength at break, elongation and Young's modulus) was measured at ambient temperature and humidity (21.8 ºC and 21 %) on a Linkam TST350 Tensile Stress Tester instrument at a 10 mm/min extension rate and a 5 mm/min retraction rate.

7.2 Synthesis of Catalysts

All reactions to make catalysts were carried out according to literature procedures. [2,4-6]

4-tButyl-2,6-diformylphenol.[4] 4-*t*Butyl-phenol (20.6 g, 137.1 mmol) and HMTA (30.4 g, 216.8 mmol), TFA (104 mL, 1.35 mol) were added to a round bottom flask, slowly whilst stirring, and the bright yellow solution was refluxed at 125 °C 10 h, after which the solution turned dark brown. A Dean-Stark condenser was added and the solution heated under reflux at 150 °C for 4 hours, after which the solution was allowed to cool to 100 °C and 3M HCl (200 mL) was added. The solution was refluxed for a further 40 minutes at 100 °C then cooled to -10 °C for 10 h, during which time a precipitate formed. The product was filtered, washed twice with cold (-78 °C) MeOH (30 mL) and dried under vacuum.

Yellow crystals; yield: 17.51 g, 84.1 mmol, 63%. ^{1}H NMR ($CDCl_3$); δ 11.48 (s, 1H, O*H*), 10.24 (s, 2H, C*H*O), 7.98 (s, 2H, Ar-*H*), 1.35 (s, 9H, CH_3).

[H_4Ln](ClO_4)$_2$.[4] To a round-bottomed flask, 4-*t*butyl-2,6-diformylphenol (4 g, 19.4 mmol), $NaClO_4$ (9.5 g, 77.6 mmol), acetic acid (2.3g, 38.8 mmol) and methanol (90 mL) were added. This solution was heated to 75 °C, whilst stirring. When the solution started to boil, 2,2-dimethyl-1,3-propanediamine (1.98 g, 19.4mmol) in methanol (30 mL) was added slowly. The reaction mixture was refluxed for 2 h, and left to stand for 16 h, after which time a

precipitate formed. This was then was filtered and washed with cold (-78 °C) methanol (20 mL).

Orange crystals; yield: 5.8 g, 7.47 mmol, 63%. ^{1}H NMR (d_6-DMSO); δ 13.60 (br s, 4H, N*H*/O*H*), 8.68 (d, 4H, N=C*H*), 7.65 (s, 4H, Ar-*H*), 3.87 (s, 8H, CH_2), 1.28 (s, 12H, CH_3), 1.14 (s, 18H, CH_3).

H_2L^4. $[H_4L^n](ClO_4)_2$ (6.00 g, 8.01 mmol) was suspended in methanol (600 mL). The suspension was cooled to 0 °C and $NaBH_4$ (9.08 g, 240 mmol) was added slowly. As $NaBH_4$ was added, the red-orange suspension turned to a clear solution. The solution was allowed to stir at 25 °C for 1 h, after which water (300 mL) was added slowly, and the solution turned cloudy. Once the precipitate started to form, the mixture was left for 10 h. The product was filtered, washed with water and dried under vacuum to yield a white precipitate. The precipitate was recrystallized from methanol (30 mL) and water (10 mL) to give white crystals. White crystals; yield: 3.66 g, 6.62 mmol, 83%. ^{1}H NMR ($CDCl_3$); δ 6.94 (s, 4H, Ar-*H*), 3.75 (s, 8H, CH_2), 2.53 (s, 8H, CH_2), 1.25 (s, 18H, CH_3), 1.00 (s, 12H, CH_3). EA: calculated for $C_{34}H_{56}N_4O_2$: C 73.87, H 10.21, N 10.13; Found: C 73.85, H 10.08, N 10.24.

$[LZn_2(OCOCF_3)_2]$ 6 . $Zn(CF_3COO)_2.xH_2O$ was dried under a vacuum at 40 °C in the presence of P_2O_5 for 24 h. H_2L (0.80 g, 1.45 mmol) was dissolved in methanol (70 mL) and $Zn(CF_3COO)_2.xH_2O$ (0.85 g, 2.91 mmol) was added. The mixture was stirred for 18 h and the methanol removed *in vacuo*. The product was taken up in dichloromethane (10 mL), filtered, and the solvent removed *in vacuo*. The white powder was the azeotroped with toluene (3 x 20 mL). The product, a white powder, was dried, under a vacuum at 40 °C, in the presence of P_2O_5, for 18 h.

White powder; yield: 0.96 g, 1.05 mmol, 74%. ^{1}H NMR ($CDCl_3$); δ 6.92(s, 4H, Ar-*H*), 4.32-4.26 (m, 4H, Ar-CH_2-N), 3.25 (d, *J* = 12.0 Hz, 4H, Ar-CH_2-N), 3.01(m, 4H, N-CH_2-C), 2.68 (d, *J* = 11.5 Hz, 4H, N-CH_2-C), 2.40 (t, *J* = 12.7 Hz, 4H, N*H*), 1.24 (s, 18H, Ar-CH_3), 1.18 (s, 6H, N-C-CH_3), 1.03 (s, 6H, N-C-CH_3) EA: calculated for $C_{38}H_{54}F_6N_4O_6Zn_2$: C 50.29, H 6.00, N 6.17; Found: C 45.64, H 6.76, N 5.24 calculated for $C_{38}H_{54}F_6N_4O_6Zn_2 \cdot 5H_2O$: C 46.75, H 6.47, N 5.62

[LZn_2Ph_2]^2. Under anaerobic conditions, $ZnPh_2$ (0.33 g, 1.50 mmol) in THF (2 mL) was filtered through a 2 μL filter and the solution was added to H_2L (0.41 g, 0.73 mmol) dissolved in THF (4 mL). The mixture was stirred for 18 h, and filtered and evaporated to yield a white solid. The white solid was washed with hexane and dried under vacuum at 40 °C for 18 h.

White Powder; Yield: 0.53 g, 86%: ^{1}H NMR (TCE-d_2, 403 K) d: 7.40 (br, aryl-H, 6H), 7.00 (br, aryl-H, 4H), 5.22-3.90 (br, 4H), 3.60-2.30 (br, 16 H), 1.36 (br, t Bu, 18H), 1.31 (br, CH3, 6H), 1.06 (br, CH3, 6H).

7.3 Exemplar Polymerisation Reactions:

Ring opening copolymerisation of CHO/CO_2

[$LZn_2(OCOCF_3)_2$] (0.01 g, 0.01 mmol), CHO (1.1 mL, 11 mmol) and toluene (1.1 mL) were placed in a Schlenk tube charged with a stirrer bar, under nitrogen. The relative molar ratios of [$LZn_2(OCOCF_3)_2$]:[CHO] were 1:1000. The reaction mixture was de-gassed and then heated to 80 °C at 1 bar CO_2 pressure. After the allotted reaction time, the mixture was exposed to air and a ^{1}H NMR spectrum of the crude mixture was recorded. The CHO was removed, under vacuum, and the polymer was purified by precipitation of a THF solution into methanol.

Ring opening copolymerisation of CHO/CO_2/MEG

[$LZn_2(OCOCF_3)_2$] (0.01 g, 0.01 mmol), CHO (1.1 mL, 11 mmol), MEG (0.054 mL, 0.66 mmol) and toluene (1.1 mL) were placed in a Schlenk tube charged with a stirrer bar, under nitrogen. The relative molar ratios of [[$LZn_2(OCOCF_3)_2$]]:[CHO]:[MEG] were 1:1000:30. The reaction mixture was de-gassed and then heated to 80 °C at 1 bar CO_2 pressure. After the allotted reaction time, the mixture was exposed to air and a ^{1}H NMR spectrum of the crude

mixture was recorded. The CHO was removed, under vacuum, and the polymer was purified by precipitation of a THF solution into methanol.

Ring opening polymerisation of ε-CL.

$[LZn_2(OCOCF_3)_2]$ (0.01 g, 0.01 mmol), ε-CL (0.48 mL, 4.8 mmol) and CHO (1.1 mL, 11 mmol) were placed in a vial, charged with a stirrer bar, under nitrogen. The relative molar ratios of $[[LZn_2(OCOCF_3)_2]$ 1]/[ε-CL]/[CHO] was 1/400/1000. The reaction mixture was heated to 80 °C. After the allotted reaction time, the mixture was exposed to air and a ^1H NMR spectrum of the crude mixture was recorded. The polymer was purified by precipitation of a THF solution into methanol.

Terpolymerisation of CHO/CO_2/ε-CL

$[LZn_2(OCOCF_3)_2]$ (0.04 g, 0.04 mmol), CHO (2.2 mL, 22 mmol), ε-CL (1.97 mL, 17.6 mmol), and toluene (2.2 mL) were placed in a Schlenk tube, charged with a stirrer bar, under nitrogen. The relative molar ratios of $[[LZn_2(OCOCF_3)_2]]$:[CHO]:[ε-CL] were 1:500:400. The reaction mixture was de-gassed and then heated to 80 °C at 1 bar CO_2 pressure. After the allotted time, the CO_2 was removed by six vacuum/nitrogen cycles. The reaction was monitored by ^1H NMR spectroscopy and when the ring opening polymerisation had reached ~70 %, the crude reaction mixture was exposed to air and a ^1H NMR spectrum of the crude mixture was recorded. The CHO was removed, under vacuum, and the polymer was purified by precipitation of a THF solution into methanol.

Ring opening of polymerisation of δ-VL

$[LZn_2(Ph)_2]$ (0.02 g, 0.024 mmol), δ-VL (0.89 mL, 9.6 mmol) and iPrOH(3.96 μL, 0.048 mmol) were placed in a vial with toluene (3 mL), charged with a stirrer bar, under nitrogen. The relative molar ratios of $[[LZn_2(Ph)_2]]$/[δ-VL]/[i-PrOH] was 1/400/2. The reaction mixture was heated to 80 °C. After the allotted reaction time, the mixture was exposed to air and a ^1H

NMR spectrum of the crude mixture was recorded. The polymer was purified by precipitation of a THF solution into methanol.

Terpolymerisation of CHO/CO_2/δ-VL

[$LZn_2(Ph)_2$] (0.02 g, 0.02 mmol), CHO (2.28 mL, 24 mmol), δ-VL (0.89 mL, 9.6 mmol), and toluene (2.2 mL) were placed in a Schlenk tube, charged with a stirrer bar, under nitrogen. The relative molar ratios of [[$LZn_2(Ph)_2$]]:[CHO]:[δ-VL] were 1:1000:400. The reaction mixture was de-gassed and then heated to 80 °C at 1 bar CO_2 pressure. After the allotted time, the CO_2 was removed by six vacuum/nitrogen cycles. The reaction was monitored by ^{1}H NMR spectroscopy and when the ring opening polymerisation had reached ~70 %, the crude reaction mixture was exposed to air and a ^{1}H NMR spectrum of the crude mixture was recorded. The CHO was removed, under vacuum, and the polymer was purified by precipitation of a THF solution into methanol.

Terpolymerisation of CHO/CO_2/ε-DL

[$LZn_2(Ph)_2$] (0.02 g, 0.02 mmol), CHO (4.57 mL, 48 mmol) and ε-DL (1.72 mL, 9.6 mmol) were placed in a Schlenk tube, charged with a stirrer bar, under nitrogen. The relative molar ratios of [[$LZn_2(Ph)_2$]]:[CHO]:[ε-DL] were 1:2000:400. The reaction mixture was de-gassed and then heated to 100 °C at 1 bar CO_2 pressure. After the allotted time, the CO_2 was removed by six vacuum/nitrogen cycles. The reaction was monitored by ^{1}H NMR spectroscopy and when the ring opening polymerisation had reached ~70 %, the crude reaction mixture was exposed to air and a ^{1}H NMR spectrum of the crude mixture was recorded. The CHO was removed, under vacuum, and the polymer was purified by precipitation of a THF solution into methanol.

Terpolymerisation of CHO/CO_2/ε-CL to form a multiblock copolymer

[$LZn_2(OCOCF_3)_2$] (0.02 g, 0.02 mmol), CHO (1.78 mL, 17.6 mmol), ε-CL (0.97 mL, 8.8 mmol), and toluene (2.5 mL) were placed in a Schlenk tube, charged with a stirrer bar, under nitrogen. The relative molar ratios of [[$LZn_2(OCOCF_3)_2$]]:[CHO]:[ε-CL] were 1:800:400. The reaction mixture was de-gassed and then heated to 80 °C at 1 bar CO_2 pressure. After ~16 h, the CO_2 was removed by six vacuum/nitrogen cycles. The nitrogen atmosphere was maintained for 1 h before being replaced with carbon dioxide. After ~5 h the CO_2 was removed by six vacuum/nitrogen cycles. The nitrogen atmosphere was maintained for 1 h before the crude reaction mixture was exposed to air and a ^{1}H NMR spectrum of the crude mixture was recorded. The CHO was removed, under vacuum, and the polymer was purified by precipitation of a THF solution into methanol.

Ring opening copolymerisation of CHO and PA

[$LZn_2(Ph)_2$] (0.01 g, 0.012 mmol), PA (0.08 g, 0.57 mmol) and a stock solution of CHD (55.0 μL of a 0.43 M solution in CHO) were dissolved in CHO (0.6, 6.1mmol), under nitrogen, in a screw-cap vial, charged with a stirrer bar. The relative molar ratios of [[$LZn_2(Ph)_2$]]:[CHD]:[PA]:[CHO] were 1:2:50:500. The solution was then heated to 100 °C. After the allotted reaction time, the polymerization was terminated by cooling down to ambient temperature a ^{1}H NMR spectrum of the crude mixture was recorded. The CHO was removed, under vacuum, and the polymer was purified by precipitation of a THF solution into methanol.

Terpolymerisation of CHO/PA/CO_2

[$LZn_2(Ph)_2$] (0.01 g, 0.012 mmol), PA (0.08 g, 0.57 mmol) and a stock solution of CHD (55.0 μL of a 0.43 M solution in CHO) were dissolved in CHO (2.4 mL, 24.5 mmol), under nitrogen, in a Schlenk tube, charged with a stir bar. The relative molar ratios of [[$LZn_2(Ph)_2$]]:[CHD]:[PA]:[CHO] were 1:2:50:2000. The Schlenk was then charged with 1 atm of carbon dioxide. The solution was then heated to 100 °C, and left to react for 24 h.

Aliquots for ^{1}H NMR spectroscopy were taken during the polymerisation. After the allotted reaction time, the polymerization was terminated by cooling down to ambient temperature a ^{1}H NMR spectrum of the crude mixture was recorded. The CHO was removed, under vacuum, and the polymer was purified by precipitation of a THF solution into methanol.

Terpolymerisation of CHO/PA/CO_2/ε-CL

[$LZn_2(Ph)_2$] (0.01 g, 0.012 mmol), PA (0.08 g, 0.57 mmol), ε-CL (0.53mL, 4.6 mmol) and a stock solution of CHD (55.0 μL of a 0.43 M solution in CHO) were dissolved in CHO (1.75 mL, 17.8 mmol), under nitrogen, in a Schlenk tube, charged with a stirrer bar. The relative molar ratios of [[$LZn_2(Ph)_2$]]/[CHD]/[PA]/[CHO]/[ε-CL] were 1/2/50/1550/400.The Schlenk tube was then charged with 1 atm of carbon dioxide. The solution was heated to 100 °C. Aliquots for ^{1}H NMR were taken during the polymerisation. After the allotted time, the atmosphere was changed to nitrogen using short N_2/vacuum cycles. After the allotted reaction time, the polymerization was terminated by cooling down to ambient temperature, a ^{1}H NMR spectrum of the crude mixture was recorded. The CHO was removed, under vacuum, and the polymer was purified by precipitation of a THF solution into methanol.

Terpolymerisation of VCHO/PA/CO_2/ε-CL

[$LZn_2(Ph)_2$] (0.01 g, 0.012mmol), PA (0.08 g, 0.57 mmol), ε-CL (0.53mL, 4.6 mmol) and a stock solution of CHD (55.0 μL of a 0.43 M solution in CHO) were dissolved in VCHO (2.51 mL, 17.8 mmol), under nitrogen, in a Schlenk tube, charged with a stirrer bar. The relative molar ratios of [[$LZn_2(Ph)_2$]]/[CHD]/[PA]/[VCHO]/[ε-CL] were 1/2/50/1550/400.The Schlenk tube was then charged with 1 atm of carbon dioxide. The solution was heated to 100 °C. Aliquots for ^{1}H NMR were taken during the polymerisation. After the allotted time, the atmosphere was changed to nitrogen using short N_2/vacuum cycles. After the allotted reaction time, the polymerization was terminated by cooling down to ambient temperature, a ^{1}H NMR spectrum of the crude mixture was recorded. The VCHO was removed, under vacuum, and the polymer was purified by precipitation of a THF solution into methanol.

Terpolymerisation of VCHO/PA/CO_2/ε-DL

[$LZn_2(Ph)_2$] (0.01 g, 0.012 mmol), PA (0.08 g, 0.57 mmol), ε-DL (0.86 mL, 4.6 mmol) and a stock solution of CHD (55.0 μL of a 0.43 M solution in CHO) were dissolved in CHO (2.51 mL, 17.8 mmol), under nitrogen, in a Schlenk tube, charged with a stirrer bar. The relative molar ratios of [[$LZn_2(Ph)_2$]]/[CHD]/[PA]/[VCHO]/[ε-DL] were 1/2/50/1550/400.The Schlenk tube was then charged with 1 atm of carbon dioxide. The solution was heated to 100 °C. Aliquots for ^{1}H NMR were taken during the polymerisation. After the allotted time, the atmosphere was changed to nitrogen using short N_2/vacuum cycles. After the allotted reaction time, the polymerization was terminated by cooling down to ambient temperature, a ^{1}H NMR spectrum of the crude mixture was recorded. The VCHO was removed, under vacuum, and the polymer was purified by precipitation of a THF solution into methanol.

Terpolymerisation of CHO/PA/CO_2/LA

[$LZn_2(Ph)_2$] (0.01 g, 0.012 mmol), PA (0.08 g, 0.57 mmol), LA (0.34 g, 2.4 mmol) and a stock solution of CHD (55.0 μL of a 0.43 M solution in CHO) were dissolved in CHO (1.77 mL, 17.8 mmol), under nitrogen, in a Schlenk tube, charged with a stirrer bar. The relative molar ratios of [[$LZn_2(Ph)_2$]]/[CHD]/[PA]/[CHO]/[LA] were 1/2/50/1550/400.The Schlenk tube was then charged with 1 atm of carbon dioxide. The solution was heated to 100 °C. Aliquots for ^{1}H NMR were taken during the polymerisation. After the allotted reaction time, the polymerization was terminated by cooling down to ambient temperature, a ^{1}H NMR spectrum of the crude mixture was recorded. The CHO was removed, under vacuum, and the polymer was purified by precipitation of a THF solution into pentane.

Terpolymerisation of VCHO/PA/CO_2/LA

[$LZn_2(Ph)_2$] (0.01 g, 0.012 mmol), PA (0.08 g, 0.57 mmol), LA (0.34 g, 2.4 mmol) and a stock solution of CHD (55.0 μL of a 0.43 M solution in CHO) were dissolved in VCHO (2.51 mL, 17.8 mmol), under nitrogen, in a Schlenk tube, charged with a stir bar. The relative molar ratios of [[$LZn_2(Ph)_2$]]/[CHD]/[PA]/[VCHO]/[LA] were 1/2/50/1550/400.The Schlenk

tube was then charged with 1 atm of carbon dioxide. The solution was heated to 100 °C. Aliquots for ^{1}H NMR were taken during the polymerisation. After the allotted reaction time, the polymerization was terminated by cooling down to ambient temperature, a ^{1}H NMR spectrum of the crude mixture was recorded. The VCHO was removed, under vacuum, and the polymer was purified by precipitation of a THF solution into pentane.

Ring opening of rac-LA

[$LZn_2(Ph)_2$] (0.01 g, 0.012 mmol), was dissolved in CHO (1 mL, 10 mmol) in a Schlenk tube, charged with a stirrer bar, under nitrogen. A solution of *rac*-LA (0.34 g, 2.4 mmol) dissolved in CHO (1.26 mL, 13 mmol) at 100 °C, was injected. The relative molar ratios of [[$LZn_2(Ph)_2$]]/[CHD]/[PA]/[CHO]/[LA] were 1/2000/200. Aliquots for ^{1}H NMR were taken during the polymerisation. After the allotted reaction time, the polymerization was terminated by cooling down to ambient temperature. A ^{1}H NMR spectrum of the crude mixture was recorded. The CHO was removed, under vacuum, and the polymer was purified by precipitation of a THF solution into pentane.

Terpolymerisation of CHO/CO_2/LA (1 atm)

[$LZn_2(Ph)_2$] (0.01 g, 0.012 mmol), was dissolved in CHO (1 mL, 10 mmol) in a Schlenk tube, charged with a stirrer bar, under nitrogen. The Schlenk tube was then charged with 1 atm of carbon dioxide and heated to 100 °C. A solution of *rac*-LA (0.34 g, 2.4 mmol) dissolved in CHO (1.26 ml, 13 mmol) at 100 °C, was injected. The relative molar ratios of [[$LZn_2(Ph)_2$]]/[CHD]/[PA]/[CHO]/[LA] were 1/2000/200. Aliquots for ^{1}H NMR were taken during the polymerisation. After the allotted reaction time, the polymerization was terminated by cooling down to ambient temperature. A ^{1}H NMR spectrum of the crude mixture was recorded. The CHO was removed, under vacuum, and the polymer was purified by precipitation of a THF solution into pentane.

Terpolymerisation of CHO/CO_2/LA (20 atm)

A 25 mL Parr reactor was dried in an oven for 16 h at 140 °C. The reactor was then cooled to room temperature by venting CO_2 through it, three times. [$LZn_2(Ph)_2$] (0.03 g, 0.036 mmol) was dissolved in CHO (3 mL, 32 mmol), under nitrogen at 80 °C. LA (0.52 g, 3.6 mmol) was dissolved in CHO (3.85 mL, 39 mmol) under nitrogen, at 80 °C. The relative molar ratios of [[$LZn_2(Ph)_2$]]:[CHO]:[LA] were 1:2000:100. The two mixtures was transferred to the 25 mL Parr reactor and charged with 20 bar of CO_2 and stirred. The reactor was then heated to 80 °C for 16 h. The reactor was cooled to room temperature by placing it in ice and then vented slowly to prevent CHO evaporation. A ^{1}H NMR spectrum of the crude reaction mixture was recorded. The crude mixture was then taken up in DCM and poured into a Schlenk tube and evaporated to dryness. The resulting polymer was purified by precipitation of a THF solution into methanol.

7.4 Other Reactions

Diisocyanate coupling of polymers

The polymer polyol (2.75 g, 0.77 mmol of OH endgroups) was dissolved in toluene (~10 mL). Methylene diphenyl diisocyanate (0.19 g, 0.77 mmol) and tin(II) 2-ethylhexanoate (0.027 g, 0.067 mmol) were added to the polymer solution. The mixture was heated to 60 °C for 2 h. The mixture was then poured into cold methanol to precipitate the polymer.

^{31}P NMR end group analysis

The preparation procedure carried out followed that reported by Spyros *et al*.[7] A stock solution was prepared by dissolving bisphenol A (BPA) (400mg) and of [$Cr(acac)_3$] (5.5 mg) in of pyridine (10mL). A polymer solution in $CDCl_3$ (100 mg/mL) was then prepared. The polymer solution (400 μL) and the stock solution (40 μL) were mixed in an NMR tube. Thereafter, excess 2-chloro-4,4,5,5-tetramethyl dioxaphospholane (40 μL) was transferred

into the NMR tube. The mixture was allowed to react for at least 6 h, before the ^{31}P NMR spectrum was measured.

7.5 NMR Spectra of Polymers

PCHC

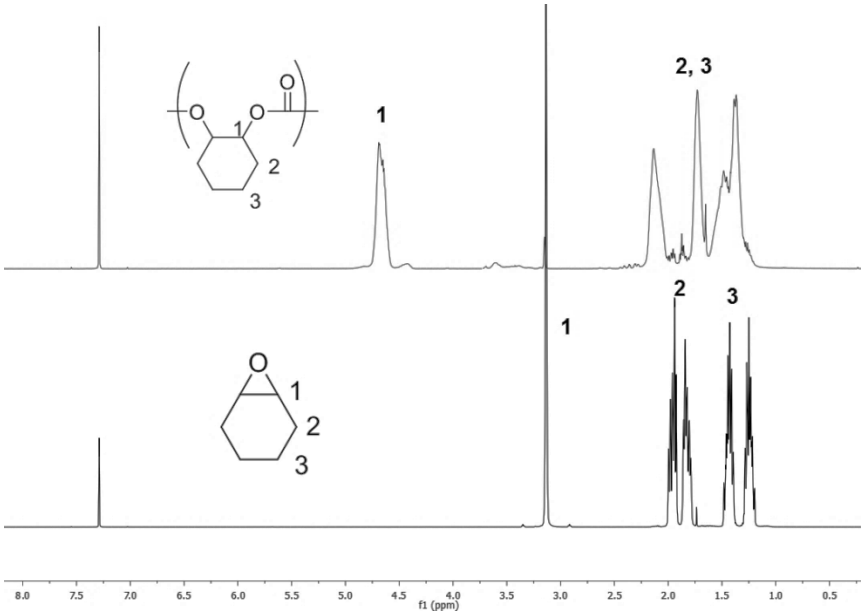

The conversion of PCHC was calculated from the comparison of the relative integrals of the methine protons (1) of CHO at 3.10 ppm and the methine protons (1) of PCHC at 4.65 ppm.

PVCHC

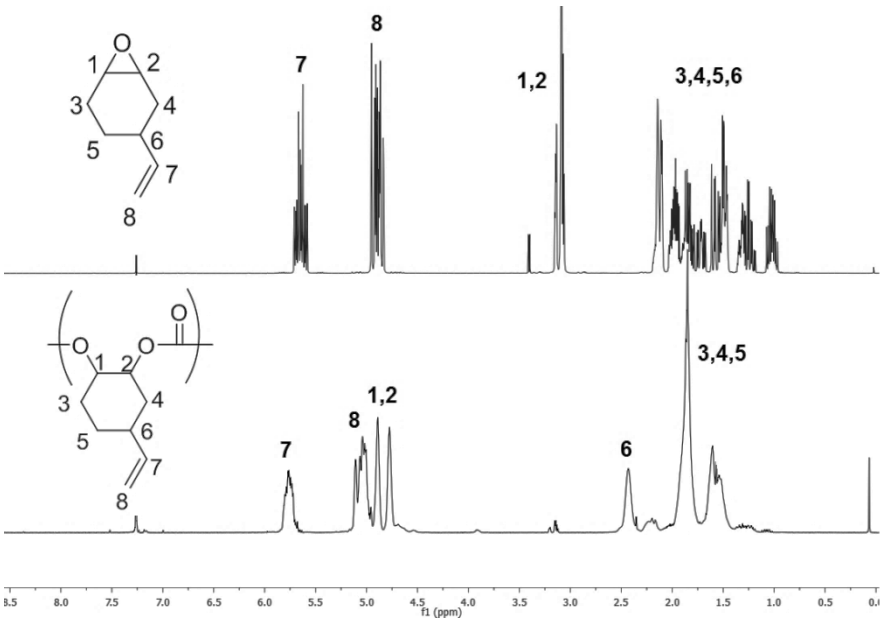

The conversion of PVCHC was calculated from the comparison of the relative integrals of the methine protons (1,2) of VCHO at 3.10 ppm and the methine protons (1) of PVCHC at 4.65 ppm.

PCL

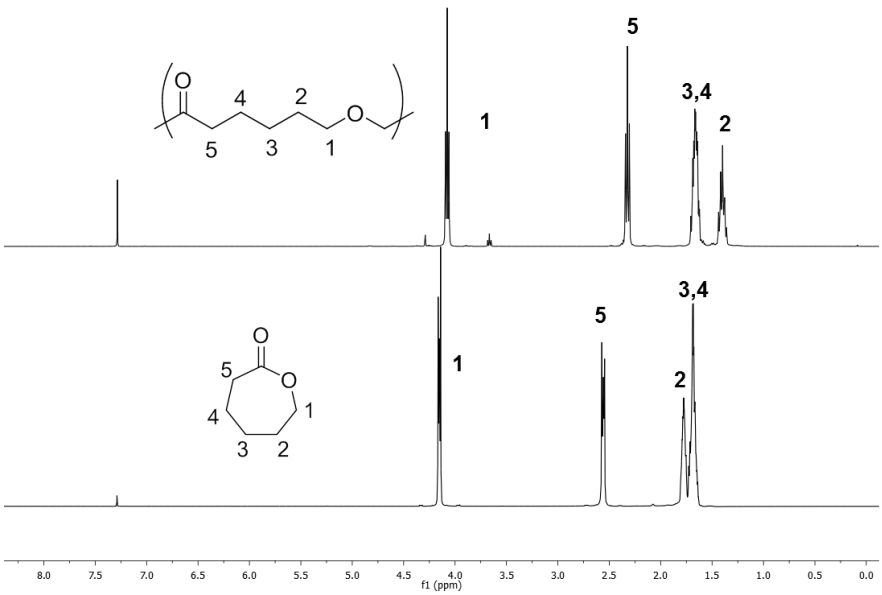

The conversion of PCL was calculated from the comparison of the relative ratios of the methylene protons (1) in ε-CL at 4.20 ppm and the methylene protons (1) in PCL at 4.05 ppm

PVL

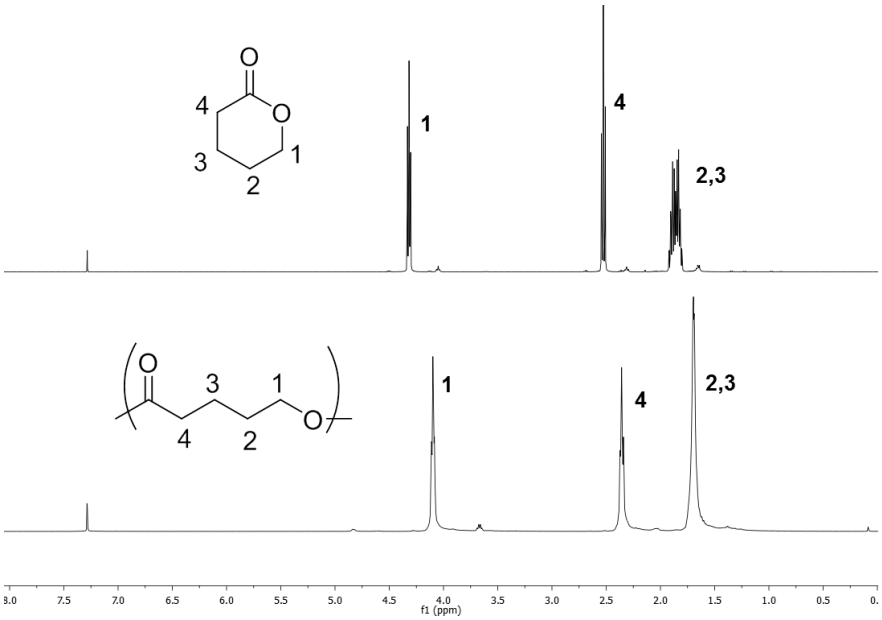

The conversion of PVL was calculated from the comparison of the relative ratios of the methylene protons (1) in δ-VL at 4.28 ppm and the methylene protons (1) in PVL at 4.0 ppm

PDL

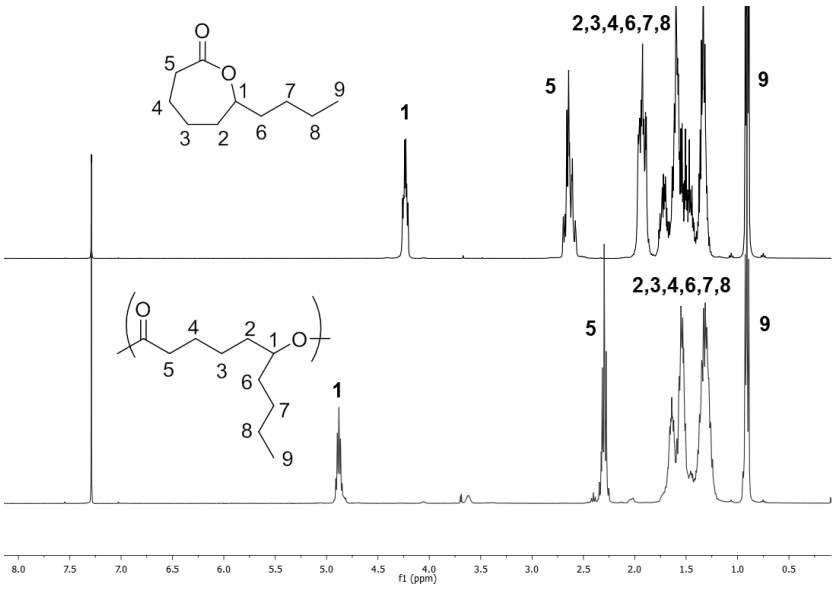

The conversion of PDL was calculated from the comparison of the relative ratios of the methylene protons (1) in ε-DL at 4.20 ppm and the methylene protons (1) in PDL at 4.85 ppm

PCHPE

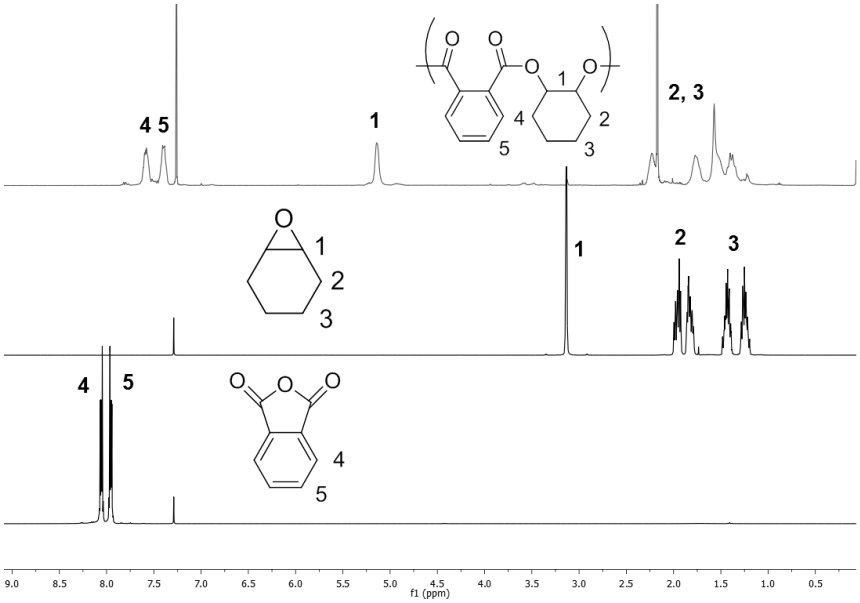

The conversion of PCHPE was calculated from the comparison of the relative ratios of the aryl protons of PA at 8.50 and 7.95 ppm and the aryl protons of PCHPE at 7.55 and 7.35 ppm

PVCHPE

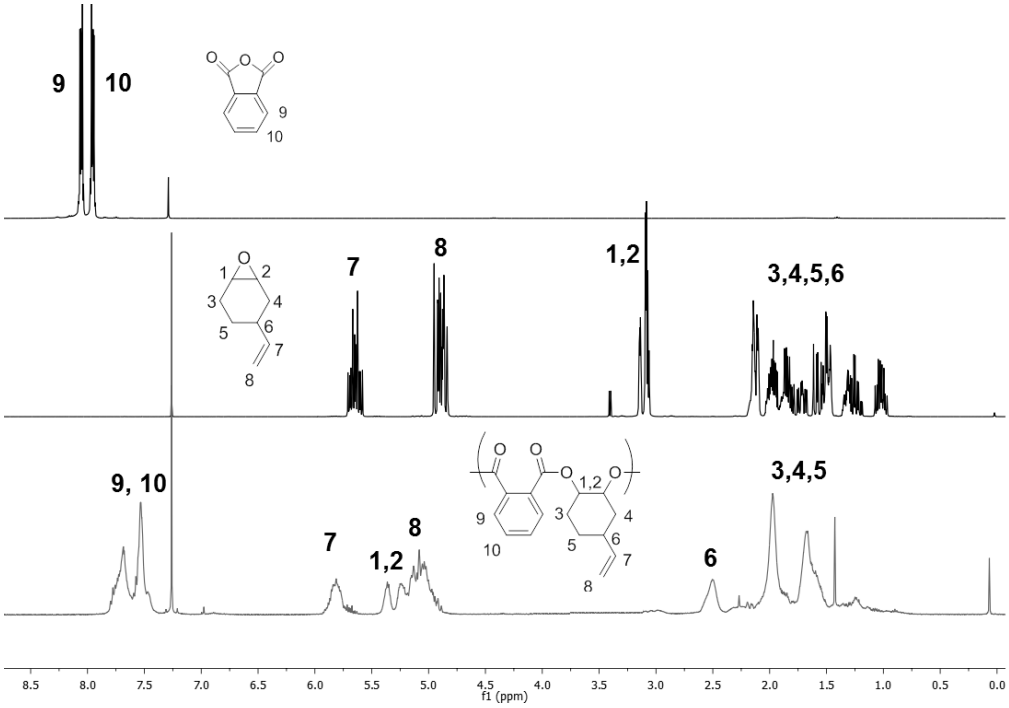

The conversion of PVCHPE was calculated from the comparison of the relative ratios of the aryl protons of PA at 8.50 and 7.95 ppm and the aryl protons of PVCHPE at 7.70 and 7.54 ppm

PLA

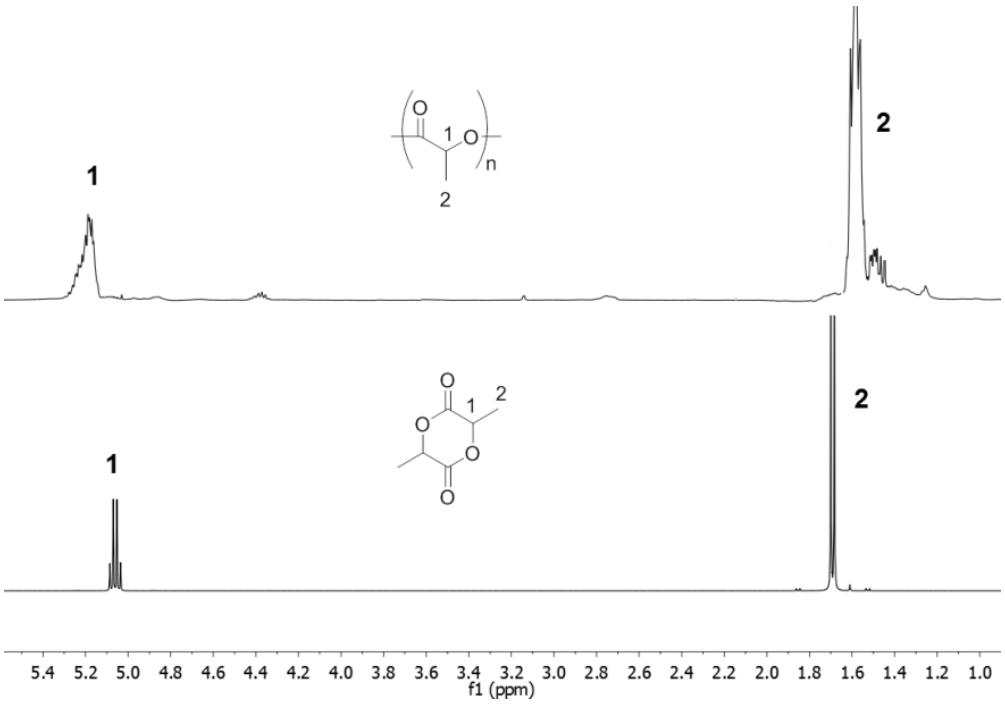

The conversion of PLA was calculated from the comparison of the relative ratios of the methine proton of LA at 5.03 ppm and the methine proton of PLA at 5.16 ppm.

7.6 References

(1) Save, M.; Schappacher, M.; Soum, A. *Macromol. Chem. Phys.* **2002**, *203*, 889.

(2) Zhu, Y.; Romain, C.; Williams, C. K. *J. Am. Chem. Soc.* **2015**, *137*, 12179.

(3) Kowalski, A.; Duda, A.; Penczek, S. *Macromolecules* **1998**, *31*, 2114.

(4) Kember, M. R.; Knight, P. D.; Reung, P. T. R.; Williams, C. K. *Angew. Chem. Int. Ed.* **2009**, *48*, 931.

(5) Buchard, A.; Kember, M. R.; Sandeman, K. G.; Williams, C. K. *Chem. Commun.* **2011**, *47*, 212.

(6) Kember, M. R.; Copley, J.; Buchard, A.; Williams, C. K. *Polym. Chem.* **2012**, *3*, 1196.

(7) Spyros, A.; Argyropoulos, D. S.; Marchessault, R. H. *Macromolecules* **1997**, *30*, 327.

Appendix

Appendix A – Chapter 1

JOHN WILEY AND SONS LICENSE TERMS AND CONDITIONS

Sep 02, 2016

This Agreement between shyeni paul ("You") and John Wiley and Sons ("John Wiley and Sons") consists of your license details and the terms and conditions provided by John Wiley and Sons and Copyright Clearance Center.

License Number	3930781088058
License date	Aug 16, 2016
Licensed Content Publisher	John Wiley and Sons
Licensed Content Publication	Wiley oBooks
Licensed Content Title	Carbon Dioxide: Utilization Options to Reduce its Accumulation in the Atmosphere
Licensed Content Author	Michele Aresta
Licensed Content Date	Jan 25, 2010
Licensed Content Pages	13
Type of use	Dissertation/Thesis
Requestor type	University/Academic
Format	Print and electronic
Portion	Figure/table
Number of figures/tables	1
Original Wiley figure/table number(s)	Figure 1.8
Will you be translating?	No
Title of your thesis / dissertation	Switchable Catalysis to make novel copolymers
Expected completion date	Oct 2016
Expected size (number of pages)	250
Requestor Location	shyeni paul 14 Chelwood Court, Westbridge ROad London, SW11 3NH United Kingdom Attn: shyeni paul

Publisher Tax ID	EU826007151
Billing Type	Invoice
Billing Address	shyeni paul 14 Chelwood Court, Westbridge ROad London, United Kingdom SW11 3NH Attn: shyeni paul
Total	0.00 GBP

Terms and Conditions

TERMS AND CONDITIONS

This copyrighted material is owned by or exclusively licensed to John Wiley & Sons, Inc. or one of its group companies (each a"Wiley Company") or handled on behalf of a society with which a Wiley Company has exclusive publishing rights in relation to a particular work (collectively "WILEY"). By clicking "accept" in connection with completing this licensing transaction, you agree that the following terms and conditions apply to this transaction (along with the billing and payment terms and conditions established by the Copyright Clearance Center Inc., ("CCC's Billing and Payment terms and conditions"), at the time that you opened your RightsLink account (these are available at any time athttp://myaccount.copyright.com).

Figure A1: Permission to reproduce figure 1.8 from 'Carbon Dioxide: Utilization Options to Reduce its Accumulation in the Atmosphere' 2010, Michele Aresta.

Appendix B - Chapter 2

Figure A2: ^{1}H NMR spectrum of PCHC ($CDCl_3$) (Table 2.1, Run 3). It is notable that there are no signals for any ring-opened caprolactone species, 4.0 ppm, consistent with the selective formation of polycarbonate under these conditions.

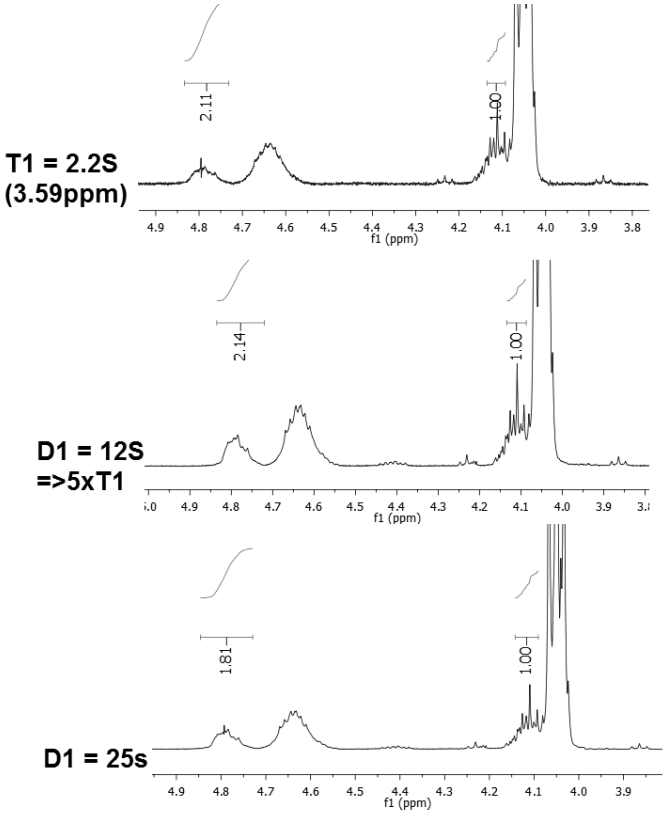

Figure A3: Excerpts of ^{1}H NMR spectra of PCHC-PCL-PCHC (C2, Table 2.4, Run 4), with different relaxation times. Comparison of the integrals of the peaks for the carbonate and ester junction (4.85 and 4.11 ppm respectively) shows little change.

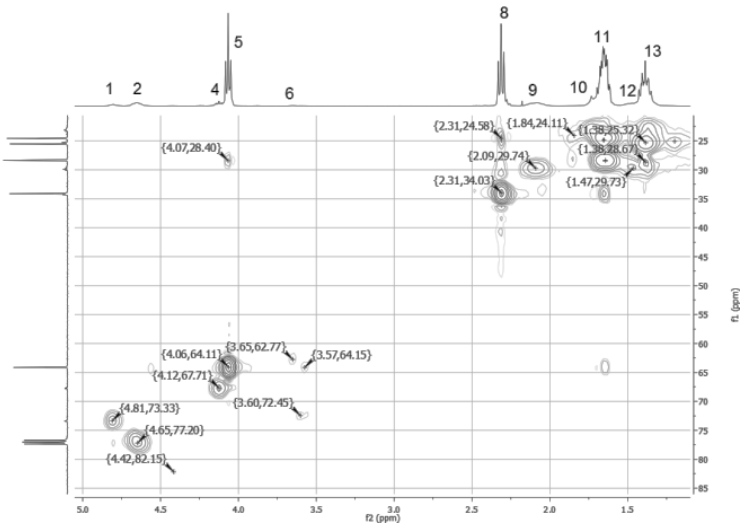

Figure A4: HSQC spectra ($CDCl_3$) of PCL-PCHC-PCL (C2, Table 2.4, Run 5)

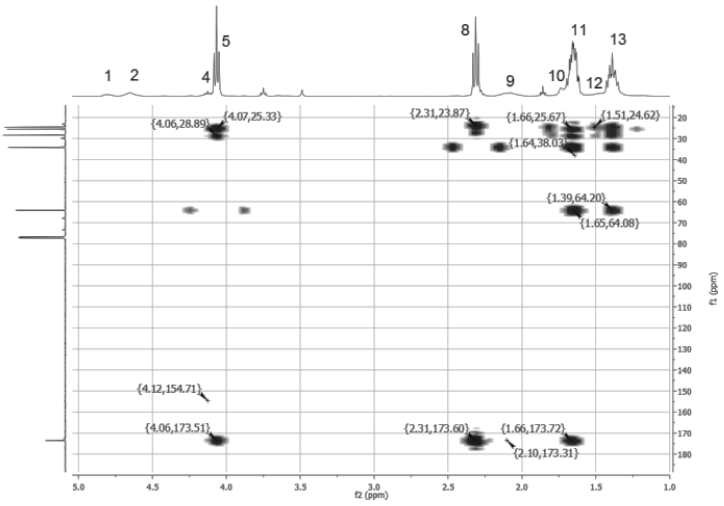

Figure A5: HMBC spectra ($CDCl_3$) of PCL-PCHC-PCL (C2, Table 2.4, Run 5)

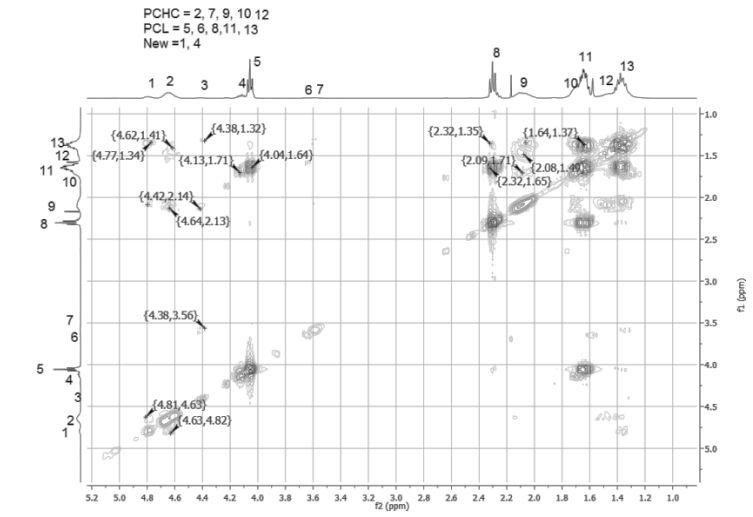

Figure A6: COSY spectrum ($CDCl_3$) of PCL-PCHC-PCL (C2, Table 2.4, Run 5)

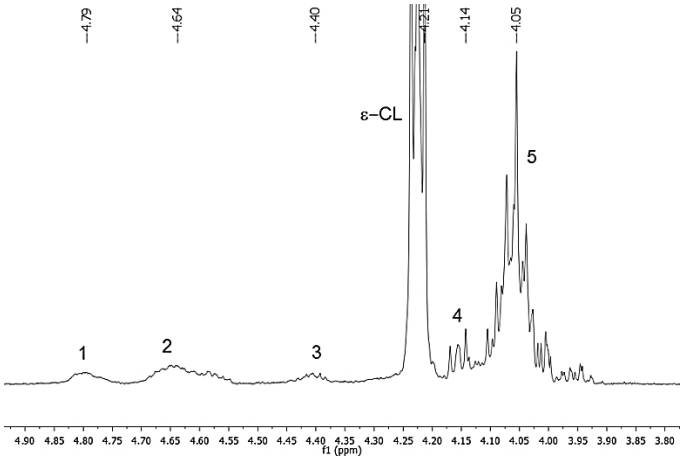

Figure A7: ^{1}H NMR spectrum of the filtrate from the purification of PCL-PCHC-PCL. Peaks are present at 4.65 ppm (2) and 4.055 ppm (5) corresponding to PCHC and PCL as well as at 4.79 (1) and 4.11ppm (4) which correspond to the carbonate and ester junction units. This indicates that the majority of material removed by fractionation is small block copolymer chains.

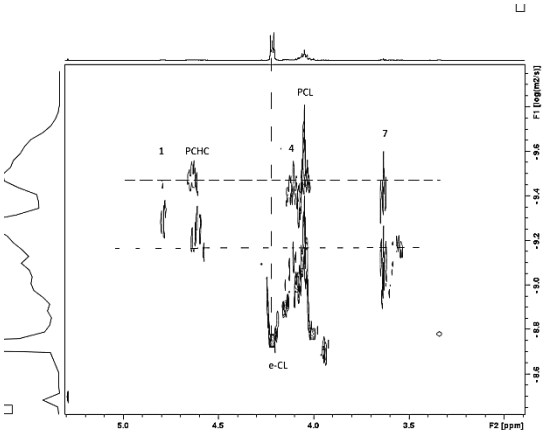

Figure A8: ^{1}H DOSY NMR spectra of the filtrate from the purification of PCL-PCHC-PCL. Several species are present as there are several diffusion coefficents. However all the species contain both PCHC and PCL.

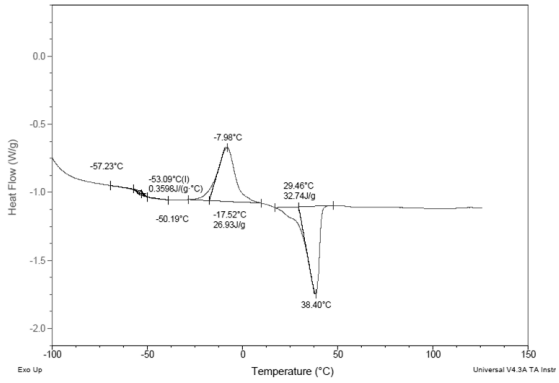

Figure A9: A representative DSC thermogram (third heating cycle) of PCL-PCHC-PCL (Table 2.4, run 5).

JOHN WILEY AND SONS LICENSE TERMS AND CONDITIONS

Sep 02, 2016

This Agreement between shyeni paul ("You") and John Wiley and Sons ("John Wiley and Sons") consists of your license details and the terms and conditions provided by John Wiley and Sons and Copyright Clearance Center.

License Number	3924140611074
License date	Aug 08, 2016
Licensed Content Publisher	John Wiley and Sons
Licensed Content Publication	Angewandte Chemie International Edition
Licensed Content Title	Chemoselective Polymerization Control: From Mixed-Monomer Feedstock to Copolymers
Licensed Content Author	Charles Romain,Charlotte K. Williams
Licensed Content Date	Jan 22, 2014
Licensed Content Pages	4
Type of use	Dissertation/Thesis
Requestor type	University/Academic
Format	Print and electronic
Portion	Figure/table
Number of figures/tables	1
Original Wiley figure/table number(s)	Figure S3
Will you be translating?	No
Title of your thesis / dissertation	Switchable Catalysis to make novel copolymers
Expected completion date	Oct 2016
Expected size (number of pages)	250
Requestor Location	shyeni paul 14 Chelwood Court, Westbridge ROad London, SW11 3NH United Kingdom Attn: shyeni paul
Publisher Tax ID	EU826007151
Billing Type	Invoice
Billing Address	shyeni paul 14 Chelwood Court, Westbridge ROad London, United Kingdom SW11 3NH Attn: shyeni paul
Total	0.00 EUR
Terms and Conditions	

TERMS AND CONDITIONS

particular work (collectively "WILEY"). By clicking "accept" in connection with completing this licensing transaction, you agree that the following terms and conditions apply to this transaction (along with the billing and payment terms and conditions established by the Copyright Clearance Center Inc., ("CCC's Billing and Payment terms and conditions"), at the time that you opened your RightsLink account (these are available at any time athttp://myaccount.copyright.com).

Figure A10: Permission to reproduce figure S3 from 'Chemoselective Polymerization Control: From Mixed-Monomer Feedstock to Copolymers' Angewandte Chemie International Edition 2014, Vol: 53, Pages: 1607-1610

Title:	Tailored Living Block Copolymerization: Multiblock Poly(cyclohexene carbonate)s with Sequence Control
Author:	Jeung Gon Kim, Christina D. Cowman, Anne M. LaPointe, et al
Publication:	Macromolecules
Publisher:	American Chemical Society
Date:	Mar 1, 2011

Logged in as:
shyeni paul
LOGOUT

PERMISSION/LICENSE IS GRANTED FOR YOUR ORDER AT NO CHARGE

This type of permission/license, instead of the standard Terms & Conditions, is sent to you because no fee is being charged for your order. Please note the following:

- Permission is granted for your request in both print and electronic formats, and translations.
- If figures and/or tables were requested, they may be adapted or used in part.
- Please print this page for your records and send a copy of it to your publisher/graduate school.
- Appropriate credit for the requested material should be given as follows: "Reprinted (adapted) with permission from (COMPLETE REFERENCE CITATION). Copyright (YEAR) American Chemical Society." Insert appropriate information in place of the capitalized words.
- One-time permission is granted only for the use specified in your request. No additional uses are granted (such as derivative works or other editions). For any other uses, please submit a new request.

If credit is given to another source for the material you requested, permission must be obtained from that source.

Figure A11: Permission to reproduce figure 3 from‘Tailored Living Block Copolymerization: Multiblock Poly(cyclohexene carbonate)s with Sequence Control’ Macromolecules, 2011, 44 (5), pp 1110–1113

JOHN WILEY AND SONS LICENSE TERMS AND CONDITIONS

Sep 02, 2016

This Agreement between shyeni paul ("You") and John Wiley and Sons ("John Wiley and Sons") consists of your license details and the terms and conditions provided by John Wiley and Sons and Copyright Clearance Center.

License Number	3939260475515
License date	Aug 31, 2016
Licensed Content Publisher	John Wiley and Sons
Licensed Content Publication	Angewandte Chemie International Edition
Licensed Content Title	Chemoselective Polymerization Control: From Mixed-Monomer Feedstock to Copolymers
Licensed Content Author	Charles Romain,Charlotte K. Williams
Licensed Content Date	Jan 22, 2014
Licensed Content Pages	4
Type of use	Dissertation/Thesis
Requestor type	University/Academic
Format	Print and electronic
Portion	Figure/table
Number of figures/tables	1
Original Wiley figure/table number(s)	figure 1
Will you be translating?	No
Title of your thesis / dissertation	Switchable Catalysis to make novel copolymers
Expected completion date	Oct 2016
Expected size (number of pages)	250

Requestor Location	shyeni paul 14 Chelwood Court, Westbridge ROad London, SW11 3NH United Kingdom Attn: shyeni paul
Publisher Tax ID	EU826007151
Billing Type	Invoice
Billing Address	shyeni paul 14 Chelwood Court, Westbridge ROad London, United Kingdom SW11 3NH Attn: shyeni paul
Total	0.00 USD

Terms and Conditions

TERMS AND CONDITIONS

This copyrighted material is owned by or exclusively licensed to John Wiley & Sons, Inc. or one of its group companies (each a"Wiley Company") or handled on behalf of a society with which a Wiley Company has exclusive publishing rights in relation to a particular work (collectively "WILEY"). By clicking "accept" in connection with completing this licensing transaction, you agree that the following terms and conditions apply to this transaction (along with the billing and payment terms and conditions established by the Copyright Clearance Center Inc., ("CCC's Billing and Payment terms and conditions"), at the time that you opened your RightsLink account (these are available at any time athttp://myaccount.copyright.com).

Figure A12: Permission to reproduce figure 1 from ‘Chemoselective Polymerization Control: From Mixed-Monomer Feedstock to Copolymers’ Angewandte Chemie International Edition 2014, Vol: 53, Pages: 1607-1610

Species	Absorption /cm^{-1}
PCHC	1010; 100; 1240; 1767; 935; 1275; 1823
PVCHC	1264
PA	1857; 1800-1770; 1790
PCHPE	1727; 1070; 1720-1740; 1065-1068; 1775
PVCHPE	1070
ε-CL	694
PCL	1190; 1176; 1760
δ-VL	1085
PVL	1186
ε-DL	1015; 1735
PDL	1190
LA	
PLA	1180; 1191
CO_2	2340

Figure A13: Table showing the absoprtions used to moniter different species when using the ATR-IR pectroscopy.

Appendix B – Chapter 3

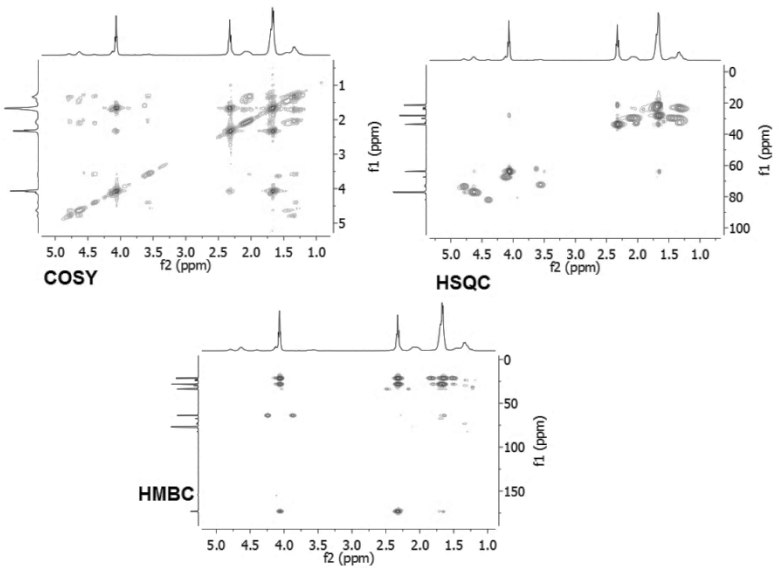

Figure A13: COSY, HSQC and HMBC NMR spectra of PVL-PCHC-PVL (C3, Table 3.4, Run 2)

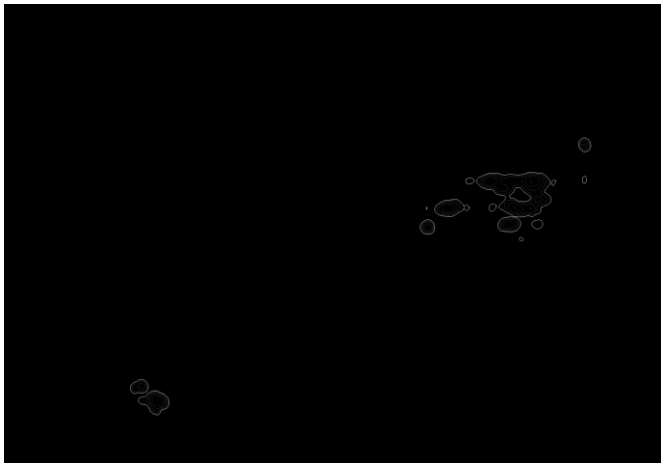

Figure A14: HSQC NMR spectra of PDL-PCHC-PDL (C3, Table 3.5, Run 1)

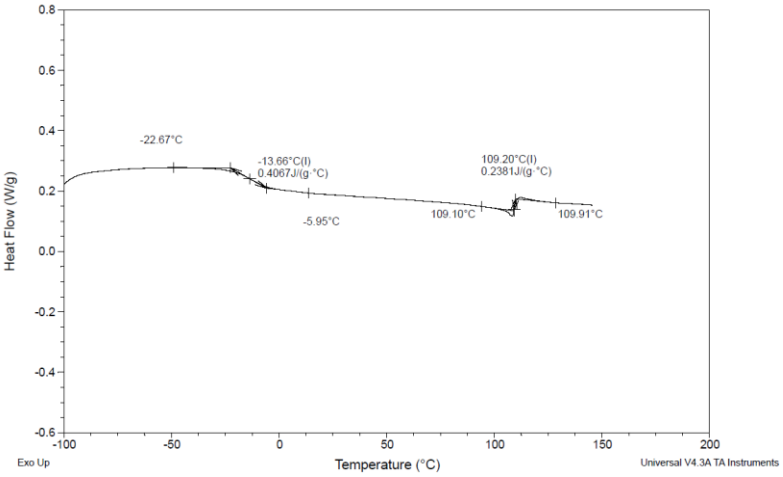

Figure A15: DSC plot of PVL-PCHC-PVL (C3, Table 3.6, Run 5)

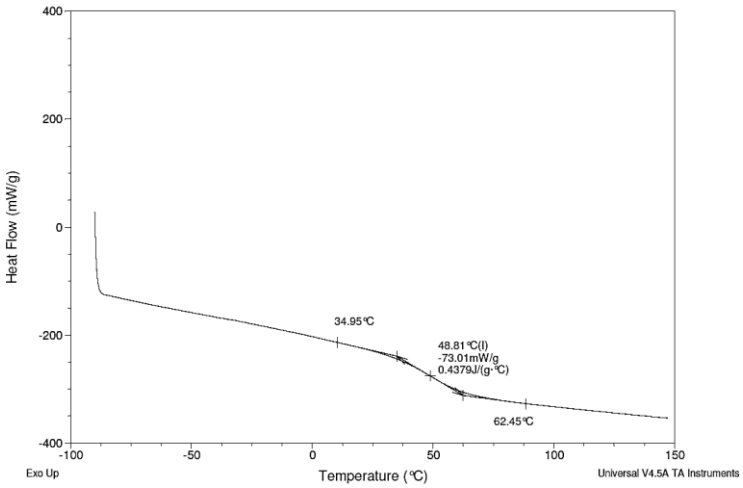

Figure A16: DSC Plot of PDL-PCHC-PDL (C3, Table 3.5, Run 7)

Appendix C – Chapter 4

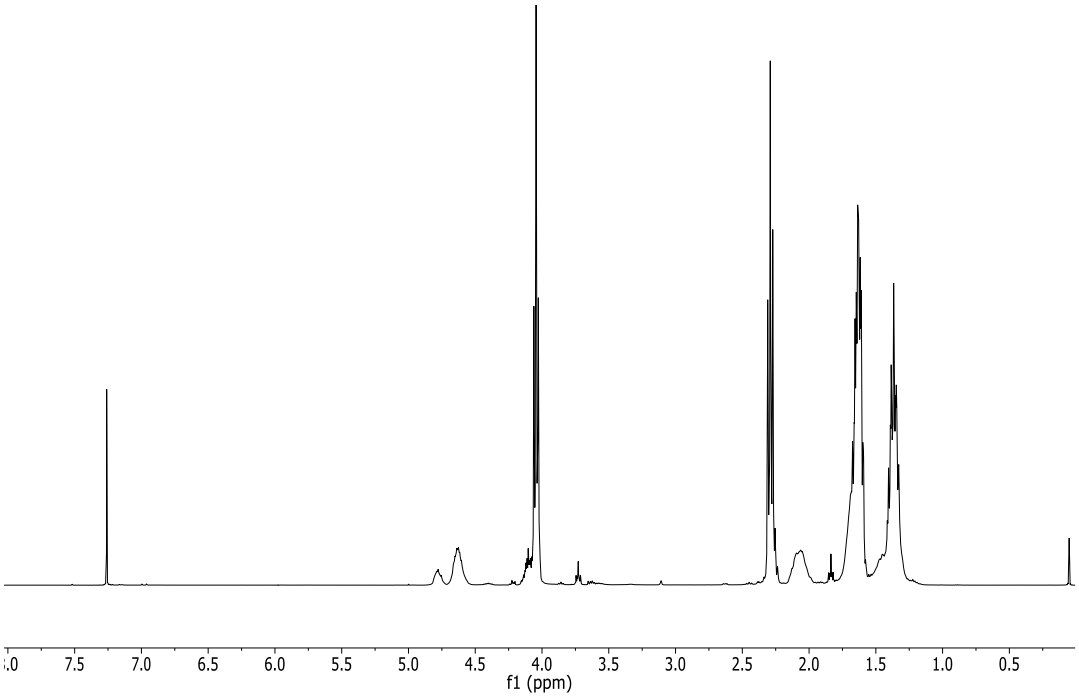

Figure A17: ^{1}H NMR of the PCHC-PCL multiblock copolymer

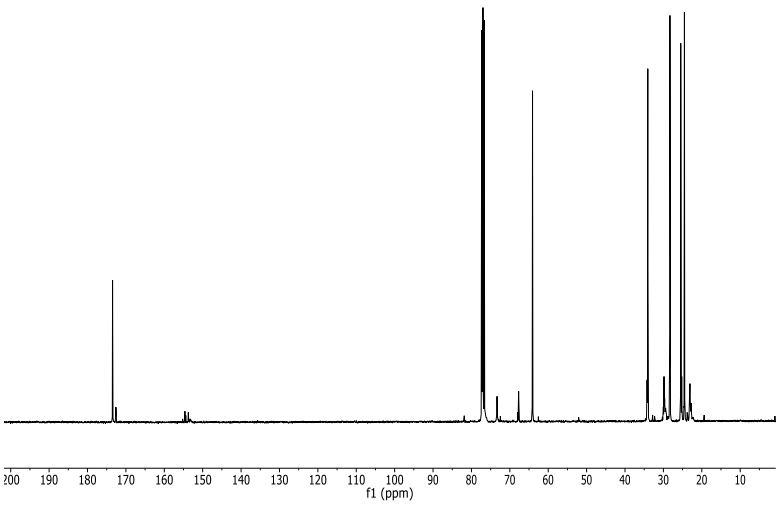

Figure A18: ^{13}C {^{1}H} NMR of the PCHC-PCL multiblock copolymer

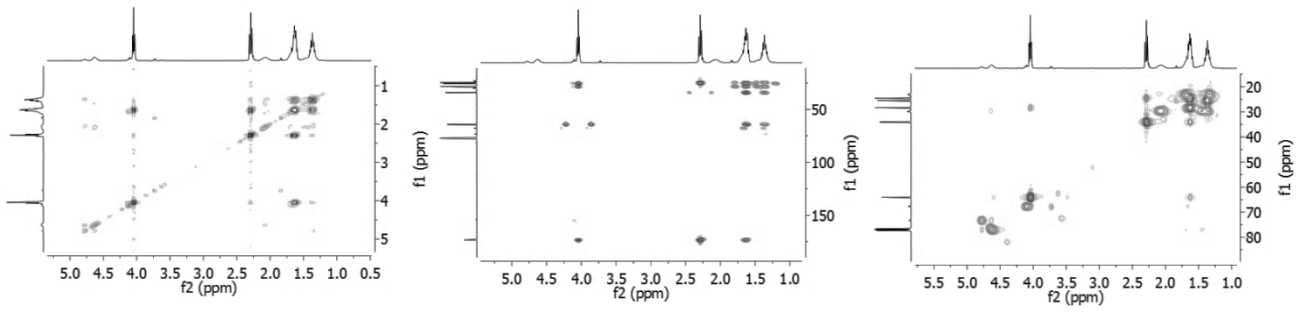

Figure A19: COSY, HSQC and HMBC NMR spectra of the PCHC-PCL multiblock copolymer

Appendix D – Chapter 5

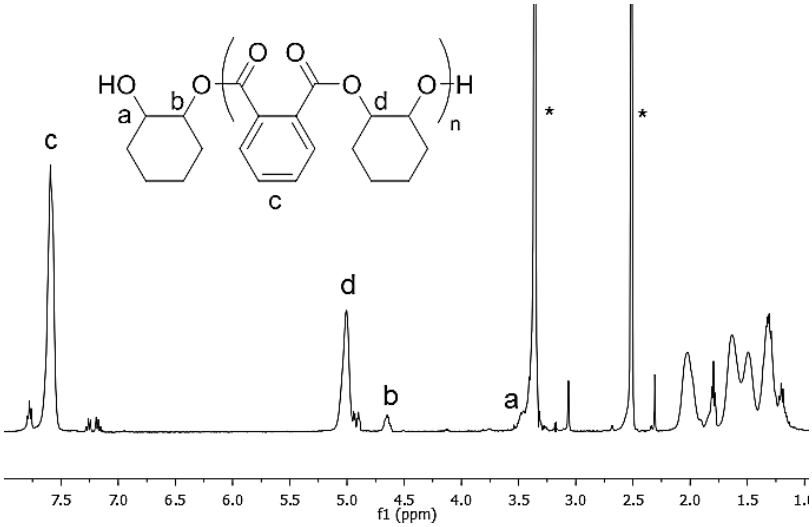

Figure A20: ^{1}H NMR (DMSO) of PCHPE, synthesised using [$LZn_2(OCOCF_3)_2$]

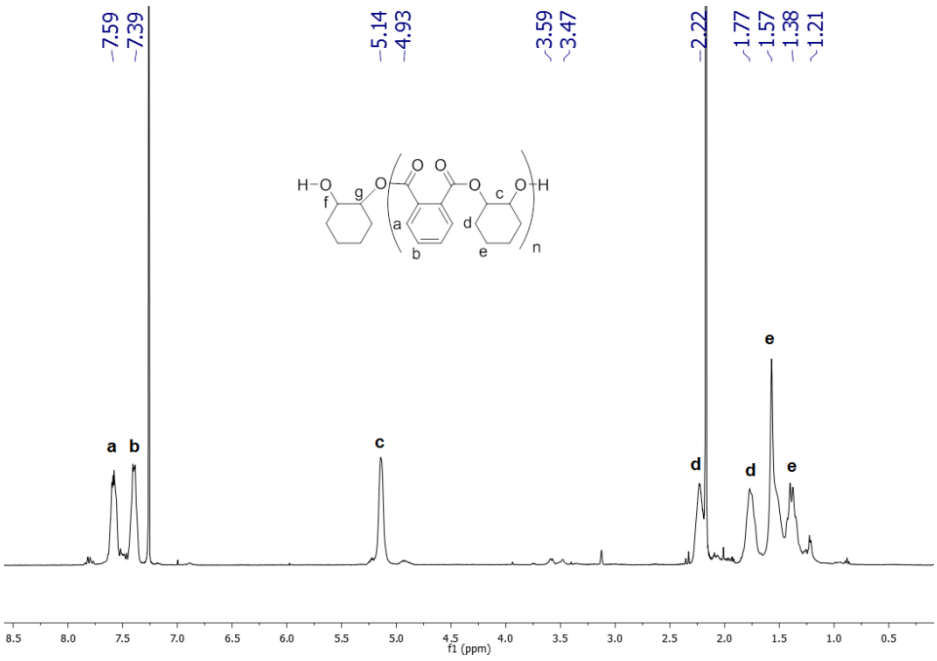

Figure A21: ^{1}H NMR ($CDCl_3$) of PCHPE, synthesised using [$LZn_2(Ph)_2$]

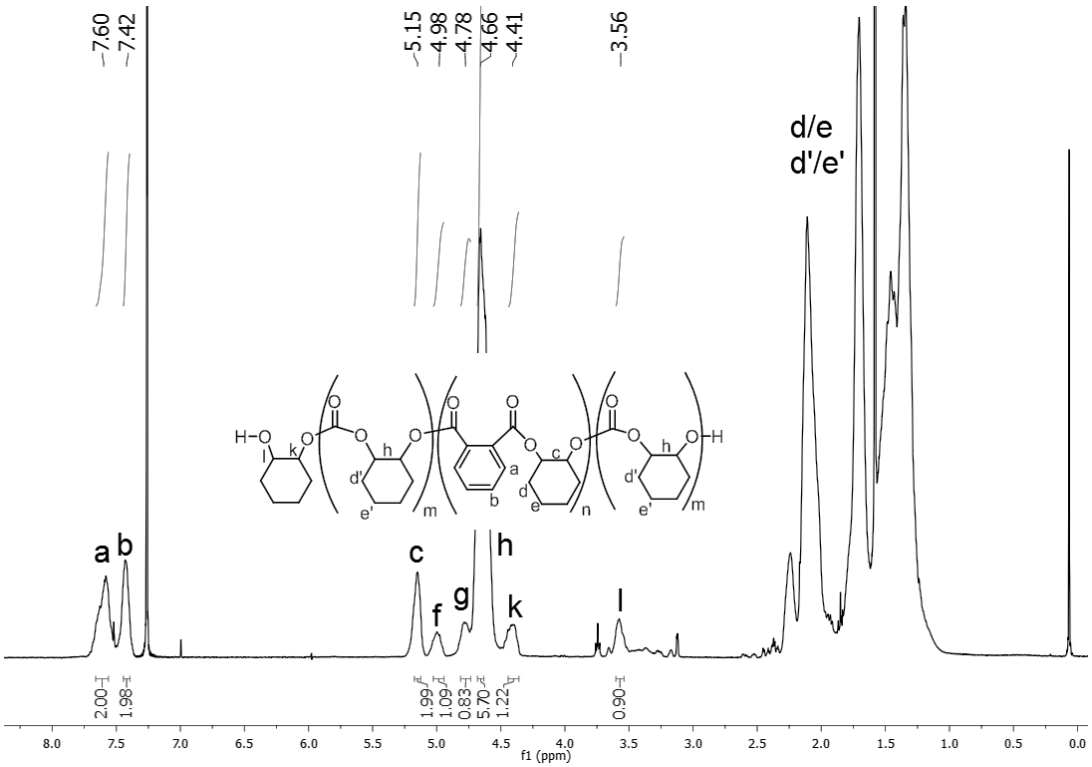

Figure A22: ^{1}H NMR spectrum of Triblock poly (carbonate-*b*-ester-*b*-carbonate) from the terpolymerisation of PA/CHO/CO_2 using [$LZn_2(Ph)_2$] and CHD.

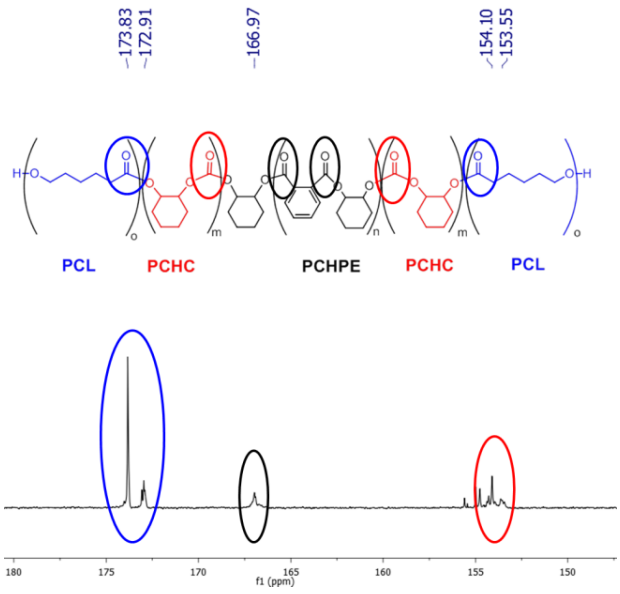

Figure A23: $^{13}C\{^{1}H\}$ of the pentablock copolymer synthesised according to C5, Table 5.2, Run 1.

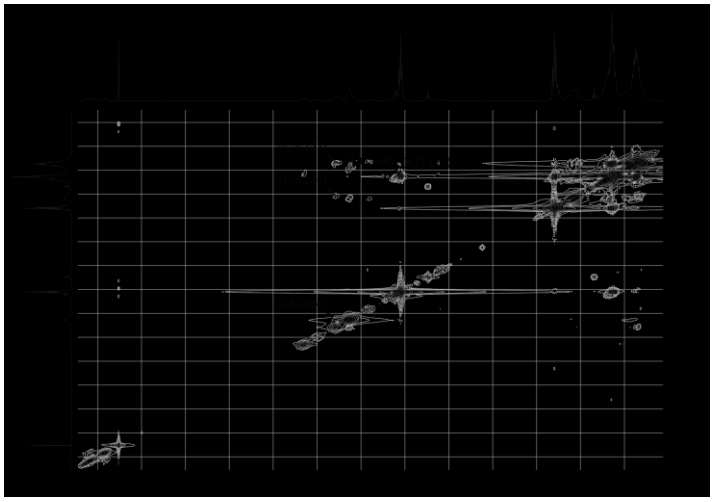

Figure A24: COSY spectrum of the pentablock copolymer synthesised according to C5, Table 5.2, Run 1.

Figure A25: HSQC spectrum of the pentablock copolymer synthesised according to C5, Table 5.2, Run 1.

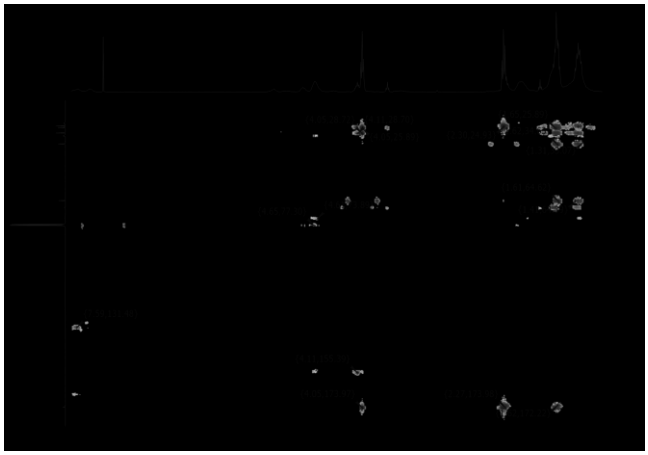

Figure A26: HMBC spectrum of the pentablock copolymer synthesised according to C5, Table 5.2, Run 1.

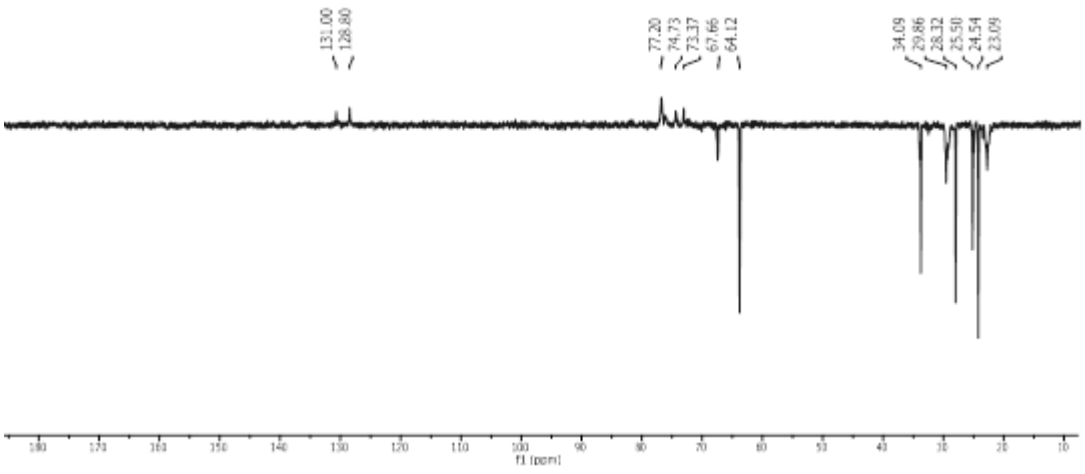

Figure A27: ^{135}DEPT spectrum of the pentablock copolymer synthesised according to C5, Table 5.1, Run 1.

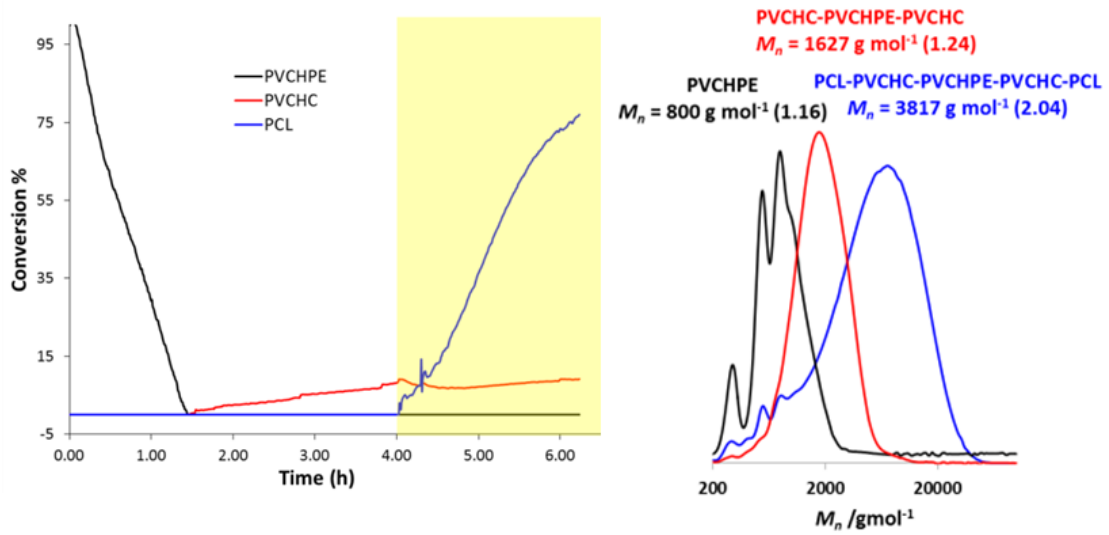

Figure A28: Left: Plot of conversion *versus* time for the formation of the pentablock copolymers (C5, Table 5.2, Run 2). Right: SEC analysis.

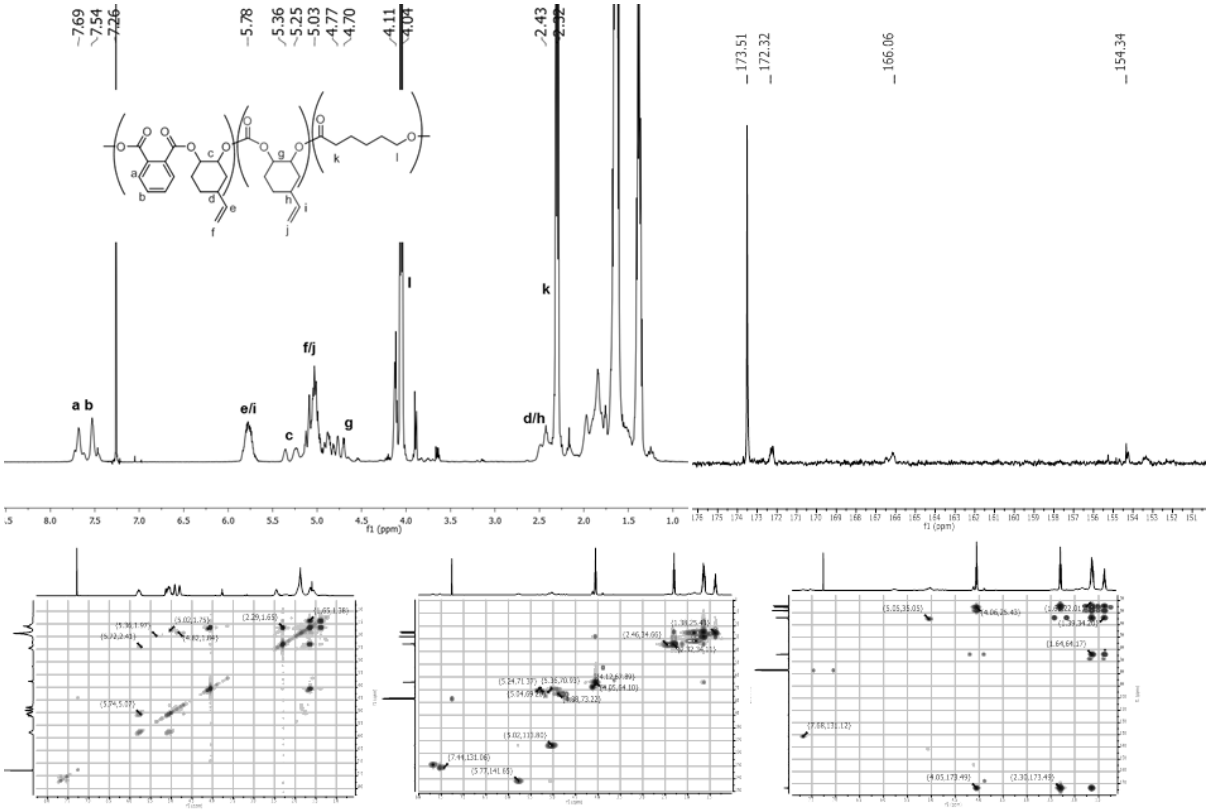

Figure A29: NMR spectra of the pentablock copolymer synthesised according to C5, Table 5.2, Run 2

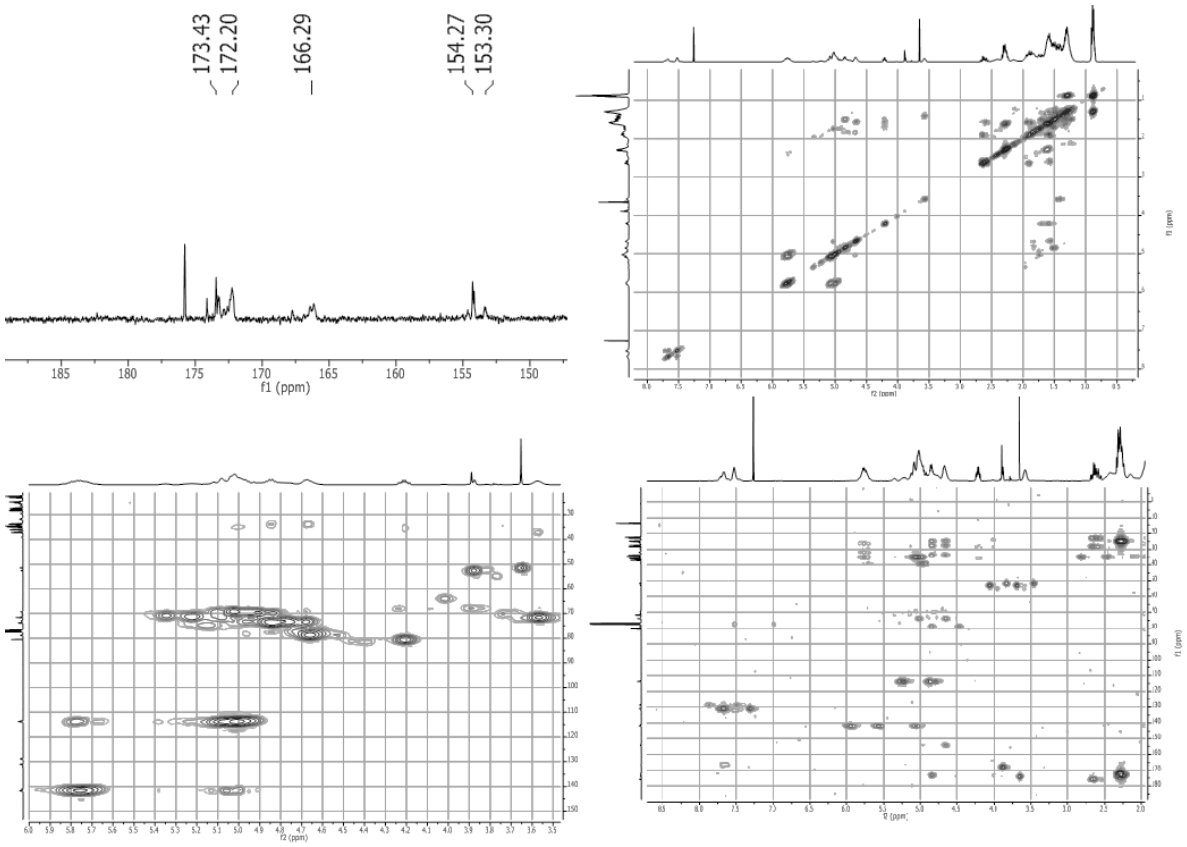

Figure A30: NMR spectra of the pentablock copolymer synthesised according to C5, Table 5.2, Run 3

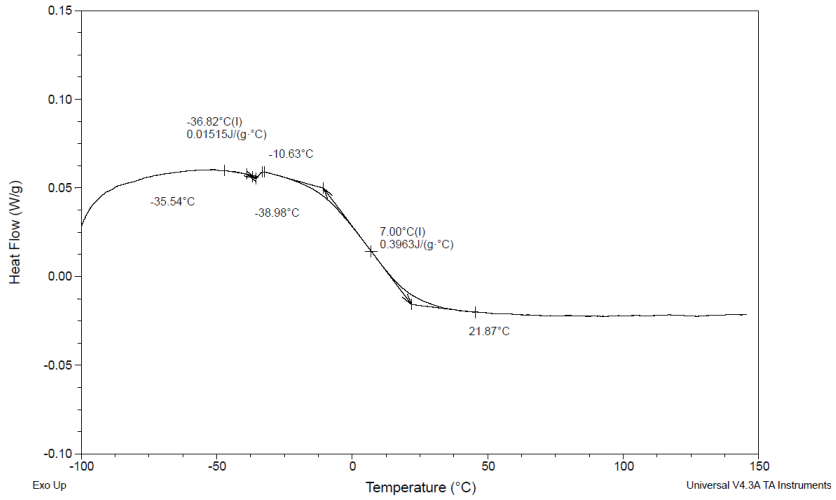

Figure A31: DSC plot of the pentablock copolymer synthesised according to C5, Table 5.3, Run 1

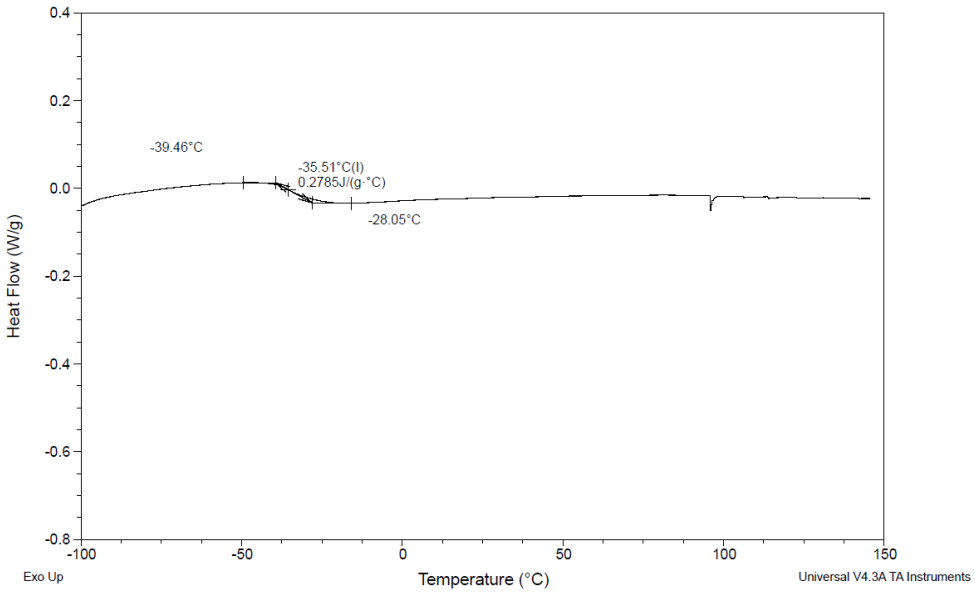

Figure A32: DSC plot of the pentablock copolymer synthesised according to C5, Table 5.3, Run 2

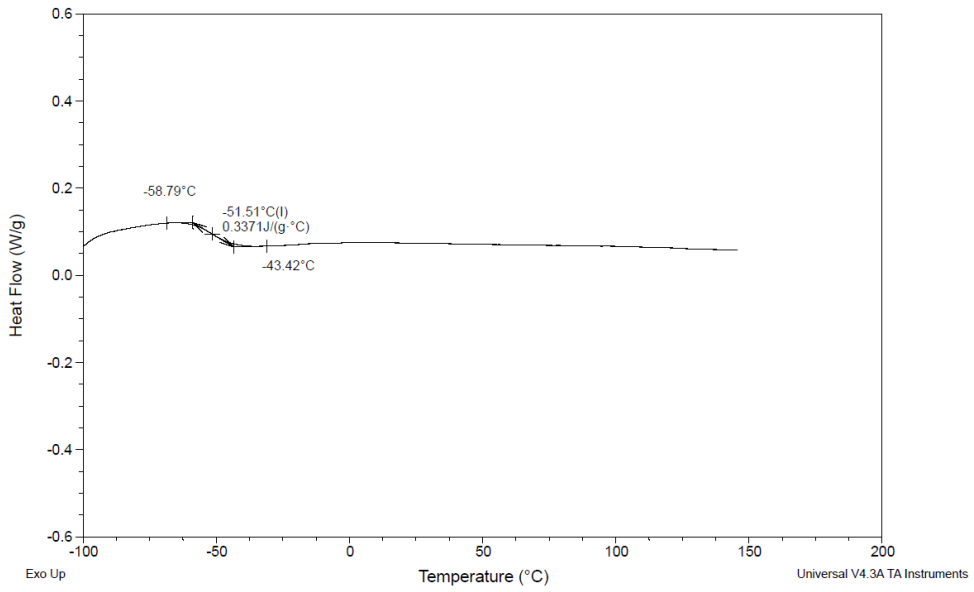

Figure A33: DSC plot of the pentablock copolymer synthesised according to C5, Table 5.3, Run 3

Figure A34: $^{13}C\{^{1}H\}$ NMR spectrum of PLA (C5, Table 5.5, Run 1)

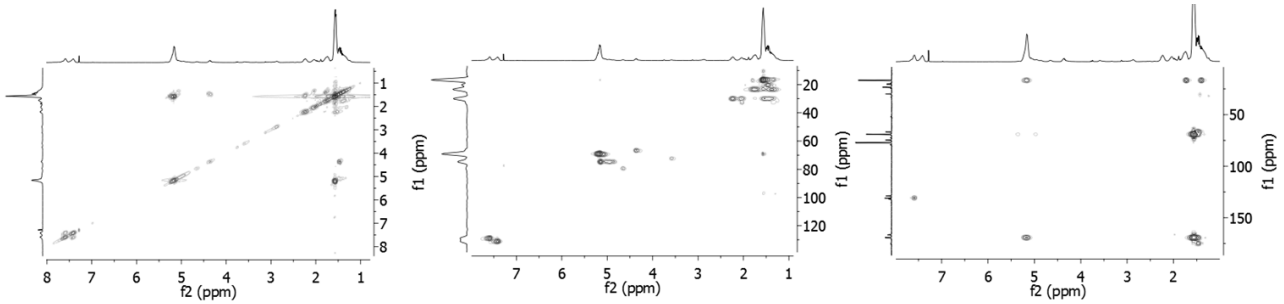

Figure A35: COSY, HSQC and HMBC NMR spectra of PLA-PCHPE-PLA (C5, Table 5.6)

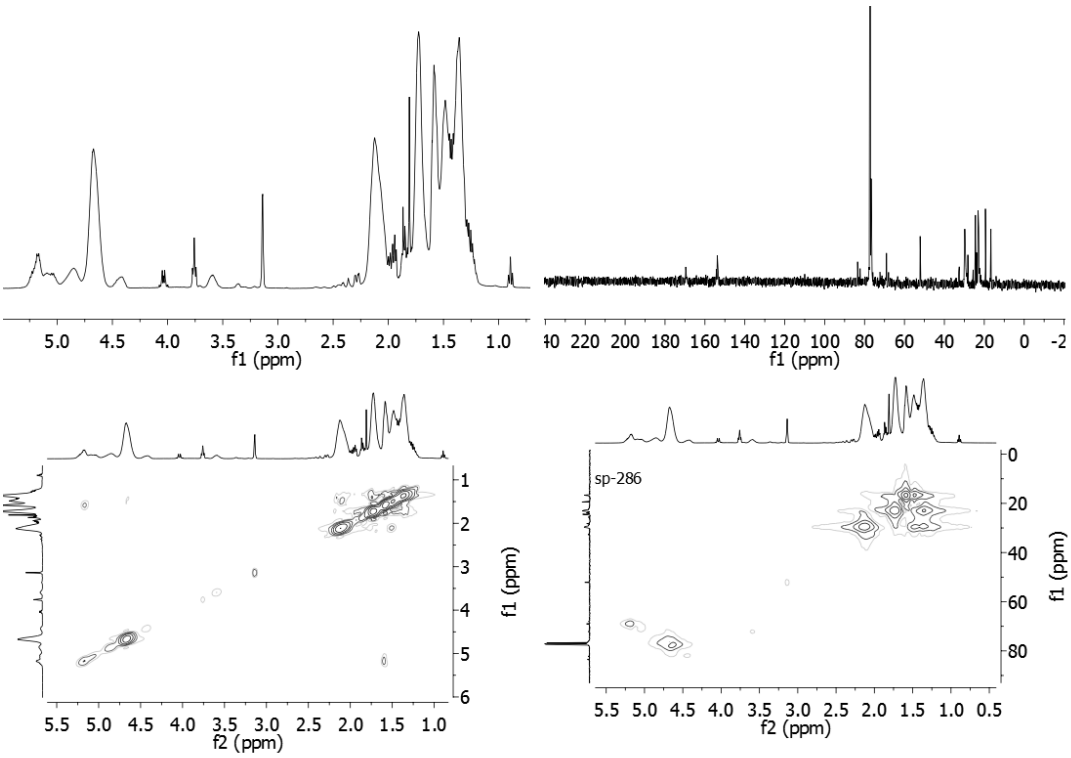

Figure A36: NMR spectra of PCHC-PLA-PCHC (C5, Table 5.7, Run 1)

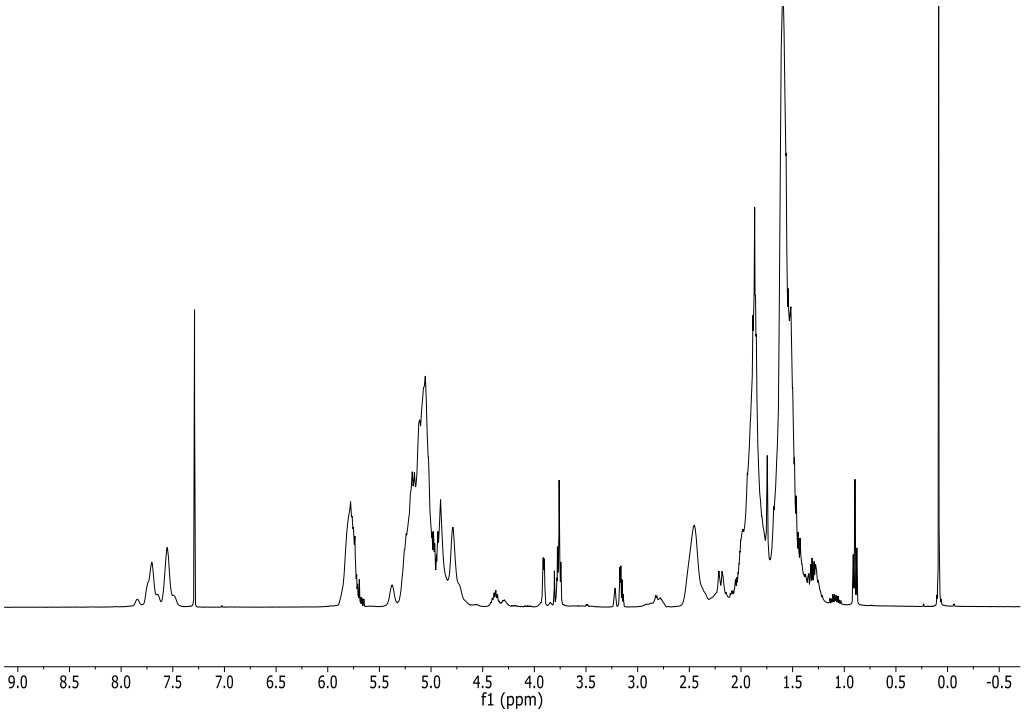

Figure A37: ^{1}H NMR spectrum of pentablock copolymer (C5, Table 5.4, Run 3)

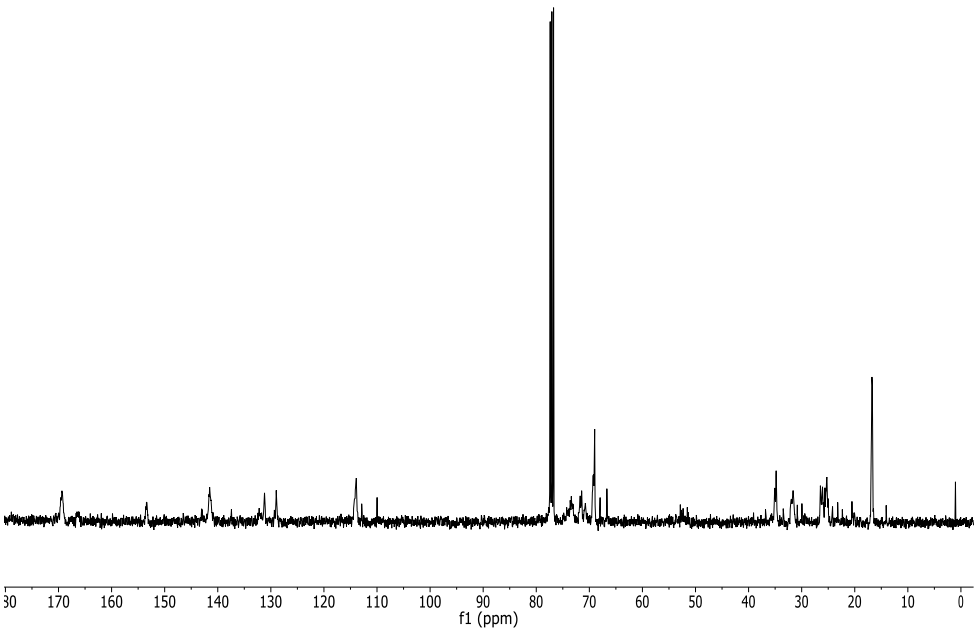

Figure A38: ^{13}C {^{1}H} NMR spectrum of pentablock copolymer (C5, Table 5.4, Run 3)

Appendix E –Chapter 6

THE AMERICAN ASSOCIATION FOR THE ADVANCEMENT OF SCIENCE LICENSE TERMS AND CONDITIONS

Sep 02, 2016

This Agreement between shyeni paul ("You") and The American Association for the Advancement of Science ("The American Association for the Advancement of Science") consists of your license details and the terms and conditions provided by The American Association for the Advancement of Science and Copyright Clearance Center.

License Number	3940821100204
License date	Sep 02, 2016
Licensed Content Publisher	The American Association for the Advancement of Science
Licensed Content Publication	Science
Licensed Content Title	Multiblock Polymers: Panacea or Pandora’s Box?
Licensed Content Author	Frank S. Bates,Marc A. Hillmyer,Timothy P. Lodge,Christopher M. Bates,Kris T. Delaney,Glenn H. Fredrickson
Licensed Content Date	Apr 27, 2012
Licensed Content Volume Number	336
Licensed Content Issue Number	6080
Volume number	336
Issue number	6080
Type of Use	Thesis / Dissertation
Requestor type	Scientist/individual at a research institution
Format	Print and electronic
Portion	Figure
Number of figures/tables	1
Order reference number	
Title of your thesis / dissertation	Switchable Catalysis to make novel copolymers
Expected completion date	Oct 2016
Estimated size(pages)	250

Requestor Location	shyeni paul 14 Chelwood Court, Westbridge ROad London, SW11 3NH United Kingdom Attn: shyeni paul

Figure A39: Permission to reproduce figure 1 from Multiblock Polymers: 'Panacea or Pandora's Box ' Science , 2012 ,336, pp. 434-440

Papers